

UNIVERSITY OF BIRMINGHAM

EXPERIMENTAL INVESTIGATION OF A PREMIXED COMPRESSION IGNITION ENGINE

By

Soheil Zeraati Rezaei

A thesis submitted to
The University of Birmingham
for the degree of
DOCTOR OF PHILOSOPHY

The University of Birmingham
School of Engineering, Department of Mechanical Engineering
September 2016

UNIVERSITY OF
BIRMINGHAM

University of Birmingham Research Archive

e-theses repository

This unpublished thesis/dissertation is copyright of the author and/or third parties. The intellectual property rights of the author or third parties in respect of this work are as defined by The Copyright Designs and Patents Act 1988 or as modified by any successor legislation.

Any use made of information contained in this thesis/dissertation must be in accordance with that legislation and must be properly acknowledged. Further distribution or reproduction in any format is prohibited without the permission of the copyright holder.

ABSTRACT

Premixed compression-ignition (PCI) combustion techniques using low-cetane fuels, including Dieseline (mixture of diesel-gasoline) and naphtha, were investigated in a light-duty multi-cylinder CI-engine focusing mainly on reducing emissions while maintaining or improving the brake-thermal-efficiency. Different fuel-injection and intake/exhaust handling strategies were investigated in a wide engine operating load range from 1.4 to 17.3 bar BMEP. Moreover, an out-cylinder emission reduction technique through using a diesel-oxidation-catalyst (DOC) was investigated. Hot (uncooled) exhaust-gas-recirculation (EGR) combined with low fuel-injection-pressure (as low as 150 bar) significantly enhanced combustion-performance (COV<5%) and reduced carbon-monoxide and hydrocarbon emissions at lower loads, when using low-cetane fuelled PCI techniques. At 1.4 to 6 bar BMEP, particulate emissions were reduced by >99% with respect to the diesel-CI baseline, in terms of number and mass, while maintaining brake-specific-NO_x below 0.4 g/kWh. At loads more than 6 bar BMEP, double-injection strategy advanced combustion-phasing, where the first injection-event was shown to be significantly influential. Due to narrower boiling-range of naphtha compared to Dieseline, naphtha PCI resulted in high-COV at low loads, while it resulted in rapid-combustion at medium/high loads. Utilisation of the hot-EGR is a "win-win" strategy to enhance the combustion-process of the PCI-engine and reduction of the volatile/semi-volatile compounds using the DOC.

Dedicated to my beloved family - Zohreh, Manouchehr and Saadat

ACKNOWLEDGEMENTS

I would like to express my gratitude towards my principal supervisor, Prof. Hongming Xu, for his generous support and supervision. I would like to thank my co-supervisor, Dr Oluremi Olatunbosun, for providing valuable hints. Special appreciations go to Prof. Akbar Ghafourian, Prof. Roy M. Harrison, Prof. Miroslaw L. Wyszynski and Prof. Gautam Kalghatgi for all invaluable scientific discussions and comments. Support from colleagues at Jaguar Land Rover, in particular Mr. Ben Neaves, regarding engine research, and at Shell, especially Prof. Roger Cracknell, regarding fuel research is appreciated. I would like to thank the University of Birmingham for my Ph.D. scholarship and European Research Council for funding the FASTER project which supported part of this work. Thanks go to technicians, Mr. Carl Hingley, Mr. Rickie Creegan, Mr. Peter Thornton, Mr. Jack Garrod and Mr. Lee Gauntlett for their help when I was designing and manufacturing the new engine test facility.

I would like to thank Mr. Yasser Al Qahtani, my close friend and colleague who has always motivated me and was cooperative in different stages of this work. Thanks go to my friends and colleagues, Dr Jose Martin Herreros and Dr Mohammed S. Alam for acting as my mentors. Furthermore, thanks go to Mr. Omid Doustdar, Dr Fan Zhang, Dr Isaline Lefort, Dr Chongming Wang, Dr Asish Sarangi, Dr Ekarong Sukjit, Ms. Maria Bogarra Macias, Dr Manju Tanwar, Dr Daliang Jiang and many more who made my work and spare time joyful.

Very special thanks to my brother, Saadat, for making living easier for me. Finally and most importantly, I would like to thank my mother and father, Zohreh and Manouchehr, for their unconditional love, support and understanding which cannot be described by words.

Soheil Zeraati Rezaei

September 2016

CONTENTS

CONTENTS I

ABBREVIATIONS VIII

LIST OF FIGURES XII

LIST OF TABLES XXI

Chapter 1 INTRODUCTION 1

1.1. Background 1

1.2. Growing energy demand and associated environmental and human health complications 3

1.3. Legislative controls of transportation emissions 4

1.4. Current automotive fuel/fleet technology and future outlook 6

1.5. Advanced compression ignition combustion engines 9

1.6. Research objectives 11

1.7. Thesis outline and approach 12

Chapter 2 LITERATURE REVIEW 17

2.1. Introduction 17

2.2. Fundamental properties of automotive fuels 17

2.2.1. Hydrocarbons composition 18

2.2.2. Auto-ignition quality 20

2.2.3. Volatility/distillation profile 21

2.2.4. Flash point 21
2.3. Conventional diesel compression ignition combustion 22
2.3.1. Pre-ignition events 23
2.3.2. Auto-ignition and premixed combustion period 23
2.3.3. Mixing-controlled combustion period 24
2.4. Premixed low temperature compression ignition combustion 26
2.4.1. Low temperature combustion (LTC) mechanism 27
2.4.2. Unburnt hydrocarbons and carbon monoxide sources 28
2.5. Low reactivity fuels for homogeneous, premixed and partially-premixed compression ignition combustion 29
2.5.1. Homogeneous charge compression ignition (HCCI) 32
2.5.2. Premixed and partially-premixed compression ignition (PPCI) 33
2.5.3. Gasoline compression ignition (GCI) 34
2.5.4. In-cylinder fuel blending for dual-fuel PPCI 36
2.6. Particulate emissions from vehicular engines 37
2.6.1. Organic fraction 38
2.6.2. Carbonaceous fraction 41
2.7. Emission abatement techniques 41
2.7.1. CO, HC and particulates after-treatment systems 42
2.7.2. NO_x after-treatment systems 48
2.8. Summary 49
Chapter 3 EXPERIMENTAL SYSTEM SETUP 50

3.1. Introduction 50

3.2. CR-15.5 engine test cell 50

3.2.1. CR-15.5 engine 50

3.2.2. Engine control unit 53

3.2.3. Dynamometer and control unit 53

3.2.4. Test cell control and conditioning 54

3.2.5. Diesel oxidation catalyst (DOC) 55

3.2.6. Intake and exhaust sampling ports design and locations 56

3.3. Instrumentations 56

3.3.1. In-cylinder pressure measurement and acquisition system 57

3.3.2. Engine and test cell pressure and temperature measurement 59

3.3.3. Fuel consumption measurement 59

3.4. CR-16.6 engine test cell 60

3.5. Emissions measurement 61

3.5.1. On-line gaseous emissions characterisation 61

3.5.2. On-line particulate emissions characterisation 62

3.5.3. Off-line gaseous and particulate emissions collection and characterisation 64

3.6. Data analysis and calculations 67

3.6.1. In-cylinder pressure based parameters calculation procedure 67

3.6.2. Specific performance and emission terms calculation procedure 68

3.7. Studied fuels 70

3.8. Uncertainties of experimental parameters 72

3.9. Summary 74

Chapter 4 PARAMETRIC ANALYSIS OF SPLIT-INJECTION STRATEGIES FOR PREMIXED COMPRESSION IGNITION 75

4.1. Introduction 75

4.2. Background 76

4.3. Experimental plan 77

4.4. Screening experiments 80

4.5. Design of experiment and analysis at 1.37 bar BMEP 82

4.5.1. Validation Experiments 84

4.5.2. Comparison of single and double injection strategies at 1.37 bar BMEP 86

4.6. Design of experiment and analysis at 2.97 bar BMEP 87

4.6.1. Comparison of single and double injection strategies at 2.97 bar BMEP 90

4.7. Summary/Conclusions 94

Chapter 5 DIESELINE FUELLED PREMIXED COMPRESSION IGNITION COMBUSTION ENGINE 97

5.1. Introduction 97

5.2. Investigation of different EGR strategies for lower engine operating loads 99

5.2.1. Effects of different EGR cooling strategies 100

5.2.2. Effects of EGR rate variation 107

5.3. Investigation of single-injection strategies for Dieseline PCI combustion 112

5.3.1. Results at 1.4 and 3 bar BMEP with application of hot-EGR and low IP 112

5.3.2. Results at 6 bar BMEP 131

5.3.3. Results at 12 bar BMEP 145

5.3.4. Results at 17.3 bar BMEP 150

5.4. Investigation of double-injection strategies for Dieseline PCI combustion 153

5.4.1. Results at 1.4 bar BMEP 154

5.4.2. Results at 3 bar BMEP 157

5.4.3. Results at 6 bar BMEP 159

5.4.4. Results at 12 bar BMEP 163

5.5. Summary/Conclusions 167

5.5.1. Effects single-injection with different injection and intake/exhaust handling strategies 168

5.5.2. Effects of double-injection strategies 170

Chapter 6 NAPHTHA FUELLED PREMIXED COMPRESSION IGNITION COMBUSTION ENGINE 173

6.1. Introduction 173

6.2. Investigation of single-injection strategy at different operating loads 173

6.2.1. Investigation of different injection pressures and timings at 1.4 bar BMEP 174

6.2.2. Investigation of different EGR rates at 1.4 bar BMEP 176

6.2.3. Investigation of different injection pressures and timings at 3 bar BMEP 178

6.2.4. Results at 6 bar BMEP 182

6.2.5. Results at 12 bar BMEP 185

6.2.6. Results at 17.3 bar BMEP 190

6.3. Investigation of double-injection strategies at different operating loads 191

6.3.1. Results at 1.4 bar BMEP 192

6.3.2. Results at 3 bar BMEP 192

6.3.3. Results at 6 bar BMEP 194

6.3.4. Results at 12 bar BMEP 196

6.4. Summary/Conclusions 199

6.4.1. Results of single-injection strategies 199

6.4.2. Results of double-injection strategies 201

Chapter 7 EFFECTS OF THE DOC ON EMISSIONS FROM A PREMIXED COMPRESSION IGNITION ENGINE 204

7.1. Introduction 204

7.2. Test Procedure 205

7.3. Effects of the DOC on emissions of Dieseline and diesel CI combustion at 1.4 bar BMEP 206

7.3.1. Results for G75-Dieseline operation 206

7.3.2. Results for diesel operation 217

7.4. Effects of the DOC on emissions of Dieseline and diesel CI combustion at 3 bar BMEP 225

7.4.1. Results for G75-Dieseline operation 226

7.4.2. Results for diesel operation 228

7.5. Effects of the DOC on emissions of Dieseline and diesel CI combustion at 6 bar BMEP 231

7.5.1. Results for G75-Dieseline operation 232

7.5.2. Results for diesel operation 234

7.6. Summary/Conclusions 237

Chapter 8 SUMMARY, CONCLUSIONS & FUTURE WORK 241

8.1. Introduction 241

8.2. Summary and conclusions 241

8.3. Possible implications for fuel/automotive industries and suggested future work 248

AUTHOR'S PUBLICATIONS RELATED TO THIS WORK 251

REFERENCES 253

APPENDIX 261

A1. Engine control with ATI VISION interface 261

A2. Electrical and signal connections of the engine test cell 263

A3. Extraction Procedure for GC×GC-TOF-MS Analysis 265

ABBREVIATIONS

Acc. C	Accumulation mode concentration (particles)
Acc. CMD	Accumulation mode count median diameter (particles)
Acc. PM	Accumulation mode particulate mass
ACE	Acenaphthene
ACY	Acenaphthylene
AFR	Air-fuel ratio
AHR-50	CAD at which 50% of accumulated heat release is achieved
AL_2O_3	Alumina
ANOVA	Analysis of variance
ANT	Anthracene
aTDC	After top dead centre
BEV	Battery electric vehicle
BS	Brake specific
BSFC	Brake specific fuel consumption
BTE	Brake thermal efficiency
C Dur	Combustion duration
CAD	Crank angle degrees (sometimes it is denoted as ^{o})
CDC	Conventional diesel combustion
CI	Compression ignition
CLD	Chemi-luminescence detection
CLIC	Computer language for identifying chemical
CMD	Count median diameter
CN	Cetane number
CO	Carbon monoxide
$CO(NH_2)_2$	Urea
COV	Coefficient of variation
D	Sometimes refers to diesel fuel
DAQ	Data acquisition board
DCN	Derived cetane number
DI	Direct-injection
Dieseline	Blend of diesel and gasoline fuels
DMS	Differential mobility spectroscopy
DOC	Diesel oxidation catalyst
DOE	Design of experiment
DPF	Diesel particulate filter
DR	Dilution ratio
EC/OC	The ratio of the elemental carbon to organic carbon
ECU	Engine control unit
EGR	Exhaust gas recirculation
EOI	End of injection
EPT	Electro-pneumatic transducer
Equivalence ratio	Ratio of actual fuel/air ratio to stoichiometric fuel/air ratio
EU	European union

FAME	Fatty acid methyl ester
FCEV	Fuel-cell electric vehicle
FID	Flame ionisation detector
FIE	Fuel injection equipment
FLR	Fluoranthene
FLU	Fluorene
FSN	Filter smoke number
FT	Fischer-tropsch
GC	Gas chromatography
GCI	Gasoline compression ignition
GDCI	Gasoline direct injection compression ignition
GDI	Gasoline direct injection
GHG	Green-house gas
H_2CO	Formaldehyde
H_2O_2	Hydrogen peroxide
HC	Hydrocarbons
HCCI	Homogeneous charge compression ignition
HD	Heavy duty
HEV	Hybrid electric vehicle
HMW	High molecular weight
HRR	Heat release rate
IBP	Initial boiling point
ICE	Internal combustion engine
ID	Ignition delay
IEA	International energy agency
Ignition dwell	CAD duration between EOI and SOC
IMEP	Indicated mean effective pressure
IP	Injection pressure
IQ	Injection-quantity
IT	Injection-timing (it is the same as SOI)
LD	Light duty
LMW	Low molecular weight
LTC	Low temperature combustion
MON	Motor octane number
MPA	Magneto-pneumatic
MPCI	Multiple premixed compression ignition
MPRR	Maximum pressure rise rate
MS	Mass spectrometry
n-	Normal (straight chain) HC
n-alkanes	Normal alkanes
NAP	Naphthalene
NDIR	Non-dispersive Infra-Red
NEDC	New European driving cycle
NH_3	Ammonia
NI	National instruments
NIMEP	Net indicated mean effective pressure

nm	Nano-meter
NO_x	Oxides of nitrogen
O_2	Oxygen
OA	Orthogonal array
OEM	Original equipment manufacturer
OH	Hydroxide
PAH	Polycyclic aromatic hydrocarbons
PCCI	Premixed charge compression ignition
PCI	Premixed compression ignition
Pd	Palladium
PFI	Port fuel injection
PGM	Platinum group metals
PHE	Phenanthrene
PID controller	Proportional-integral-differential controller
PLIF	Planar laser-induced fluorescence
PM	Particulate mass
PN	Particulate number
PPCI	Partially premixed compression ignition
ppm	Parts per million
ppmv	Volumetric parts per million
Pt	Platinum
PTFE	Polytetrafluoroethylene
PTO	Power take off
PYR	Pyrene
RCCI	Reactivity controlled compression ignition
RDE	Real driving emissions
RF	Response factor
RON	Research octane number
RPM	Revolutions per minute
S.T.P	Standard temperature and pressure
SC	Supercritical
SCR	Selective catalytic reduction
SD	Standard deviation
SI	Spark ignition
SOA	Secondary organic aerosol
SOC	Start of Combustion
SOF	Soluble organic fraction
SOI	Start of injection (it is the same as IT)
SVOC	Semi-volatile organic compounds
TD	Thermal desorption
TDC	Top dead centre
THC	Total hydrocarbons
TIC	Total ion chromatogram
TOF	Time of flight
TPN	Total particulate number
TWC	Three-way catalyst

UCM	Unresolved complex mixture
UK	The United Kingdom
ULSD	Ultra-low sulphur diesel
μm	Micro-meter
UNIBUS	Uniform bulky combustion system
VGT	Variable-geometry turbocharger
VNT	Variable-nozzle-turbine
WEO	World energy outlook
WLTP	Worldwide harmonized light vehicles test procedure
WTW	Well-to-wheel
XRF	X-ray fluorescence
λ	Specific (relative) air-fuel ratio

LIST OF FIGURES

Figure 1-1 Number of publications versus year covering the period from the beginning of year 2000 to (*) the end of June of year 2016 (this data was obtained from the Web of Science searching for publications in all databases containing the exact phrases illustrated)..... 11

Figure 3-1 The CR-15.5 engine test cell 51

Figure 3-2 Schematic of the CR-15.5 engine test cell..... 52

Figure 3-3 Exhaust sampling port design: (a) before and (b) after welding to the pipe with holes at different cross sectional area of the sampling port..... 57

Figure 3-4 In-cylinder pressure (white), crank shaft encoder (green) and cam shaft encoder (red) signals versus time created in the LabVIEW interface..... 58

Figure 3-5 Schematic of the CR-16.6 engine test cell..... 61

Figure 3-6 Schematic of the exhaust dilution and sample collection system..... 65

Figure 3-7 Comparison of different fuels in terms of their boiling profile measured with either ASTM D86 or DIN EN ISO 3405 methods 72

Figure 3-8 Particulate number and size distribution results for random error experiments..... 74

Figure 4-1 Effect of the injection parameters on smoke emissions at 2.97 bar BMEP. (~ indicates approximate value, Q and T are Injection Quantity-ratio and Timing, respectively. ^{o} aTDC is equal to CAD aTDC) 80

Figure 4-2 Taguchi and validation experiments results of $BSNO_x$ and smoke for 1.37 bar BMEP 85

Figure 4-3 Accumulation mode particulate number and size distribution of single and double injection strategies at 2.97 bar BMEP 91

Figure 4-4 Particulate number and size distribution for three first injection quantity-ratios with fixed injection-timing (at -68 CAD aTDC) and combustion phase (at 3 CAD aTDC) at 2.97 bar BMEP [43] 93

Figure 4-5 Particulate number and size distribution for four first injection-timings with fixed first injection quantity-ratio (at 70%) and combustion phase (at 3 CAD aTDC) at 2.97 bar BMEP [43] 93

Figure 5-1 Effect of different EGR cooling strategies at different injection pressures (IPs) on the intake manifold temperature at 1.4 and 3 bar BMEP and 1800 RPM 102

Figure 5-2 Effect of different EGR cooling strategies at different injection pressures (IPs) on BSTHC and BSCO at 1.4 and 3 bar BMEP and 1800 RPM 104

Figure 5-3 Effect of different EGR cooling strategies at different injection pressures (IPs) on smoke at 1.4 and 3 bar BMEP and 1800 RPM 105

Figure 5-4 Effect of different EGR cooling strategies at different injection pressures (IPs) on $BSNO_x$ at 1.4 and 3 bar BMEP and 1800 RPM 106

Figure 5-5 Effect of different EGR cooling strategies at different injection pressures (IPs) on the exhaust gas temperature at 1.4 and 3 bar BMEP and 1800 RPM 107

Figure 5-6 Comparison of $BSNO_x$ emissions of G75-Dieseline and diesel (D) at different EGR rates 109

Figure 5-7 Comparison of smoke emissions of G75-Dieseline and diesel (D) at different EGR rates 110

Figure 5-8 Comparison of BTE of G75-Dieseline and diesel (D) at different EGR rates 111

Figure 5-9 Comparison of BSTHC emissions of G75-Dieseline and diesel (D) at different EGR rates 112

Figure 5-10 In-cylinder pressure, heat release rate and injection pulse results for G75-Dieseline and diesel (D) combustion at: (a) 3 bar BMEP and (b) 1.4 bar BMEP 114

Figure 5-11 Results of smoke emissions for G75 and diesel at 3 bar BMEP with different injection-timings and injection pressures; (a) illustrates the full range and (b) illustrates a zoomed view to show smoke values below 0.2 FSN 116

Figure 5-12 Results of smoke emissions for G75 and diesel at 1.4 bar BMEP with different injection-timings and injection pressures; (a) illustrates the full range and (b) illustrates a zoomed view to show smoke values below 0.2 FSN 119

Figure 5-13 Results of $BSNO_x$ emissions for G75 and diesel with different injection-timings and injection pressures at: (a) 3 bar BMEP and (b) 1.4 bar BMEP 120

Figure 5-14 Coefficient of variation (COV) of net indicated mean effective pressure (NIMEP) for G75 and diesel with different injection pressures and timings at: (a) 3 bar BMEP and (b) 1.4 bar BMEP 121

Figure 5-15 Comparison of G75 and diesel at 3 bar BMEP with different injection-timings and pressures, in terms of: BTE, brake specific fuel consumption (BSFC) and combustion efficiency 123

Figure 5-16 Comparison of G75 and diesel at 1.4 bar BMEP with different injection-timings and pressures, in terms of: BTE, brake specific fuel consumption (BSFC) and combustion efficiency 124

Figure 5-17 Comparison of G75 and diesel with different injection pressures and timings at 3 bar BMEP, in terms of: (a) ignition delay (ID), (b) brake specific total hydrocarbons (BSTHC), (c) combustion delay (CD) and (d) brake specific carbon monoxide (BSCO) 125

Figure 5-18 Comparison of G75 and diesel with different injection pressures and timings at 1.4 bar BMEP, in terms of: (a) ignition delay (ID), (b) brake specific total hydrocarbons (BSTHC), (c) combustion delay (CD) and (d) brake specific carbon monoxide (BSCO) 127

Figure 5-19 Combustion duration (C Dur) of G75 and diesel with different injection pressures and timings at: (a) 3 bar BMEP and (b) 1.4 bar BMEP 128

Figure 5-20 Engine exhaust temperature for G75 and diesel with different injection pressures and timings at: (a) 3 bar BMEP and (b) 1.4 bar BMEP 130

Figure 5-21 BTE and $BSNO_x$ for single-injection of G75 with different EGR valve positions and injection-timings with injection pressure of: (a) 500 bar, (b) 600 bar and (c) 700 bar at 6 bar BMEP; red circles in the figures mark the highest achieved BTE while $BSNO_x$ is below 0.4 g/kWh 132

Figure 5-22 BTE and $BSNO_x$ for single-injection of diesel with different EGR valve positions and injection-timings with injection pressure of: (a) 800 bar, (b) 1000 bar and (c) 1200 bar at 6 bar BMEP 134

Figure 5-23 Smoke emissions in terms of filter smoke number (FSN) for G75, left column, and diesel, right column, at different injection pressures, injection-timings and EGR valve positions at 6 bar BMEP 136

Figure 5-24 Brake specific accumulation mode particulate mass (Acc. PM) for G75, left column, and diesel, right column, at different injection pressures, injection-timings and EGR valve positions at 6 bar BMEP (it should be noted that this graph is a semi-logarithmic plot) 137

Figure 5-25 Brake specific total particulate number (TPN) for G75, left column, and diesel, right column, at different injection pressures, injection-timings and EGR valve positions at 6 bar BMEP (it should be noted that this graph is a semi-logarithmic plot) 139

Figure 5-26 Particulates count median diameter (CMD) for G75, left column, and diesel, right column, at different injection pressures, injection-timings and EGR valve positions at 6 bar BMEP 140

Figure 5-27 Brake specific particulate number and size distributions for G75 and diesel at 6 bar BMEP; (a) semi-logarithmic plot and (b) log-log plot 141

Figure 5-28 Brake specific total hydrocarbons (BSTHC) for G75, left column, and diesel, right column, at different injection pressures, injection-timings and EGR valve positions at 6 bar BMEP 143

Figure 5-29 Brake specific carbon monoxide (BSCO) for G75, left column, and diesel, right column, at different injection pressures, injection-timings and EGR valve positions at 6 bar BMEP 144
Figure 5-30 In-cylinder pressure, heat release rate and injection pulse for G75 and diesel at 6 bar BMEP using single-injection 145
Figure 5-31 Comparison of results of G75 single-injection with the results of base line diesel single-injection at 12 bar BMEP with fixed injection pressure of 1000 bar 147
Figure 5-32 In-cylinder pressure, heat release rate and injection pulse for G75 and diesel at 12 bar BMEP, IP of 1000 bar and EGR rate of 15% 148
Figure 5-33 Brake specific particulate number and size distributions for G75 and diesel at 12 bar BMEP and IP of 1200 bar 149
Figure 5-34 In-cylinder pressure, heat release rate and injection pulse for G75 and diesel at 12 bar BMEP and IP of 1200 bar 150
Figure 5-35 In-cylinder pressure, heat release rate and injection pulse for G75 and diesel at 17.3 bar BMEP 153
Figure 5-36 Comparison of G75 and diesel when using double-injection strategy at 1.4 bar BMEP 156
Figure 5-37 Comparison of G75 and diesel when using double-injection strategy at 3 bar BMEP 158
Figure 5-38 Comparison of G75 and diesel when using double-injection strategy at 6 bar BMEP; IP of G75 and diesel were fixed at 500 and 1200 bar, respectively 160
Figure 5-39 In-cylinder pressure, heat release rate and injection pulse for G75 and diesel at 6 bar BMEP with double-injection strategies 162
Figure 5-40 Particulate number and size distribution for G75 and diesel at 6 bar BMEP with double-injection strategies 162

Figure 5-41 Comparison of G75 and diesel when using double-injection strategy at 12 bar BMEP; IP of G75 and diesel were fixed at 1000 and 1200 bar, respectively, and IT2 was maintained at -5 CAD aTDC for G75 and at -3 CAD aTDC for diesel and EGR rate was fixed at 15% for both fuels 164
Figure 5-42 In-cylinder pressure, heat release rate and injection pulse for G75 and diesel at 12 bar BMEP with double-injection strategies. Injection pressures of G75 and diesel were fixed at 1000 bar and 1200 bar, respectively 165
Figure 5-43 Particulate number and size distribution for G75 and diesel at 12 bar BMEP with double-injection strategies. Injection pressures of G75 and diesel were fixed at 1000 bar and 1200 bar, respectively 165
Figure 5-44 In-cylinder pressure, heat release rate and injection pulse for G75 at 12 bar BMEP with different injection pressures and double-injection strategy 167
Figure 6-1 Combustion and emissions characterises of naphtha compression ignition at 1.4 bar BMEP while using single-injection strategy 176
Figure 6-2 Effect of varying EGR rate for naphtha compression ignition at 1.4 bar BMEP while using single-injection 177
Figure 6-3 Combustion and emissions characterises of naphtha compression ignition at 3 bar BMEP while using single-injection 179
Figure 6-4 Effect of varying injection pressure for naphtha compression ignition at 3 bar BMEP while using single-injection 181
Figure 6-5 Brake thermal efficiency (BTE) and brake specific NO_x ($BSNO_x$) of naphtha compression ignition with different injection pressures and EGR settings at 6 bar BMEP ... 184
Figure 6-6 BTE, $BSNO_x$, BSTHC and BSCO of naphtha compression ignition with the injection pressure of 400 bar and different EGR settings at 6 bar BMEP 185

Figure 6-7 Combustion and emission characteristics of naphtha compression ignition with varying injection-timing at 12 bar BMEP; λ and EGR rate were fixed at around 1.25 and 8%, respectively. 187
Figure 6-8 In-cylinder pressure, heat release rate and injection pulse for naphtha and G75 at 12 bar BMEP when using single-injection 188
Figure 6-9 Particulate number and size distribution of naphtha and G75 at 12 bar BMEP when using single-injection 188
Figure 6-10 Combustion and emission characteristics of naphtha compression ignition with varying injection pressure at 12 bar BMEP 189
Figure 6-11 Combustion and emission characteristics of naphtha at 3 bar BMEP with double-injection strategies 193
Figure 6-12 Combustion and emission characteristics of naphtha at 6 bar BMEP with double-injection strategies 194
Figure 6-13 Combustion and emission characteristics of naphtha at 12 bar BMEP with double-injection strategies 197
Figure 7-1 Injection pressure (IP) sweep effect on particulate number and size distribution for G75-Dieseline at 1.4 bar BMEP at two injection-timings (IT) 207
Figure 7-2 Particulate number and size distribution before and after DOC when using G75 at 1.4 bar BMEP 210
Figure 7-3 Three-dimensional plots of the total ion chromatogram (TIC) for gas phase SVOC emissions from G75 combustion at 1.4 bar BMEP, (a) before DOC and (b) after DOC 212
Figure 7-4 Normal alkanes (n-alkane) and total alkanes emissions before and after the DOC when using G75 fuel at 1.4 bar BMEP 213
Figure 7-5 Normal (n)-alkyl-cyclohexanes and total alkyl-cycloalkanes emissions before and after the DOC when using G75 fuel at 1.4 bar BMEP 216

Figure 7-6 PAH emissions before and after the DOC when using G75 fuel at 1.4 bar BMEP 217
Figure 7-7 Particulate number and size distribution before and after DOC when using: (a) diesel and (b) G75 at 1.4 bar BMEP 219
Figure 7-8 Particulate number and size distribution before and after DOC when using hot-EGR for diesel at 1.4 bar BMEP 221
Figure 7-9 Normal alkanes (n-alkane) and total alkanes emissions before and after the DOC when using diesel fuel at 1.4 bar BMEP 223
Figure 7-10 Normal (n)-alkyl-cyclohexanes and total alkyl-cycloalkanes emissions before and after the DOC when using diesel fuel at 1.4 bar BMEP 224
Figure 7-11 PAH emissions before and after the DOC when using diesel fuel at 1.4 bar BMEP 225
Figure 7-12 Particulate number and size distribution before and after DOC when using G75 at 3 bar BMEP 227
Figure 7-13 Alkanes emissions before and after the DOC when using G75 fuel at 3 bar BMEP 228
Figure 7-14 Particulate number and size distribution before and after DOC when using diesel at 3 bar BMEP 230
Figure 7-15 Alkanes emissions before and after the DOC when using diesel fuel at 3 bar BMEP 231
Figure 7-16 Particulate number and size distribution before and after DOC when using G75 at 6 bar BMEP 233
Figure 7-17 Alkanes emissions before and after the DOC when using G75 fuel at 6 bar BMEP 234

Figure 7-18 Particulate number and size distribution before and after DOC when using diesel at 6 bar BMEP 235
Figure 7-19 Alkanes emissions before and after the DOC when using diesel fuel at 6 bar BMEP 236

LIST OF TABLES

Table 1-1 EU emission standards for light-duty compression ignition (Diesel) Vehicles from [9] 6

Table 2-1 Breakdown of the fractions of the particulates emissions sourced from vehicles [24]. 38

Table 3-1 CR-15.5 engine specifications 51

Table 3-2 CR-16.6 engine specifications 60

Table 3-3 Properties of the utilised fuels 71

Table 3-4 Measured parameters with their average value and standard deviation for random error experiments 74

Table 4-1 Taguchi L9 orthogonal array for fractional factorial analysis of 3 factors with 3 variation levels (9 experiments must be conducted) 78

Table 4-2 Taguchi fractional factorial DOE factors and levels for 1.37 bar BMEP 81

Table 4-3 Taguchi fractional factorial DOE factors and levels for 2.97 bar BMEP 81

Table 4-4 Fractional factorial Taguchi-DOE results at 1.37 bar BMEP 83

Table 4-5 The optimum two-stage and single-stage injection strategies results at 1.37 bar BMEP, AHR-50: 3 CAD aTDC 86

Table 4-6 Taguchi fractional factorial DOE results at 2.97 bar BMEP 88

Table 4-7 The optimum two-stage and single-stage injection strategies results at 2.97 bar BMEP, AHR-50: 2 CAD aTDC 91

Table 5-1 Test conditions of the EGR cooling strategy experiments to investigate effects of the EGR temperature on the combustion performance and emission characteristics while using single-injection 98

Table 5-2 Test conditions of the EGR rate variation experiments to investigate effects of the EGR rate on the combustion performance and emission characteristics while using single-injection 98
Table 5-3 Test conditions of the single-injection strategy experiments 99
Table 5-4 Test conditions of the double-injection strategy experiments 99
Table 5-5 Effect of the variation of SOI at 1.4 bar BMEP with IP of 450 bar on G75-Dieseline PCI 113
Table 5-6 Comparison of G75 and diesel at 12 bar BMEP with fixed injection pressure and combustion-phasing; IT for G75 and diesel were -5 and -3 CAD aTDC, respectively 149
Table 5-7 G75 combustion performance and emissions results at 17.3 bar BMEP and IP of 1100 bar 151
Table 5-8 Comparison of G75 and diesel at 17.3 bar BMEP with the same AHR-50; IT of G75 and diesel were fixed at -3 and 0 CAD aTDC, respectively 152
Table 5-9 Results of selected operating points of G75 and diesel fuels at 1.4 bar BMEP using single-injection strategy 156
Table 5-10 Results of selected operating points of G75 and diesel fuels at 3 bar BMEP using single-injection strategy 159
Table 5-11 Results of selected operating points of G75 and diesel fuels at 6 bar BMEP using single-injection strategy 160
Table 5-12 Comparison of different injection pressures for G75 double-injection at 12 bar BMEP. First and second injection-timings were fixed at -40 and -5 CAD aTDC, respectively. EGR rate was fixed at 15% and 10 % of the total injected fuel was injected in the first injection 166

Table 6-1 Combustion and emission characteristics of naphtha compression ignition with varying EGR rate at 12 bar BMEP; IT and IP were fixed at -7 CAD aTDC and 1000 bar, respectively 190

Table 6-2 Combustion and emissions characteristics of naphtha compression ignition at 17.3 bar BMEP; IP and EGR rate are fixed at 1100 bar and 5.5%, respectively 191

Table 6-3 Variation of second injection-timing (IT2) for naphtha at 12 bar BMEP while first injection-timing was fixed at -100 CAD aTDC 198

Table 7-1 Emissions and exhaust temperature before and after DOC when using G75 at 1.4 bar BMEP 208

Table 7-2 Particulate emissions physical concentration characteristics for G75 at 1.4 bar BMEP 211

Table 7-3 Emissions and exhaust temperature before and after DOC when using diesel at 1.4 bar BMEP 218

Table 7-4 Particulate emissions physical concentration characteristics for diesel at 1.4 bar BMEP 220

Table 7-5 Emissions and exhaust temperature before and after DOC when using hot-EGR for diesel at 1.4 bar BMEP 220

Table 7-6 Particulate emissions physical concentration characteristics for hot-EGR diesel at 1.4 bar BMEP 221

Table 7-7 Emissions and exhaust temperature before and after DOC when using G75 at 3 bar BMEP 226

Table 7-8 Particulate emissions physical concentration characteristics for G75 at 3 bar BMEP 227

Table 7-9 Emissions and exhaust temperature before and after DOC when using diesel at 3 bar BMEP 229

Table 7-10 Particulate emissions physical concentration characteristics for diesel at 3 bar BMEP 230

Table 7-11 Emissions and exhaust temperature before and after DOC when using G75 at 6 bar BMEP 232

Table 7-12 Particulate emissions physical concentration characteristics for G75 at 6 bar BMEP 233

Table 7-13 Emissions and exhaust temperature before and after DOC when using diesel at 6 bar BMEP 234

Table 7-14 Particulate emissions physical concentration characteristics for diesel at 6 bar BMEP 235

Chapter 1
INTRODUCTION

1.1. Background

Concerns regarding the possible scarcity of fossil fuel reserves and adverse effects of primary and secondary emissions originated from combustion engines have motivated research into more efficient and clean energy-convertors. The importance and extent of these issues has forced regulatory bodies to enforce drastic reductions in emissions limits during the past two decades. The research into these energy conversion systems covers a spread from clean fuel research to internal combustion engines (ICE) to emissions after-treatment systems.

Conventionally, diesel compression ignition (CI) engines are more fuel efficient compared to their gasoline spark ignition (SI) engines counterparts. This is due to less throttling losses, higher utilised compression ratio and more close to ideal operating cycle [1]. However, conventional diesel CI engines emit higher levels of particulates and oxides of nitrogen (NO_x) while emitting lower levels of carbon monoxide (CO) and hydrocarbons (HC). This is due to properties of the diesel fuel and its combustion in the globally-lean but heterogeneous CI combustion mode. Attempts for avoiding/reducing particulates and NO_x emissions in the engine cylinder or with exhaust after-treatment systems have been always accompanied with fundamental issues. Simultaneous in-cylinder reduction of these emissions has been always a challenge due to the well-known NO_x-particulates emissions trade-off. While these issues exist for conventional diesel CI engines, possible in-cylinder abatement techniques are favoured over using costly, complex and fuel-economy deteriorating exhaust after-treatment

systems. The best foreseeable solution for an ICE is: an ICE with diesel-engine-like efficiency but much less emissions.

Premixed compression ignition (PCI) techniques have shown to be very promising in simultaneously reducing NO_x and particulates emissions inside the engine cylinder. NO_x emissions are mainly reduced by lower intake O_2 concentration and combustion temperature while in-cylinder particulates formation is mainly reduced by improving the local air-fuel mixture quality. However, PCI engines normally emit more CO and HC emissions required to be controlled by an exhaust oxidation catalyst. Generally, engine operating window is another challenge to overcome when using PCI techniques as they are normally limited to low, not very low though, to medium load operation. Misfire at low loads and high combustion noise at high loads are the major issues to be addressed. Fuel properties, mainly low auto-ignition tendency (low cetane number) and high volatility, can play important roles in achieving the objectives of PCI type combustion in a wider operating load range [2]. The overall aim of this research, therefore, is to investigate utilisation of low cetane number fuels to develop a combustion technique for in-cylinder reduction of NO_x and particulates and in-cylinder coupled with out-cylinder (using exhaust after-treatment) reduction of CO and HC emissions while maintaining high brake thermal efficiency. The objectives of the case studies presented in this thesis are to improve understanding of PCI combustion technique and provide solutions in order to benefit from efficient and clean combustion in a wide engine operating load range in a production multi-cylinder diesel engine.

1.2. Growing energy demand and associated environmental and human health complications

Energy production and usage, chiefly combustion of fossil fuels and bio-mass, are known to be the major anthropogenic sources of air pollution which can be partly attributed as the cause of around 6.5 million premature deaths per year [3]. Currently, the energy sector is the main source of global green-house gas (GHG) emissions and CO_2 levels as the main GHG emission is expected to increase by 16% by 2040 [4]. Based on the main expected future scenario for world energy outlook (WEO) by the international energy agency (IEA) in 2015 [4, 5], energy consumption is expected to grow by one-third between 2013 to 2040. Although it is expected that the energy required for this increasing demand may be partly sourced from clean energy sources such as nuclear, hydro, wind and solar power [3], the role of fossil fuels, at least in the transportation sub-sector, seems to stay very significant [2].

In 2014, fossil fuels provided almost 81% of the total energy required for the global demand [3]. Transportation, as an energy sub-sector, uses oil by more than 90% for its energy requirements. Globally, using roads as the way of transportation has increased by 25% during the last decade and currently in Europe more than half of the road transport is supplied by diesel fuelled vehicles [3]. Apart from contributions to CO and HC emissions, more than half of the NO_x global emissions are sourced from combustion of fuels, mainly diesel, in vehicles used for all means of transportation [3]. The role of energy usage for transportation in producing fine particulate matter (with aerodynamic diameters less than 2.5 μm ($PM_{2.5}$) containing many fractions such as black carbon and organic compounds) is currently ranked after the roles of energy usage in buildings and industries [3]. Currently, 10% of the primary $PM_{2.5}$ emissions, originated from energy production and usage, is from transportation sub-sector [3]. Within these figures for total global NO_x and $PM_{2.5}$ emissions from transportation,

more than 50% for NO_x and almost 10% for $PM_{2.5}$, road transport is the major contributor to both, 58% and 73% respectively. Apart from several illnesses which can be caused by exposure to NO_x emissions, fine particulate matter penetrating to the deepest points of the lung is the most harmful known pollutant to the human health [3].

NO_x emissions can cause lung problems and asthma attacks [6] while particulate emissions, apart from lung cancer, can be attributed as a trigger to chronic obstructive pulmonary disease (COPD), heart and cardiovascular diseases [3, 7]. Furthermore, nano-particles (with aerodynamic diameters less than 50 nm) can enter the blood stream and lead to some other health problems [6]. CO, a colourless and odourless gas, can change haemoglobin of the blood to carboxyhaemoglobin and hence carriage of oxygen through blood streams can be reduced; at high concentrations (around 400 parts per million (ppm)), CO can lead to fatal consequences [6]. Some of the HC, e.g. benzene and polycyclic aromatics, are believed to have some degrees of being carcinogen, genotoxic and neurotoxic [6]. These HC can be found in the diesel exhaust both in gas and condensed/adsorbed phase. Human health is not the only direct and in-direct victim of the air pollution; it can put environment in danger as well [6], which can be linked with problems such as food and economy issues [3]. Namely, issues such as lower yield of agricultural activities, higher chance of acid rain and eutrophication are some of the adverse outcomes of air pollution [3]. These highlight the importance of understanding and avoiding the sources of these emissions.

1.3. Legislative controls of transportation emissions

Importance and scale of the aforementioned issues related to energy use for transportation have made governments to make a positive move by imposing emissions limits for on-road and off-road vehicles. The reducing trend of these limits has been forcing vehicles to be

cleaner and cleaner year by year over the last two decades. In addition to emissions standards, factors affecting vehicle out emissions have been regulated for years; for instance, diesel fuel cetane number, volatility and sulphur content currently have regulatory limiting ranges around the world [8].

Emissions limits are different for different types of engines (CI or SI). Currently, vehicular emissions assessment is done by placing the vehicle over a chassis dynamometer and driving it over a predefined vehicle speed versus time matrix. In Europe, new European driving cycle (NEDC) is currently being used for this purpose, while it is going to be replaced by an under-development worldwide harmonized light vehicles test procedure (WLTP) in the near future [9]. Due to the fact that these procedures are lab-based and not necessary representative of the real-world driving cycles, a real driving emissions (RDE) testing requirement, not lab-based, is planned to be imposed between 2017 and 2021 [9].

As an example under discussion, Table 1-1 lists previous and current emission regulations in the European Union (EU) for light-duty (LD) CI engines. This table shows regulation number, its enforcement year and the limiting value of each emission. It can be observed that NO_x and particulate mass (PM) limits for LD CI engines have been considerably reduced from Euro 3 to Euro 6, by 84% and 90% respectively, in a 14-years period. Introduction of particulate number (PN) limits in Euro 5 (b) and Euro 6 has had the benefit of controlling lighter weight emitted particulates which do not considerably contribute to the PM and therefore may be uncounted. These bring the necessity of in-cylinder and/or out-cylinder reduction of NO_x and particulates emissions. However, usage of the after-treatment (out-cylinder) techniques is accompanied by several issues which are discussed in Chapter 2. Even with after-treatment systems, achievement of emissions reduction under real-world conditions is challenging. Studies have shown that under real-world driving conditions, emissions can be

higher; for example NO_x emissions of a Euro 6 diesel vehicle was higher than its regulatory limit by 7.5 times as reported in [3] and the references within.

Table 1-1 EU emission standards for light-duty compression ignition (Diesel) Vehicles from [9]

Regulation number and enforcement year	**$HC+NO_x$**	**NO_x**	**CO**	**PM**	**PN**
	g/km				number/km
Euro 1, 1992	0.97	-	2.72	0.14	-
Euro 2 (DI), 1996 [(a)]	0.9 [(b)]	-	1.0	0.10 [(c)]	-
Euro 3, 2000	0.56	0.50	0.64	0.05	-
Euro 4, 2005	0.3	0.25	0.50	0.025	-
Euro 5, 2009 [(d)]	0.23	0.18	0.50	0.005	- [(e)]
Euro 6, 2014	0.17	0.08	0.50	0.005	6.0×10^{11}

(a) In the same year, a regulation for IDI engines was enforced
(b) 0.7 for IDI engines
(c) 0.08 for IDI engines
(d) A secondary Euro 5 (Euro 5 (b)) was introduced in 2011
(e) 6.0×10^{11} for Euro 5 (b) was introduced in 2011

1.4. Current automotive fuel/fleet technology and future outlook

Globally, around 95% of the transportation energy is supplied by petroleum liquid fuels at the moment and some believe this will remain the scenario for the forecastable future [2, 10]. In order to reduce emissions and dependency on fossil fuels, a considerable amount of research efforts has been devoted to look into clean and/or bio-based fuels. An example is the usage of Fischer-Tropsch (FT) process which was first used during the Second World War to produce diesel fuel from coal and later was upgraded to produce bio-fuels from bio-mass and syngas [8]. So far, the low price of the crude oil and its availability for many years have made the FT process an uneconomical option [8]. Another challenge to consider is the fact that bio-fuel production should go towards using non-edible stock rather than edible stock. For example, unlike the biodiesel being produced from plant seeds, fatty acid methyl ester (FAME), future fuels must be produced from more non-edible sources [8]. However, there is still a great scope

for bio-fuels to contribute in providing energy for the automotive sector and reduce the load on fossil fuels in some countries such as Brazil.

Some other promising technologies for reducing emissions such as hybridisation incorporating an ICE and other types of energy-convertors, e.g. mechanical-flywheels and/or electrical-motors, have already reached the markets. Usage of fuel-cell electric vehicle (FCEV), mainly using hydrogen, is under research and development as well. Even some companies are looking into cryogenic engine concepts utilising liquid air or liquid nitrogen as their fuel [11]. However, the practicality of these options for the long term future and the extent to which they can contribute to satisfy market needs are under question.

Currently, the transportation fuel market is dominated by diesel and gasoline fuels and the major product of crude oil refineries is gasoline [12]. Some projections of future demands suggest that there may be a surplus of light distillation fraction (gasoline-like) fuels due to the fact that demand is going towards heavier distillation fractions mainly driven by the increasing need for the commercial transport [2, 10]. Around 35% of today's transportation energy is provided by diesel fuel which is forecasted to increase to 40% in 2040 surpassing the share of gasoline [10]. Apart from diesel engines dominating the market for heavy-duty (HD) vehicle fleet, light-duty (LD) sector is shifting towards diesel-engine-powered vehicles in some parts of the world. In 2014, 50% of the newly-registered LD vehicles in the United Kingdom (UK) were diesel-engine-powered cars [13]. These highlight the necessity of the better fuel economy for normal diesel and gasoline (gasoline direct injection (GDI)) engines which is expected to be continually improved over the upcoming years [10], while there is a great scope for incorporating other available and under-development options such as electrification of vehicles.

Electrification of a vehicle is chiefly referred to using electricity as an energy source to power its wheels. Full (all) electric option (battery electric vehicle (BEV)) uses a large battery-pack charged from the electricity-grid and/or regenerative charging during vehicle operation. If a vehicle has an ICE or a fuel-cell beside the electric motors, either in series, parallel or complex configuration, it is a hybrid electric vehicle (HEV). If the battery-pack of a HEV can be charged from the electricity-grid as well as on-board, then it is called plug-in HEV (PHEV). All these platforms have benefits in terms of reducing emissions in the usage phase [14]. Another factor that highlights the benefit of electrification is the opportunity to shift emissions from congested urban areas to rural areas. Pollutions from vehicles are in much closer proximity to individuals compared to those from power plants where the utilised electricity is generated [15]. Moreover, in the case of BEV and partly PHEV, grid-electricity used for charging the battery-pack can be produced from renewable sources and help total GHG emissions reduction. However, the main question to ask is "where does electricity or hydrogen come from and how much total CO_2 will be emitted well-to-wheel (WTW)?"

Depending on the method by which electricity or hydrogen is produced, total cycle (WTW) CO_2 emissions will be different [14]. Other current problems with most of the electrified options are customer's vehicle-range-anxiety, long charging time, charging infrastructure availability limitations and heavy weight of the batteries. However, based on [10], it is projected that almost 40% of new cars to be sold in 2040 will be HEV while BEV and PHEV will account for less than 10% globally. It is expected that ICE will still have the dominant share of the light-duty market by 2040 [10]. Even hybrid platforms will still need an ICE and these indicate the continuous requirement of research into improving fuels, ICE and after-treatment technologies.

Referring back to the aforementioned expected gasoline-like fuels surplus in the future and considering the fact that by far CI engines are the most efficient ICE, an economical way

(considering refinery and usage phases) of using these extra gasoline-like fuels is actually to combust them in a CI engine, if possible [2]. If this happens, less processed gasoline-like fuel, such as naphtha, will be used in a more efficient engine and in turn CO_2 emissions from both production and usage phase of the fuel will be reduced [2]. This, furthermore, will help to overcome the possible light-heavy fraction imbalance. More discussions on this topic and possibility of using gasoline-like fuels in CI engines are provided in the next section as well as other chapters of this thesis.

1.5. Advanced compression ignition combustion engines

Recent diesel engines are equipped with some cutting-edge technologies such as variable nozzle turbochargers and common-rail high pressure fuel direct-injection systems. However, still high emissions of NO_x and particulates from the conventional diesel combustion have motivated research into some unconventional advanced CI strategies. Part of the problem is due to the high reactivity of the diesel fuel towards auto-ignition in the engine cylinder which, for example, results in high particulate emissions simply by not allowing enough time for air and fuel to be mixed completely. One approach is to reduce this reactivity either by using normal diesel fuel and in-cylinder techniques or by using a totally different fuel and combustion strategy. For instance, gasoline-like fuels are less reactive towards auto-ignition [2] and therefore have longer periods of mixing with in-cylinder gases prior to the main combustion event. Following the idea of improving fuel-air mixing, several techniques for in-cylinder simultaneous reduction of NO_x and particulates under the generic concept of premixed compression ignition (PCI) low temperature combustion (LTC) were proposed. The most recent trend is to use low reactivity fuels for these techniques, e.g. homogeneous charge CI (HCCI), reactivity controlled CI (RCCI), partially premixed CI (PPCI) and its extension

gasoline CI (GCI). A considerable amount of text in Chapter 2 of this thesis is dedicated to review these techniques in details. The main motivation behind this research is the new trend in fuel and automotive industries focusing on utilisation of PCI/GCI engines in the near future for meeting stringent imposed emissions and fuel-economy legislations [2].

In PCI/GCI combustion, it is possible to use less-processed (low-octane) gasoline-like fuels for higher fuel-economy and less harmful emissions when compared to conventional and low-temperature diesel combustion [2]. Figure 1-1 illustrates the recent publications trend for each year from year 2000 to the end of June of year 2016 which is representative of the increased interest in these concepts and possible gaps to be covered. Based on this figure, HCCI concept is being mainly addressed in the literature. While the number of publications about PCI, RCCI and especially GCI concepts is not very high, there seems to be an increasing interest in these concepts recently.

Among the readily available options, mixing of diesel with gasoline (named as Dieseline) seems to be a very promising option to reduce the reactivity of the original diesel fuel and this idea is used in the current research work. In this thesis, different blending ratio for Dieseline is indicated with the prefix of the gasoline volumetric content in Dieseline; e.g. 50% gasoline mixed in diesel based on volume is called G50-Dieseline. Moreover, low reactivity Naphtha fuel is studied as a futuristic option which is discussed in Chapters 2 and 6.

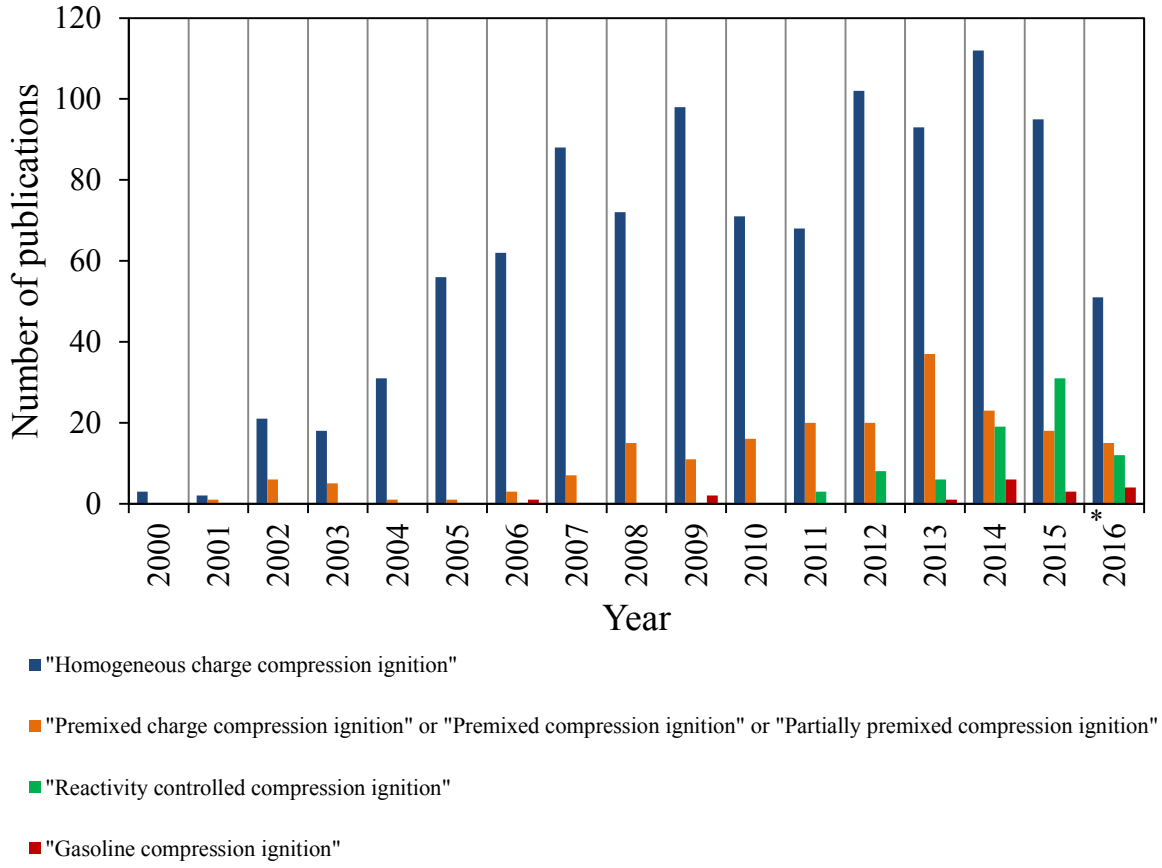


Figure 1-1 Number of publications versus year covering the period from the beginning of year 2000 to (*) the end of June of year 2016 (this data was obtained from the Web of Science searching for publications in all databases containing the exact phrases illustrated)

1.6. Research objectives

The overall aim of this research work is to develop and/or investigate low-cost fuelling, combustion and exhaust after-treatment techniques to reduce emissions, with particular focus on the simultaneous reduction of NO_x and particulates, from the stock compression ignition (CI) engine while maintaining its high fuel conversion efficiency. This includes investigation into the concept of premixed CI (PCI) and its extension gasoline CI (GCI) combustion by understanding their detailed combustion and emissions characteristics while operating on

different low-cetane (gasoline-like) fuels at different engine operating and controlling modes. Furthermore, the role of a diesel oxidation catalyst (DOC) in influencing emissions from the PCI combustion is investigated. The particular objectives of the current research are:

1. To investigate effects of different fuel injection, e.g single and split injection, and intake/exhaust handling strategies on combustion performance and emission characteristics of PCI/GCI combustion when using low-cetane fuels considering effects of fuel properties, e.g. boiling range profile, in a wide engine operating load range;
2. To develop techniques which help reduce CO and hydrocarbons (HC) emissions and fuel consumption at lower operating loads and assess their effects on other emissions, engine operation and DOC efficiency;
3. To investigate effects of the DOC on volatile and non-volatile emissions by comprehensively characterising exhaust compounds upstream and downstream of the DOC;
4. To conduct a benefit-analysis for PCI/GCI combustion compared to diesel fuelled combustion at the same operating modes.

1.7. Thesis outline and approach

In order to address the aforementioned research objectives, this thesis incorporates eight chapters which are outlined separately (excluding the current chapter) below.

- ***Chapter 2***

  In this chapter, fundamental background and advanced concepts available in the literature related to the case-studies conducted in this research work are reviewed. The review firstly starts with discussing some fundamental physical and chemical properties of automotive fuels. Then, conventional diesel CI combustion mechanism followed by the "generic" advanced premixed low temperature CI combustion mechanism and emissions formation processes in both are reviewed. Subsequently, more advances in the premixed CI combustion, including homogenous and partially-homogeneous concepts, when utilising low reactivity fuels, such as gasoline compression ignition (GCI) combustion, are discussed. Afterwards, the discussion is focused on characteristics of vehicular particulate emissions focusing mostly on organic and carbonaceous fractions. Finally, CI engine emissions abatement techniques including exhaust after-treatment systems, with the main focus on the DOC, are reviewed.

- ***Chapter 3***

  This chapter describes experimental setup and methods used in this research work. These include detailed description of the designed, manufactured, commissioned and utilised engine and after-treatment test cells, gaseous and particulate emissions measurement and analysis techniques, combustion-related characteristics calculation procedure and specifications of the studied fuels.

- ***Chapter 4***

  This chapter investigates some techniques using various fuel injection strategies to improve fuel-air premixing quality compared to the single-injection at low-medium

engine loads. It discusses the results of a parametric analysis of split-injection strategies when using G50-Dieseline fuel for partially premixed CI combustion. The study of split-injection involving injection quantity-ratios and timings aims to achieve optimised charge premixing and consequently reduce NO_x and particulate emissions simultaneously. Effects of key injection parameters on combustion and emission characteristics of the engine are quantitatively identified by the Taguchi design-of-experiment method. Furthermore, optimum operating values of injection parameters for obtaining the minimum and maximum of combustion and emission characteristics are identified. Based on the results, optimum minimum values of NO_x and smoke are found and are compared to the single-injection results.

- ***Chapter 5***

  Applying the information and understandings achieved in Chapters 2 and 4, this chapter investigates the viability and benefits of using a low cetane number (CN) fuel with a wide boiling range (G75-Dieseline, with CN less than 30) for premixed CI combustion at different operating loads, from 1.4 to 17.3 bar BMEP. This study incorporates different fuel injection and intake/exhaust handling strategies and results are compared to the results obtained when using diesel fuel at the same operating loads as the base-lines. Challenges with the combustion stability faced at the low load operation when using G75-Dieseline in a multi-cylinder stock CI engine motivated the author to develop some techniques using high hot exhaust gas recirculation (EGR) rates and very low injection pressures for significantly enhancing the premixed combustion and reducing its emissions. Comprehensive results of combustion performance and emission characteristics when using single-injection and double-injection strategies are compared for both of the fuels.

- ***Chapter 6***

  Conclusions from Chapter 5 helped to investigate naphtha premixed CI combustion in this chapter. Naphtha fuel used in this study has a similar CN to the G75-Dieseline used in the previous chapter while its boiling range is narrower and similar to the market gasoline. The main objective of this chapter, through comparison of naphtha with G75-Dieseline, is to identify the effects of the boiling range on the degree of charge stratification and consequently combustion performance and emission characteristics of premixed CI at various operating conditions. Same operating conditions used in Chapter 5 while using both single and double injection strategies were utilised to perform a detailed comparison between naphtha, G75-Dieseline and diesel combustion.

- ***Chapter 7***

  Generally, low particulates and NO_x emissions from premixed compared to conventional diesel CI combustion are accompanied with high emissions of CO and HC suggesting the requirement for an oxidation catalyst. This chapter discusses the effects of a production DOC on emissions from G75-Dieseline and high-EGR diesel CI combustions. Therefore, Chapters 4, 5 and 6 develop and discuss in-cylinder techniques to reduce emissions and this chapter discusses an out-cylinder reduction technique for coping with the short-coming of the premixed combustion. The effectiveness of the developed hot-EGR technique on improving the emission reduction efficiency of the DOC at low loads is examined in this chapter. Apart from studying regulated gaseous emissions and physical characteristics of particulate emissions upstream and downstream of the DOC, a comprehensive characterisation of semi-volatile organic compounds in gas phase through application of a state-of-the-art comprehensive gas-chromatography and mass-spectrometry is conducted.

- ***Chapter 8***

  This final chapter summarises the main conclusions drawn from different case-studies presented in this thesis and suggest some scopes for future research as a continuation of this work.

Chapter 2
LITERATURE REVIEW

2.1. Introduction

This research focuses on three main factors affecting engine performance and vehicle-out emissions: fuel properties, in-cylinder emission reduction strategies and out-cylinder emission reduction strategies. Although each of these factors can incorporate various options, in this chapter the aim has been to review some fundamental and advanced concepts available in the literature to support the philosophy of selecting the conducted case-studies. Investigation of all possible options was out of the scope and resources of this research. Firstly, fundamentals of automotive fuels are briefly reviewed. Secondly, conventional and advanced compression ignition (CI) combustion phenomena and emissions formation mechanisms while operating on both are reviewed. Thirdly, recent concepts of advanced compression ignition combustion using low reactivity fuels are surveyed. Finally, exhaust after-treatment systems, with the main focus on the diesel oxidation catalyst (DOC), are briefly reviewed.

2.2. Fundamental properties of automotive fuels

Fuel properties (both physical and chemical) are known to influence engine combustion performance and emission characteristics [2]. Current diesel and gasoline fuels are mainly mixtures of thousands of various hydrocarbons (HC) with different properties [16] and depending on the compound types present in the mixture and their concentrations, fuel can have different properties [8]. These hydrocarbon species and their transitional forms, as

unburnt fuel and combustion by-products, respectively, are found in the exhaust gas of the automotive engines. Therefore, they can affect the engine combustion event itself and once released from engine exhaust valves, affect processes inside the exhaust pipe and processes in the environment. These highlight the possibility and importance of controlling/tailoring HC content to design fuels which are suitable for both in-cylinder and out-cylinder processes. In order to address the abovementioned points, it is attempted to separately review some of the major properties of fuels in the following paragraphs, although it is obvious that fuel properties are inter-linked. It is appreciated that some other fuel properties, not discussed here, such as density, energy content, biofuel content, viscosity and lubricity can have effects on the performance of a fuel in a vehicle. However, discussion of all these properties will be lengthy and therefore properties that are directly related to this research are discussed exclusively. Most of the discussion is directed towards the variables which can influence properties of paramount importance for the premixed type CI combustion: fuel auto-ignition tendency and volatility.

2.2.1. Hydrocarbons composition

Auto-ignition property of a fuel has a very high impact on achieving the premixed type CI combustion which is the main focus of this thesis. Thus, most of the discussion in this section is focused on relating chemical composition of the fuel to its auto-ignition tendency. Therefore, major classes of hydrocarbons present in the conventional fuels are reviewed here:

Alkane (Paraffin) content: These compounds contain only single carbon-carbon bonds and are saturated. They are present in both normal (straight-chain) and branched-chain molecular structure. Alkanes with relatively long chain (C_{10} to C_{20} [8]) are the main component of conventional diesel fuels [16] and have higher boiling points compared to compounds present

in gasoline fuel (C_4 to C_{10}). These species become more unstable as their chain length becomes longer; this is perfect for a robust auto-ignition in high pressure and temperature conditions observed in the cylinder of a CI engine [8]. These make the diesel fuel to have a better auto-ignition quality compared to gasoline. However, the effect of other hydrocarbon species and chemical structure available in the mixture should not be ignored. For instance, some iso-paraffins have very low auto-ignition tendencies compared to their same chemical formula normal alkanes [8].

Cyclo-alkane (Naphthene) content: These compounds contain only single carbon-carbon bonds similar to alkanes. However, instead of having a straight or branched molecular structure, naphthenes are ring (cyclic) hydrocarbons which have lower auto-ignition tendency compared to the normal alkanes. [8, 16]

Alkene (Olefin) content: Alkenes are open chain unsaturated hydrocarbons with carbon-carbon double-bond. Their auto-ignition tendency is between normal alkanes and cyclo-alkanes. [8, 16]

Alkyne (Acetylene) content: Alkynes are open chain unsaturated hydrocarbons containing a carbon-carbon triple-bond [16]. They are present in low concentrations in the conventional fuels.

Aromatic content: Benzene ring, a flat cyclic hydrocarbon which has alternative double-bonds between the carbons, is the building block of aromatic hydrocarbons. Despite the fact that polycyclic aromatic hydrocarbons (PAH) have low auto-ignition tendency, depending on the length of the aliphatic side chain of the aromatic hydrocarbon, their auto-ignition tendency can vary and be close to alkanes [8]. PAH are difficult to be completely oxidised in the engine and therefore can either leave the cylinder unburnt or be a source of soot formation [2].

Obviously, by varying the concentration of these different classes of compounds in the mixture (fuel), properties of the resultant mixture can be controlled. Currently, driven mainly by its chemical composition, the signature of the conventional diesel fuel is its higher auto-ignition tendency and lower volatility compared to the conventional gasoline fuel. What if it was required to alter this signature of diesel fuel in order to achieve reduced emissions when utilised in CI engines? Will blending diesel and gasoline help? This is discussed later in this chapter and supported by experimental data presented in Chapters 4, 5 and 7.

2.2.2. Auto-ignition quality

Auto-ignition quality (tendency), assessed by the cetane number (CN), of the diesel fuel can be named as one of its most important properties. Fuels with higher CN are more reactive towards auto-ignition in CI engines [2, 8, 16]. Lower CN allows more time for the fuel to be well-mixed with the air before combustion. The term "ignition delay (ID)", defined as the duration between the start of injection (SOI) of the fuel into the engine cylinder and the start of combustion (SOC), is a function of fuel CN; generally lower CN means longer ID [2]. Gasoline fuel must have a very low auto-ignition tendency when used in a spark ignition (SI) engine to avoid unwanted auto-ignition and reduce the chance of knocking [2]. Antiknock property of gasoline fuels is identified by the octane numbers (research octane number (RON) and motor octane number (MON)) [2]. There is an inverse correlation between cetane and octane numbers [2].

At the time of developing first diesel engines in late 19th century, Rudolf Diesel's realization was that the high resistance of the gasoline towards auto-ignition makes it unsuitable as a fuel for CI combustion [8]. However, with advancements of engine technologies and improved knowledge of CI combustion phenomenon, using gasoline-like fuels has been investigated in

CI engines to benefit from the prolonged ID. Blending diesel and gasoline fuels (Dieseline) at different ratios alters the relative concentration of different classes of hydrocarbons in the mixture and therefore blends have a CN between that of gasoline and diesel.

2.2.3. Volatility/distillation profile

Conventional fuels are composed of various hydrocarbons with different boiling properties. Therefore, they are identified with a boiling or distillation curve rather than a single boiling-point. Fuels with lower boiling ranges are easier to be vaporised and therefore can help to improve fuel-air mixing process in the engine cylinder. Compared to diesel, gasoline as well as having lower tendency to auto-ignite is more volatile. Volatility of the fuel is an important factor in all stages of pre-combustion, combustion and post-combustion events inside a CI engine cylinder. Lowering the final boiling point of a diesel fuel has shown the potential for improving engine performance and lowering emissions in light-duty engines [8]. Dieseline fuel has a wide boiling profile between that of gasoline and diesel [12, 17].

2.2.4. Flash point

Flash point is a fuel storage safety factor defining the lowest temperature at which enough vapour of the fuel is available in a closed volume to ignite with an ignition trigger [8]. For conventional diesel, this figure is higher than for gasoline which dictates the use of different fuel storage and transportation tank for these two fuels. This has raised some concerns about the feasibility of using mixtures of diesel and gasoline in one fuelling system. However, recent research suggests that at gasoline volumetric concentrations of more than 50%, flash

point of the Dieseline fuel is similar to that of gasoline and therefore can be safely used in a vehicle [18].

2.3. Conventional diesel compression ignition combustion

Conventional diesel combustion (CDC) is a heterogeneous process resulted from injecting fuel into a high pressure and temperature ambient close to the cylinder top dead centre (TDC). Using conventional injection and air handling strategies, high auto-ignition tendency of the conventional diesel fuel does not allow the fuel to be well-mixed with the air, simply by not allowing enough time before the combustion starts. Fuel-air mixture packets auto-ignite and proceed to combustion while it is possible that injection event continues after the combustion has started. This is more likely to occur at higher engine loads when the ambient temperature and pressures are higher and injection duration is longer compared to low loads. [2, 16, 19]

The nature of CDC makes it very difficult to reduce oxides of nitrogen (NO_x) and particulates emissions simultaneously inside the cylinder. Based on the diagrams presented in [20, 21], NO_x and particulates formations are governed by two main factors: local equivalence ratio (ratio of actual fuel/air to stoichiometric fuel/air) and local temperature. Diesel engines are normally operated under globally lean conditions (equivalence ratio<1) while local fuel-air mixture packets can be fuel-rich. The conceptual models available for CDC are discussed in the following sub-sections. These models are applied to CDC with no or low amounts of exhaust gas recirculation (EGR) while using multi-hole injectors [19]. Injection and ignition events are overlapped (negative ignition dwell – defined as the duration between the end of injection to the SOC [22]) with injection-timings close but prior to the TDC. The review discusses pre-combustion events and combustion stages separately as follows.

2.3.1. Pre-ignition events

After the fuel spray injection, in the form of a conical-shaped jet, the in-cylinder gases start to get mixed with the small fuel droplets. Each fuel spray jet gets more entrainment with the in-cylinder gases as it travels further from the injector. Therefore the local equivalence ratio along the jet axis is lower further from the injector tip. Thermal energy of the in-cylinder gas helps to vaporise the liquid fuel jet [22]. Change in the in-cylinder gas density, e.g. by intake boosting, can affect both fuel jet penetration length and liquid length inversely [22]. This fully vaporised fuel, mixed with the in-cylinder gases, travels further into the cylinder where it mixes with other less fuel-rich contents available inside the cylinder.

2.3.2. Auto-ignition and premixed combustion period

Formation of the first intermediate-reaction species (formaldehyde (H_2CO), hydrogen peroxide (H_2O_2), carbon monoxide (CO) and some altered HC) indicates the occurrence of the first-stage ignition event [22, 23]. This is the start of a chain-like process and after around 100 to 200 microseconds [22], secondary ignition event takes place, which leads to the premixed stage of the diesel combustion [16]. Secondary ignition event is a highly exothermic process which increases in-cylinder temperature and pressure considerably. It should be mentioned that fuel spray jet is still intact when combustion starts. Locally high equivalence ratio fuel-air packets undergoing this high temperature rise, to almost up to 2000 K, can be sources of soot precursors' formation, e.g. PAH. Carbonaceous species formation will be present in the downstream cross-section of the combusting jet [22, 24].

2.3.3. Mixing-controlled combustion period

At the time that premixed heat release rate reaches its peak value, on the jet boundaries where temperature and local equivalence ratios are high, a diffusion flame initiates. This diffusion flame is associated with the mixing-controlled stage of the diesel combustion [22]. The flame will not be propagated up to the injector and there will be a distance between the flame starting point and the injector tip termed as the lift-off length [22, 25, 26]. In the lift-off length, there will be a premixed reaction zone producing combusting species fed into the jet cross section to be consumed [23]. Temperature in the fuel-rich core of the jet cross section is increased by combustion of reactants sourced from the premixed reaction zone and present in the diffusion flame itself. Therefore, this core will be a source of soot formation as equivalence ratio and temperature are sufficiently high. Soot formation intensity is the highest in the region close to the end of the jet [22]. Lift-off length can strongly affect the engine-out soot emissions by influencing the fuel-air mixing upstream of the reaction zone of the diffusion flame. Higher ambient temperature and density, observed in higher loads, is known to reduce the lift-off length [26]. Increasing injection pressure increases the lift-off length while fully vaporising the liquid spray prior to the lift-off length is very important [26]. These can partly explain soot emissions variations as a result of changing injection pressure and in-cylinder charge density and temperature.

Mixing-controlled stage is important for the formation of NO_x emissions. Similar to almost every in-cylinder emission formation process, NO_x formation is a function of temperature and mixture fuel-air ratio. Thermal NO_x can be formed in temperatures more than almost 2200 K in almost stoichiometric (towards lean) equivalence ratios [20]. NO_x forms on the combusting jet hot periphery near fuel-air packets with equivalence ratios close to stoichiometry [22]. It is worthy to mention that soot, fed from inside of this well-established combusting jet towards

outside of the jet, can be oxidised near these high temperature regions. Therefore, in the CDC, any disturbance to these regions in order to reduce their temperature or oxygen concentration and consequently NO_x formation can deteriorate soot oxidation process.

The concentration of engine-out soot emissions is believed to be governed by two separate controlling mechanisms with both being important: their initial formation and their in-cylinder oxidation [2, 19, 22, 24]. Without sophisticated optical techniques, it is challenging to judge whether the observed variation trends in particulate emissions are a result variations in the formation process or oxidation process or variations of both simultaneously (which can happen at different levels) [24]. The formed soot can be oxidised where high enough temperature and oxygen content are available and long enough residence time is allowed for complete oxidation [2, 24]. In-cylinder soot oxidisers can be species such as O_2, O, hydroxide (OH), H, CO_2 and H_2O [24]. Main in-cylinder soot oxidisers are oxygen and OH radicals. For the CDC, there is debate on whether oxygen is the dominant oxidiser or OH radical is oxidising soot [24]. Nevertheless, based on the original Dec's conceptual model [19], the primary region where both of these oxidisers may attack soot is in the diffusion flame.

Reducing the in-cylinder oxygen content and temperature, e.g. by means of utilising higher EGR, can help to reduce NO_x formation while it can obviously promote possibility of increased soot emissions. Plee *et al.* [27, 28] performed some studies on NO_x formation mechanism and concluded that higher flame temperature of the diffusive combustion can explain higher NO_x formation rates. EGR can influence combustion and emission characteristics by its oxidiser reduction effect, thermal effect and chemical effect which were separately studied by Ladommatos *et al.* [29-33]. In the CDC, intake charge oxygen content reduction by using EGR, has the major effect in influencing NO_x emissions, more than the resultant prolonged ID and increased intake temperature [29, 34]. High heat capacity of CO_2, found in the EGR, has a relatively small effect on reducing NO_x emissions [30]. Water vapour

content of the EGR, which is less than its CO_2 content while having higher heat capacity, can help reduce in-cylinder peak temperature and therefore reduce NO_x emissions while intake air dilution has still the highest effect [31]. In the systems that EGR is used without reducing the intake charge oxygen content (boosted operation), NO_x can be reduced without significant increase in soot emissions [34]. Meanwhile CO and HC emissions from CDC are relatively low, and therefore are not discussed here, they can be increased in reduced O_2 conditions (when using higher EGR without boosting).

A good approach appears to be avoiding primary soot formation by improving the fuel-air mixture quality prior to the combustion while using high EGR [2]. Diffusive flame and consequently locally rich fuel-air packets can be avoided, when there is a long enough ignition dwell. In this way, fuel-air mixture packets with different strengths (not completely homogeneous) will burn in a premixed combustion [2, 35]. Therefore, possibility of overcoming the NO_x-soot reduction trade-off becomes more practical in a CI engine. This is the main concept of premixed CI (PCI) combustion discussed below which can be described by auto-ignition in multiple points of the chamber and/or local flame propagation [2]. However, low-NO_x and low-soot combustion can be linked with high CO and HC emissions [2] as discussed in the following sections.

2.4. Premixed low temperature compression ignition combustion

Combustion temperature in a CI engine can be reduced by increasing the fuel-specific heat capacity of the combusting mixture [22]. This is achieved via dilution either by using excess charge to reduce global and local equivalence ratios or simply by using exhaust gas recirculation (EGR); this is generally the basis of low temperature combustion (LTC) [22]. Based on the aforementioned mechanisms, both NO_x and carbonaceous particulate emissions

can be reduced by operating at lower combustion temperatures while the effect of oxidiser availability should not be ignored.

Musculus *et al.* [22], after reviewing and updating the CDC conceptual model by Dec *et al.* [19] (discussed in the previous section), proposed some conceptual models for the PCI LTC in diesel engines. Based on these conceptual models, compared to CDC, LTC includes more fuel-air overmixing and less soot forming regions, extended IDs and longer fuel spray penetration lengths [22]. Normally in LTC, while using the same fuel, the ignition dwell is prolonged by using higher EGR rates. Either early or late injection strategies, compared to the CDC, can be used. Both of these strategies, beside higher EGR, decelerate the rate of required chemical evolutions for the ignition event as the in-cylinder temperatures and pressures are normally lower at these injection-timings [22]. Lower fuel economy while using LTC might be an issue as higher dilution increases CO and HC emissions. Moreover, combustion-phasing needs to be altered from its optimised timing in order to avoid high combustion generated noise [22]. These are discussed in the following text and section 2.5, while in order to avoid duplication, only differences from the CDC are presented.

2.4.1. Low temperature combustion (LTC) mechanism

LTC mechanism with early fuel injection-timings, which is more relevant to the present research, is briefly reviewed here. Although initial steps of fuel spray developments are similar to the CDC, LTC conditions result in faster penetration of the fuel spray beside longer liquid length. This means that fuel spray vaporisation rate is slower. Thus, interactions between liquid fuel and piston and also liquid fuel and cylinder wall become important, especially at very early injection-timings. Liquid fuel impinging the walls can possibly leave a liquid film on them which can exist for some to many crank angle degrees (CAD) depending

on the operating conditions. In a light-duty engine unburnt hydrocarbons concentration will be high in the squish region and top ring-land crevice. These increase both UHC and CO emissions discussed in the next sub-section. [22]

Preliminary reactions leading to formation of intermediate-reaction species (for the first-stage reaction) can be observed across the entire combustion chamber. Some portions of the fuel-air mixture close to the piston bowl surface can be fuel-rich which can be a source of soot or soot precursors when main heat release occurs. However, the equivalence ratios are sufficiently low that insignificant amount of soot precursors are formed. Main heat release event is initiated from locations where these fuel-rich packets are present. Moreover, secondary ignition events can be initiated in the squish volume region after some CAD. Sharp premixed heat release rate is a signature of this type of combustion if combustion-phasing is close to the TDC. [22]

2.4.2. Unburnt hydrocarbons and carbon monoxide sources

Based on [22], it was observed that over-lean mixture packets present between different fuel spray jets can be sources of UHC. However, evidence was provided that UHC and CO emissions were mainly sourced from regions near the formed liquid films on locations close the bowl rim area on the piston surface and squish volume [36-38]. In addition, upper region of the cylinder axis, where lean packets are found, can be source of UHC and to a less extent CO [22]. The other possible source of UHC in this region can be unwanted late introduction of fuel into the cylinder by mechanisms such as fuel dribbling from the injector. Compared to the CDC, as most of the combustion happens near lower region of the combustion chamber in LTC, this UHC can contribute more significantly to the observed engine out emissions. All of these emission formation and evolution mechanisms are load dependant. CO oxidation rate

can be increased in regions with higher temperature and/or OH concentration. Heat losses in the squish volume can cause reduced ignition and oxidation rate of the lean packets.

Based on these points, it is evident that utilising longer ID to avoid locally rich fuel-air mixture packets and consequently soot production is an objective of the LTC mechanism. Longer ID is achieved by increasing EGR to large amounts in diesel LTC while this technique is limited to low loads because of the high reactivity of diesel fuel towards auto-ignition at high loads. What if a less reactive fuel is used? This is the topic of discussion in the following section. Musculus' conceptual models [22] is claimed to be not applicable to the combustion of low reactivity (gasoline-like) fuels [22]. However, compared to the CDC, the basis of the operation should be more similar to the LTC as advanced injection-timings are used for gasoline-like fuels and combustion process does not generally include diffusive flame [2].

2.5. Low reactivity fuels for homogeneous, premixed and partially-premixed compression ignition combustion

Due to the shorter ID of conventional diesel-like fuels (40<CN<60) compared to gasoline-like fuels, their achievable low-smoke and low-NO_x PCI window is only limited to the low load operation [2]. At these loads, diesel PCI is normally indicated by a single sharp peak of heat release rate and higher maximum pressure rise rate (MPRR) which increases the combustion generated noise. Pilot injection can be used as a strategy to reduce diesel PCI noise at lower operating loads while it is normally accompanied with reduced efficiency and increased smoke emissions [2, 39]. Based on the discussions provided above, it is obvious that fuel ID and volatility can play important roles for enhancing CI engine combustion and emission

characteristics mainly by influencing the quality of local air-fuel mixture packets. Utilising fuels with low CN and high volatility in a CI engine has its benefits and drawbacks which are discussed in the following sub-sections. One way to make low CN fuels, from already available fuels, is through blending liquid or gaseous hydrocarbons with different reactivity and volatility [2]. Research efforts have been devoted to investigate the usage of either online (in-cylinder) control, e.g. [40], and offline (out-cylinder) control, e.g. [41], of the fuel-air mixture reactivity. These techniques are discussed in more details later in this chapter.

Among the current petroleum-based fuel choices, blend of conventional gasoline and diesel (Dieseline) seems to be a very practical and readily available option to lower the CN of the resultant fuel. With the current engines, it seems to be challenging to combust neat conventional gasoline and a blend with a more reactive fuel seems more practical [2]. Dieseline is being considered as one of the fuel candidates for the future use [12, 17, 18, 41-51].

Dieseline blends, compared to neat diesel and gasoline fuels, have wider boiling ranges and their properties are somewhere between that of diesel and gasoline depending on the blend-ratio. Initial boiling point of the Dieseline fuel with more than 50% volumetric content of gasoline is strongly dominated by the gasoline content due to the presence of less low molecular weight (LMW) HC in the diesel fuel [12]. Based on the studies conducted in [12] for Dieseline in some heating processes, cracking and coking reactions for high MW HC can be inhibited via the solvating effect by the LMW HC that do not leave the confined volume of the studied system. This may partly explain the prolonged ID of Dieseline fuel with higher concentration of gasoline-range HC compared to the diesel fuel. Moreover, it is known that, in general, gasoline fuel has higher heat of vaporisation, more than diesel fuel, [52] which cools down the in-cylinder charge upon injection and consequently reduces the rate of chemical reactions leading to the main combustion event. Fuels with high paraffinic content, normally

with longer chain length found in diesel, have shorter IDs as the rate of decomposition and oxidation reactions involving free radicals are faster [17]. More stable ring-structure of aromatic compounds, found in gasoline, leads to longer IDs as higher pressure and temperatures are required for auto-ignition [17]. The relative concentration of different HC species can be well-controlled by the blend-ratio of diesel and gasoline. If used in a diesel-like direct injection system, variation of the fuel CN can affect the lift-off length as well; higher CN generally results in shorter lift-off length [53].

Dieseline fuel feasibility for supercritical (SC) injection and combustion has been investigated [12, 17]; it is basically heating and vaporising the fuel before the injection event. It was found that gasoline content of Dieseline fuel acts as an anti-coking agent which is useful for the fuel injection equipment (FIE), especially injectors operating at high temperatures [12]. Heavy components present in the diesel fuel can thermally decompose and form products that can block the injector holes. Gasoline was also shown to be beneficial in order to reduce the critical temperature of the fuel [12]. Although this SC system is not commercialised yet, understandings from this system is beneficial for the current CI engines, especially for their FIE.

These are properties of the Dieseline fuel achieved by blending representative diesel and gasoline available in the market. While in the future, cuts from different fractions of the refinery can be used to produce a fuel, directly in the refinery, with similar properties which might even reduce the cost of the resultant fuel. One of the petroleum options currently being investigated is a fuel which can be called, in general, “naphtha” as streams from different crude oil refinery processes [54]. It can be readily available from different cuts of the refinery which are indeed the feed-stock of gasoline [55]. Naphtha is much easier to be produced compared to the current gasoline and diesel fuels which can lower CO_2 emissions in the refinery process [55, 56]; it is the least processed refinery stream [56]. Indeed, it is required to

consume energy to increase the octane number of naphtha for using it as a high RON gasoline. However, if naphtha ("low-quality gasoline") with minimum refinery requirements can be used efficiently in a CI engine, there can be a synergy (well-to-wheel) for CO_2 reduction [54-56]. This means both fuel refinery (production) process and usage process will produce less CO_2 compared to the current processes [54-56]. Furthermore, mitigation of the possible upcoming imbalance of the demands for light and heavy fractions, as discussed in Chapter 1, while running on a cheaper fuel can be a very interesting side-benefit [54]. It can be claimed that full-range naphtha has a boiling-range similar to the currently available market gasoline [56]. These fuels can even contain bio-based fractions for achieving high efficiency and low emissions combustion [57-60].

Based on these points, with the main focus on the long ID and high volatility of the fuel, advanced CI combustion modes using low CN fuels were introduced by various researchers. These combustion modes are reviewed in the following sub-sections.

2.5.1. Homogeneous charge compression ignition (HCCI)

In general, the major target of the homogeneous charge compression ignition (HCCI) is to prepare a homogeneous lean fuel-air mixture before compressing the charge [22, 61]. This requires fuels with low CN [62] to avoid unwanted auto-ignition early in the compression stroke. In HCCI, as the injection and ignition events take place very far from each other, chemical kinetics is very important [22]. This imposes some difficulties with the control of ignition and combustion events and therefore a reliable control over phasing of the combustion [63-65]. Rapid combustion featuring high heat release rates and high pressure rise rates due to the homogenous charge is another issue with HCCI. Some techniques have been employed to intentionally reduce this charge homogeneity [66] to control this rapid heat

release rate while mixture was still everywhere fuel lean. Problems with the HCCI motivated researchers to look into a less homogenous CI mode which is reviewed below.

2.5.2. Premixed and partially-premixed compression ignition (PPCI)

Premixed compression ignition (PCI), partially premixed compression ignition (PPCI) and premixed charge compression ignition (PCCI) are the terms used, interchangeably, in the literature to define strategies which use a more heterogeneous fuel-air mixture compared to the HCCI [22]. Arbitrary, in this section the term "PPCI" was selected to discuss this mode. In PPCI, normally, fuel is injected in the compression stroke but not very close to the TDC. Although the intention is to separate EOI and SOC, injection and kinetically controlled ignition events are more linked compared to HCCI. The fuel-air mixture is more stratified compared to HCCI and therefore combustion is less rapid. In principle, the target is to avoid locally rich air-fuel packets while maintaining a reasonable degree of stratification. Indeed, the LTC conceptual model reviewed earlier in this chapter is used to understand this mode of combustion while using a normal CN diesel fuel [22].

Longer ID of the fuel can help to achieve a more premixed charge compared to CDC and diesel LTC. The ID can be prolonged by using high EGR rates as well, which helps to lower down NO_x emissions in parallel. Lower fuel CN can help to extend PPCI operating range to higher loads. Load expansion for low-emissions combustion was achieved through application of some combustion and fuelling techniques, e.g multiple injection of high RON fuels, which are presented in [67-69]. However, research in this field, as one of the unresolved challenges with PPCI, is still on progress. Some researchers, e.g. in [70-72], have introduced the concept of multiple premixed compression ignition (MPCI) where, normally, heat release rate has two separate peaks in order to reduce the intensity of single peak combustion.

Researchers at the University of Birmingham have conducted several experiments to investigate Dieseline PPCI combustion [41, 43, 46-48]. Research started with low volumetric content of gasoline in Dieseline (10% to 20%) and further increased to 50%. All these techniques are normally accompanied with reduced brake thermal efficiency and elevated CO and HC emissions, especially at low loads, which is the other challenge with PPCI. HC emissions are more affected by the ID while global equivalence ratio controls CO emissions when using low gasoline content in Dieseline [73].

While using the off-line blending technique, a suitable CN for all operating conditions is under question. A recent concept under investigation is to use PCI combustion of low processed gasoline-like fuels (or fuels with similar characteristics to low processed gasoline-like fuels), similar to naphtha discussed earlier. This concept is called gasoline compression ignition (GCI) and is discussed in the following section.

2.5.3. Gasoline compression ignition (GCI)

As Kalghatgi mentioned in his book [2], a feasible premixed type combustion termed as GCI combustion has a great potential for the future CI-engine-powered fleet in terms of engine/after-treatment, fuel and running costs reduction. Engine cost reduction can be met by reducing the need for high fuel injection pressure and costly after-treatment systems, as opposed to the requirements for the current diesel engines. Fuel and running costs reduction were discussed earlier in this section when talking about the low processed gasoline-like fuels. He suggested using fuels with 75<RON<85 with no stringent volatility requirements for GCI combustion [2]. Moreover, for the current market CI engines, he suggested addition of diesel-like HC to the gasoline fraction as a starting point. Some studies have been conducted to develop strategies to use CI of the neat market gasoline fuel [74-78]. This technique was

called gasoline direct injection compression ignition (GDCI) incorporating a new engine design concept. However, with current stock engines, it is challenging to run on the market gasoline fuel.

At low loads, when using low CN gasoline-like fuels with single-injection strategy, advancing injection-timing has a limit when combustion-phasing starts to retard sharply, as opposed to advancing the injection-timing, and combustion starts to be unstable [2, 79]. This is due to the fact that premixing will continually improve and become similar to the HCCI type operation (very lean local packets) and gasoline is difficult to auto-ignite under these conditions [2]. As mentioned earlier, when advanced injection-timings are used, in-cylinder temperature and pressure are lower and therefore chemical kinetics can be completely or partly frozen. If the injection event happens after this timing limit, control of combustion-phasing is more linked with the injection-timing and combustion will happen in a less premixed environment (local mixture packets have a wider strength – more stratified). Retarding the injection-timing outside the operable range will result in very late combustion-phasing and unstable combustion. Long ID of the fuels at low loads can be useful in bringing the local air-fuel ratio closer to the global air-fuel ratio. This can consequently make leaner packets which proceed slower for combustion and therefore reduce peak of heat release rate, MPRR and NO_x emissions. However, this comes with a downside of increased THC and CO emissions as discussed earlier [2, 80]. At higher loads, when using low CN fuels, as the global and local equivalence ratios are higher, closer to stoichiometric strength, auto-ignition of multiple points happens more rapidly leading to high peak heat release rates, MPRR and NO_x emissions [2, 35]. This is partly due to the fact that diffusive combustion is avoided by separating injection and combustion events.

Auto-ignition characteristics of a fuel depend on the engine it is being used for. Compression ratio of the engine seems to be of paramount importance. Results from experiments conducted

in a light-duty single cylinder research CI engine with a compression ratio of 16:1 indicated that a fuel with 75<RON<85 can be beneficial for achieving low smoke and NO_x emissions [81]. Fuels outside this RON range faced difficulties in achieving these emission reduction targets either at low load, misfire with high RON fuel, or at high load, high smoke with low RON fuel. Lower compression ratio engines require lower RON fuels to achieve auto-ignition at low loads [55]. Optimised multiple injection strategies have been shown to be beneficial for making a better mixture stratification which can therefore reduce peak heat release rate and its accompanying issues [2, 74-77]. Through reducing possibility of overmixing and over-leaning lower injection pressures have illustrated to be beneficial for low load GCI operation [2, 81].

Kalghatgi [2] claims that in GCI combustion, although fuel auto-ignition resistance is the most important parameter for achieving a stable and low-emissions combustion in a wide engine operating load range, volatility of the fuel can play a role as well in creating a more stratified mixture. Mixture of diesel and gasoline, which have a wider distillation range compared to neat diesel and gasoline fuels, seems to be beneficial in order to increase the chance of achieving GCI at higher EGR rates and engine speeds [2, 82]. An interesting case study would be to identify the effects of distillation range of the fuel on the PCI/GCI combustion while keeping the CN the same. Naphtha (with gasoline-like distillation range) and Dieseline (with wide distillation range) introduced in the beginning of this section were selected for this study and results are discussed in Chapters 5 and 6.

2.5.4. In-cylinder fuel blending for dual-fuel PPCI

Fuel properties can be controlled on-line (in the engine cylinder) when injecting two fuels of different characteristics at different ratios. This can be useful in the PPCI combustion mode where research has suggested benefits in using high-CN fuel for low load and low-CN fuel for

high load [40, 83]. One of the possible proposed techniques is to inject low CN fuel with a port fuel injection (PFI) system in the intake stroke and high CN fuel early in the cycle directly in the cylinder with a direct injection (DI) system, which can use multiple injections. In other words, reactivity of the resultant fuel can be controlled and thus the generic name of "reactivity controlled compression ignition (RCCI)" was given to these strategies [40, 84]. In this way fuel-air mixture stratification level can be controlled and consequently a robust control over combustion event is achieved. The main role of the high reactivity fuel is to ignite the premixed mixture [40]. RCCI has been proven to achieve high thermal efficiencies benefiting from the dynamic control over fuel properties.

Apart from the obvious benefits of RCCI, or similar concepts, the main issue is the fact that two separate fuel injection system are required. For mobile applications, at least light-duty, this is not favourable as it means that in fuel-stations two fuel tanks of the vehicle should be filled with two different fuels. Two different sets of injection pumps, injectors and controllers are needed. This increases the cost and questions practicality of the RCCI for the future mobile fleet. Moreover, the fuel injected in the intake manifold can replace the air going to the cylinder and therefore there will be a need for higher intake boost. However, this technique seems very promising for stationary applications.

2.6. Particulate emissions from vehicular engines

As discussed earlier, one of the challenges with the CDC is reducing its particulate emissions. Moreover, although particulates from the PCI modes are lower, they still need to be characterised. Therefore, this section reviews the main properties of particulate emissions from vehicular engines. Particulates emitted from the exhaust of an internal combustion engine (ICE) powered vehicle can be of three forms: nucleation mode, accumulation mode

and coarse mode [24, 85]. Nucleation mode particulates are believed to be of volatile nature with geometries similar to a sphere and generally contain minute/no solid core. Accumulation mode particulates are a combination of carbonaceous solid core embedded with oily/wet volatile and semi-volatile compounds. Formation of coarse mode particulates is less frequent in a vehicle system [24] and therefore is not discussed in the results section of this work.

Vehicular particulate matter emissions have two main parts: volatile fraction and non-volatile fraction. Volatile part has sub-fractions of organic, nitrate and sulphate. Non-volatile part has carbonaceous fraction (soot) and ash fraction. Among these, organic and carbonaceous fractions are the most pronounced part of the particulates emitted from the engines, as shown in Table 2-1 [24], and therefore the focus of this research. It should be noted that this breakdown is extremely engine operating mode, fuel, lubricating oil and measurement technique dependant and these figures are just general approximations [24].

Table 2-1 Breakdown of the fractions of the particulates emissions sourced from vehicles [24].

Fraction (-)	Contribution Percentage (%)
Organic	10 to 90
Carbonaceous	10 to 90
Sulphate*	<5
Ash	<1 to 2
Nitrate	<1

* It was assumed that no oxidation catalyst is used. No data was reported on the sulphur content of the assumed fuel and engine lubricating oil.

2.6.1. Organic fraction

Organic fraction of the engine particulate emissions is one of its most complex portions as it can be sourced from thousands of HC compounds in fuel, engine lubricating oil and from

transitional compounds resulting from their partial combustion. This fraction is the dominant factor in defining the chemical properties of the particulates [24]. The organic fraction sourced from the fuel can be from unburned fuel compounds or compounds which results from the partial pyrolysis of the fuel molecules [24]. Engine lubricating oil contribution to the particulates organic fraction is also significant [24, 85, 86]. Oil can enter the combustion chamber from different locations, such as piston rings and valves, and either get involved in the combustion process or leave the cylinder unburned [24, 87].

Organic fraction is believed to be mainly composed of carbon and hydrogen (hydrocarbons) and some levels of oxygen, nitrogen and sulphur. Funkenbusch *et al.* [88], in 1979, conducted some tests in order to characterise the organic fraction of the particulates emitted from a medium-duty diesel engine. Although engine technology, testing and emission analysis are very different now, this study reports some interesting findings. Paraffinic content (alkanes) were the most dominant mass fraction (up to 65%). Maximum contributions of the other studied portions were: 15% for oxygenated, 15% for acidic, 14% for aromatic and 6% for transitional compounds [88]. These results are indicative of the importance of alkanes within the organic fraction due to their high contribution. As reported in [89] and [86], a bimodal distribution of HC, based on the apparent carbon number, is found in the particulate phase of diesel emissions. Diesel fuel and lubricating oil are the sources of these two peaks; first peak is from lighter HC in the fuel and second peak is from heavier HC in the oil.

When the exhaust gas leaves engine exhaust valves, containing the carbonaceous fraction, due to temperature drop at first in the exhaust system and combination with dilution after leaving the tailpipe to the atmosphere, various particulate and gas phase evolutions can occur. There can be some links to the gaseous HC emissions, where higher HC emissions suggests higher organic fraction of the particulate matter. Nucleation and condensation of the gaseous volatile species in the presence of temperature gradients are possible which can change the number

and mass balance of particulates. Particulate number (PN) and particulate mass (PM) are increased by HC nucleation while HC condensation/adsorption increases PM [90]. Exhaust gas HC have different volatility and vapour pressure which makes the knowledge of their detailed composition necessary. Gas-particulate partitioning is strong in these conditions and this is where the effect of semi-volatile organic compounds (SVOC) becomes very significant [86, 91].

More than one percent of the mass of SVOC is found in both condensed and gas phase [91] while their vapour pressure in the atmosphere is between 10^{-11} and 10^{-5} atm [86]. SVOC can contribute to the formation of secondary organic aerosol (SOA) [86]. Studies, such as [92, 93] have shown that organic fraction is composed of various compounds: normal and branched alkanes, alkyl-cycloalkanes, various aromatics and PAH while few studies have addressed SVOC with high carbon numbers (C>15) in both qualitative and quantitative manner [86]. The similarity between the composition of the fuel and that of the organic fraction is obvious. SVOC in diesel exhaust gas is normally attributed to HC with carbon number between C_{15} and C_{25}. The reason behind the aforementioned lack of substantial qualitative and quantitative data is the fact that using conventional gas chromatography (GC) techniques for identifying heavier compounds is problematic [86, 94]. This is due to the fact that they are largely unresolved by conventional GC techniques and create an unresolved complex mixture (UCM) in the chromatogram [86, 94]. However, using a more comprehensive technique, such as GC×GC used in this work, will help to overcome this issue. This technique is explained in Chapter 3 and was used to characterise gas phase SVOC emissions discussed in Chapter 7.

2.6.2. Carbonaceous fraction

Carbonaceous (soot or elemental carbon) fraction, with a very high carbon to hydrogen ratio, is mainly formed due to in-cylinder pyrolysis reactions of fuel molecules and to a less extent oil molecules [24]. Similar to the organic fraction, carbonaceous fraction is believed to contain carbon, hydrogen, oxygen, nitrogen and sulphur while being dominated by carbon (C_8H, C_9H and $C_{10}H$) as the name indicates [24]. Drawing a line between different fractions can be challenging due to the limitations in the fractionation methods [24]. This fraction is mainly responsible for the graphite nature of particulate emissions.

2.7. Emission abatement techniques

Some of the in-cylinder emission abatement techniques for CI engines were reviewed earlier in this chapter. Techniques such as optimised fuel injection strategy (including injection pressure, timing, number of events and type of fuel), engine intake pressure and temperature, EGR rate and combustion chamber geometry can be used to restrict emissions formation processes and also improve their diminishing processes [22, 95]. For instance, injection strategy modification for enhancing the PCI while using even diesel-type fuels seems promising. For example, Toyota uniform bulky combustion system (UNIBUS) [96] utilises double-injection strategies with the first injection early in the compression stroke and the second near the TDC. This technique is useful for improving the fuel-air mixing quality. However, it is limited to low ratios of the first injection-quantity and low loads due to the fact that intense heat release early in the compression stroke must be avoided [2]. Modulated kinetics (MK) is another system [97-99] which utilises high ratios of cold-EGR coupled with high swirl ratios while retarded injection-timings are used to reduce NO_x and smoke

simultaneously. High swirl ratio helps the fuel-air mixing in the short time available for the late injection strategies and consequently reduces HC emissions [99]. Some techniques for reducing the engine-out emissions were developed in this work and are presented in Chapters 4, 5 and 6. However, the main focus of this section is to provide some background for exhaust after-treatment systems and their associated challenges to support discussions provided in this thesis.

2.7.1. CO, HC and particulates after-treatment systems

Diesel oxidation catalyst (DOC) basics

The production diesel oxidation catalyst (DOC), a see-through (monolith) catalytic convertor, is used to reduce CO, HC and soluble organic fraction (SOF) of the particulate emissions by accelerating their reaction rates with oxidisers. NO to NO_2 conversion can be another benefit of the DOC as NO_2 can be used as a good oxidiser in the after-treatment systems placed after the DOC, e.g. in particulate filters. DOC is popular due to its simplicity, minimal effect on the engine performance (low back pressure), low cost and ease of use [95]. On the other hand, there are some issues to be addressed before benefiting from this technique, including its performance dependence on the temperature and possible loss of activity by various roots such as poisoning [95]. The other problem can be the unwanted conversion of SO_2 to SO_3 (please refer to [100] for more details), but as, in general, the sulphur content of the fuels are low currently, this is not discussed here.

DOC design and operating factors

DOC, in general, consists of five main parts: steel canister (packaging), packing mat, catalyst substrate, catalyst wash-coat and catalytic material. DOC performance, related to the design of the DOC itself, is a function of its physical and chemical properties. Physical properties include substrate material selection, geometry/structure and dimensions while chemical properties include wash-coat selection, precious metal preparation, loading and coating technique [101]. The substrate is normally made of cordierite ceramic or meal alloys. The wash-coat is generally highly porous alumina (Al_2O_3). Catalytic material is "normally" precious (noble) metal. In a "production DOC", these are from the platinum group metals (PGM) which are normally platinum (Pt) or palladium (Pd) or a combination of these [102]. Kim *et al.* [100] found that the light-off temperature (defined as the temperature at which 50% reduction efficiency is achieved) and thermal instability, after being aged, of the DOC is normally lower when a bimetallic version is used. Apart from the DOC design parameters effect, the condition at which it is operating is very important for its performance. These external factors are basically exhaust gas properties, either physical including temperature and flow rate or chemical which are mainly concentrations of different exhaust gas constituents. The utmost important external parameter affecting the performance of a DOC is its operating temperature. Conversion efficiency of each exhaust gas compound is defined as:

$$Conversion\ Efficiency = \frac{Inlet\ Concentation - Outlet\ Concentation}{Inlet\ Concentration}$$

Equation 2-1

Operating temperature can either be controlled by the exhaust gas temperature entering the DOC or by other external heat treatment methods. Exhaust gas temperature entering the DOC is a function engine operating speed and load, engine control parameters such as injection-timing and valve timing, engine design such as compression ratio and exhaust pipe insulation [95]. In modern diesel engines, DOC is normally located just after the turbocharger to utilise high exhaust temperature before it cools down by passing longer path of the exhaust pipe. Turbocharger itself is placed close to the engine exhaust valve. Heat drawn in the turbocharger to generate intake air boost reduces the gas temperature entering the DOC and this can reduce conversion efficiency of the DOC. External heat treatment methods are normally more problematic in terms of complexity, cost, space, weight, engine efficiency and vehicle component durability [95, 101]. These can include external heating or insulation of the piping and DOC. Between these techniques, control of the exhaust temperature by means of engine control parameters without the need for any major hardware modification is outstanding. This strategy is partly addressed in Chapters 5 and 7 of this thesis.

Exhaust flow rate is important as well, since it can affect the space velocity [95] which in simple words can affect the interaction time between the exhaust gas and active sites of the DOC. Obviously, shorter interaction time means less chance of complete conversion of the targeted species. Exhaust gas composition can affect the performance of a DOC. Exhaust oxygen concentration is an important factor for the CO and HC catalytic reduction. Normally, as diesel engines operate under lean conditions, oxygen is found in sufficient concentrations in the exhaust gas. However, some techniques such as using high EGR rate, e.g. for PCI strategies, will reduce engine exhaust gas oxygen content.

Species conversion mechanism inside a DOC

The principle of oxidation in a catalytic convertor involves both mass transfer and chemical reaction kinetics. These involve transport of the reactants to the active site of the catalyst and consequently their diffusion followed by chemisorption (covalent bonding) of some reactants. Then, there will be a chemical reaction between either the species themselves or with other adsorbed species in different phases followed by the reverse of adsorption and diffusion processes [103]. Technically, Langmuir-Hinshelwood and Eley-Rideal mechanisms may be used to generally define complete oxidation of CO and HC involving the dissociative adsorption of oxygen [103]. Langmuir-Hinshelwood can be used for reactions where the reactant is first adsorbed and then reacts with either other reactants or adsorbed oxygen species [104]. Eley-Rideal can be used for reactions where the reactant is oxidised in the gas by an adsorbed oxygen specie [104].

Importantly, conversion efficiency of different HC is not similar while it depends on the element itself and the mixture it is present when passing the DOC [104]. Oxidation theory cannot always support the reduction mechanism, suggesting that there are other removal mechanisms [95]. In theory, once the catalyst reaches the light-off temperature for a specific exhaust constituent, the rate of oxidation is controlled by the rate of mass transfer or diffusion rate of that specie. This means, in theory, there is more diffusion of LMW HC with higher volatility compared to HMW HC. However, short chain HC are known to have higher light-off temperatures compared to longer chain HC. As opposed to theory, interestingly, longer chain hydrocarbons have shown to be removed more efficiently over a catalyst [24, 105].

This brings the question of: “why would longer chain HC be converted easier?” Considering n-alkanes for the sake of simplicity, research shows that decreasing C-H bond strength of n-alkanes with increasing their chain length reduce their surface ignition temperature on a

catalyst [106-108]. This means longer chain n-alkanes are more reactive over a catalyst. It is interesting that this trend is similar to what is observed for auto-ignition tendency of different HC in a CI engines as discussed earlier. In addition, this behaviour of DOC might be partly explained by the fact that there are possibilities that heavier HC can be catalytically cracked into lighter HC [95]. This makes the conversion efficiency definition difficult as it is not confirmed whether compounds observed after the DOC are "oxidised" or "synthesised".

Another mechanism for HC reduction, albeit if it can be called reduction, is through HC adsorption or condensation on the cold catalyst when operating temperature is below the light-off temperature [24, 95]. These stored HC can be either oxidised when the temperature is high enough or just desorb without being oxidised not necessarily when temperature is high [24]. Uncertainty in these, arise a scope to a further detailed characterisation of HC before and after the DOC especially in the case of premixed type combustion with different fuel properties where less literature is available.

The SOF of particulate emissions is also affected by the DOC. As discussed earlier in this chapter, a contributor to the SOF, understood by far, is the adsorbed HC on the carbonaceous cores (in the accumulation mode) or nucleated organic species in the exhaust (nucleation mode). As the DOC reduces the gas phase HC, SOF can be reduced as well. This is valid if gas phase HC has not been adsorbed/condensed on the particulates before the DOC. Based on the discussion provided earlier in this chapter, the role of the DOC for reducing emissions from the PCI combustion is obvious.

Diesel particulate filter (DPF)

Despite of many efforts [24], the conventional DOC is not very efficient in removing soot mainly due to the fact that soot is in the solid phase rather than gas phase and therefore harder to enter the active sites. However, the only way they can be reduced is by getting stuck to the monolith walls of the DOC. These stuck particulates cannot be catalytically converted and therefore may only be oxidised under high temperature conditions. They also can inhibit proper oxidation of CO and HC as they mask the active sites of the DOC [95]. The carbonaceous fraction of particulates is mainly physically filtered by a diesel particulate filter (DPF) in diesel vehicles. DPF uses a channelled wall-flow monolith made from ceramic with precisely controlled porosity and adjacent channels being alternatively plugged at each end [95]. Filtration mechanism can be explained by diffusional deposition, inertial deposition and flow-line interception of particulates on the filter media [95].

As particulates are accumulated in the DPF, exhaust back pressure is increased and obviously engine operation will be affected, e.g. pumping losses will increase. In order to avoid filter clogging, frequent filter regeneration (by burning the loaded particulates) must be performed. Regeneration strategies need to increase the low temperature of the diesel exhaust gas or filter to the levels sufficient for soot oxidation [95]. It should be mentioned that DOC can help DPF in a manner to increase the exhaust gas temperature entering the DPF, by exothermic reactions inside the DOC, and consequently help soot oxidation inside the DPF. High rate of soot oxidation by oxygen in a DPF is achieved at temperatures in excess of almost 600 ^{o}C while oxidation by NO_2 (which can be partly produced by the DOC as discussed earlier) can happen at around half of this temperature [95, 102]. While regeneration with NO_2 seems promising, there are some factors to be met before achieving successful regeneration such as a certain limits of NO_x/particulates ratio and fuel sulphur content [95]. It should be mentioned that these techniques are possible within a combined system comprised of both DOC and

DPF. However, regeneration has its accompanying issues [95]. For instance, increased exhaust temperature, e.g by using post fuel injection into the cylinder, can have adverse effects on the fuel economy and engine out emissions. These issues highlight the benefits of in-cylinder strategies for soot reduction.

2.7.2. NO_x after-treatment systems

Currently, NO_x emitted from diesel engines can be reduced by the selective catalytic reduction (SCR) using nitrogen containing compounds, ammonia or urea SCR, or exhaust HC, HC SCR ($deNO_x$ catalyst) [95]. This is possible through the reaction of NO_x ($NO+NO_2$) with either ammonia or HC; and resultants are nitrogen and water under temperature and pressure conditions of the diesel exhaust. However, NO_x reduction in the fuel-lean exhaust of a light-duty diesel vehicle has been problematic [95]; there are several problems associated with each technology. The use of relatively complex and expensive current ammonia SCR systems is accompanied with issues such as the need for supplying, carrying and refilling ammonia – a toxic compound. Moreover, similar to the urea SCR, its efficient operation depends on the temperature which is low in the exhaust of a CI engine [95, 109]. HC SCR, which relies on the HC content available in the exhaust, either from the engine or from the extra injected HC directly into the exhaust, has issues such as not having enough HC available for the NO_x reduction at all the operating modes or fuel economy penalty [95]. These highlight the advantages of the safe, cheap and less complex in-cylinder reduction techniques for a mobile application.

2.8. Summary

In summary, some fundamental and advanced concepts in the areas related to conventional and advanced clean CI combustion engines are reviewed in this chapter. Trends in this research field indicate the scope for investigating techniques such as utilising low reactivity fuels to reduce emissions, especially NO_x and particulates, from the CI engine while keeping its high fuel conversion efficiency when running on the PCI combustion mode. Furthermore, use of an exhaust catalytic converter seems to be a good option to cope with the shortcoming of the PCI combustion: high CO and HC emissions. It is clear that fuel, engine, combustion mode and exhaust after-treatment strategy must be properly matched to achieve these targets. Based on the literature survey, there is a scope for further research into fuelling, intake/exhaust handling and exhaust after-treatment strategies to expand the currently limited operating window of the PCI combustion and reduce (both in-cylinder and out-cylinder) CO and HC emissions while using a production multi-cylinder CI engine.

Chapter 3
EXPERIMENTAL SYSTEM SETUP

3.1. Introduction

This chapter describes details of the experimental and analytical systems used for the current research work. This includes description of setting up and using engine test cells, measurement and analysis of engine performance and emission characteristics and utilised fuels. Two engine test cells were used for this research: CR-15.5 and CR-16.6 which are described below. CR-15.5 was used for the experiments presented in Chapters 5, 6 and 7. CR-16.6 was used for experiments presented in Chapter 4. CR-15.5 engine test cell is described first.

3.2. CR-15.5 engine test cell

This engine test cell (Figure 3-1) was mainly designed, manufactured and commissioned by the author. The major components and operating factors of the test cell are presented below:

3.2.1. CR-15.5 engine

Most of the experiments were conducted on a 2.2 L, 4-cylinder in-line compression ignition (CI) engine equipped with a common rail direct-injection (DI) system and a variable-nozzle-turbine (VNT) turbocharger. This engine is a production engine, as found in the market, without any major changes to its original settings. It is a DURATORQ L316 diesel engine

from the Ford Puma family and its production application is in Land Rover Defender 2012. However, due to some control facility limitations, solenoid injectors (from older generation of these engines) instead of piezoelectric injectors (originally assembled on the engine) were used. Major specifications of the engine are listed in Table 3-1.

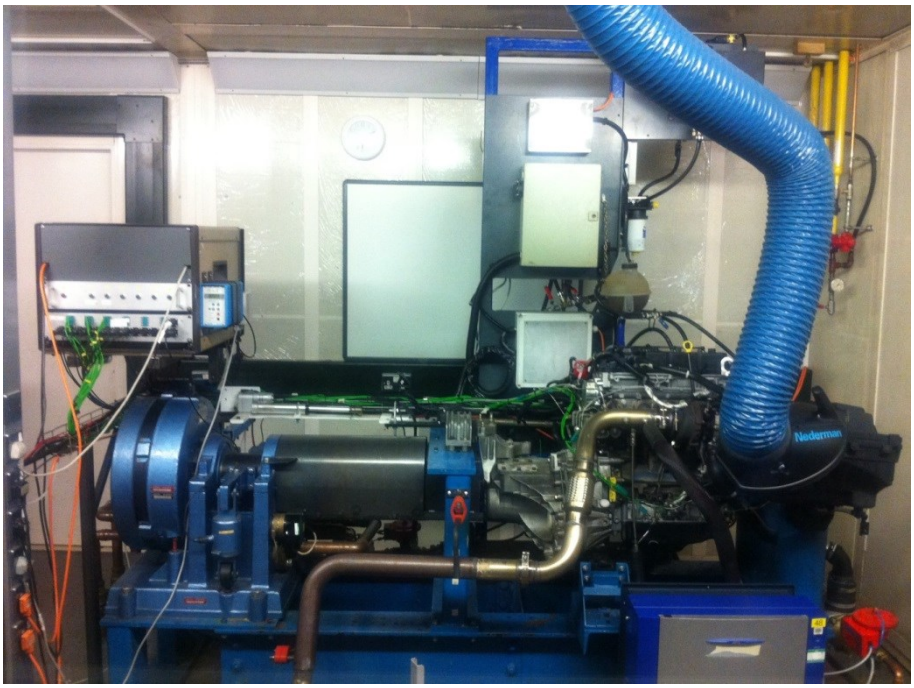


Figure 3-1 The CR-15.5 engine test cell

Table 3-1 CR-15.5 engine specifications

Bore (mm)	86
Stroke (mm)	94.6
Connecting Rod Length (mm)	155
Capacity (cc)	2198
Compression Ratio	15.5:1
Injection System	DI Common Rail
Injectors	Solenoid, 7 Holes (0.15mm diameter)

A schematic of the CR-15.5 engine test cell is illustrated in Figure 3-2. The exhaust gas recirculation (EGR) cooling system was upgraded in order to be able to control the cooling intensity of the exhaust gas before being looped back to the intake manifold. This was achieved by means of placing a simple ball-valve in the outlet of the cooling circuit of the EGR heat exchanger. As it is shown later in thesis, especially in Chapter 5, EGR temperature can play an important role in the attainment of the robust premixed compression ignition (PCI). It should be mentioned that some of the auxiliary units including power steering pump, vacuum pump, alternator, coolant pump and air-conditioning compressor are not connected to the engine.

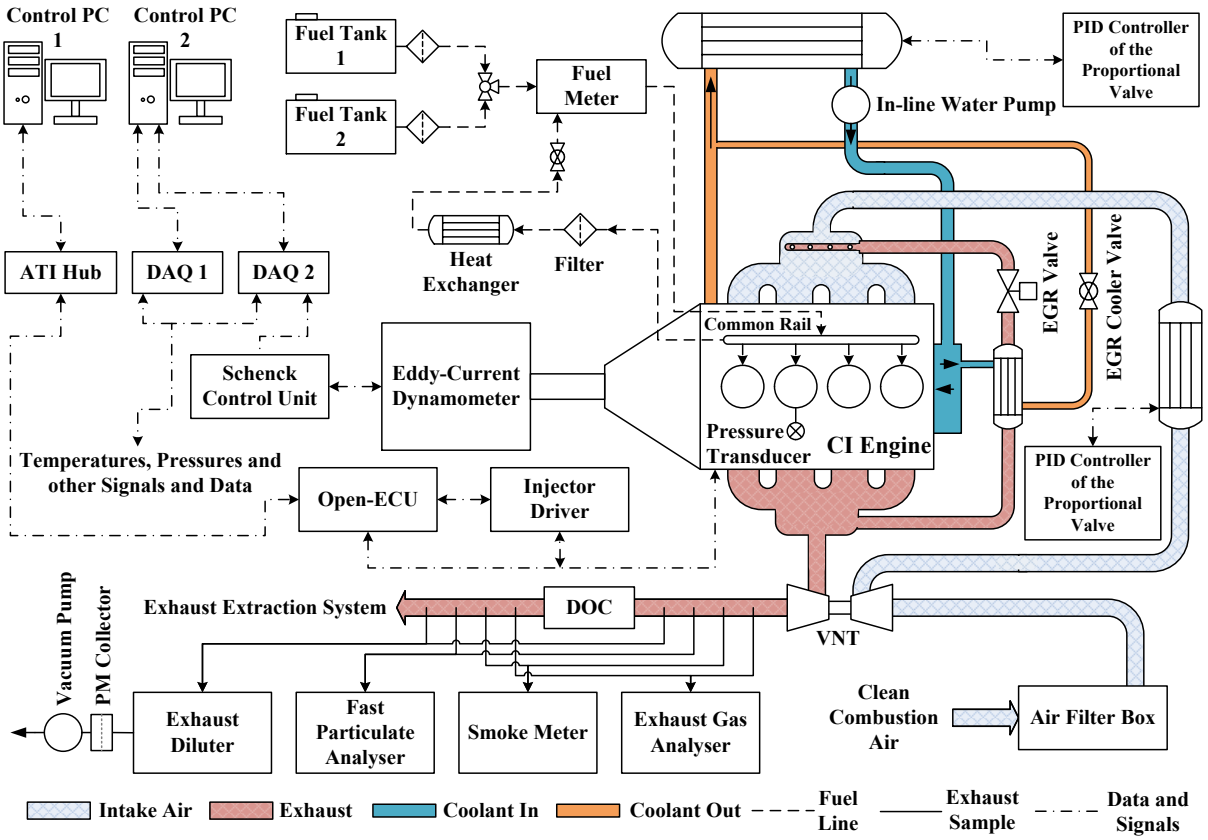


Figure 3-2 Schematic of the CR-15.5 engine test cell

3.2.2. Engine control unit

The engine control unit (ECU) used in this test cell is a M250 Open-ECU platform from Pi-Innovo [110] and it is equipped with a Pi-Innovo S070 solenoid injector driver [110]. The Open-ECU has two H-Bridges which were used to control VNT turbocharger actuator and EGR valve. An external H-bridge from Axiomatic (AX10060X [111]) was used to control the intake manifold throttle valve of the engine. Most of the control terms of the control strategy in the Open-ECU are based on feed-forward terms (open-loop), typically maps, accompanied with feed-back terms, mostly proportional–integral–derivative (PID) terms, (closed-loop).

The Open-ECU and injector driver communicate with the control PC through a Vision Network Hub (VNI2) from Accurate Technologies (ATI) [112]. ATI VISION software [113] was used to develop the data acquisition and control interface (shown in Figure A-1 in the Appendix) which allows flexible control of the engine operating settings, e.g. injection events, EGR valve settings, VNT settings, etc. PID controllers and controller loops in the strategy file of the Open-ECU were optimised either by Pi-Innovo or the author. Main electrical and signal connections of the test cell are shown in Figure A-2 which shows the location of the Open-ECU in the loop.

3.2.3. Dynamometer and control unit

A water cooled eddy current dynamometer from Froude Consine (EC38TA) [114] was used to measure crank shaft torque and rotational speed of the engine. The engine is connected to the dynamometer by means of a dual-mass flywheel, a clutch, a power take off (PTO) unit and a universal-joint shaft assembly. The dynamometer is controlled by a Schenck series 2000 D/W controller [114] which allows two main control modes: fixed speed and fixed torque.

3.2.4. Test cell control and conditioning

The test cell is controlled by a combination of computer-based and stand-alone controllers. Most of the computer based controllers are written in the LabVIEW software (some were written by the previous doctoral researchers: Fan Zhang [48] and Jun Zhang [114] and were upgraded by the author). Description of each of the in-house software for control and data acquisition (which is not discussed in this section) is provided in the appropriate sections later in this chapter.

Intake air (clean combustion air shown in Figure 3-2) of the engine was provided from lab air supply system which keeps the clean air temperature at 22 ± 1 ^{o}C. A heat exchanger was used as the intake air intercooler after the compressor of the VNT turbocharger (shown in Figure 3-2). The heat exchanger is a FG17 from BOWMAN (shell and tube type) and its cooling intensity was controlled by a closed loop control system (designed and manufactured by the author) to maintain the air temperature going to the intake manifold at a defined target level. The components of this system are:

1. A pneumatic Northvale Korting three-way proportional control valve (75AK-M26824-15/20DN) placed at the outlet of the heat exchanger which allows control over the lab water flow through the heat exchanger. This valve receives a pneumatic signal from an electro-pneumatic transducer (EPT).
2. The EPT is an EP-8000-4 (high volume output) from Johnson Controls which receives its electric control signal from a PID controller.
3. The PID controller is a Fuji Electric PXG.4E and its output, set by the temperature input from a K-type thermocouple placed just after the heat exchanger, is electric current between 4 to 20 mA-DC depending on the cooling intensity required.

Engine coolant loop (used for cooling the engine, EGR and lubricating oil) has a similar closed loop control system as the air intercooler system. The only two differences are the heat exchanger and the control valve: a BOWMAN GL320 heat exchanger and a 74AK-M26815-25DN pneumatic Northvale Korting three-way proportional control valve. With these settings, engine out coolant temperature can be controlled in a flexible manner. For the current research work, coolant temperature was maintained at 90 ± 1 ^{o}C.

The test cell has both fresh air supply and extraction system to reduce fumes and maintain cell temperature at the ambient level while the engine is being operated. Exhaust pipe of the engine is connected to an exhaust extraction system.

Engine start and stop (including ignition and cranking) is controlled by a LabVIEW interface (originally designed by Jun Zhang [114] and upgraded by the author to fit to the new test cell). The LabVIEW interface is connected to the data acquisition board (DAQ), from the National Instruments (NI) USB-6218 [115], which controls a set of relays and electrical currents (connections diagram are provided in Figure A-2).

3.2.5. Diesel oxidation catalyst (DOC)

The CR-15.5 engine used in this work is equipped with a production diesel oxidation catalyst (DOC). The DOC package contains two honeycombs: one has a circular profile and the other one is oval. The circular honeycomb has a diameter of 144 mm and length of 96 mm. The oval honeycomb is 157 mm in length and 188 mm and 153 mm in cross sectional profile. Both of these honeycombs have 20×20 (400) cells per square inch (CPSI). The circular honeycomb is catalysed and the other honeycomb is un-catalysed (just the ceramic monolith); circular honeycomb is placed closer to the engine. In order to identify the precious metal

content of these, samples were taken from the honeycombs and analysed by means of X-ray fluorescence (XRF) technique. Platinum (Pt) to palladium (Pd) weight ratio of the catalysed DOC was found to be approximately 3:1.

3.2.6. Intake and exhaust sampling ports design and locations

Samples were required to be collected from both intake and exhaust streams of the engine. Intake air, after the entry of the EGR tube to the intake manifold, was sampled to calculate the EGR percentage by measuring the CO_2 concentration. Exhaust steam was sampled at different locations of the exhaust system, mainly before (for Chapters 5, 6 and 7) and after the DOC (for Chapter 7). All of the exhaust sampling was conducted by using heated lines, unless not required by the measurement instrument, with temperature maintained at 191 ± 3 ^{o}C. In order to avoid sampling artefacts caused by sampling in the vicinity of the exhaust pipe wall, sampling ports were designed to collect exhaust gas from either the centre of the pipe or a number of locations in the cross-section of the pipe. Figure 3-3 illustrates an example of the exhaust sampling port design.

3.3. Instrumentations

This section explains the major instrumentations used for this study.



(a)



(b)

Figure 3-3 Exhaust sampling port design: (a) before and (b) after welding to the pipe with holes at different cross sectional area of the sampling port

3.3.1. In-cylinder pressure measurement and acquisition system

A Kistler 6058A non-cooled piezo star pressure transducer equipped with a 6544Q192 glow-plug adaptor is used to measure in-cylinder pressure of the engine (cylinder number 3). The pressure transducer was calibrated before the start of the experiments by the Kistler Company;

its sensitivity and linearity are -17.68 pico-Coulomb/bar and ≤ ± 0.05% of full scale output (FSO), respectively. These values are used in the Kistler charge amplifier (Type 5011B10Y50) incorporating the drift compensation (Drco). The output from the charge amplifier is linked to a NI PCI-6251 card and is referenced to the crank angle degree (CAD) by using signals from the crank shaft encoder and cam shaft encoder. Two signals from the shaft encoder (AMI-Elektronik/Art.No:41500043-00360) for each CAD and each revolution were used in an in-house LabVIEW interface (upgraded by the author) to show in-cylinder pressure and calculated heat release rate (HRR) on-line. In the LabVIEW interface, using DAQmx Start Trigger, crank shaft encoder (for each revolution) and cam shaft encoder signals are used to identify the start point of data logging (Figure 3-4).

In-cylinder pressure data were recorded for 200 consecutive engine operating cycles for each sample and was used to calculate some of the terms discussed later in this chapter.

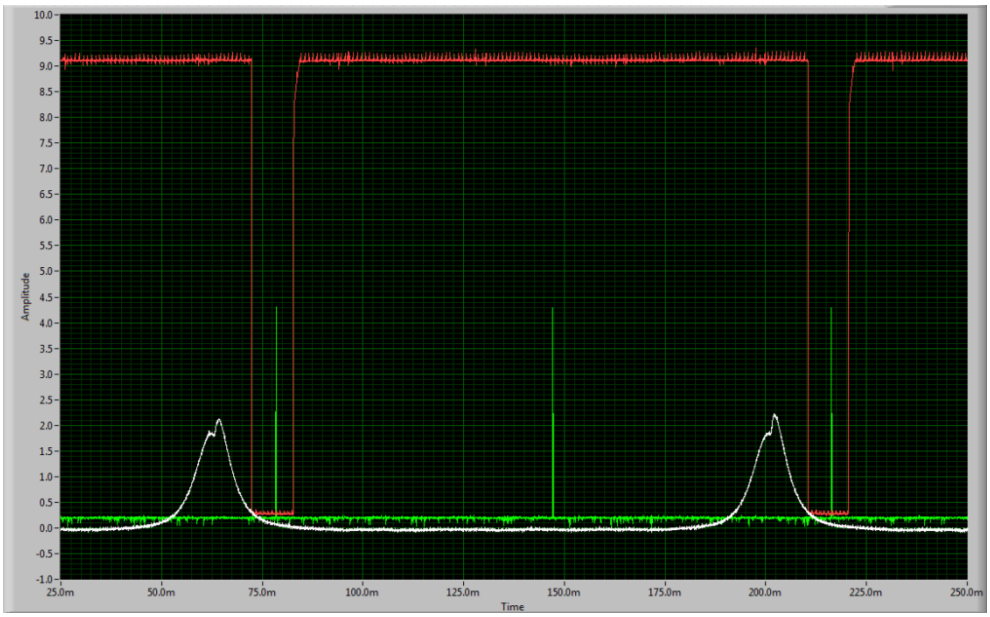


Figure 3-4 In-cylinder pressure (white), crank shaft encoder (green) and cam shaft encoder (red) signals versus time created in the LabVIEW interface

3.3.2. Engine and test cell pressure and temperature measurement

Calibrated K-type thermocouples from RS Company, with mostly 3 mm diameter, were used to measure temperatures at different locations of the test cell. Some examples of the key locations of temperature measurement are: exhaust before VNT, exhaust after VNT, exhaust after DOC, oil sump, fuel feed-line and intake manifold. The signals from the amplifier (thermocouple amplifier shown in Figure A-2) were recorded using the NI USB-6218 card via an in-house LabVIEW interface and data were averaged for 180 s at each test point.

Pressure data were measured at different locations using Variohm EuroSensor EPT 3100 pressure transducers (max 2 bar) [116]. These pressure transducers were calibrated frequently by using a Druck DPI 601 portable pressure indicator/calibrator. Scales for each utilised pressure transducer (voltage output with respect to actual pressure (linear scale calibration)) was updated frequently in the LabVIEW interface.

3.3.3. Fuel consumption measurement

The fuelling system, incorporating auto-filling and over-flow detection/control sub-systems, was designed and manufactured by the author. Fuel consumption was measured by an AVL 733s dynamic fuel meter. The test cell has two fuel tanks with separate filters and the fuel stream can be switched by a three-way valve (Figure 3-2). Return fuel line from the engine has an in-line fuel filter before being introduced to an AVL 752-60 fuel cooler. Fuel temperature in the feed and return lines was monitored and controlled to assure repeatable fuel consumption measurements. The fuel meter was calibrated frequently using a build-in function. For all of the experiments, unless specified, fuel consumption was measured and averaged over 180 s. A ball-valve was needed to be placed after the fuel cooler (before the

fuel meter inlet). This valve was used to throttle the fuel return line when less viscous and more volatile fuels were used. In this manner, measurement fluctuations related to using gasoline-like fuels in a CI engine were minimised.

3.4. CR-16.6 engine test cell

This engine test cell was mainly prepared by Jun Zhang [114] and Fan Zhang [48] and the author helped to modify and upgrade the cell. This test cell was used to collect experimental results presented in Chapter 4 of this thesis. It had a 4-cylinder in-line 2.2 L DURATORQ Ford Puma CI engine equipped with a common rail DI system and a variable-geometry turbocharger (VGT). It had a prototype ECU which allowed full control over different operating parameters of the engine. Major engine specifications are listed in Table 3-2. A 6056A Kistler non-cooled pressure transducer equipped with a 6542Q18 Kistler glow-plug adaptor was used to measure the in-cylinder pressure. Engine test cell schematic is illustrated in Figure 3-5 and more information about this test cell can be found in [43, 48, 114].

Table 3-2 CR-16.6 engine specifications

Bore (mm)	86
Stroke (mm)	94.6
Connecting Rod Length (mm)	166
Capacity (cc)	2198
Compression Ratio	16.6:1
Injection System	DI Common Rail
Injectors	Solenoid, 7 Holes (0.15mm diameter)

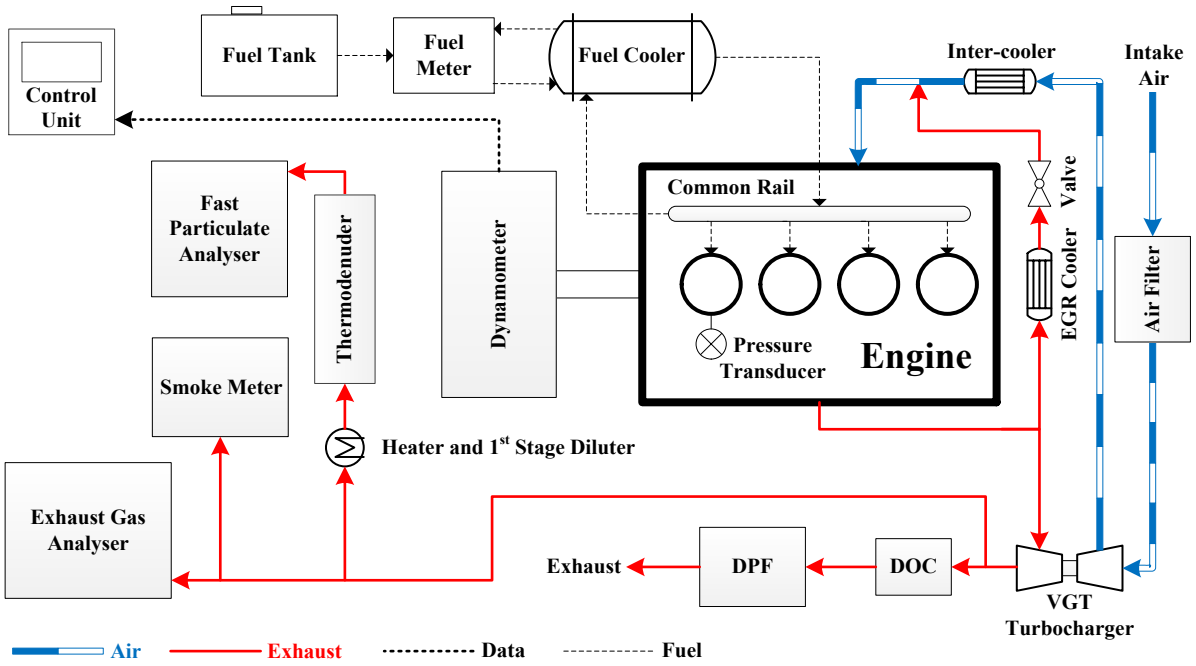


Figure 3-5 Schematic of the CR-16.6 engine test cell

3.5. Emissions measurement

This section describes the techniques utilised for either on-line or off-line emissions measurement.

3.5.1. On-line gaseous emissions characterisation

Gaseous emissions were measured by a Horiba MEXA-7100-DEGR exhaust gas analyser and averaged over 180 measurements (each measurement takes 1 s) directly from the exhaust pipe at different locations. Before any measurement, the instrument was calibrated using the zero and span gases. It uses dry chemi-luminescence detection (CLD) technique for oxides of nitrogen (NO_x) and nitric oxide (NO), dry non-dispersive Infra-Red (NDIR) technique for carbon monoxide (CO) and carbon dioxide (CO_2), hot-wet (uncondensed) flame ionisation

detector (FID) technique for total hydrocarbons (THC) and magneto-pneumatic (MPA) technique to measure oxygen (O_2). Specific air-fuel ratio (λ) is calculated based on the concentrations of the exhaust constituents. However, carbon-normalised ratios of H/C and O/C of each fuel needs to be inserted in the control software by the operator for correct measurement of λ. Fuels used in this study had very low O_2 content and therefore the reduced sensitivity of the FID for measurement of the oxygenated HC [117] was ignored.

3.5.2. On-line particulate emissions characterisation

Particulate emissions were measured on-line by two instruments in this work as below:

AVL smoke meter

An AVL smoke meter (model 415S) was used to measure smoke emissions in the exhaust by collecting samples on a paper filter. It incorporates a reflectometer which indicates the soot content using the blackening number (can vary from 0 to 10 for clean and fully loaded filter), equivalent to the filter smoke number (FSN), of the filter relative to its un-blackened state [118]. "Auto-Range Online" measurement method (with automatic number of measurements) was selected for this work which is suitable for steady state smoke measurements [119]. The instrument was warmed-up and purged before any measurement.

CAMBUSTION fast particulate analyser

CAMBUSTION DMS500 MKII fast particulate analyser (working based on differential mobility spectroscopy (DMS)) was used to measure, primarily, particulates number and size

distribution. The utilised DMS500 has a two-stage integrated dilution system using hot compressed air for the first diluter (low dilution ratio) and cleaned exhaust gas (by a carbon high-efficiency-particulate-air (HEPA) filter) for the second dilution (high dilution ratio). The diluted aerosol is then introduced to a classifier column operating at vacuum pressure (0.25 bar absolute) where particulates are first charged with a corona charger. The column has a high voltage electrode in the centre. Particulates are mixed with a clean sheath air stream and are attracted towards the grounded electrode rings on the outer diameter of the column. Depending on the charge and aerodynamic drag, particulates land on different rings of the column. This is used for characterising their size and number distribution. [120]

Different moments based on the particulate equivalent aerodynamic diameter distribution can be calculated. Mass calculation can be conducted by separating nucleation and accumulation modes based on the log normalisation and applying Equation 3-1 for agglomerates and Equation 3-2 for spherical particulates [121]:

$$Mass\ (\mu g) = 2.20 \times 10^{-15} \times {d_p}^{2.65}\ (nm)$$

Equation 3-1

$$Mass\ (\mu g) = 5.20 \times 10^{-16} \times {d_p}^{3}\ (nm)$$

Equation 3-2

All the particulate number and size distribution data presented in this thesis are averaged over 60 s for a single measurement, unless specified to be different. The instrument was auto-zeroed frequently.

3.5.3. Off-line gaseous and particulate emissions collection and characterisation

Some of the characterisations were needed to be conducted outside the engine labs are described below.

Exhaust dilution and sample collection system for gaseous and particulate emissions

An in-house exhaust dilution and sample collection system, designed and manufactured by the author, was used to collect engine exhaust particulate and gas phase samples to be analysed by some lab-based techniques discussed later in this section. A schematic of this system is shown in Figure 3-6.

This system incorporates a modified TSI model 3302A diluter. The diluter was modified to use compressed air passed through a high flow rate moisture trap and two HEPA filters. The undiluted hot exhaust sample, delivered via a heated line maintained at 191^{o}C, mixes with an external airstream at ambient temperature. For the current research, dilution ratio (DR) was kept at around 1:30±5 confirmed by measurements of NO before and after the dilution system. The pressure difference gauge, shown in Figure 3-6, was utilised to ensure there is a positive engine exhaust sample flow and maintain the DR at a fixed level.

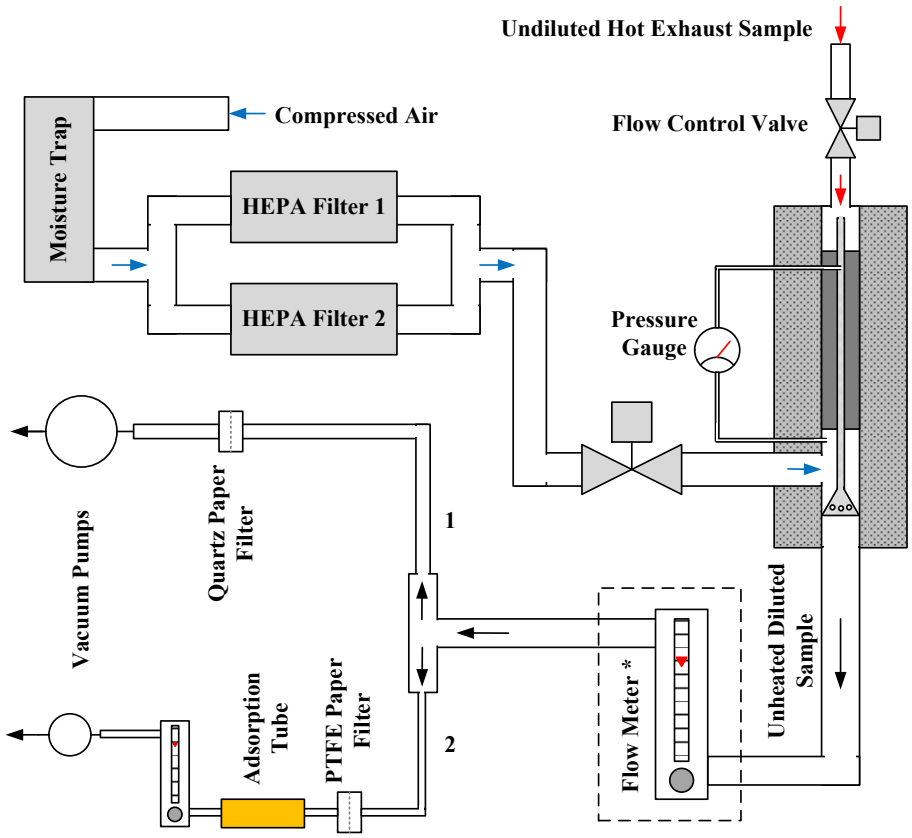


Figure 3-6 Schematic of the exhaust dilution and sample collection system

The diluted sample is divided into two flow streams, 1 and 2 as shown in Figure 3-6. Stream 1, with a flow rate of 9 L/min, is created by a vacuum pump and is used for sampling particulates via a prebaked quartz filter (47 mm). A calibrated rotameter, marked with the dashed rectangle in Figure 3-6, was used to measure the flow rate and was removed while sampling to avoid any possible particle losses. Stream 2, with a flow rate of 1.8 L/min, created by a small vacuum pump is used for sampling particulates on a polypropylene backed polytetrafluoroethylene (PTFE) paper filter 47 mm (Whatman) followed by the collection of gas phase compounds using stainless steel gas absorption tubes filled with quartz wool and 300 mg Carbograph 2TD 40/60 (Markes International). The temperatures at the sampling points were 25 ±5 ^{o}C. For all of the experiments, samples were collected for 30 minutes at steady-state conditions.

TD-GC×GC-TOF-MS analyses for gas phase SVOC

Thermal desorption (TD) coupled to comprehensive gas chromatography time of flight mass spectrometry (GC×GC-TOF-MS) was used to characterise gas phase SVOC emissions. These analyses were conducted in collaboration with researchers at the School of Geography, Earth and Environmental Sciences at the University of Birmingham. In this technique, effluents from the first GC column (which are separated based on volatility like conventional GC) are injected into a secondary column to be separated on the basis of polarity. More details about this state-of-the-art technique can be found in [122, 123].

For quantification and considering the losses of the analysis method, tubes were spiked with 1 ng of a deuterated internal standard mix (the list is provided in Appendix section A3). Gas phase emitted species collected on the stainless steel adsorption tubes were desorbed by means of a TD system (Unity 2, Markes International). Then the sample was analysed by means of a two-column GC, 7890A, Agilent Technologies gas chromatograph equipped with a cryogenic modulator (Zoex ZX2). The first and second column were SGE DBX5, non-polar capillary column (30 m, 0.25 mm ID, 0.25 μm – 5% phenyl polysilphenylene-siloxane), and SGE DBX50 (4.0 m, 0.1 mm ID, 0.1 μm – 50% phenyl polysilphenylene-siloxane), respectively. The GC×GC was connected to a Bench-ToF-Select (Markes International) and the scan speed was set at 50 Hz with a mass range of 35 to 525 m/z (mass to charge ratio). Ionisation energy that was used in this work was 70 eV. Details about the temperature ramp settings are provided in [86]. Data obtained were processed and post-processed via GC Image v2.3 (Zoex Corporation). Computer language for identifying chemical (CLIC) was used to characterise different classes of hydrocarbons within each sample.

Organic-carbon/elemental-carbon (OC/EC) analyses

Particulate emissions collected on the quartz paper filters were analysed to identify absolute amount and ratio of organic carbon (OC) and elemental carbon (EC) species. For this purpose an OCEC Lab Instrument Model 5 (Sunset-Laboratory) which works based on a thermal-optical method was used [124].

3.6. Data analysis and calculations

This section explains some of the data processing conducted by means of using different in-house codes in different platforms, e.g. MATLAB and Microsoft Excel, developed by the author. Related combustion performance and emission terms such as heat release rate (HRR), brake thermal efficiency (BTE), combustion efficiency, specific air-fuel ratio, brake specific emissions, etc. are calculated for each experiment as follows.

3.6.1. In-cylinder pressure based parameters calculation procedure

In-cylinder pressure data was pegged using the concept of having the same in-cylinder pressure at the bottom dead centre of the intake stroke as the intake manifold pressure [125]. HRR was calculated for each CAD from the averaged in-cylinder pressure data (for 200 consecutive engine operating cycles) by Equation 3-3 [1, 16]:

$$\frac{dQ_n}{d\theta} = \frac{\gamma}{\gamma - 1} p \frac{dV}{d\theta} + \frac{1}{\gamma - 1} V \frac{dp}{d\theta}$$

Equation 3-3

Where γ is the ratio of the specific heats (C_p/C_v), θ is CAD and p (Pa) and V (m^3) are the in-cylinder pressure and volume, respectively. Based on the results of this calculation procedure, other parameters are calculated. Combustion-phasing (AHR-50) is defined as the CAD at which 50% of accumulated heat release is achieved. Combustion duration is the CAD duration between AHR-10 and AHR-90. Ignition delay is the CAD duration between start of injection (SOI) and start of combustion (SOC). SOC is defined as the CAD at which HRR rate curve passes the zero level from a negative value to a positive value after SOI [19]. Combustion delay is defined as the CAD duration between SOI and AHR-50. The coefficient of variation (COV) of net indicated mean effective pressure (NIMEP) is the ratio of the standard deviation in NIMEP divided by its mean value over a defined number of cycles [16].

3.6.2. Specific performance and emission terms calculation procedure

Different brake performance characteristics can be calculated by knowing data such as fuel consumption, engine brake torque output and emission concentrations. As an example, BTE (fuel conversion efficiency) is calculated based on the Equation 3-4 [16].

$$Brake\ thermal\ efficiecncy = 100 \times \frac{2\pi NT}{\dot{m}_f Q_{HV}}$$

Equation 3-4

Where N is engine crank shaft speed (rev/s), T is brake torque (N m), $\dot{m}_f$ is the fuel consumption rate (kg/s) and Q_{HV} is the fuel net calorific value (J/kg).

Some of particulate and gaseous emissions results presented in this thesis are brake-specific normalised. For particulate emissions measured by the DMS500, the brake-specific conversion procedure is via using the ideal gas law and assuming that exhaust gas is an ideal gas. As an example, Equation 3-5 shows the calculation of specific normalised particulate concentration (dN/dlogdp/kWh) based on particulates volumetric concentration, exhaust mass flow rate, exhaust density and engine power. It should be borne in mind that all DMS500 measurements are valid for standard temperature and pressure (S.T.P) conditions and therefore any subsequent conversions should be conducted at S.T.P conditions. For this reason, standard temperature (273 K) and pressure (100 kPa) are considered for these set of conversions.

$$Specific\ normalised\ concentration \left(\frac{\frac{dN}{dlogdp}}{kWh}\right)$$
$$= Normalised\ concentration \left(\frac{\frac{dN}{dlogdp}}{m^3}\right)$$
$$\times Exhaust\ mass\ flow\ rate \left(\frac{kg}{h}\right) \times \frac{1}{Exhaust\ density} \left(\frac{m^3}{kg}\right)$$
$$\times \frac{1}{Engine\ power} \left(\frac{1}{kW}\right)$$

Equation 3-5

Gas phase species measured by Horiba MEXA-7100-DEGR exhaust gas analyser in ppmv were needed to be converted into the brake specific terms (g/kWh). In this study, the technique of determining λ from the exhaust constituents was utilised. Brettschneider/Spindt

method [126] combined with the algorithm suggested by [16] for wet HC measurement was used to calculate λ considering NO_x emissions and assuming there is no CO_2 and H_2O in the ambient air. Another assumption is that no water remains in the condenser, used for dry measurements, of the Horiba MEXA-7100-DEGR exhaust gas analyser. These assumptions are not completely ideal but effects of their variation on the calculated value are very low [126]. Brake-specific CO emission (as an example) was calculated based on Equation 3-6 [16].

$$Brake\ specific\ CO\ \left(\frac{g}{kWh}\right) = \frac{Mass\ flow\ rate\ of\ CO\ \left(\frac{g}{h}\right)}{Brake\ power\ output\ (kW)}$$

Equation 3-6

Mass flow rate of CO is calculated based on its molar mass, its volumetric concentration in the exhaust and the total exhaust mass flow rate and mean molar mass [16].

3.7. Studied fuels

Three liquid fuels were used in this work:

1. Diesel: neat normal European ultra-low sulphur diesel (ULSD) (specification EN 590).
2. Dieseline: blend of diesel, same specifications as fuel 1, and neat normal European RON95 unleaded gasoline (ULG95) (specification EN 228). Different blend-ratios were studied with the major focus on the G75-Dieseline fuel which is a blend of 75% of ULG95 in ULSD by volume. Before starting the blending work, ULG was enriched with 300 volumetric parts per million (ppmv) of the Paradyne R655 fuel lubricity

improver to prevent failure of the production diesel engine fuel injection equipment (FIE). FIE of the diesel production engines are designed to work with diesel-like fuels which normally possess higher lubricity and viscosity compared to gasoline-like fuels.

3. Light naphtha: a synthetic fuel produced on a special order to mimic the properties of the low processed light naphtha fuel available in the refineries, as discussed in Chapter 2.

Table 3-3 shows the specifications of ULSD (diesel), G75-Dieseline and naphtha as well as neat ULG95 (gasoline). Analysis of the fuel properties were conducted by some external labs.

Table 3-3 Properties of the utilised fuels

	Diesel	**G75-Dieseline**	**Naphtha**	**Gasoline**
Density at 15 ^{o}C (kg/m^{3})	835.1	768.2	742.5	742.8
RON (-)	-	~75*	74.5	95.4
MON (-)	-	-	73.6	86.6
CN (-)	52.6	-	-	-
Derived CN (-) ×	-	30.0	27.4	-
Cetane Index (-)	-	27.2	-	-
Net Calorific Value (MJ/kg)	42.72	42.52	43.86	42.34
Total Paraffins (v/v %)	-	57.8	56.9	47.1
Olefins (v/v %)	-	7.2	0.3	7.9
Naphthenes (v/v %)	-	-	15.0	6.3
Aromatics (v/v %)	-	31.7	18.0	26

* this value is estimated

× DCN measurement is certified for 33<DCN<64; at DCN: 34, reproducibility is ± 2.21

- means the value is not available

Figure 3-7 illustrates boiling curve of the studied naphtha and G75-Dieseline in comparison to diesel and gasoline fuels. It can be observed that, as expected, G75-Dieseline has a wide boiling curve and boiling curve of naphtha is narrower while their DCN is in the same range (RON is believed to be in the same range as well).

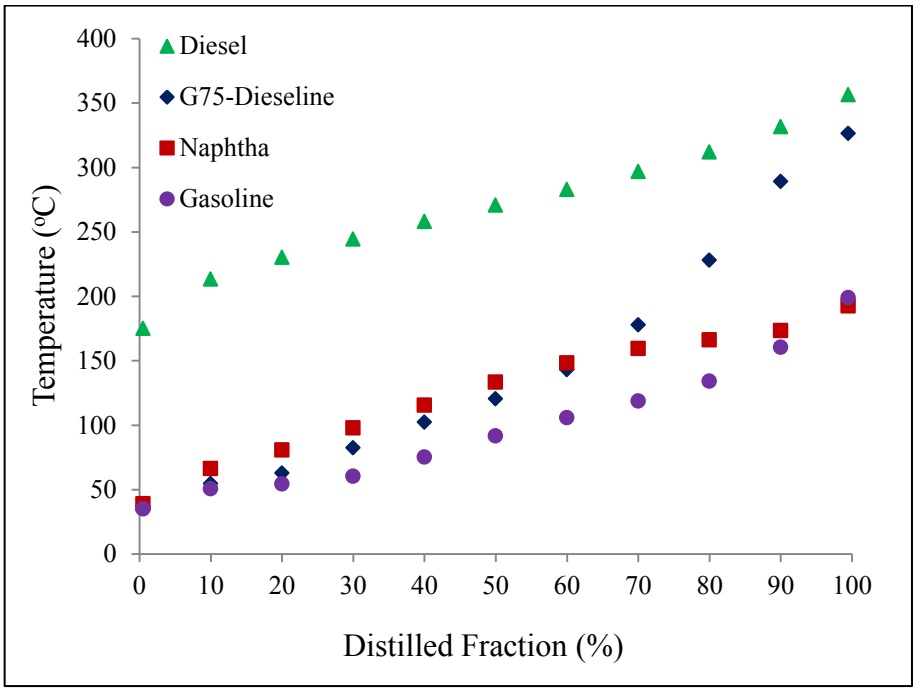


Figure 3-7 Comparison of different fuels in terms of their boiling profile measured with either ASTM D86 or DIN EN ISO 3405 methods

3.8. Uncertainties of experimental parameters

Some level of error/uncertainty is an undeniable part of all experimental results. This section provides information (if not mentioned earlier in this chapter) on the accuracy of the utilised instruments (based on the guidelines provided by the manufacturers) and discusses an example about the repeatability of the experimental results.

In normal conditions, the Schenck controller used for the dynamometer shows 0 ± 1 newton meter (N m) at the zero speed. This was checked before the start of experiments and in case of higher deviation, the calibration key was used to correct for errors. Fuel consumption measurement error by AVL 733s is from 0.12 % to 0.2 % of measured values depending on the fuel consumption. As mentioned before, the linearity of the Kistler 6058A pressure transducer is ≤ ± 0.05% of FSO. The typical error in the measurements by the Kistler 5011B10Y50 charge amplifier is less than ± 2% and ± 0.5% for <±100 pC and ≥±100 pC range, respectively, while linearly is ≤ ± 0.05%. Measurements linearity related to using analysers included in the Horiba MEXA-7100-DEGR are all ≤ ± 1% of FSO. Standard deviation (SD) of the measurements (for repeatability) with the AVL smoke meter 415S is less than ± 0.005 FSN + 3% of measured value.

It should be mentioned that all of the experimental data presented in this thesis are averages of multiple measurements in the steady-state conditions. The repeatability of the results was carefully monitored by considering the SD of multiple measurements. As an example, the SD of BTE results was mostly ≤ ± 0.2%. In order to show the repeatability of the experimental data (to show the random uncertainty (apart from the fixed uncertainties presented in the above paragraph) in measurements), an example is provided below.

Fifteen different experiments in the same day but different times of the day were conducted at the engine load of 1.4 bar brake mean effective pressure (BMEP) and speed of 1800 revolutions per minute (RPM) using diesel fuel. Table 3-4 lists some results of these experiments. Each experiment was averaged over 60 s of sampling (except smoke results which was measured for a single measurement of 6 s). It can be seen that variations are relatively minimal. Particulate number and size distribution results for the same experiments are illustrated in Figure 3-8. Variations in smaller particulates (nucleation mode) were higher than larger particulates (accumulation mode), although variations are minimal.

Table 3-4 Measured parameters with their average value and standard deviation for random error experiments

Parameter	CO	THC	NO_x	CO	THC	NO_x	smoke	Fuel*
Unit	ppmv			g/kWh			FSN	Kg/h
Average	1016.67	763.84	203.53	25.55	9.53	6.39	0.027	1.529
SD (±)	7.77	17.37	1.32	0.38	0.27	0.06	0.002	0.003

* Fuel is equivalent to fuel consumption rate.

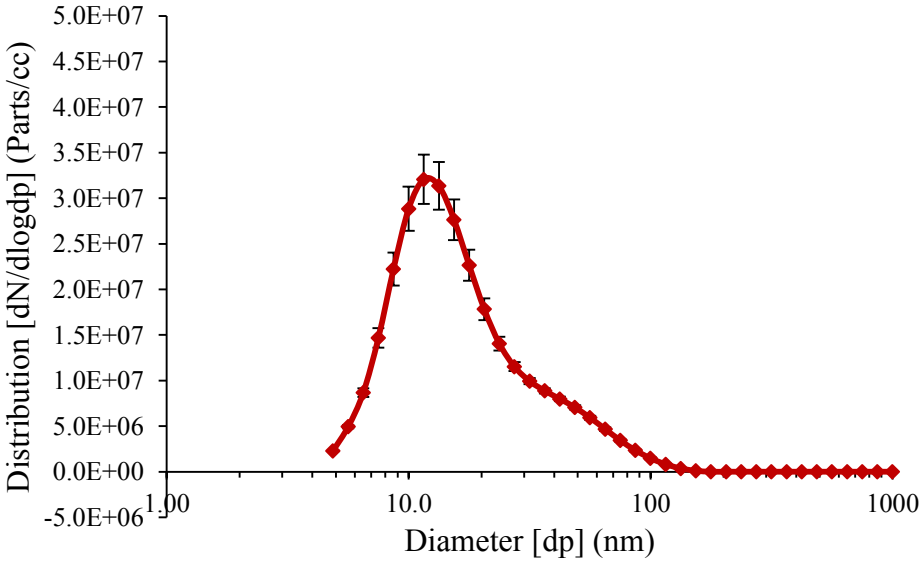


Figure 3-8 Particulate number and size distribution results for random error experiments

3.9. Summary

This chapter described the experimental system setup used in this research work. Two different engine test cells were described briefly followed by the description of the instrumentation, measurement and analysis techniques utilised for different case studies of this thesis.

Chapter 4
PARAMETRIC ANALYSIS OF SPLIT-INJECTION STRATEGIES FOR PREMIXED COMPRESSION IGNITION

4.1. Introduction

As discussed in details in Chapter 2, some properties of Dieseline fuel compared to diesel fuel, such as longer ignition delay, help enhance fuel-air premixing and combustion processes. Some investigations conducted by a former doctoral researcher at the University of Birmingham on "Spray, Combustion and Emission Characteristics of Dieseline Fuel" [48] illustrated that using Dieseline helps reduce NO_x and smoke simultaneously. A group of researchers, including the current author, studied the effects of gasoline blend-ratio in the Dieseline fuel on the combustion and emission characteristics when operating on the partially premixed compression ignition (PPCI) mode [41, 47]. Based on these studies, focusing mostly on the single-injection and including gasoline volumetric blend-ratios from 0% to 70%, 50% of gasoline in diesel (G50-Dieseline) was found to be the optimum blend-ratio considering the test engine, operating points and selected control strategies. Using blend-ratios below 50% faced difficulties in achieving low smoke emissions at medium-high engine operating loads, e.g. 7.85 bar brake mean effective pressure (BMEP), while using blend-ratios above 50% resulted in a very unstable combustion at lower operating loads [41]. However higher gasoline blend-ratios were suggested to be studied to benefit from PPCI combustion at higher operating loads which is the focus of Chapter 5 of this thesis.

Single-injection of Dieseline fuel (with gasoline volumetric blend-ratios less than or equal to 50%) at low-medium loads has been studied comprehensively at the University of Birmingham [41, 46, 48]. Results showed outstanding reductions of NO_x and smoke emissions, by up to 90%, compared to the neat diesel operation. Further to these studies, and in order to avoid duplication, focus of this chapter is on the parametric analysis of the double-injection strategies when using G50-Dieseline and its comparison to the single-injection strategy. This study aims to achieve improved fuel-air premixing and better control over combustion-phasing suitable for PPCI operation. Most of the materials presented in this chapter have been published in [43].

4.2. Background

Fuel injection strategy can effectively govern fuel-air mixing process and consequently control combustion and emission characteristics [76]. When advanced injection-timings are utilised, apart from some associated issues discussed later in this chapter, possibility of achieving more locally lean mixture packets increases and this is due to a more prolonged ignition delay [61]. Two-stage split-injection (double-injection) strategy incorporating advanced injection-timings such as uniform bulky combustion system (UNIBUS) [64], allows the injected fuel to be well-mixed with air prior to the combustion event. A well-planned split-injection strategy in combination with other controlling factors, e.g. fuel properties and EGR ratio, can be used to govern the premixing process and consequently chemical kinetics and combustion-phasing for the CI combustion fuelled with gasoline-like fuels [127]. Therefore, a parametric study of the effects of each injection parameter on controlling combustion performance and emission characteristics of the PPCI combustion is an

interesting research case study. Taguchi fractional factorial design of experiment (DOE) is regarded as a cost-effective and efficient method for conducting parametric analysis [128].

4.3. Experimental plan

Individual effects of injection quantity-ratios and injection-timings in the double-injection strategy for a G50-Dieseline fuelled PPCI engine were investigated via application of the Taguchi DOE. These experiments were carried out on the CR-16.6 engine described in Chapter 3. Experiment groups were conducted at three different loads of 1.37, 2.97 and 5.19 bar BMEP at a fixed engine speed of 1800 revolutions per minute (RPM). However, experiments were limited at the engine load of 5.19 bar BMEP due to unsatisfactory results and the reason will be discussed in section 4.4. The studied load and speed conditions were selected from a testing matrix provided by the original equipment manufacturer (OEM) for evaluating the engine performance and fuel economy in a vehicle new European driving cycle (NEDC) test. More details related to each experimental group will be provided in their relevant sections.

It should be mentioned that investigation of the effects of all controlling parameters on engine performance and emissions is beyond the scope of this work. It is well-appreciated that variations of factors such as compression ratio, EGR rate, valve timing, boost pressure, injection pressure, etc. can control engine outputs considerably. In this study, while fixing all other variation sources, the target was to investigate individual effects of first injection quantity-ratio, first injection-timing and second injection-timing on the combustion and emission characteristics of the PPCI engine at each studied load. Moreover, optimum levels of the studied injection parameters which result in either minimum or maximum value of a typical engine output were identified. In order to investigate the aforementioned research

requirements, Taguchi fractional factorial design analysis [129] coupled with Pareto analysis of variance (ANOVA) [130] was used.

As the first step, first injection quantity-ratio (percentage to the total injected quantity), first injection-timing (crank angle degrees (CAD) after top dead centre (aTDC)) and second injection-timing (CAD aTDC) were selected as the three controllable under-study factors. There was no need to consider second injection quantity-ratio since the effect is already included in the first injection quantity-ratio as it was selected to be based on percentage. In the second step, levels of variation must be carefully assigned to each controllable factor. Three practical levels of variation, based on some screening experiments presented later in section 4.4, were selected for each factor. Study of three factors with three variation levels (which normally requires 3^3=27 experiments) in a fractional factorial Taguchi-DOE method requires only 9 experiments using L9 orthogonal array (OA) which randomises factors and levels in a specific order [129]. Table 4-1 shows L9 OA which includes experiment numbers with the assigned variation level in the parenthesis for each studied factor. For each experiment, three trials were conducted to incorporate the effect of noise on the study [129, 130].

Table 4-1 Taguchi L9 orthogonal array for fractional factorial analysis of 3 factors with 3 variation levels (9 experiments must be conducted)

Exp. No.	1st Quantity (%)	1st Timing (CAD aTDC)	2nd Timing (CAD aTDC)
1	(1)	(1)	(1)
2	(1)	(2)	(2)
3	(1)	(3)	(3)
4	(2)	(1)	(2)
5	(2)	(2)	(3)
6	(2)	(3)	(1)
7	(3)	(1)	(3)
8	(3)	(2)	(1)
9	(3)	(3)	(2)

As mentioned earlier, practical variation levels for each factor need to be selected with caution as these levels can partly influence the quality of the DOE. In this manner experimental plan of this parametric study was selected to be as follows:

1) Some screening experiments were conducted at both 1.37 and 2.97 bar BMEP in order to select practical variation levels for each studied factor.
2) DOE analysis at 1.37 bar BMEP were conducted. The optimum results were compared to the results achieved by using the single-injection strategy.
3) DOE analysis at 2.97 bar BMEP were conducted. The optimum results were compared to the results achieved by using the single-injection strategy.

For all of the experiments, the end of final injection was before the start of combustion (SOC). In other words, premixed combustion with single peak heat release rate, without any significant diffusive or two-stage combustion, was observed in all of the experiments. Boost pressure was maintained at 1.1 bar and EGR rates were fixed at 53%, 45% and 30% for 1.37, 2.97 and 5.19 bar BMEP, respectively. These levels were selected to keep the specific (relative) air-fuel ratio or λ between 1.2 and 1.6. These settings allow combustion temperature of the fuel-air mixtures to be within the temperature range needed for achieving simultaneous low NO_x emissions and high combustion efficiency [64]. Injection pressure (IP) was kept at 520, 580 and 850 bar for 1.37, 2.97 and 5.19 bar BMEP, respectively, which are the same levels in the engine control unit (ECU) maps for each studied load and speed.

4.4. Screening experiments

Screening experiments were conducted to select some practical variation levels for the studied injection parameters in the Taguchi-DOE analysis. Selection of the levels was performed based on the general response trend of the engine to the variation of the controllable factors indicated by changes in the combustion and emission characteristics. As an example, the response of the engine in terms of smoke emissions when varying injection parameters is illustrated in Figure 4-1.

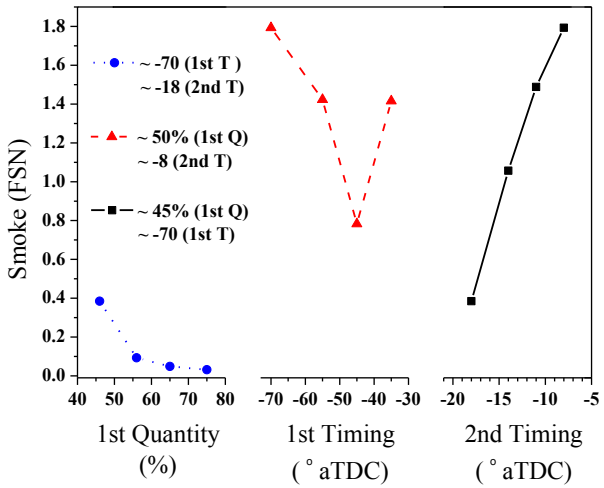


Figure 4-1 Effect of the injection parameters on smoke emissions at 2.97 bar BMEP. (~ indicates approximate value, Q and T are Injection Quantity-ratio and Timing, respectively. ^{o} aTDC is equal to CAD aTDC)

It can be seen that changes in the first injection quantity-ratio and second injection-timing resulted in almost linear variation of smoke emissions. In contrast, changes in the first injection-timing (within the studied range) resulted in a non-monotonic variation trend of smoke emissions. Therefore, by selecting three variation levels such as -30, -60 and -70 CAD aTDC, a local minimum point for smoke emissions will be missed (i.e. smoke at -45 CAD

aTDC) and consequently this will result in a low-quality DOE analysis. This is indicative of the fact that practical references are required for the variation level selection procedure. For both engine loads of 1.37 and 2.97 bar BMEP, similar approach was applied in order to select practical variation levels of factors considering all of the investigated combustion and emissions characteristics. Outcomes and conclusions of the screening experiments in the form of selected factors and their corresponding variation levels are listed in Table 4-2 and Table 4-3 for 1.37 and 2.97 bar BMEP, respectively. For each experiment of the fractional factorial Taguchi-DOE analysis, these levels were randomised based on the L9 OA.

Table 4-2 Taguchi fractional factorial DOE factors and levels for 1.37 bar BMEP

Level	1st Quantity (%)	1st Timing (CAD aTDC)	2nd Timing (CAD aTDC)
(1)	50	-40	-10
(2)	60	-50	-14
(3)	70	-60	-18

Table 4-3 Taguchi fractional factorial DOE factors and levels for 2.97 bar BMEP

Level	1st Quantity (%)	1st Timing (CAD aTDC)	2nd Timing (CAD aTDC)
(1)	50	-40	-10
(2)	60	-55	-14
(3)	70	-70	-18

Aforementioned limitations for conducting experiments at the engine load of 5.19 bar BMEP are explained here. The main reason was the fact that application of double-injection strategy, even at low to moderate first injection quantity-ratios (e.g. 15%) and relatively early first injection-timings (e.g. -50 CAD aTDC), resulted in obtaining a two-stage combustion. This was indicated by the two separate heat release rate peaks while the first peak was too early

before TDC which was not satisfactory for the purpose of these experiments. This is believed to be due to the shorter ignition delay of the G50-Dieseline fuel at this load compared to lower studied loads. Higher temperature of the combustion chamber parts coupled with higher average temperature of the in-cylinder residual gases, as load is increased, can shorten the ignition delay [16]. For this reason, experiments at this load were not further pursued. In order to overcome this issue, it is suggested that some other engine controlling factors such as optimised valve profiles and lower cetane fuels can be used. The idea of lowering the cetane number of Dieseline fuel by increasing its gasoline content as well as testing another low-cetane fuel (naphtha) is the topics of discussion for Chapters 5 and 6. Study of all other controlling parameters was out of scope and resources of this work.

4.5. Design of experiment and analysis at 1.37 bar BMEP

Results of the Taguchi-DOE analysis at 1.37 bar BMEP are listed in Table 4-4. In this table, contribution of each studied injection parameter (in terms of percentage of total contributions) for affecting a specific characteristic is shown. Moreover, settings with which optimum minimum and maximum value of a specific combustion or emission characteristic is obtained are presented.

At this load, brake specific (BS) NO_x variations were mostly influenced by changing injection quantity-ratio and first injection-timing. In the presence of enough oxygen, high-temperature zones of combustion can help generate NO_x emissions [63]. Increasing first injection quantity-ratio and advancing its timing resulted in a condition helpful for achieving more fuel-air premixing. Therefore local combustion temperature and consequently $BSNO_x$ can be reduced. Second injection-timing can influence the combustion-phasing (AHR-50) and therefore can control the temperature at which combustion starts and proceeds and consequently can affect

$BSNO_x$ emissions. Smoke emissions variations were mainly influenced by the injection-timings which confirm the importance of premixing quality (local air-fuel ratio (AFR) in the charge) and AHR-50.

Table 4-4 Fractional factorial Taguchi-DOE results at 1.37 bar BMEP

Parameter	Contribution (Percentage)			Optimum Min. Condition (Level and Value)			Optimum Max. Condition (Level and Value)		
	1st Q*	1st T*	2nd T*	1st Q (%)	1st T (°aTDC)	2nd T (°aTDC)	1st Q (%)	1st T (°aTDC)	2nd T (°aTDC)
$BSNO_x$	46.1%	46.1%	7.8%	(3) 70	(3) -60	(1) -10	(1) 50	(1) -40	(2) -14
Smoke	13.0%	43.4%	43.6%	(3) 70	(1) -40	(3) -18	(2) 60	(2) -50	(1) -10
BSCO	10.0%	85.4%	4.6%	(2) 60	(1) -40	(3) -18	(3) 70	(3) -60	(2) -14
BSTHC	2.2%	97.2%	0.6%	(1) 50	(1) -40	(3) -18	(3) 70	(3) -60	(1) -10
$BSCO_2$	10.6%	86.8%	2.6%	(1) 50	(1) -40	(3) -18	(3) 70	(3) -60	(1) -10
BTE	6.7%	91.4%	1.9%	(3) 70	(3) -60	(1) -10	(1) 50	(1)-40	(3) -18
AHR-50	14.9%	15.2%	69.9%	(3) 70	(1) -40	(3) -18	(2) 60	(2) -50	(1) -10
MPRR	39.1%	34.6%	26.3%	(3) 70	(3) -60	(1) -10	(1) 50	(2) -40	(3) -18

* Q and T are abbreviations for Injection Quantity-ratio and Timing, respectively.

Variations of BSCO and BSTHC were mainly influenced by the first injection-timing changes. Results indicate that more premixing with earlier injection-timings results in higher levels of these emissions. Similarly, variations of brake thermal efficiency (BTE) and $BSCO_2$ were governed by the first injection-timing by 86.8% and 91.4% respectively. These trends are observed due the fact that combustion efficiency changes with the variation of the studied injection factors. It should be noted that these experiments were conducted at a fixed engine brake torque. Therefore, in order to overcome the issue of combustion efficiency variation and consequently load variation, total injected fuel quantity had to be modified. This requirement of adjusting the total injected fuel quantity was fulfilled while keeping the defined injection

quantity-ratios for first and second injection events at each experiment. More fuel consumption in a fixed load condition means less BTE and this is well supported by the results listed in Table 4-4.

In-line with findings of other researchers [64], AHR-50 variations were mainly governed by the second injection-timing with a contribution of 69.9%. At this load, injecting more fuel in the first injection event with more retarded timings, while second injection-timing is advanced results in a more advanced AHR-50. This can be linked to the fact that operation under premixed compression ignition conditions is significantly controlled by chemical kinetics. Therefore in-cylinder temperature and pressure as well as available fuel concentration at the time of injection can play important roles for triggering the combustion and controlling its progression rate [22]. Variations of maximum pressure rise rate (MPRR) were controlled by changes of all the injection parameters, while the first injection-timing had the highest contribution to the variations (39.1%).

4.5.1. Validation Experiments

In order to validate the Taguchi-DOE method, some validation experiments were conducted. Figure 4-2 illustrates the results of Taguchi L9 OA experiments as well as two of the validation experiments focusing on $BSNO_x$ and smoke emissions as the main emissions under study for this case study. In this figure, $BSNO_x$ in terms of g/kWh and smoke in terms of filter smoke number (FSN) are reported versus the experiment number.

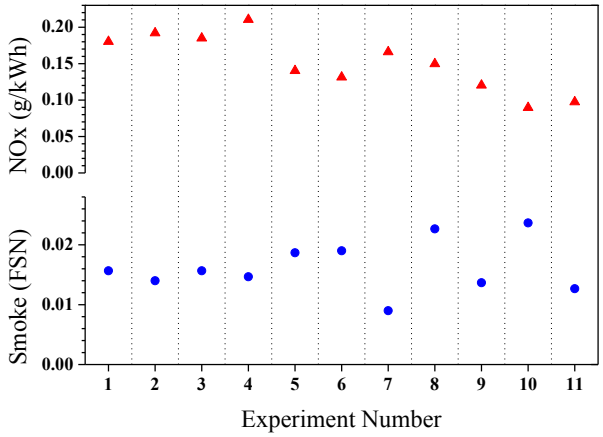


Figure 4-2 Taguchi and validation experiments results of $BSNO_x$ and smoke for 1.37 bar BMEP

The optimum minimum conditions at which Taguchi-DOE predicts that minimum smoke level is achieved was included in the 9 experiments (1 to 9) conducted for the L9 OA; which is experiment number 7. Based on the Taguchi-DOE, the optimum condition for minimum $BSNO_x$ was not selected when the levels of injection parameters were randomised by the application of the L9 OA. Therefore, a validation experiment for obtaining minimum $BSNO_x$ based on the levels suggested by the Taguchi-DOE was conducted (experiment number 10). Based on the results of experiments number 7 and 10, a compromise for simultaneously achieving low $BSNO_x$ and smoke was conducted (experiment number 11). Levels for experiment number 11 was selected through considering common-levels and the intermediate of uncommon-levels of injection parameters for minimum $BSNO_x$ and smoke indicated by the Taguchi-DOE. At the experiment number 10, $BSNO_x$ was found to be 0.09 g/kWh which was the minimum value in all the conducted experiments. The experiment number 7 showed that smoke was also the minimum in all the experiments with a value of 0.009 FSN. Results achieved at the experiment number 11 were close to the optimum minimum values of $BSNO_x$ and smoke emissions. Thus, efficiency of the Taguchi-DOE analysis for this load was confirmed through the mentioned validation experiments.

4.5.2. Comparison of single and double injection strategies at 1.37 bar BMEP

Results of the experiment number 11, as a condition at which minimum $BSNO_x$ and smoke are achieved simultaneously using the developed double-injection strategy, were compared to the corresponding single-injection strategy with the same combustion-phasing fixed at 3 CAD aTDC. Fixing the AHR-50 at the same CAD helps to omit its considerable effect on influencing combustion and emission characteristics [131]. Results of double-injection and the corresponding single-injection strategies are listed in Table 4-5.

Table 4-5 The optimum two-stage and single-stage injection strategies results at 1.37 bar BMEP, AHR-50: 3 CAD aTDC

Injection Mode	Injection Q and T (%) and (^{o}aTDC)	BTE (%)	MPRR (bar/^{o})	$BSNO_x$ (g/kWh)	Smoke (FSN)	BSCO (g/kWh)	BSTHC (g/kWh)
Single (Main)	(100%, -14)	19.36	3.77	0.221	0.072	43.17	10.04
Two-stage	(70%, -50) , (30%, -14)	17.70	2.58	0.097	0.012	45.11	23.91

Via using the developed double-injection strategy, $BSNO_x$ and smoke levels were reduced by around 56% and 83%, respectively, compared to the single-injection strategy. Combustion generated noise is believed to be lower when using the developed double-injection strategy since the MPRR was reduced by around 31%. There was a penalty of lower BTE (around 1.6% less, in absolute value) and it is believed to be due to higher BSCO (by around 4.5%) and THC (around 2.4 times more). However, it cannot be concluded that the double-injection strategy has considerably lower BTE at every possible condition compared to the single-injection strategy. For example, results of the optimum maximum condition for BTE, predicted by the Taguchi-DOE, showed a value of 19.17%.

Based on these results, using the developed double-injection strategy helped to improve premixing quality and consequently reduce $BSNO_x$ and smoke emissions. Utilising relatively long ignition delay (low reactivity) of G50-Dieseline at this load combined with advanced injection-timings, for the first portion of the injected fuel, resulted in achieving more locally lean mixture packets. Higher THC emissions, seemingly due to lowered combustion efficiency, can be linked with overmixing and/or under-mixing [16, 22]. Fuel spray jets impinging on the cylinder walls and piston in early injections can affect the mixing process and emissions [22, 132-134]. Based on the Taguchi-DOE analysis, first injection-timing is the dominant factor for affecting THC emissions. Thus, it can be hypothesised that one possible reason for the increasing trend of THC, as earlier injection-timings are used, is fuel wall-impingement. As the injection-timing is advanced, due to lower in-cylinder pressure and temperature, fuel spray can travel further into the cylinder and form a liquid film on the walls – a potential source of unburnt HC [22, 37, 135, 136]. Kashdan *et al.* [37] conducted some optical studies to identify the origins of unburnt HC emissions in a homogeneous compression ignition engine. They proposed that this formed liquid film might detach from the hot walls when there is a sudden decrease in the in-cylinder pressure during the expansion stroke by the flash boiling mechanism. Using optimised IP and included-angle of the injectors can help reduce THC emissions sourced from fuel wall-impingement. Results when using lower IPs with even higher gasoline content in the Dieseline fuel are discussed in Chapter 5.

4.6. Design of experiment and analysis at 2.97 bar BMEP

Results of the Taguchi-DOE analysis at 2.97 bar BMEP are listed in Table 4-6. Due to higher accumulation mode particulate concentration at this load, accumulation mode particulate size and distribution were also investigated. Results of accumulation mode concentration (Acc. C)

and accumulation mode count median diameter (Acc. CMD) are presented in the table. It should be noted that a thermo-denuder was used to remove volatile species and moisture from the aerosol before being introduced to the second stage diluter of the DMS500. In this way, it was aimed to achieve a more repeatable measurement of accumulation mode particulates without considering nucleation mode particles [137]. Volatile hydrocarbons are known to contribute to increasing particulate size and mass during temperature drop and dilution [90]. It should be mentioned that engine speed was the same as for the lower studied load while it was required to inject more fuel and therefore the contribution of each injection parameter was different.

Table 4-6 Taguchi fractional factorial DOE results at 2.97 bar BMEP

Parameter	Contribution (Percentage)			Optimum Min. Condition (Level and Value)			Optimum Max. Condition (Level and Value)		
	1st Q*	1st T*	2nd T*	1st Q (%)	1st T (°aTDC)	2nd T (°aTDC)	1st Q (%)	1st T (°aTDC)	2nd T (°aTDC)
$BSNO_x$	33.8%	43.6%	22.6%	(3) 70	(3) -70	(1) -10	(1) 50	(1) -40	(3) -18
Smoke	37.3%	4.0%	58.7%	(3) 70	(2) -55	(3) -18	(1) 50	(1) -40	(1) -10
BSCO	9.9%	87.5%	2.6%	(1) 50	(1) -40	(2) -14	(3) 70	(3) -70	(1) -10
BSTHC	10.8%	89.2%	0.0%	(1) 50	(1) -40	(1) -10	(3) 70	(3) -70	(3) -18
$BSCO_2$	57.7%	40.7%	1.6%	(1) 50	(1) -40	(3) -18	(3) 70	(3) -70	(1) -10
Acc. CMD†	64.5%	35.2%	0.3%	(3) 70	(2) -55	(2) -14	(1) 50	(1) -40	(1) -10
Acc. C‡	32.9%	6.1%	61.0%	(3) 70	(3) -70	(3) -18	(1) 50	(1) -40	(1) -10
BTE	31.7%	66.2%	2.1%	(3) 70	(3) -70	(1) -10	(1) 50	(1) -40	(3) -18
AHR-50	9.9%	11.3%	78.8%	(2) 60	(1) -40	(3) -18	(3) 70	(3) -70	(1) -10
MPRR	4.4%	35.3%	60.3%	(2) 60	(3) -70	(1) -10	(3) 70	(1) -40	(3) -18

* Q and T are abbreviations for Injection Quantity-ratio and Timing, respectively.
† Acc. CMD is accumulation particulate count median diameter.
‡ Acc. C is accumulation particulate total concentration.

$BSNO_x$ variations were mainly dominated by the changes of first injection-timing (43.6%) while injection quantity-ratio had a considerable contribution (33.8%). Compared to the lower

studied load, second injection-timing had a higher contribution (22.6%). This can be described by the fact that as load increases larger quantity of the fuel must be injected while the time for premixing is approximately similar to the lower load. Moreover, global in-cylinder temperature is higher and changes in the combustion-phasing, through changing the second injection-timing, can result in a more observable $BSNO_x$ variation as the temperature during pre-combustion and combustion events is higher. Second injection-timing had the highest effect on the variations of the smoke emissions followed by the quantity-ratio.

Similar to the previous load, variations of BSCO and BSTHC were governed by the first injection-timing. $BSCO_2$ variations were mostly influenced by changes of first injection quantity-ratio (57.7%) and the first injection-timing (40.7%). Acc. CMD variations were mostly depended on the first injection quantity-ratio. Accumulation mode particulates with smaller diameters were produced if higher percentage of the total injected fuel is introduced in the first injection event. Similar to the case for smoke emissions, variations of the Acc. C were mainly due to change of the second injection-timing (by 61%) while retarding the second injection-timing reduced the accumulation mode particulate concentration. This is a good indication that smoke and accumulation mode particulate concentration are directly correlated. Based on the fact that carbonaceous particulate formation is temperature dependant [20], lower in-cylinder temperature as the combustion-phasing is retarded can reduce the chance of soot formation.

BTE was mainly affected by the changes of first injection-timing with a contribution of 66.2%. Less premixing resulted in higher BTE as there are less BSCO and BSTHC emissions. Similar to the previous load, AHR-50 variations were mainly governed by the second injection-timing. Second injection-timing with a contribution of the 60.3% was the dominant parameter for MPRR variations. MPRR can be correlated to the rates at which combustion

proceeds and in-cylinder pressure increase which are functions of AHR-50. As expected, retarded second injection-timing resulted in lower MPRR at this load.

4.6.1. Comparison of single and double injection strategies at 2.97 bar BMEP

Similar to the lower studied load, apart from conducting validation experiments, results of an optimum double-injection strategy for simultaneous minimum $BSNO_x$ and smoke emissions were compared to the results of a corresponding single-injection strategy. Levels of the factors for the double-injection strategy were selected based on the common levels and intermediate of uncommon levels of the parameters for minimum $BSNO_x$ and smoke emissions from the Taguchi-DOE. $BSNO_x$ emissions at this load were mainly influenced by the first injection-timing while smoke emissions were not greatly influenced by this parameter. Therefore, the priority was given to the level of first injection-timing more suitable for minimum $BSNO_x$ achievement. Table 4-7 reports results of both of the strategies.

The developed double-injection strategy reduced $BSNO_x$ emissions by around 39% compared to the single-injection strategy with the same combustion-phasing fixed at 2 CAD aTDC. Smoke emissions were reduced by around 96% when using the double-injection strategy compared to the single-injection strategy. Figure 4-3 illustrates accumulation mode particulate number and size distribution for the single and double-injection strategies shown in Table 4-7. Apart from an obvious reduction in the accumulation mode particulate concentration, the developed double-injection strategy reduced the Acc. CMD by 25.9 nm. Smaller particulates, compared to larger particulates, are more dangerous due to their more reactivity (as a result of higher surface to volume ratio), expected prolonged suspension time and reduction issues (as they are more difficult to be trapped) [85]. However, the observed Acc. CMD reduction was

due to total particulate concentration reduction rather than increased number of smaller particulates.

Table 4-7 The optimum two-stage and single-stage injection strategies results at 2.97 bar BMEP, AHR-50: 2 CAD aTDC

Injection Mode	Injection Q and T (%) and (^{o}aTDC)	BTE (%)	MPRR (bar/^{o})	$BSNO_x$ (g/kWh)	Smoke (FSN)	BSCO (g/kWh)	BSTHC (g/kWh)
Single (Main)	(100%, -15)	29.32	6.61	0.164	2.10	22.61	1.74
Two-stage	(70%, -70) , (30%, -14)	26.47	6.32	0.100	0.07	21.45	13.91

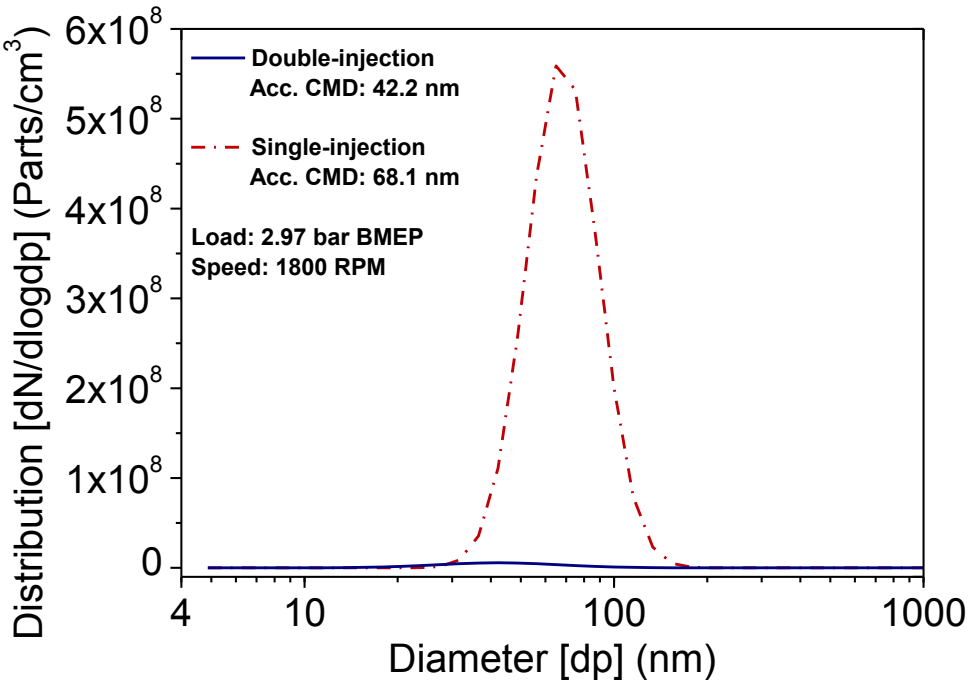


Figure 4-3 Accumulation mode particulate number and size distribution of single and double injection strategies at 2.97 bar BMEP

These reductions were accompanied by a considerable penalty of reduced BTE (by around 2.85 less, in absolute value). While BSCO was reduced by around 5%, BSTHC was raised by around 8 times for the double-injection strategy. It can be hypothesised that increased BSTHC

emissions when using the double-injection strategy are mainly unburnt fuel which did not have a chance to be converted into other species in the cylinder; therefore possibility of CO formation is reduced. MPRR was lowered slightly by around 4.5%. Similar to what was discussed for the previous load, lower BTE at this optimum condition does not mean that split-injection strategy generally results in very low BTE levels; the condition discussed in Table 4-7 is not designed for maximum achievable BTE as well as low NO_x and smoke.

Advancing the first injection-timing, further than what was tested for the Taguchi-DOE at the load of 2.97 bar BMEP, was examined for three first injection quantity-ratios of 50%, 60% and 70%. For these experiments combustion-phasing was fixed. Results, discussed in detail in [43], indicated that all the gaseous emissions can increase if the first injection-timing is advanced further. As combustion efficiency decreases due to excessive premixing and/or fuel wall-impingement, more fuel must be injected to compensate for the drop in engine brake output torque. Therefore, the effect of higher injected fuel quantity can be more than the premixing for influencing combustion and emission characteristics. In addition, increased levels of coefficient of variation (COV) of indicated mean effective pressure (IMEP) were observed. Higher COV of IMEP is a sign of cycle-by-cycle variation when the engine experiences misfire and/or not complete combustion conditions for some operating cycles and suddenly a high temperature firing cycle which will burn accumulated fuel in the cylinder in a not-optimised way. However, accumulation mode particulate emissions always stayed at lower levels compared to the single-injection strategy as shown in Figure 4-4 and Figure 4-5. In these figures, C is the abbreviation for concentration and reductions in both Acc. CMD and concentrations are obvious when using the double-injection strategy.

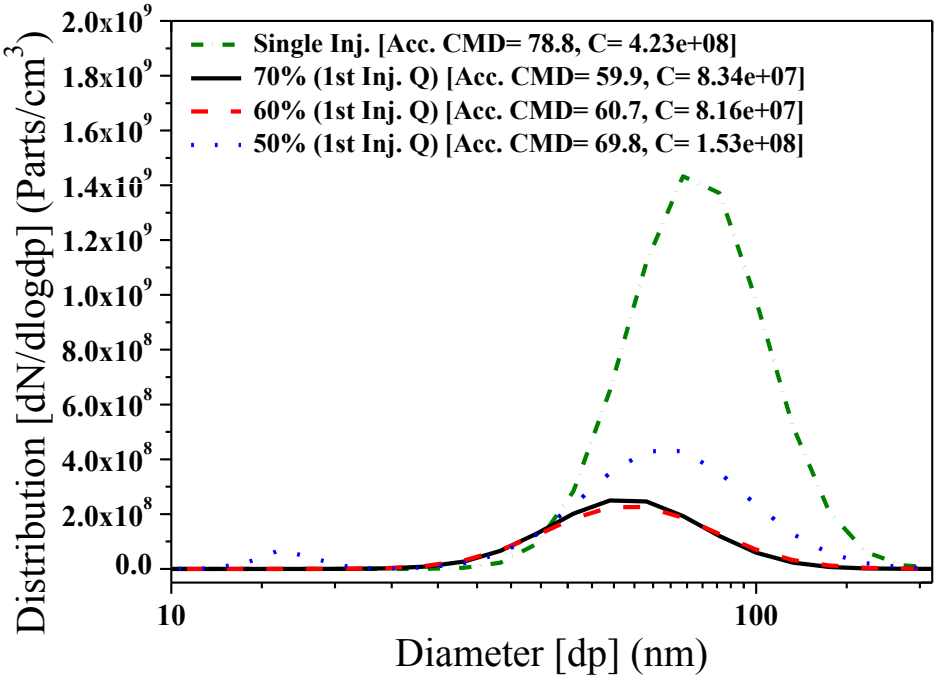


Figure 4-4 Particulate number and size distribution for three first injection quantity-ratios with fixed injection-timing (at -68 CAD aTDC) and combustion phase (at 3 CAD aTDC) at 2.97 bar BMEP [43]

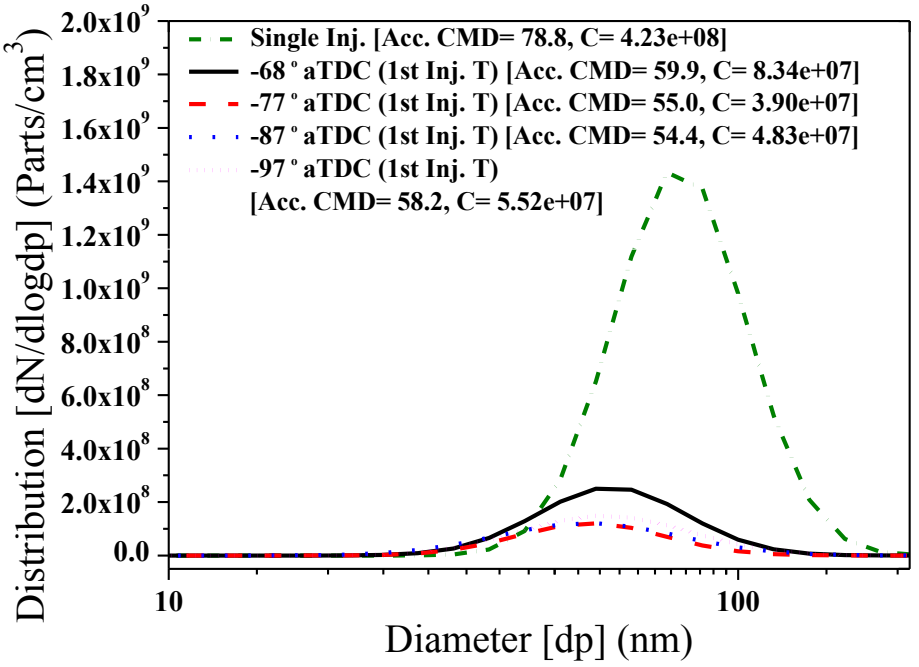


Figure 4-5 Particulate number and size distribution for four first injection-timings with fixed first injection quantity-ratio (at 70%) and combustion phase (at 3 CAD aTDC) at 2.97 bar BMEP [43]

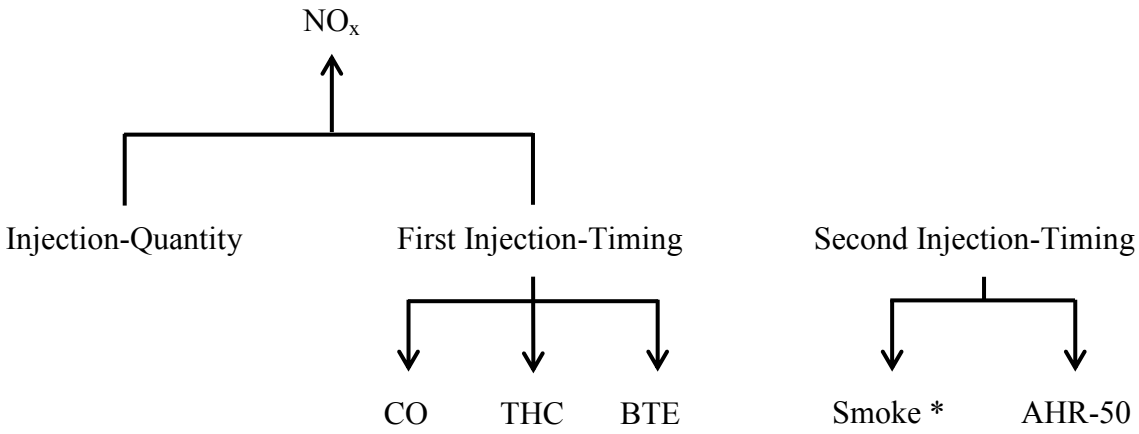
Finally, it was demonstrated that the developed double-injection strategy has the potential of helping to achieve low-NO_x and low-smoke PPCI combustion through improving the premixing quality. Various enhancements, such as optimised combustion chamber geometry and injection system, can be further studied to benefit from low HC emissions which is conventionally high from PPCI combustion strategies [22]. Lower CN fuels, e.g. high gasoline content Dieseline, while using high EGR and boost pressure can be used to benefit from this strategy at higher engine operating loads which are investigated in Chapters 5 and 6 of this thesis.

4.7. Summary/Conclusions

The effects of varying key parameters of the double-injection strategy, including injection quantity-ratios and timings, on the combustion performance and emission characteristics of a G50-Dieseline fuelled PPCI engine were investigated. A parametric analysis, by using the Taguchi-DOE, was conducted to identify individual effects of each under-study injection parameter. Moreover, optimum levels of injection parameters at which minimum and maximum combustion or emission characteristics are achieved, were identified. The main focus was to achieve enhanced fuel-air premixing process and consequently achieve simultaneous reductions in $BSNO_x$ and smoke emission at two different load groups of 1.37 and 2.97 bar BMEP. The main findings of this investigation are as follows:

- At both of the studied loads, variations of NO_x emissions were dominated by the first injection event (timing and quantity-ratio, while absolute contributions of each were load dependant). Variations of the brake thermal efficiency (BTE), CO and total hydrocarbons (THC) were mainly influenced by the first injection-timing. Variations of the

combustion-phasing (AHR-50) were governed by the second injection-timing. A graphical illustration of the major effects of the studied injection parameters is shown below:



* Smoke variations are influenced mostly by the second injection-timing but also first injection quantity and timing depending on the operating load.

- At 1.37 bar BMEP, changes in the smoke emissions were affected by varying both of the injection-timings. At 2.97 bar BMEP, after the high contribution of the second injection-timing, the most influential parameter was first injection quantity-ratio.
- With the developed double-injection strategy, $BSNO_x$ and smoke emissions were reduced by around 50% and 90% compared to the single-injection strategy. At these conditions, there can be a penalty of reduced BTE mainly due to increased THC emissions. However, double-injection strategy cannot be linked with low BTE at all of the possible injection settings.
- Premixing and injected fuel-quantity are two competing factors for the PPCI engine operation. At very early first injection-timings, due to possible fuel wall-impingement and overmixing with air which results in lower combustion efficiency and load drop,

premixing process can reach a limit where the effect of required higher injected fuel quantity is dominant in determining combustion and emission characteristics.

- The utilised Taguchi-DOE method for performing a parametric analysis was proved to be cost-effective and efficient in these studies.

Double-injection strategies developed in this chapter for G50-Dieseline fuel was proved to help improve the fuel-air premixing process when compared to the single-injection strategy in a PPCI engine. Simultaneous reduction of smoke and NO_x was accompanied with higher THC emissions. Refinement of the fuel injection system and combustion chamber geometry to be suitable for PPCI combustion using low-cetane fuels is expected to reduce THC emissions. Moreover, improved intake/exhaust handling strategies can be helpful for reducing THC and CO emissions. Less reactive fuels, compared to G50-Dieseline, coupled with higher intake pressure and EGR can be utilised to achieve double-injection strategy at higher engine operating loads. Single-injection strategy might be beneficial for less reactive fuels as the ignition dwell is longer compared to G50-Dieseline. Some of these ideas are investigated in Chapters 5 and 6 of this thesis.

Chapter 5
DIESELINE FUELLED PREMIXED COMPRESSION IGNITION COMBUSTION ENGINE

5.1. Introduction

Conclusions drawn from the results presented in Chapter 4 suggest that there is a scope for using higher gasoline content in the Dieseline fuel to lower its reactivity and use it for higher operating loads. Moreover, as discussed in Chapter 2, the general trend of research topics in the premixed compression ignition (PCI) combustion area is going towards utilising low quality gasoline-like fuels which have lower octane number compared to the market gasoline. Therefore, this chapter investigates the feasibility and benefits of using 75% gasoline volumetric content in the Dieseline fuel (G75-Dieseline) for the PCI combustion mode in various operating loads. Detailed properties of this blended fuel are reported in Chapter 3. Based on Kalghatgi [2], using this fuel with an estimated RON of around 75 for achieving a low-NO_x and low-smoke combustion can be classified under gasoline compression ignition (GCI) combustion. However, arbitrary in this chapter the term "PCI" is used to describe Dieseline premixed combustion.

In this chapter, first some techniques developed to achieve G75-Dieseline (G75) PCI combustion in a multi-cylinder stock CI engine at lower engine operating loads are presented and discussed. Then, effects of utilising different fuel injection, exhaust gas recirculation (EGR) and intake boosting strategies on combustion performance and emission characteristics at 1.4, 3, 6, 12 and 17.3 bar BMEP and 1800 RPM are discussed. Results are compared to the

combustion performance and emission characteristics results of diesel CI combustion at each operating mode. Table 5-1, Table 5-2, Table 5-3 and Table 5-4 list the summary of test conditions used for the main experiment groups discussed in this chapter. More details about each experiment group and additional experiments conducted are presented in the appropriate section. For all of these studies, the CR-15.5 engine described in Chapter 3 was utilised.

Table 5-1 Test conditions of the EGR cooling strategy experiments to investigate effects of the EGR temperature on the combustion performance and emission characteristics while using single-injection

Fuel	**Engine Load**	**Engine Speed**	**Injection Pressure**	**Injection Timing ***	**EGR Strategy (cold (C) and hot (H))**
-	bar BMEP	RPM	bar	CAD aTDC	%
Diesel	1.4	1800	350 to 900	-8.5 to -5.5	52 (C) & (H)
	3	1800	350 to 1400	-9.5 to -5.5	45 (C) & (H)

* Injection timing was varied to maintain AHR-50 at the same CAD at each engine load.

Table 5-2 Test conditions of the EGR rate variation experiments to investigate effects of the EGR rate on the combustion performance and emission characteristics while using single-injection

Fuel	**Engine Load**	**Engine Speed**	**Injection Pressure**	**Injection Timing**	**EGR Strategy (cold (C) and hot (H))**
-	bar BMEP	RPM	bar	CAD aTDC	%
G75	1.4	1800	250	-30	~ 45 to 60 (H)
	3	1800	250	~ -42	~ 40 to 49 (H)
Diesel	1.4	1800	500	~ -9 to -7 *	~ 40 to 60 (C)
	3	1800	700	~ -9 to -7 *	~ 40 to 50 (C)

* Injection timing was varied to maintain AHR-50 at the same CAD at each engine load.

Table 5-3 Test conditions of the single-injection strategy experiments

Fuel	Engine Load	Engine Speed	Injection Pressure	Injection Timing	EGR Strategy (cold (C) and hot (H))
-	bar BMEP	RPM	bar	CAD aTDC	%
G75	1.4	1800	150 to 350	-40 to -20	52 (H)
	3	1800	150 to 350	-52.5 to -32.5	45 (H)
	6	1800	500 to 700	-27 to -18	30 to 34 (C)
	12	1800	1000 &1200	-7 to -3	15 & 18 (C)
	17.3	1800	1100	-3 to -1	~ 5 (C)
Diesel	1.4	1800	150 to 900	-13 to -6	52 (C)
	3	1800	150 to 1400	-16.5 to -5.8	45 (C)
	6	1800	800 to 1200	-12 to 0	30 to 34 (C)
	12	1800	1000 & 1200	-3	15% (C)
	17.3	1800	1200	0	~ 5 (C)

Table 5-4 Test conditions of the double-injection strategy experiments

Fuel	Engine Load	Engine Speed	Injection Pressure	First Injection Quantity *	First Injection Timing	Second Injection Timing	EGR Strategy (cold (C) and hot (H))
-	bar BMEP	RPM	bar	%	CAD aTDC		%
G75	1.4	1800	150	10 to 50	-100 to -60	-40	52 (H)
	3	1800	350	10 to 50	-100 to -60	-32.5	~ 45 (H)
	6	1800	500	10 to 50	-100 to -60	-26	32 (C)
	12	1800	900 to 1100	10 & 30	-140 to -20	-5	15 (C)
Diesel	1.4	1800	500	10 to 50	-100 to -20	-10	52 (C)
	3	1800	700	10 to 50	-100 to -20	-8	~ 45 (C)
	6	1800	1200	10 to 50	-100 to -20	-3	32 (C)
	12	1800	1200	10 & 30	-100 to -20	-3	15 (C)

* First injection quantity in % refers to the ratio of the first injected fuel portion to total injected fuel.

5.2. Investigation of different EGR strategies for lower engine operating loads

Several researchers, e.g. in [2, 41, 138], have reported that it is difficult to avoid misfire and uncontrollable combustion at lower operating loads when using low cetane number (CN) fuels

for the CI combustion modes. This is due to the fact that long-ignition delay of the fuel coupled with low temperature and pressure of the in-cylinder charge reduces the reaction rates leading to a stable combustion [138]. It might be worthy to mention that, indeed, this has been one of the challenges with the homogenous charge compression ignition (HCCI) combustion [2, 22]. Higher levels of EGR required to supress NO_x formation in the PCI modes normally reduce the combustion temperature and oxygen availability and thus can "add insult to the injury". Therefore, this section discusses the effects of EGR variation on the combustion and emission characteristics of G75-Dieseline PCI and diesel CI at low loads. The objective is to answer this question: "can a modified EGR strategy be used to improve combustion process of the PCI/GCI mode?"

5.2.1. Effects of different EGR cooling strategies

Apart from increasing the compression-ratio, one efficient method to overcome the aforementioned challenges and to enhance low CN fuelled PCI combustion at low loads, utilised by the majority of researchers, is by heating the intake air before it enters the combustion chamber [138]. As PCI combustion modes are kinetically controlled [22], elevated in-cylinder temperature increases the rate of the required reactions leading to ignition and combustion of the combustible fuel-air packets which increases total combustion efficiency. However, intake heating decreases the mass of air going to the cylinders due to reduced density and therefore needs to be compensated by more boosting, if required.

Currently, intake air heating seems practical when testing engines in the labs; however, it is accompanied with several issues for an on-road vehicle. These issues can be energy consumption, response time, space limitation, weight, complexity, cost, etc. which are not favoured by the original equipment manufacturers and consumers. Moreover, if the heater is

not to be used all the time, for all loads and speed or at least the majority of them, there is no incentive to have it on a vehicle. Deactivating the intake air intercooler, normally placed after the turbocharger of a diesel engine, to increase intake air temperature may be an option. However, normally at low loads gas temperature after the turbocharger compressor is not high enough to elevate the intake temperature substantially. Considering all of the aforementioned issues and focusing on the PCI combustion mode at lower engine operating loads, varying EGR temperature by dynamically controlling the cooling intensity of its cooler seems an interesting option.

Normally EGR system is equipped with a cooler [95] in order to reduce intake temperature and also reduce thermal throttling effect caused by hot-EGR [34]. However, utilising hot-EGR coupled with deactivated air intercooler can help omit the necessity of assembling an external air heating system on the engine for low load low-CN fuelled PCI. Side-benefits of hot-EGR can be reduced chances of cooler fouling [95] and condensation of the volatile species in the intake system. It should be mentioned that the engine test bed used in this study does not have any air heater and the only modification was to place a valve, shown in Figure 3-2 in Chapter 3, to stop/restrict coolant flow through the EGR cooler.

Initial experiments with the G75-Dieseline (G75) fuel either without EGR or with cold-EGR showed very high combustion instability accompanied with high hydrocarbons (HC) and carbon monoxide (CO) emissions. For this reason, hot-EGR technique was utilised and results showed very considerable improvements which are discussed in details in sub-sections 5.2.2 and 5.3.1. In order to investigate the effects of utilising either hot or cold EGR on combustion and emissions results, neat diesel fuel was chosen as it was not possible to achieve combustion with G75 when using cold-EGR. These experiments were conducted at two engine operating loads of 1.4 and 3 bar BMEP while engine rotational speed, AHR-50 and intake boost pressure were fixed. At the engine load of 1.4 bar BMEP, EGR was fixed at 52%

while injection pressure (IP) was varied at 350, 500 and 900 bar. At the engine load of 3 bar BMEP, EGR was fixed at 45% while IP was varied at 350, 700 and 1400 bar. The reasons for selecting these values are explained in the following sections. In the figures of this section, letters "A", "NA" and "PA" are abbreviations for activated, not activated and partially activated, respectively, indicating the status of the EGR cooler. When EGR cooler is NA or PA, air intercooler is completely deactivated.

Figure 5-1 illustrates the air intake manifold temperature measured at 100 mm after the EGR tube entrance into the intake manifold while air temperature before the engine intake filter box was fixed at 22 ± 0.5 ^{o}C. At 3 bar BMEP, full deactivation of the EGR cooler resulted in very high manifold temperatures, more than 150 ^{o}C, and therefore it had to be PA due to concerns regarding melting and deflection of plastic parts of the stock manifold. It can be seen that intake temperature values are considerably higher, between 42 ^{o}C and 43.5 ^{o}C at 1.4 bar BMEP and 27.5 ^{o}C and 31.5 ^{o}C at 3 bar BMEP, when using hot-EGR instead of cold-EGR.

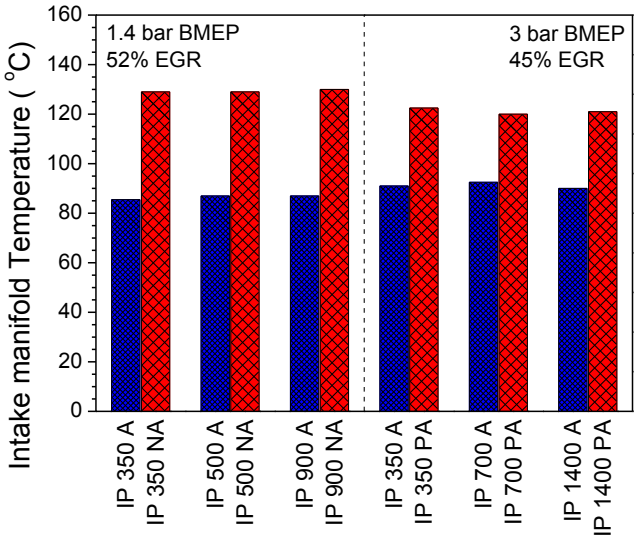


Figure 5-1 Effect of different EGR cooling strategies at different injection pressures (IPs) on the intake manifold temperature at 1.4 and 3 bar BMEP and 1800 RPM

Effects of using hot and cold EGR on brake specific total hydrocarbons (BSTHC) and BSCO emissions can be seen in Figure 5-2. Using hot-EGR instead of cold-EGR for neat diesel fuel combustion at 1.4 bar BMEP reduced both BSTHC and BSCO by 32.7% at the IP of 500 bar which is a representative IP for this load for this family of engines [48]. With PA EGR cooler at 3 bar BMEP and IP of 700 bar, BSTHC and BSCO emissions were reduced by 29.6% and 37.2%, respectively. It might be worthy to mention that generally changes in the brake thermal efficiency (BTE) were minor (below 0.5%) when comparing results of using hot and cold EGR.

CO and HC emissions can originate from incomplete combustion of the fuel where the fuel-air mixture is either over-lean or over-rich and when temperature is not enough to initiate and complete their combustion [16]. Elevated intake temperature is an important factor for reducing these emissions especially at low loads when using high EGR rates for PCI combustion. In the case of low CN fuels, such as G75, the importance of this factor becomes more obvious as they are less reactive towards auto-ignition and also gasoline-like fuels have higher heat of evaporation (higher cooling effect) compared to diesel [52]. At both loads with either of hot and cold EGR, BSTHC and BSCO emissions were increased as higher IP was used. Increase of IP can reduce the fuel droplet size and consequently contribute to fuel-air over-mixing. Moreover, longer liquid length and spray penetration length when using higher IP can increase possibility of liquid-fuel wall-impingement under PCI conditions [22]; another source of CO and unburnt HC emissions.

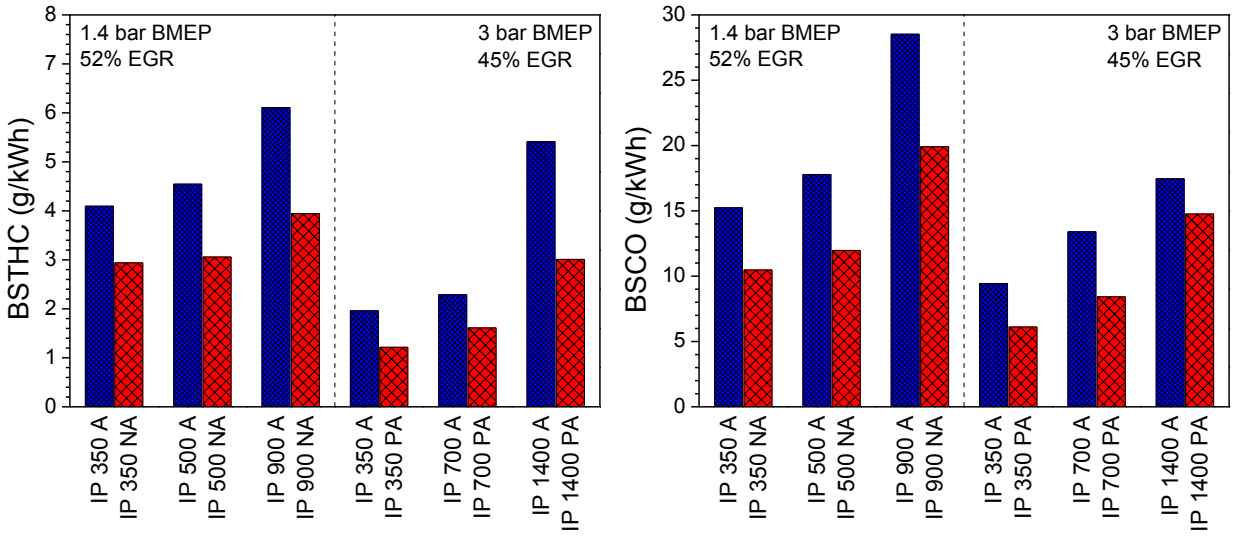


Figure 5-2 Effect of different EGR cooling strategies at different injection pressures (IPs) on BSTHC and BSCO at 1.4 and 3 bar BMEP and 1800 RPM

Although there are reductions in BSTHC and BSCO emissions, smoke was increased when hot-EGR was used as shown in Figure 5-3. At 1.4 bar BMEP and IP of 500 bar, smoke was increased by around 3.9 times when using hot-EGR compared to cold-EGR. These increases might be due to heightened overall in-cylinder temperature which may assist soot formation [20] and/or by reduced intake O_2 concentration (confirmed by λ values reduction) due to EGR thermal throttling effect [34] which can help soot formation and reduce in-cylinder oxidation rate [24]. Increasing IP helps reducing smoke emissions to compensate for the effect of hot-EGR; however, increased IP is accompanied with reduced BTE and increased cyclic variations.

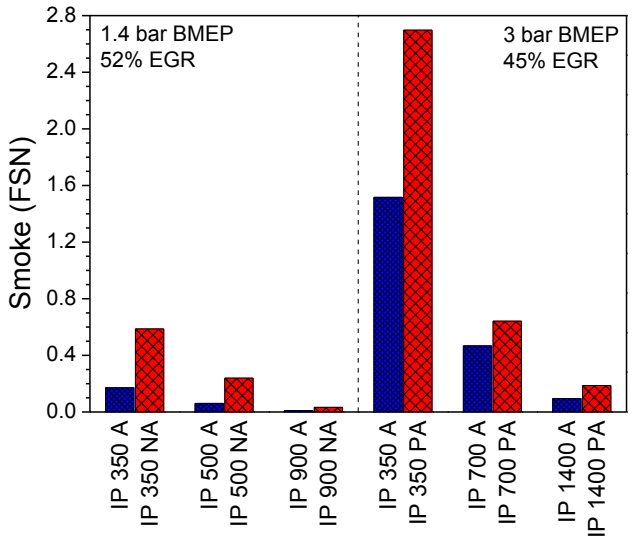


Figure 5-3 Effect of different EGR cooling strategies at different injection pressures (IPs) on smoke at 1.4 and 3 bar BMEP and 1800 RPM

Figure 5-4 shows that $BSNO_x$ emissions are almost in the same range with hot and cold EGR. Normally higher in-cylinder temperature at the end of compression stroke and during combustion caused by increased intake temperature results in higher NO_x emissions [34]. However, thermal throttling when using hot-EGR reduces intake O_2 concentration [34], which is known to substantially reduce NO_x emissions [20, 34], even more than lower intake temperature [34]. Therefore, it can be hypothesised that there is a balance between these two mechanisms: higher intake temperature and reduced intake oxygen. Considering results of NO_x and smoke in parallel, it seems that the thermal throttling had the dominant effects.

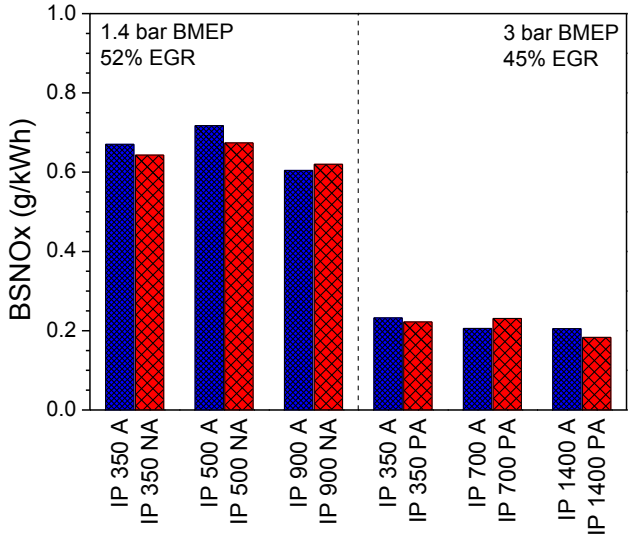


Figure 5-4 Effect of different EGR cooling strategies at different injection pressures (IPs) on $BSNO_x$ at 1.4 and 3 bar BMEP and 1800 RPM

As expected by thermodynamic analysis, exhaust temperature was elevated by increasing the intake temperature using hot-EGR as shown in Figure 5-5. These temperatures are measured after the turbine side of the turbocharger. This is the location that normally after-treatment systems of diesel engines are placed. This temperature increase can help improve conversion efficiency of the after-treatment systems if enough oxidiser is present in the exhaust, for instance diesel oxidation catalyst (DOC), which is discussed in details in Chapter 7.

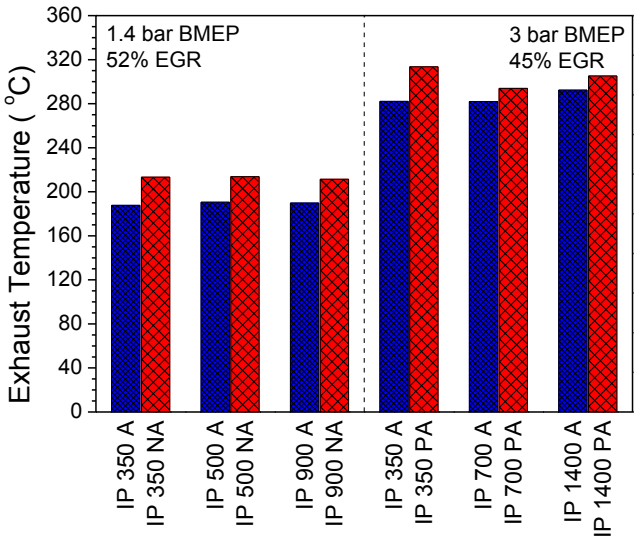


Figure 5-5 Effect of different EGR cooling strategies at different injection pressures (IPs) on the exhaust gas temperature at 1.4 and 3 bar BMEP and 1800 RPM

5.2.2. Effects of EGR rate variation

From the results presented in the previous sub-section, it was concluded that using hot-EGR strategy for the neat diesel fuel combustion can increase already undesirably high smoke emissions further. Screening experiments showed that achieving acceptable combustion efficiency, while the engine is operating on G75 fuel at 1.4 and 3 bar BMEP, without hot-EGR is not possible. Therefore, for these two relatively low engine operating loads, hot-EGR strategy was selected for G75 fuel and cold-EGR strategy (normally used in diesel engines) was utilised for diesel fuel. Combustion performance and emission characteristics of G75 PCI and neat diesel combustion at various EGR rates were compared. These experiments were conducted to identify a reasonable EGR rate in order to meet a $BSNO_x$ emission target. This target for $BSNO_x$ was arbitrary defined to be values less than 0.4 g/kWh; indeed this is the target for Euro VI $BSNO_x$ limit for heavy-duty diesel engines at steady-state testing condition [139]. Moreover, these tests can help identify the effects of using lower and higher hot-EGR

rates on the performance of G75 fuel in PCI mode; to understand which factor is more influential: higher intake temperature or more dilution when increasing hot-EGR rate.

These experiments were conducted at 1.4 and 3 bar BMEP and a fixed engine rotational speed of 1800 RPM. IP was fixed at 250 bar for G75 at both loads and at 500 and 700 bar for 1.4 and 3 bar BMEP, respectively, for diesel. Selection of lower IP for G75 was based on some preliminary experiments indicating that using higher IPs, e.g. 450 bar, result in excessive cyclic variation for which experimental data are presented later in this chapter. Using G75 resulted in much longer ignition delays and this is discussed in details in the next section. Injection-timing (IT) for G75 was around -30 and -42 CAD aTDC at 1.4 and 3 bar BMEP, respectively, and was between -9 to -7 CAD aTDC for diesel at both studied loads. The slight variation of IT was used to fix AHR-50 at around 11 CAD aTDC for both loads and fuels.

$BSNO_x$ emissions from combustion of G75 and diesel (D) fuels with different EGR rates are illustrated in Figure 5-6[1]. As expected, for both fuels, there is a monotonic reduction trend of $BSNO_x$ emissions as EGR rate is increased. Generally, $BSNO_x$ values for diesel fuel are higher than G75, although this is less evident at 3 bar BMEP. One possible reason can be less intake air thermal throttling effect when using cold-EGR for diesel fuel and therefore more oxygen available which can increase NO_x formation. Furthermore, using a low reactivity fuel like G75 at these engine operating loads will result in a very good premixing of fuel and air and therefore more of the local fuel-air packets are close to the overall mixture strength which is lean. This can reduce the burning rate and reduce sudden peak temperature rise in the cylinder which can result in the thermal production of NO_x [2]. Heat release rate data presented in the next section, comparing G75 and diesel combustion at 1.4 bar BMEP, prove this claim. Although intake temperature is increasing as EGR rate is increased, especially for

[1] It should be noted that at 1.4 bar BMEP, first presented EGR rate is slightly different for the two fuels due to experimental system limitations at the time of conducting these experiments.

G75 fuel using hot-EGR, and this can increase the peak cylinder temperature, NO_x is reduced. For NO_x emissions reduction, it seems that higher intake dilution when using higher EGR rate is more important compared to the elevated intake temperature. Based on this figure, target of 0.4 g/kWh for $BSNO_x$ is achievable for both fuels at the studied IPs and EGR rates.

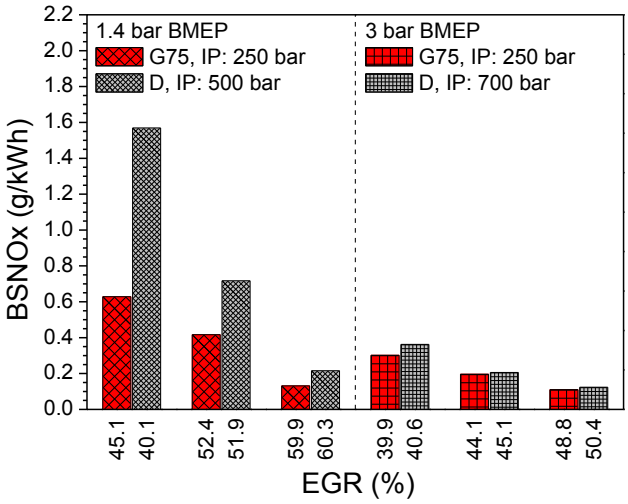


Figure 5-6 Comparison of $BSNO_x$ emissions of G75-Dieseline and diesel (D) at different EGR rates

Effect of EGR rate variation on smoke emissions is illustrated in Figure 5-7. Combustion of diesel fuel, even with using cold-EGR and higher fuel IP compared to G75, resulted in higher smoke emissions at both studied loads. In general, variation of smoke emissions from G75 combustion were decoupled from the EGR rate as smoke values always stayed at very low levels (below 0.008 FSN and 0.05 FSN at 1.4 and 3 bar BMEP, respectively). Good premixing of G75 fuel with air results in less locally rich fuel-air packets which reduces the possibility of particulate formation in the first place. Smoke emissions from diesel combustion, on the other hand, increased as EGR rate was increased. It can be seen that well-known trade-off between NO_x and smoke reduction exists for the diesel fuel combustion.

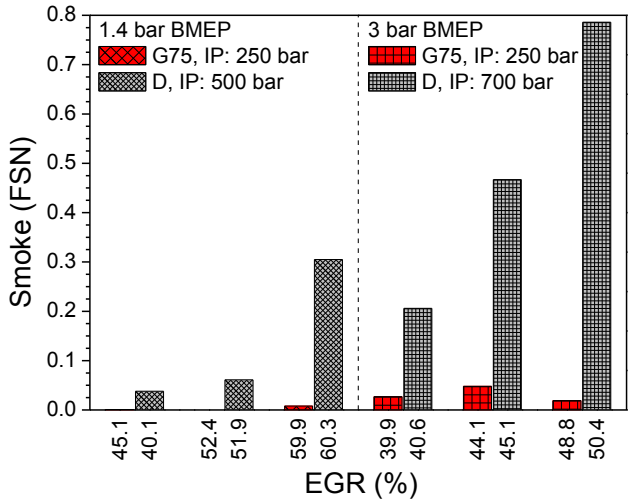


Figure 5-7 Comparison of smoke emissions of G75-Dieseline and diesel (D) at different EGR rates

BTE results are shown in Figure 5-8 to mainly assess the effect of increased hot-EGR rate on the G75 combustion performance. At 1.4 bar BMEP, BTE values were generally in the same range for G75 while for diesel fuel, BTE was slightly decreased as EGR rate was increased. At 3 bar BMEP, BTE was not following a specific trend as EGR rate was changed. However, it was the lowest at the EGR rate of 49% for G75; it was reduced by around 1.73% in absolute value compared to 44% EGR rate.

Based on these results and some more screening experiments, although changes in BTE are minor, it can be hypothesised that higher intake temperature when the EGR rate is increased does not help gain BTE for G75 fuel as the charge becomes more diluted at the same time. It might be worthy to mention that coefficient of variation (COV) of net indicated MEP (NIMEP) when using G75 was generally reduced as EGR rate was increased; e.g. at 1.4 bar BMEP from 7.33% at EGR rate of 45.1% to 4.97% at EGR rate of 52.4%. Diesel combustion resulted in higher BTE compared to G75 combustion; however, it should be mentioned that IP of 250 is not the best for achieving high BTE and these results are only presented to show

variation trends as EGR rate is modified. Results of a more in-depth investigation comparing G75 and diesel at different IPs are reported in the next section.

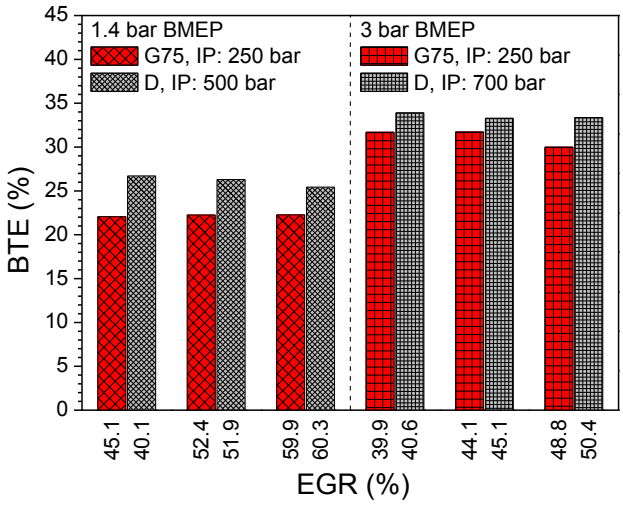


Figure 5-8 Comparison of BTE of G75-Dieseline and diesel (D) at different EGR rates

Figure 5-9 depicts BSTHC emissions as a function of EGR rate variation. Diesel fuel compared to G75 fuel combustion resulted in lower BSTHC values at both studied loads. This might be due to the fuel-air overmixing and possible fuel wall-impingement when using G75. For diesel fuel at both loads and G75 at 3 bar BMEP, there is an increasing trend of BSTHC emissions as EGR rate is elevated. For G75 at 1.4 bar BMEP, BSTHC was the lowest at the EGR rate of 52%. Increasing EGR rate from around 44% to 49% at 3 bar BMEP when using G75 resulted in a sharp increase of BSTHC by 44.7%. From results and discussions provided above, EGR rates of 52% and 45% were selected for 1.4 and 3 bar BMEP, respectively, for the studies presented in the next section. In this manner, defined $BSNO_x$ emission target (<0.4 g/kWh) in conjunction with acceptable BTE and BSTHC emissions were achieved for G75-Dieseline PCI combustion.

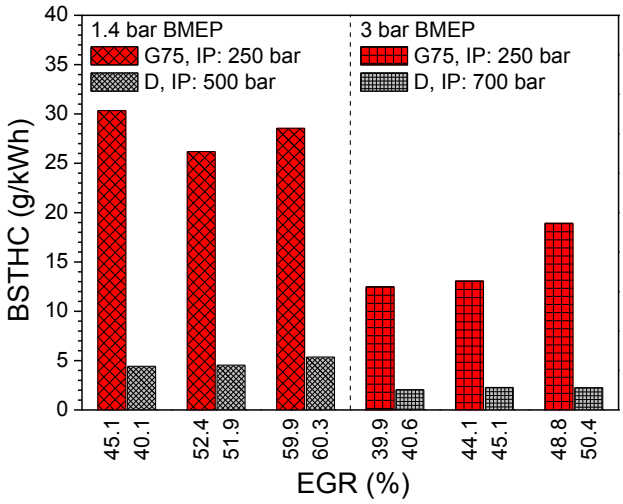


Figure 5-9 Comparison of BSTHC emissions of G75-Dieseline and diesel (D) at different EGR rates

5.3. Investigation of single-injection strategies for Dieseline PCI combustion

In this section, effects of single-injection strategy, including injection-timings and IP, on the combustion performance and emission characteristics when using G75 and diesel fuels are investigated. Additionally, at engine loads of 6, 12 and 17.3 bar BMEP, effects of EGR variation are studied.

5.3.1. Results at 1.4 and 3 bar BMEP with application of hot-EGR and low IP

In this sub-section, combustion and emission characteristics of G75 fuel injected with three low IPs of 150, 250 and 350 bar and diesel fuel injected with IPs of 150, 250, 350, 500, 700, 900 and 1400 bar at different start of injection (SOI) are compared at two loads of 1.4 and 3 bar BMEP. For all of these experiments, engine speed was fixed at 1800 RPM and EGR rate was maintained at 52% and 45% for 1.4 and 3 bar BMEP, respectively, while intake pressure was fixed. Hot-EGR technique was used for G75 and cold-EGR technique was used for diesel

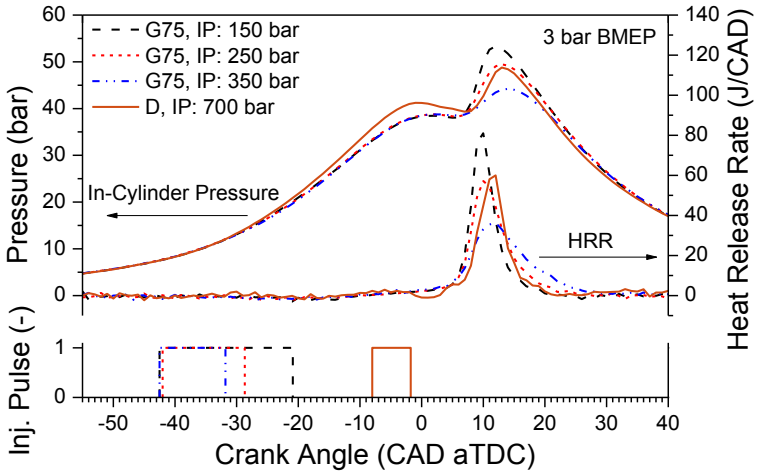
fuel. At these two loads, IP below 150 bar was not allowed by the engine control unit (ECU) and injecting fuel with IP above 350 bar resulted in unstable combustion for the G75 fuel. To prove this claim, some experimental results at the engine load of 1.4 bar BMEP, IP of 450 bar, EGR rate of 52% and different SOI are listed in Table 5-5. Unacceptably high COV of NIMEP and BSTHC and BSCO emissions are observed for all of the studied SOI which can be hypothesised to be due to overmixing and/or fuel wall-impingement. For diesel fuel, studied IPs were selected in order to:

a) investigate low IPs in order to compare the results with the results of G75 fuel at the same IPs,
b) investigate normally-practised IPs (since very low IPs are not normally practised for the diesel fuel),
c) investigate higher IPs to identify what reduction of smoke emissions can be achieved and at what cost to other combustion and emission characteristics.

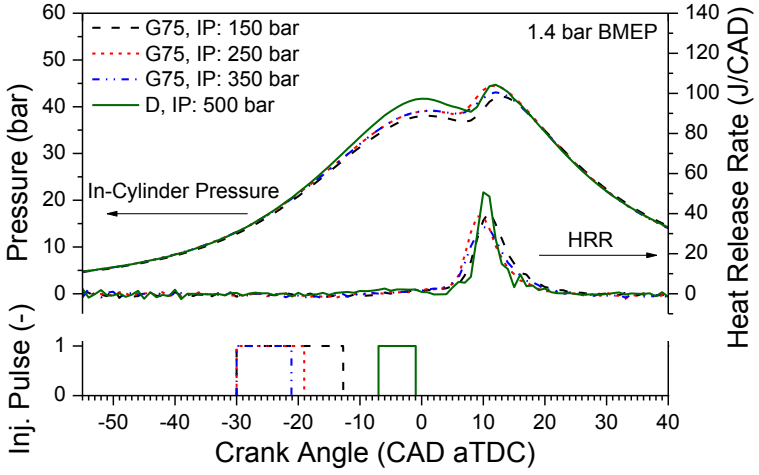
Table 5-5 Effect of the variation of SOI at 1.4 bar BMEP with IP of 450 bar on G75-Dieseline PCI

SOI	**COV of NIMEP**	**BTE**	**MPRR**	**BSNO$_x$**	**BSTHC**	**BSCO**	**smoke**
CAD aTDC	(%)	(%)	(Bar/ CAD)	(g/kWh)			(FSN)
-20	59.90	18.08	1.68	0.66	67.93	41.55	0.217
-30	53.05	20.98	1.12	0.32	40.24	60.48	0.008
-40	63.81	17.55	1.19	0.21	86.15	89.86	0.114

In-cylinder pressure, heat release rate (HRR) and injection electrical pulse (obtained from the ECU) at two loads of 3 and 1.4 bar BMEP are illustrated in Figure 5-10 (a) and (b), respectively.



(a)



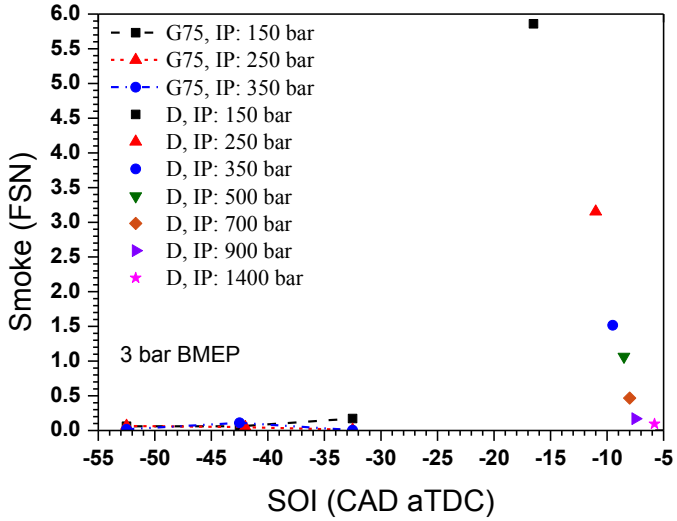
(b)

Figure 5-10 In-cylinder pressure, heat release rate and injection pulse results for G75-Dieseline and diesel (D) combustion at: (a) 3 bar BMEP and (b) 1.4 bar BMEP

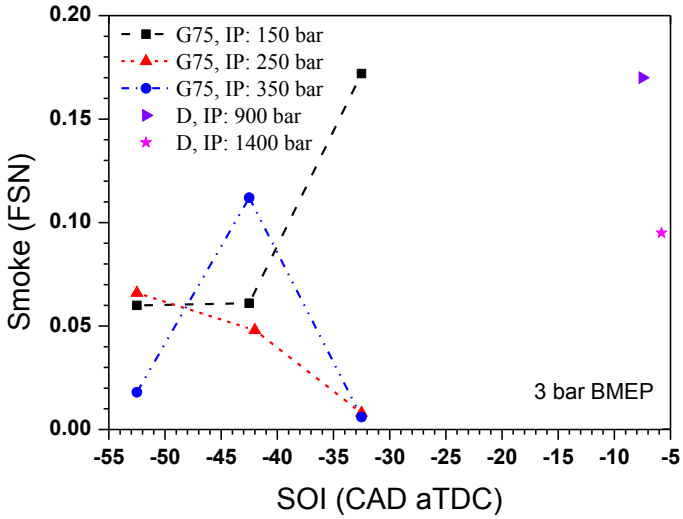
For both fuels, there is a clear separation between the end of injection (EOI) and start of combustion (SOC) and HRR has only one peak. Therefore, these can suggest that premixed combustion was achieved for both fuels while G75 has much longer ignition delay (ID) compared to diesel. AHR-50 of diesel fuel combustion was kept in the same range as for G75 by modifying the injection-timing in order to eliminate the effect of combustion-phasing variation on the results. For G75 at 3 bar BMEP while using the illustrated injection-timings,

increasing IP from 150 to 350 bar reduced in-cylinder peak pressure and peak HRR. It can be hypothesised that very low IP of 150 bar can help to form a less homogenous mixture with local packets more close to stoichiometric condition, rather than lean, and therefore more rapid and intense HRR when combustion starts [2]. However, at 1.4 bar BMEP, change of IP did not have a considerable influence on pressure and HRR. Cooling effect, effect of higher heat of evaporation, of G75 in comparison to diesel is evident by observing the reduced compression peak of in-cylinder pressure; G75 injected earlier than diesel reduced this peak.

Figure 5-11 illustrates smoke emissions at 3 bar BMEP when G75 was injected at three different IPs and three timings of -52.5, -42.5 and -32.5 CAD aTDC. Injection-timings outside this range for G75 were examined and results were not satisfactory; either excessively late AHR-50 or very high COV of NIMEP. Advancing the injection-timing for G75 beyond -52.5 CAD aTDC did not advance the AHR-50 probably due to high overmixing and/or possible fuel wall-impingement which can slow down the chemical kinetics required for ignition and then combustion events [2, 22]. Experimental results showed that at this load modifying injection-timing (within -52.5 to -32.5 CAD aTDC range) for G75 did not change the AHR-50 significantly and it was in the range of 11 to 12 CAD aTDC. This made it possible to compare diesel results and G75 results at the same AHR-50. Diesel was injected at seven different IPs, from 150 to 1400 bar, and injection-timing was set to achieve AHR-50 similar to those of G75.



(a)



(b)

Figure 5-11 Results of smoke emissions for G75 and diesel at 3 bar BMEP with different injection-timings and injection pressures; (a) illustrates the full range and (b) illustrates a zoomed view to show smoke values below 0.2 FSN

It can be seen from Figure 5-11 (a) that smoke levels of G75 are lower than diesel. With the same IP of 150 bar, when comparing G75 (with SOI of -52.5 CAD aTDC) and diesel at the same AHR-50, smoke was reduced by around 99%. However, it should be mentioned that IP of 150 bar is not normally used for diesel fuel at this operating load. Even with normally

utilised IP for diesel (700 bar), smoke emissions were around 87% lower when comparing result of G75 at 150 with that of diesel. It should be emphasised again that these low levels of smoke emissions from G75 combustion are achieved with very low IPs (for CI engines) beside using the hot-EGR technique; both are known to increase smoke emissions. This reduction of smoke emissions from G75 combustion compared to diesel combustion can be attributed to longer ignition delay and higher volatility of G75 fuel.

Lower IP imposes less mechanical load on the engine, reduces parasitic losses and requires less complex and costly fuel injection equipment (FIE). It normally results in larger liquid droplet size and therefore weakens evaporation and atomization processes. Furthermore, it requires longer injection duration which is not a positive factor for soot reduction when using highly reactive fuels, e.g. diesel, as the ignition delay is short and there is a higher chance that most of the fuel is burnt in the mixing-controlled stage. However, for G75 at low loads, it is believed that low IPs (below 350 bar) may help to achieve more degree of stratification which is useful for premixed combustion. At the early injection-timings, in-cylinder pressure and temperatures are low which will allow injected fuel spray to penetrate further into the cylinder [22]. Low IPs for the relatively volatile G75 could have reduced the spray wall-impingement. Moreover, it might be worthy to mention that higher in-cylinder temperature due to using hot-EGR may increase the evaporation rate of the spray with even low IPs. However, all of these hypotheses need to be confirmed with detailed in-cylinder optical studies.

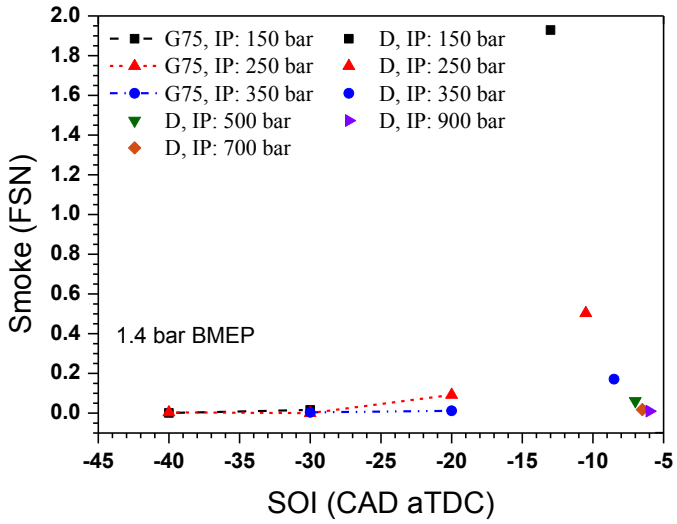
For diesel fuel combustion, increasing the IP reduced smoke emissions monotonically while injection-timing was required to be adjusted to maintain AHR-50 at the same CAD. An idea can be to use higher IP for diesel fuel at low loads in order to achieve same low levels of smoke as for G75. Figure 5-11 (b) shows a zoomed view of the smoke emissions results below 0.2 FSN when using G75 and diesel. For G75, it can be seen that the lowest smoke value (0.006 FSN) within the studied test points was achieved at SOI of -32.5 CAD aTDC and IP of

350 bar. It was not possible to achieve low levels of smoke, similar to G75, with diesel fuel without using high IPs of 900 and 1400 bar. This smoke reduction for diesel had a downside of reduced BTE values discussed later in this sub-section.

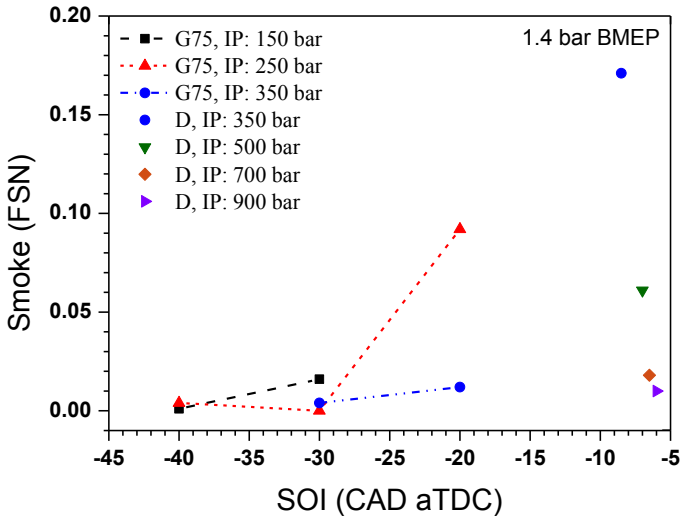
Smoke emissions results at 1.4 bar BMEP are illustrated in Figure 5-12. Results for G75 with IP of 150 bar at -20 CAD aTDC and with IP of 350 bar at -40 CAD aTDC are not presented in the rest of the figures for this load. This is due to the fact that operation of the engine in these points was not reliable indicated by high levels of COV of NIMEP. This highlights the need for intense optimisation of engine operating settings for G75 as engine performance is sensitive to their changes. Similar to 3 bar BMEP, using G75 resulted in lower smoke emissions compared to diesel. At this load, when increasing IP for diesel fuel, it was found that lower IP (compared to 3 bar BMEP) was required to achieve smoke levels similar to those of G75 combustion; with IP of higher than 500 bar, smoke emissions were less than 0.1 FSN. Particulate emissions from these operating modes are discussed in details, e.g. in terms of number and size distribution, in Chapter 7 of this thesis.

These low smoke emissions from G75 combustion were achieved simultaneously with low $BSNO_x$ emissions as shown in Figure 5-13 at both loads. At 3 bar BMEP, $BSNO_x$ emissions of G75 and diesel fuels are in the same range while at 1.4 bar BMEP, $BSNO_x$ emissions of diesel fuel combustion are generally higher than G75. At 1.4 bar BMEP, compared to diesel with IP of 500 bar, G75 PCI combustion resulted in lower $BSNO_x$ emissions by around 65% with IP of 150 bar and SOI of -40 CAD aTDC. It should be noted that for G75 fuel with hot-EGR technique, although intake temperature is higher compared to diesel, intake oxygen content is less due to the thermal throttling effect of the hot-EGR. At the lower studied load, achieving $BSNO_x$ value of less than 0.4 g/kWh was not possible for diesel fuel with EGR rate of 52% as opposed to G75. As discussed earlier, burn rate of diesel at this load is generally higher than G75 which can increase peak cylinder temperature and NO_x emissions. $BSNO_x$ reduction for

diesel fuel combustion under these conditions might be possible with increasing EGR rate. However, as shown in sub-section 5.2.2, this reduction will be accompanied with reduced BTE and increased smoke and THC emissions.

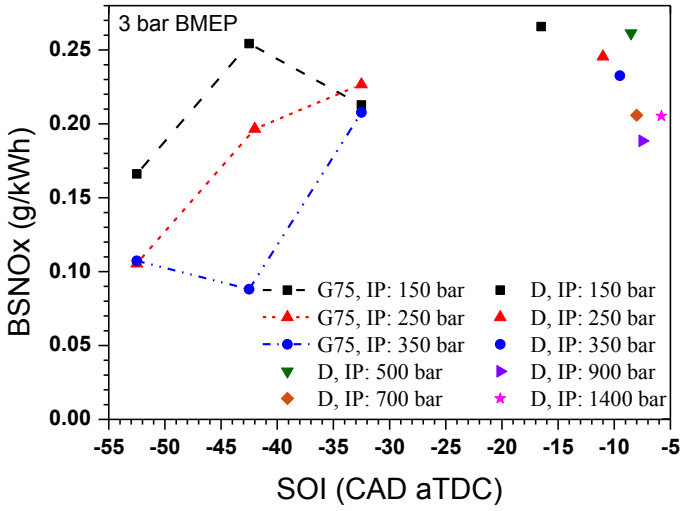


(a)

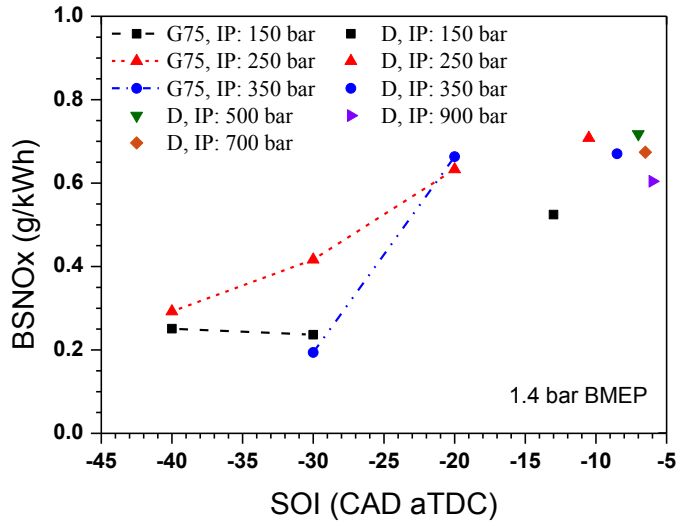


(b)

Figure 5-12 Results of smoke emissions for G75 and diesel at 1.4 bar BMEP with different injection-timings and injection pressures; (a) illustrates the full range and (b) illustrates a zoomed view to show smoke values below 0.2 FSN



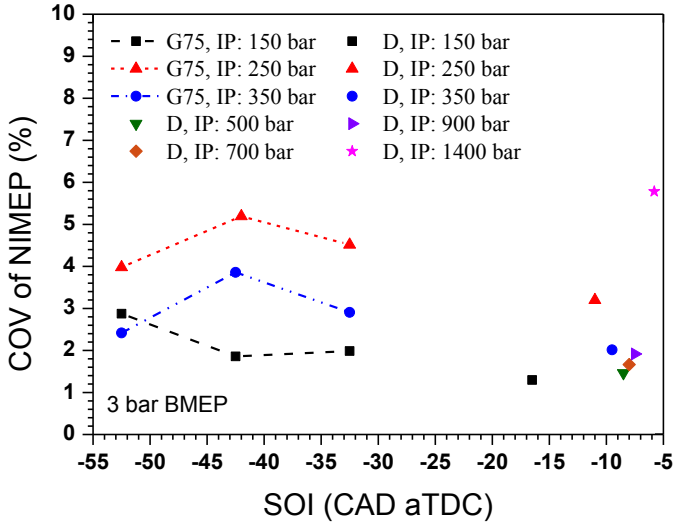
(a)



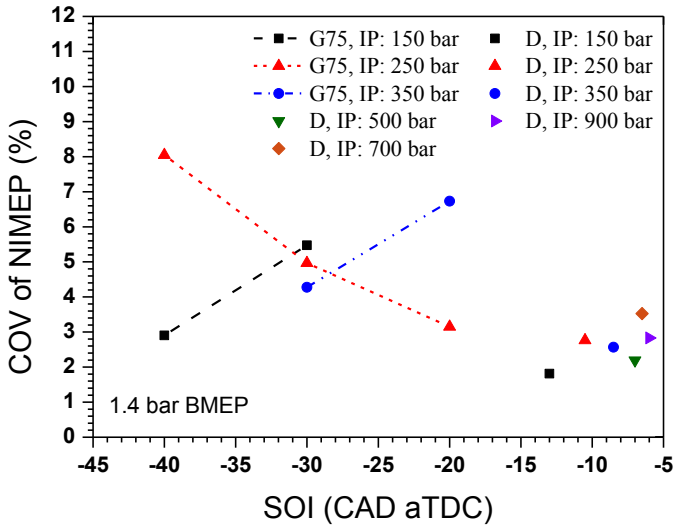
(b)

Figure 5-13 Results of $BSNO_x$ emissions for G75 and diesel with different injection-timings and injection pressures at: (a) 3 bar BMEP and (b) 1.4 bar BMEP

Cyclic variation of the combustion when operating at low loads on the PCI mode and especially with very low cetane number fuels is a very important challenge to overcome. In order to assess the cyclic variations, COV of NIMEP is illustrated for both loads in Figure 5-14.



(a)



(b)

Figure 5-14 Coefficient of variation (COV) of net indicated mean effective pressure (NIMEP) for G75 and diesel with different injection pressures and timings at: (a) 3 bar BMEP and (b) 1.4 bar BMEP

At 3 bar BMEP, generally COV is less than 5% for both fuels. Using high IP of 1400 bar for diesel fuel, to achieve low smoke values, resulted in a relatively high COV of NIMEP. These acceptable levels of COV achieved for G75, as opposed to earlier screening studies, are believed to be due to usage of hot-EGR and low IPs. At the lower studied load of 1.4 bar

BMEP, it is possible to achieve COV value of less than 5% for both fuels with the exception of some operating points for G75 fuel. It is expected that with further optimisation of engine operation controlling parameters and tailoring the cylinder geometry for the PCI operation, cyclic repeatability will be improved.

BTE, brake specific fuel consumption (BSFC) and combustion efficiency at 3 bar BMEP are shown in Figure 5-15. Generally, for G75 at this operating load, retarding the injection-timing (within the illustrated range) resulted in higher BTE and combustion efficiency. It is shown later in this chapter that BSTHC and BSCO were reduced as the injection-timing was retarded. When the fuel is injected earlier, there is higher chance for the fuel and air to be overmixed; also occurrence of wall-wetting is more likely and therefore combustion efficiency can be reduced. Except results at the injection-timing of -32.5 CAD aTDC, lower IP resulted in higher BTE and lower BSFC.

With same low IPs, diesel fuel combustion resulted in higher BTE values. Higher BTE values for diesel fuel were achieved with a considerable drawback of elevated smoke emissions as discussed earlier. In order to reduce smoke emissions of diesel fuel, IP was increased. Even with increasing IP to 900 and 1400 bar diesel combustion emitted more smoke emissions compared to G75 combustion. Increasing IP for diesel, for reducing smoke emissions, resulted in reduced BTE values as shown in Figure 5-15. This might be due to higher mechanical load on the engine and reduced combustion efficiency. With IP of 700 bar, which resulted in higher smoke values by around 7.8 times compared to G75 at 350 bar BMEP with same AHR-50, BTE of diesel and G75 operation were in the same level. These results illustrate that BSFC of less than 260 g/kWh is possible to be achieved for both of the fuels at this load. Moreover, combustion efficiency of G75 fuel can be higher than 99% and be close to the combustion efficiency of diesel fuel combustion.

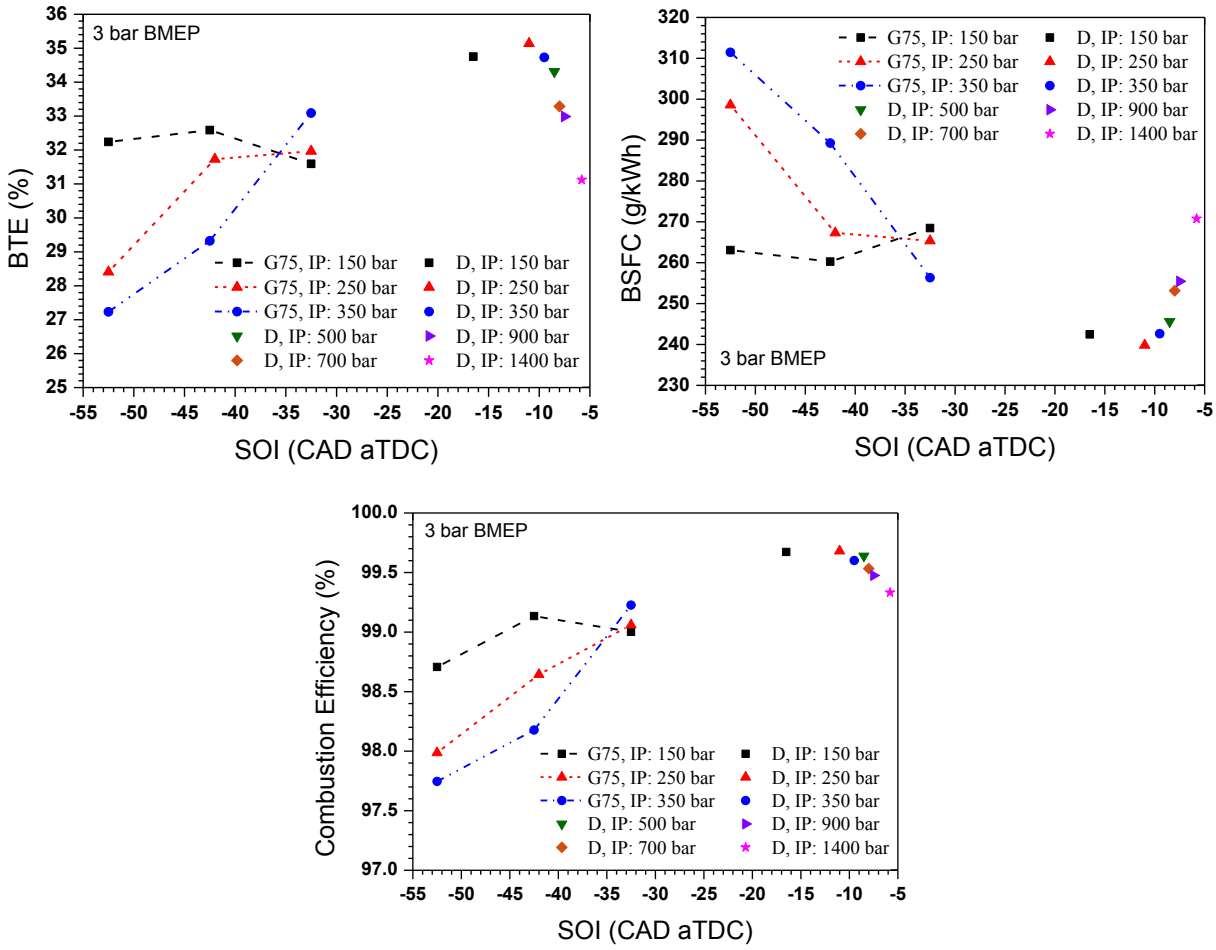


Figure 5-15 Comparison of G75 and diesel at 3 bar BMEP with different injection-timings and pressures, in terms of: BTE, brake specific fuel consumption (BSFC) and combustion efficiency

From these results, it can be concluded that reducing engine out smoke emissions of diesel fuel combustion with higher IPs has a cost of reduced BTE. Moreover, it is suggested that it is better to not compare fuels with diverse properties using the same IPs. Application of high IPs of 900 or 1400 bar will result in very unstable combustion for G75 fuel while application of low IPs of 150 to 350 bar for diesel results in high particulate emissions.

Figure 5-16 illustrates BTE, BSFC and combustion efficiency results at 1.4 bar BMEP where, in general, using diesel fuel resulted in higher BTE. However, as it was shown in Figure 5-12 and Figure 5-13, smoke and BSNO$_x$ emissions of diesel combustion are normally higher than

emissions of G75, while increasing IP resulted in lower smoke and thermal efficiency for diesel. The issue at this load was high $BSNO_x$ emissions from diesel combustion presented earlier in this section. Utilising low IP of 150 bar with injection-timing of -40 CAD aTDC resulted in the peak BTE value (24.31%) when using G75 which is around 2% lower compared to diesel with IP of 500. Regardless of the IP, combustion efficiency of G75 was improved as the injection-timing was retarded (within the illustrated range). There was a reducing trend for BTE and combustion efficiency of diesel fuel as IP was increased.

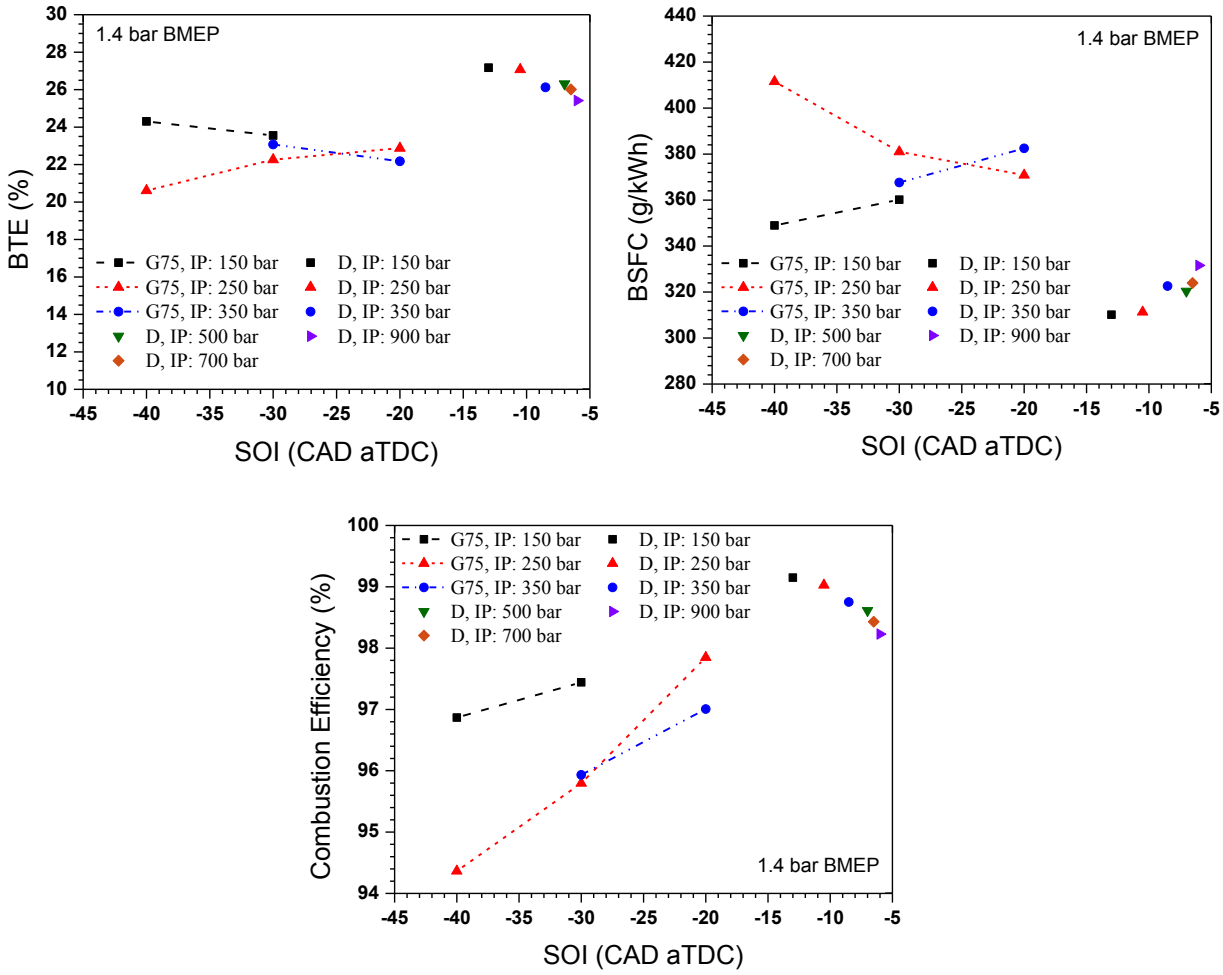


Figure 5-16 Comparison of G75 and diesel at 1.4 bar BMEP with different injection-timings and pressures, in terms of: BTE, brake specific fuel consumption (BSFC) and combustion efficiency

For G75 at 3 bar BMEP, both ignition delay (ID), defined as the CAD duration from SOI to start of combustion (SOC), and combustion delay (CD), defined as the CAD duration from SOI to AHR-50 [2], were prolonged as injection-timing was advanced (shown in Figure 5-17 (a) and (c)). This indicates that altering injection-timing, within the illustrated range, have minimal effect on changing the AHR-50 and to a lesser extent the SOC.

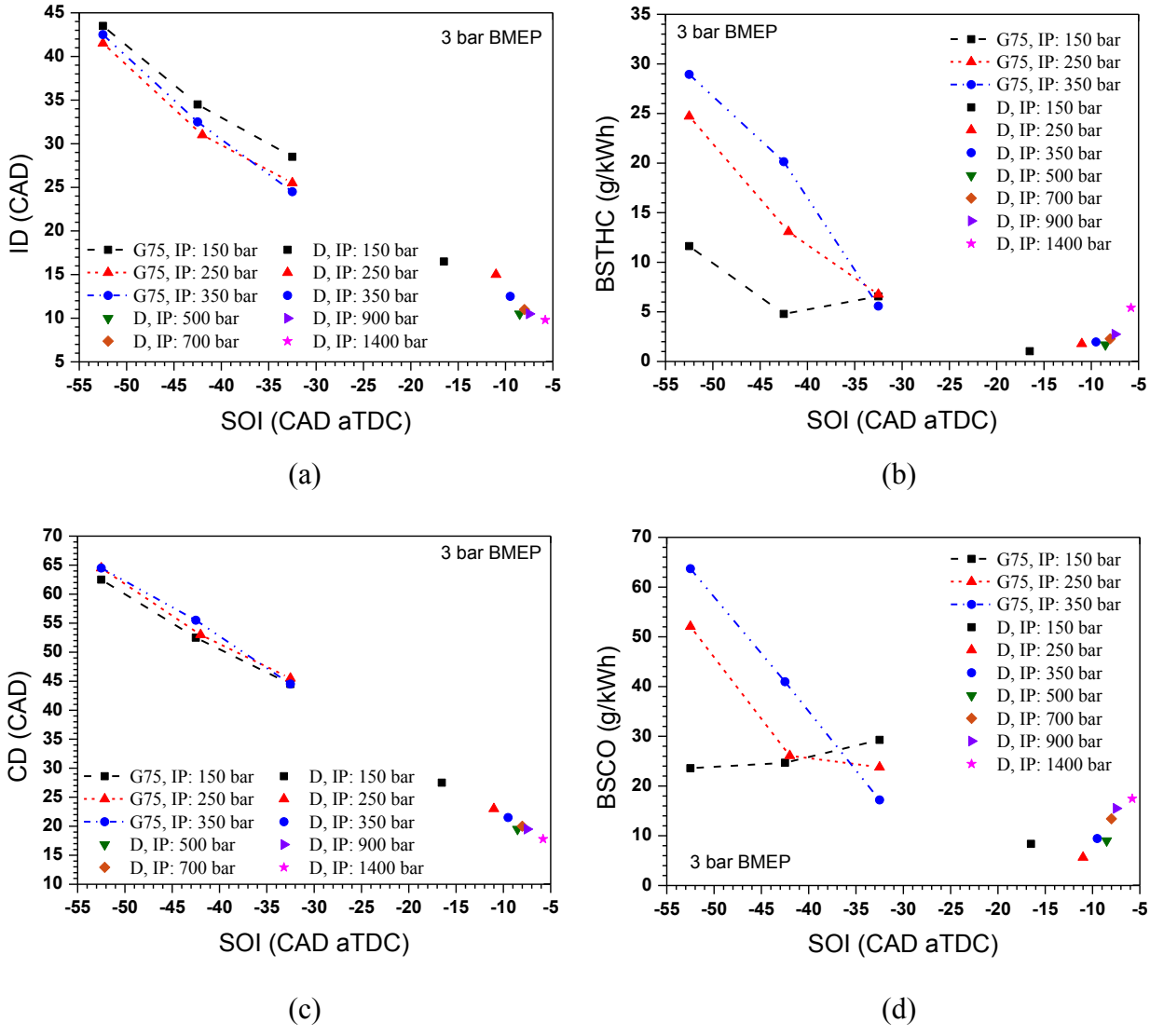


Figure 5-17 Comparison of G75 and diesel with different injection pressures and timings at 3 bar BMEP, in terms of: (a) ignition delay (ID), (b) brake specific total hydrocarbons (BSTHC), (c) combustion delay (CD) and (d) brake specific carbon monoxide (BSCO)

BSTHC emissions, in general, were reduced as the injection-timing was retarded which can show the effect of possible over-mixing of fuel and air and/or fuel wall-impingement. Except for IP of 150 bar, BSCO followed the same reduction trend similar to BSTHC. Normally higher IP resulted in higher BSTHC and BSCO emissions. Diesel fuel illustrated shorter ID and consequently lower BSTHC and BSCO. For diesel fuel, ID and CD were linked with the IP and were shortened as IP was increased. In general, BSTHC and BSCO were increased as IP was increased. It was possible to achieve similar values of diesel BSTHC and BSCO (below 6 and 17 g/kWh respectively) when using G75 with lower IP and retarded injection-timing.

At 1.4 bar BMEP, results illustrated the same trend as 3 bar BMEP with difference in the absolute values for ID, CD, BSTHC and BSCO shown in Figure 5-18. Lower IP for G75 fuel resulted in less BSTHC and BSCO emissions. Diesel, in general, has shorter ID and CD and less BSTHC and BSCO emissions. For G75, at the injection-timing of -40 CAD aTDC which corresponds to the peak BTE, presented earlier, BSTHC reached a minimum value (11.66 g/kWh) while BSCO was relatively high under the studied engine conditions. For diesel fuel, while increase of IP did not have considerable influence on the BSTHC emissions, BSCO emissions increased with increase of IP. High engine out HC and CO emissions can be efficiently controlled by a diesel oxidation catalyst (DOC). However, there are some issues related to lower engine operating loads when running on low temperature combustion modes which normally result in lower exhaust temperature.

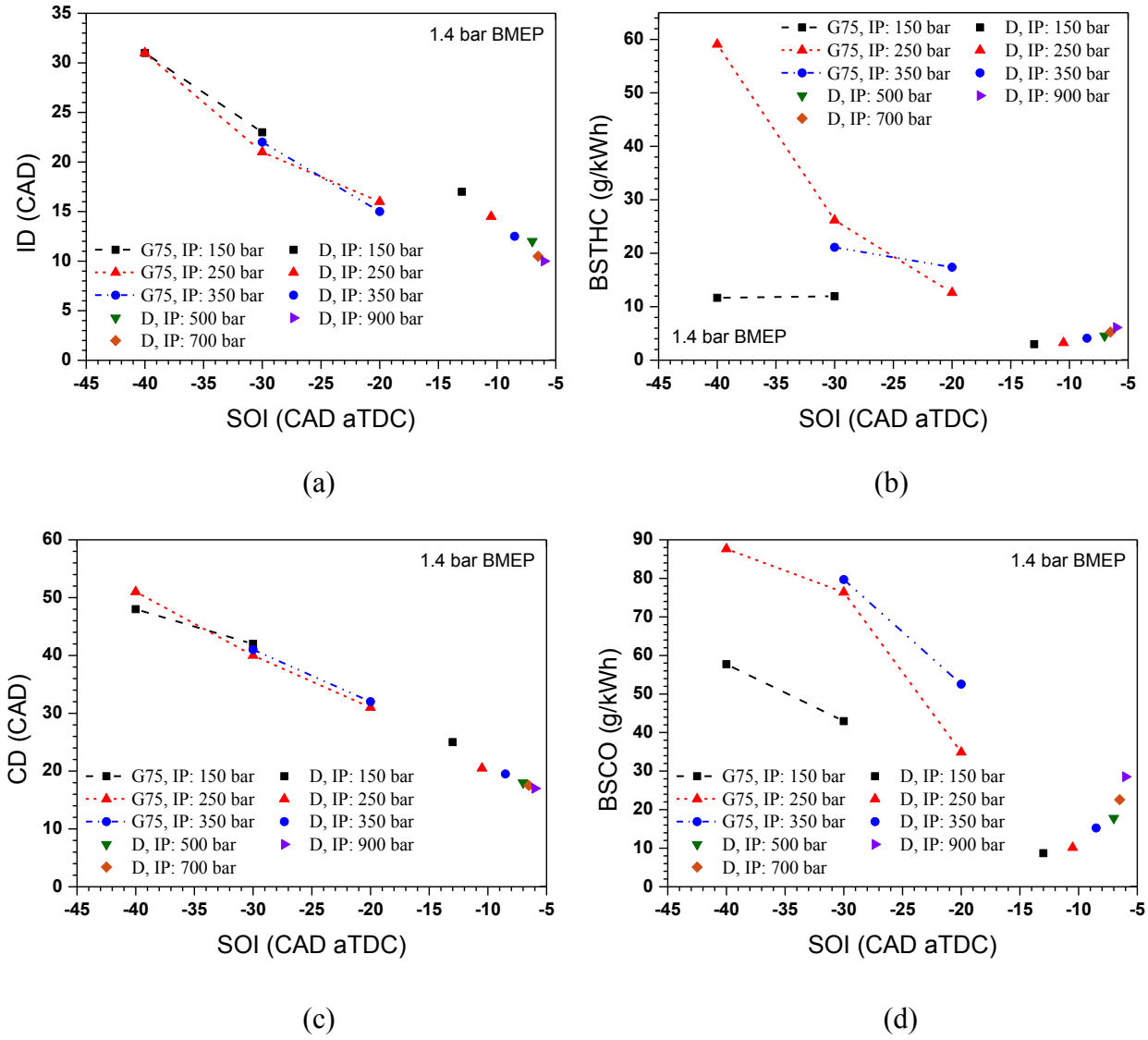
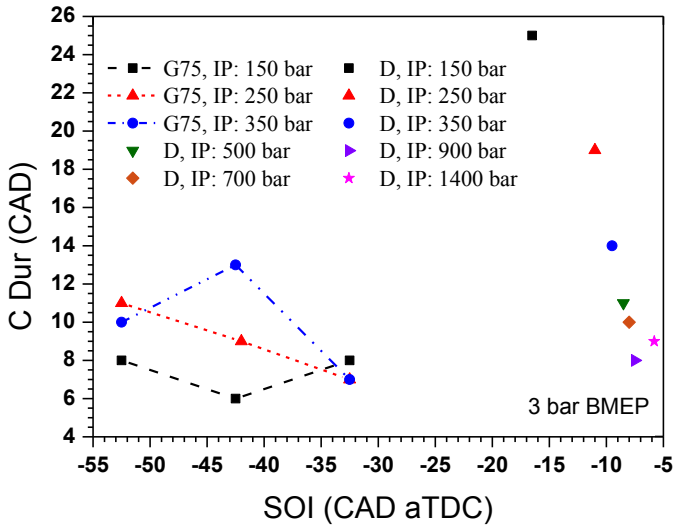


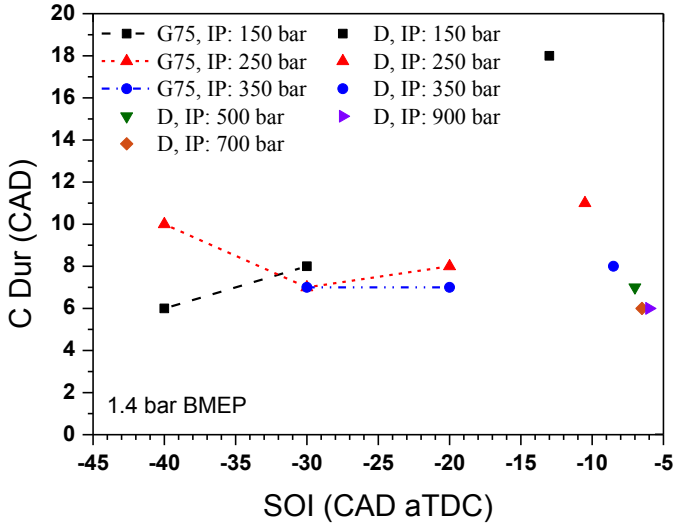
Figure 5-18 Comparison of G75 and diesel with different injection pressures and timings at 1.4 bar BMEP, in terms of: (a) ignition delay (ID), (b) brake specific total hydrocarbons (BSTHC), (c) combustion delay (CD) and (d) brake specific carbon monoxide (BSCO)

Combustion duration (C Dur), defined as the CAD duration from AHR-10 to AHR-90, is illustrated in Figure 5-19. In general, combustion durations for G75 and diesel were in the same range. There was no specific trend for G75 with respect to variation of injection pressure and timing. On the other hand for diesel fuel, lower IP prolonged C Dur; this might be related to the higher degree of stratification for diesel fuel with lower ID and possible

overlap between EOI and SOC which result in achieving mixing-controlled combustion with diffusive flame.



(a)

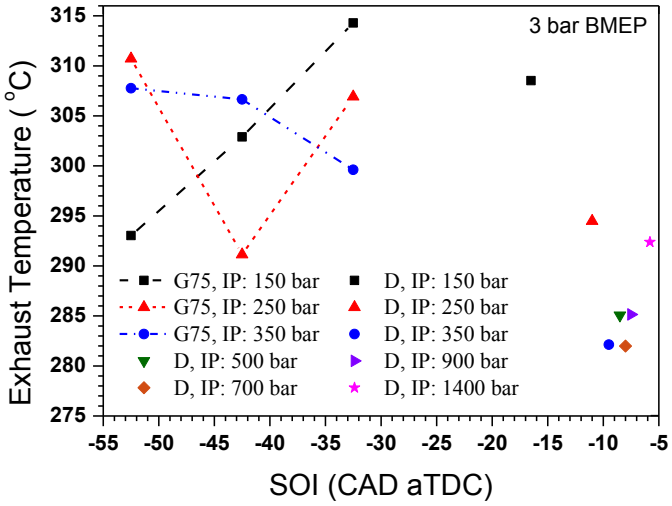


(b)

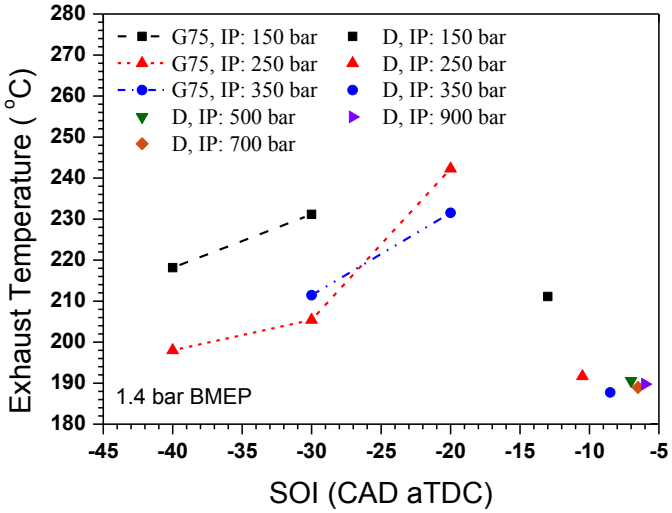
Figure 5-19 Combustion duration (C Dur) of G75 and diesel with different injection pressures and timings at: (a) 3 bar BMEP and (b) 1.4 bar BMEP

Shorter combustion duration for premixed combustion, normally, is accompanied with higher HRR peaks and higher maximum pressure rise rate (MPRR). MPRR, which can be linked to the combustion noise, for both fuels was in the range of 1 to 4.5 bar/CAD at 3 bar BMEP and 1 to 2.5 bar/CAD at 1.4 bar BMEP. As the combustion-phasing was kept constant for both fuels, MPRR values were in the same range.

As discussed briefly earlier in this chapter and in Chapter 2, exhaust temperature is a critical parameter for the good performance of DOC. For the case of proposed PCI/GCI combustion with G75 using hot-EGR technique and low IP, higher exhaust temperatures compared to diesel combustion were achieved and results are illustrated in Figure 5-20. At the lower studied load, compared to diesel combustion, G75 combustion resulted in higher exhaust temperatures (generally measured to be more than 200 ^{o}C). This is in contrast to what is normally expected from low temperature PCI combustion strategies where exhaust temperature is relatively lower compared to conventional diesel operation [140]. At 1.4 bar BMEP, engine exhaust temperature of around 190 ^{o}C was recorded for diesel combustion with IP of 500 bar while G75 combustion exhaust temperature when using IP of 150 bar and SOI of -40 CAD aTDC (settings for max achieved BTE) was around 218 ^{o}C. This increase in temperature while maintaining low soot operation is really helpful for improving the DOC efficiency at this load, in comparison to the case of diesel with cold-EGR strategy; this claim is supported by experimental results discussed in details in Chapter 7.



(a)



(b)

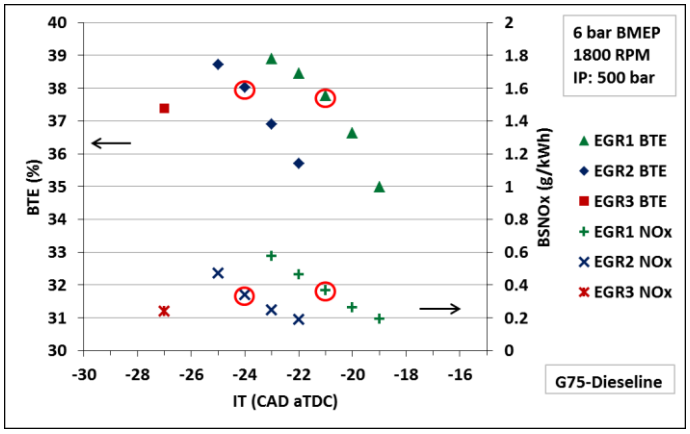
Figure 5-20 Engine exhaust temperature for G75 and diesel with different injection pressures and timings at: (a) 3 bar BMEP and (b) 1.4 bar BMEP

Lower load operation of G75 PCI/GCI combustion in the studied engine was a challenge to overcome and results discussed in this section proved its possibility with using low IP and hot-EGR. In the following sub-sections results at 6, 12 and 17.3 bar BMEP are presented and discussed to assess the benefits of G75 PCI/GCI strategy while using single-injection at medium and high loads compared to diesel operation.

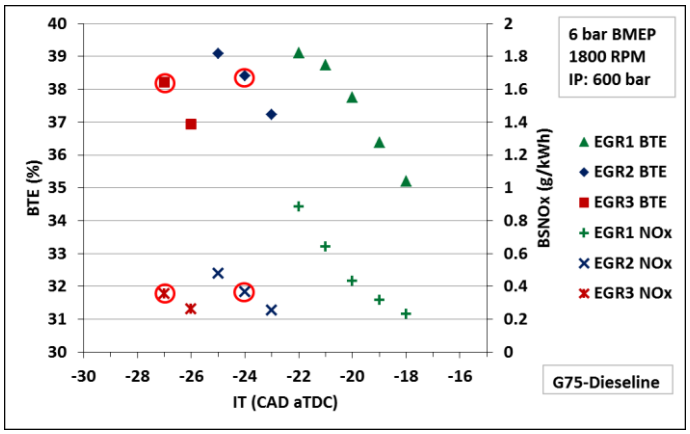
5.3.2. Results at 6 bar BMEP

Based on several screening experiments at 6 bar BMEP and 1800 RPM, using low IPs of 150, 250 and 350 bar was not suitable for achieving low smoke and NO_x emissions from the G75 PCI combustion. Therefore, based on the results, higher IPs had to be chosen which are discussed below. Moreover, screening tests showed that none of the heat-exchanger deactivation strategies (either for EGR cooler or air intercooler) were beneficial for increasing BTE and reducing $BSNO_x$ and smoke emissions simultaneously at 6 bar BMEP. Therefore, cold-EGR strategy with activated air intercooler was utilised for all of the tests conducted at this load.

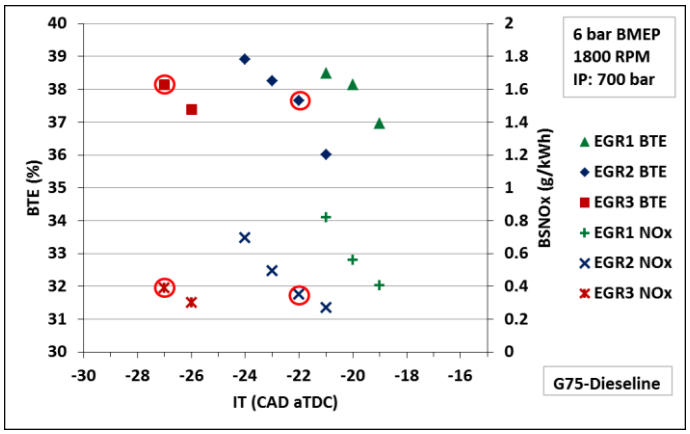
Figure 5-21 illustrates BTE and $BSNO_x$ results of single-injection strategy for G75 fuel using three IPs, three EGR valve settings and various injection-timings (ITs). The actuation level of the turbocharger valve was kept constant for all of these experiments. EGR valve setting refers to the opening level of the EGR valve. EGR1 refers to 48.5%, EGR 2 refers to 50.5% and EGR3 refers to 52.5% valve opening of the full opening position of the utilised EGR valve. The reason for selecting this strategy was the fact that maintaining the EGR rate at a fixed level when the IT is being modified was challenging since there is an interaction between the EGR valve and turbocharger valve. Therefore, it was decided to maintain valve positions at some defined settings concluded from several screening experiments and this was beneficial for maintaining specific air-fuel ratio (λ) at the desirable levels. With these settings, λ was between 1.2 and 1.4 while λ of EGR1>EGR2>EGR3 at the same combustion-phasing. EGR percentage was between 30% to 34% and boost pressure was between 1.20 to 1.28 bar absolute. The range of injection-timings used for this study was chosen based on two selected constraints: the MPRR must be less than 12 bar/CAD and BTE must be more than 33%.



(a)



(b)

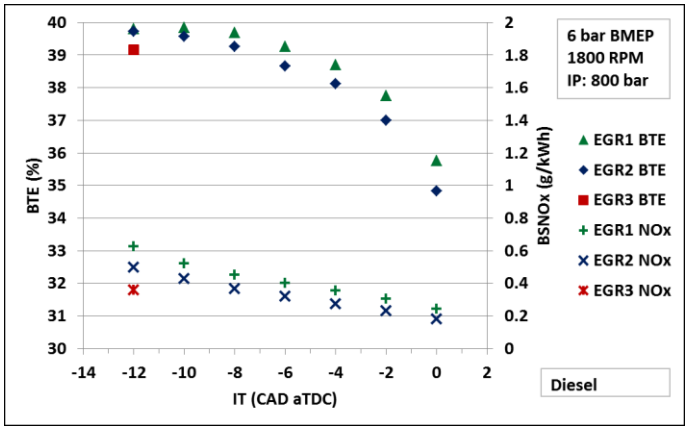


(c)

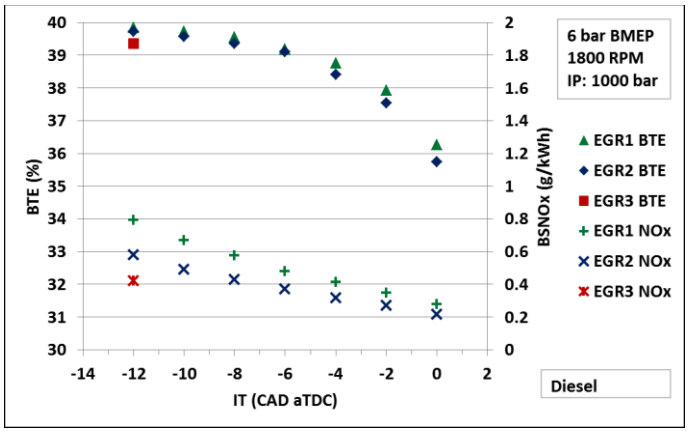
Figure 5-21 BTE and $BSNO_x$ for single-injection of G75 with different EGR valve positions and injection-timings with injection pressure of: (a) 500 bar, (b) 600 bar and (c) 700 bar at 6 bar BMEP; red circles in the figures mark the highest achieved BTE while $BSNO_x$ is below 0.4 g/kWh

Based on Figure 5-21, at each IP, BTE and $BSNO_x$ are functions of IT and EGR valve position. Advancing IT increased BTE while $BSNO_x$ emissions were also increased. This is due to the fact that combustion-phasing was advanced as earlier ITs were used. More opening of the EGR valve helped to achieve more advanced ITs without surpassing the 12 bar/CAD constraint for MPRR due to increased ignition delay. With the same IT, increasing EGR valve opening resulted in lower $BSNO_x$ and BTE. In general, with the same IT and EGR settings, increasing IP resulted in higher values of $BSNO_x$ and BTE as the AHR-50 was advanced (approached towards the TDC). Higher IP results in shorter injection duration (at a fixed engine load) and can help prepare fuel-air packets which are more readily combustible in a shorter period of time. It can be concluded that there is a trade-off between increasing BTE and reducing NO_x at this load. Considering the $BSNO_x$ target value of 0.4 g/kWh, within the studied test points when using IP of 600 bar, IT of -24 CAD aTDC and EGR rate of 32.74%, a maximum BTE of 38.41% was achieved and its corresponding $BSNO_x$ value was 0.36 g/kWh.

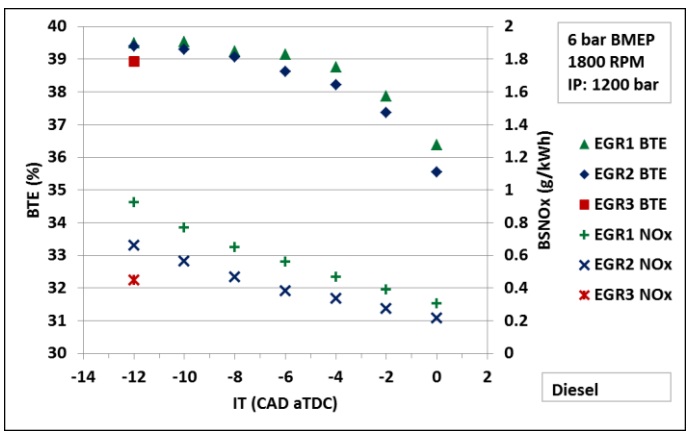
Figure 5-22 shows BTE and $BSNO_x$ results for diesel with the same EGR valve strategy as used for G75 but with different ITs and IPs. Using the same IPs for diesel as for G75 resulted in high values of smoke emissions, e.g. 3.99 FSN for IP of 500 bar and 2.19 FSN for IP of 700 bar at the same AHR-50, while $BSNO_x$ emission were around 0.4 g/kWh. Therefore, higher range of IPs were utilised which are normally used in diesel engines for this speed and load [41, 48]. With respect to G75, ITs had to be retarded to avoid high MPRR and intense combustion before the TDC due to the short ignition delay of diesel.



(a)



(b)



(c)

Figure 5-22 BTE and $BSNO_x$ for single-injection of diesel with different EGR valve positions and injection-timings with injection pressure of: (a) 800 bar, (b) 1000 bar and (c) 1200 bar at 6 bar BMEP

Considering the $BSNO_x$ target of less than 0.4 g/kWh, BTE levels for diesel are in the same range of BTEs for G75 (between around 38% to 39%) while smoke emissions are considerably higher (illustrated in Figure 5-23). Increasing the IP for diesel fuel, from 800 bar to 1200 bar, resulted in higher $BSNO_x$ values when using the same IT and EGR valve opening. Similar to the case of G75, using advanced ITs resulted in higher BTE and $BSNO_x$ values. MPRR for both of the fuels were less than 10 bar/CAD using the earliest studied IT, and dropped monotonically as IT was retarded (to values below 3 bar/CAD) due to retarded AHR-50. For diesel, in contrast to G75, increasing the IP resulted in higher MPRR which can be linked to the combustion induced noise. These results indicate the effectiveness of AHR-50, λ and IP for controlling combustion and emissions characteristics of the engine.

Smoke emissions results for both G75 and diesel are illustrated in Figure 5-23. G75 combustion resulted in very low smoke values (mostly below 0.04 FSN) using all the studied IPs, ITs and EGR valve openings. Diesel smoke emissions were higher than G75 smoke emissions. For diesel, utilising higher IP combined with retarded IT helped to reduce smoke, however smoke emissions never reached below 0.5 FSN. These reductions in FSN values were obtained with the least studied EGR valve opening (which normally resulted in higher $BSNO_x$) and retarded IT (which normally resulted in lower BTE). For example with IP of 1200 bar and IT at TDC, minimum smoke value in these experiments for diesel was achieved (0.560 FSN) while BTE was relatively low (36.37%). Thus, in the case of diesel combustion at 6 bar BMEP, simultaneous reduction of smoke and NO_x has a drawback of reduced BTE (similar to the observations at 1.4 and 3 bar BMEP).

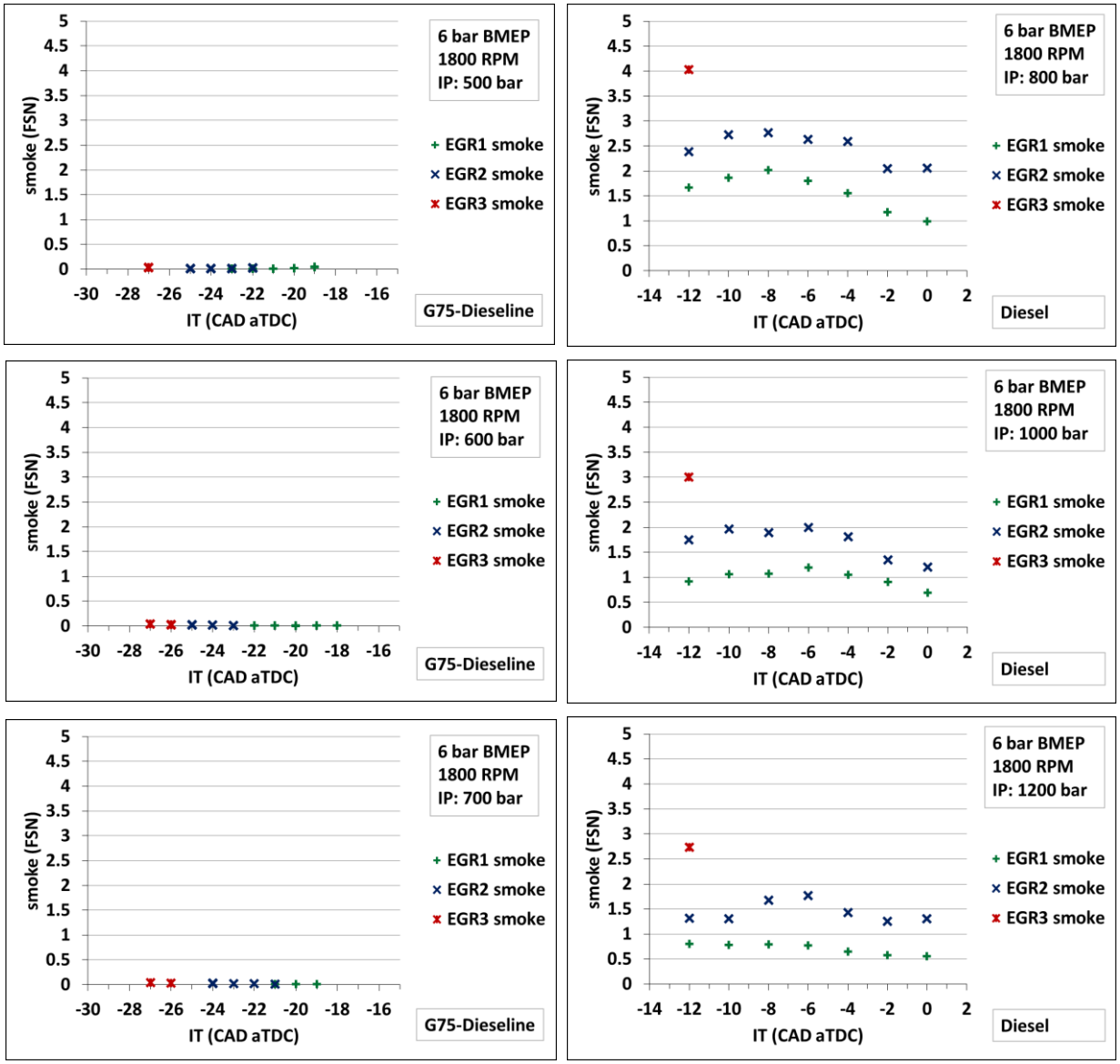


Figure 5-23 Smoke emissions in terms of filter smoke number (FSN) for G75, left column, and diesel, right column, at different injection pressures, injection-timings and EGR valve positions at 6 bar BMEP

In order to compare particulates emissions in terms of mass from combustion of G75 and diesel fuels, brake specific accumulation mode particulate mass (Acc. PM) emissions are illustrated in Figure 5-24. Agglomerates are believed to be the main contributor to the mass of total emitted particulates from an engine [85]. For G75 fuel, most of the studied engine operating conditions resulted in Acc. PM of less than 0.001 g/kWh while for diesel they were

between 0.023 to around 1 g/kWh. Variation trend of Acc. PM is similar to variation trend of smoke for both of the fuels. This figure confirms that PM emission of G75 fuel is less than diesel by orders of magnitude.

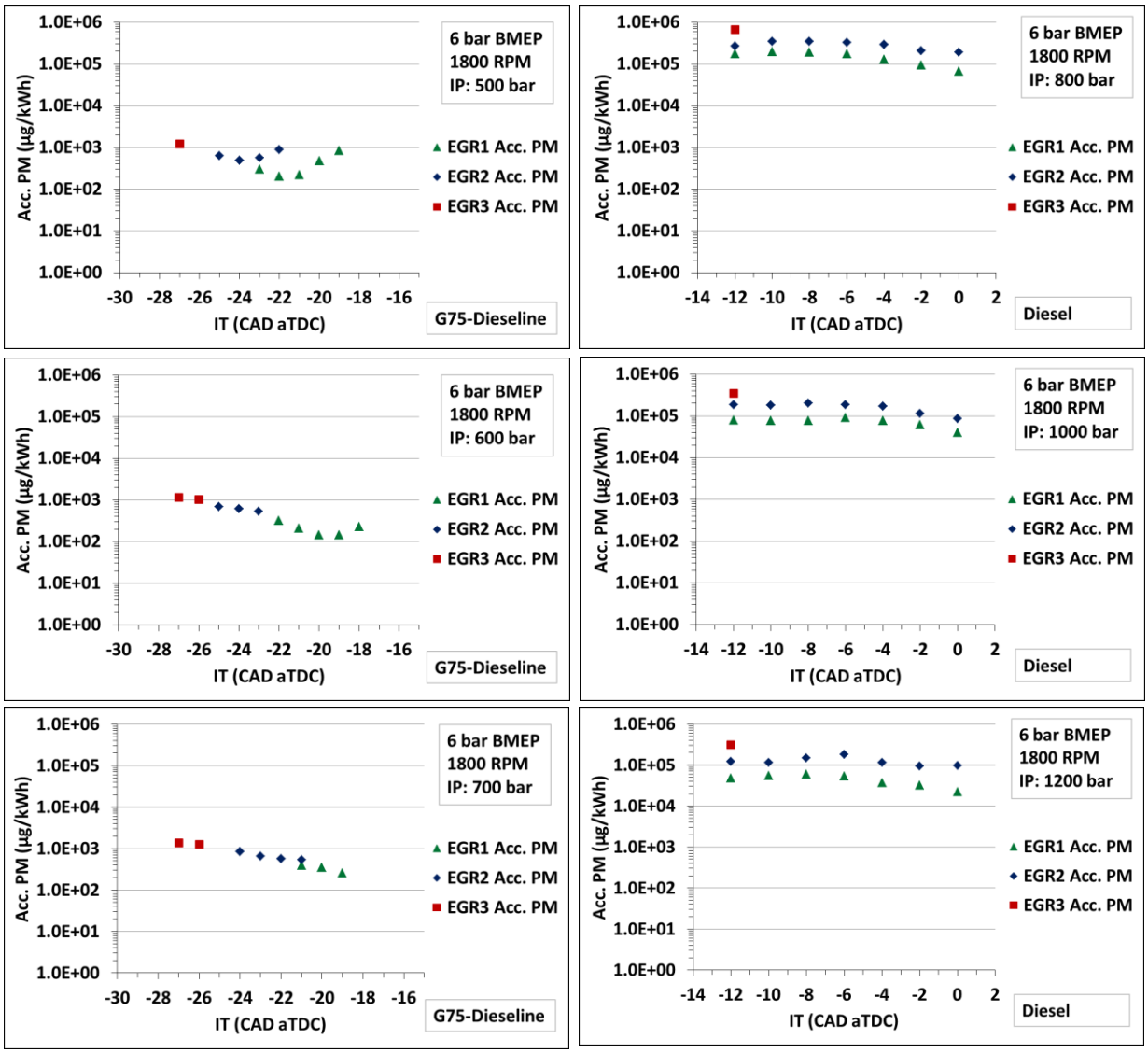


Figure 5-24 Brake specific accumulation mode particulate mass (Acc. PM) for G75, left column, and diesel, right column, at different injection pressures, injection-timings and EGR valve positions at 6 bar BMEP (it should be noted that this graph is a semi-logarithmic plot)

Brake specific total particulate number (TPN) emissions are illustrated in Figure 5-25. These results show the number of detected particulates in the diameter range of 5 to 1000 nm both in nucleation and accumulation modes. Similar to PM, TPN emissions of G75 combustion is lower than TPN emissions of diesel. Similar to PM, for diesel at a fixed IT, more EGR valve opening resulted in higher TPN. Using G75, TPN as low as 1.83×10^{12} particles/kWh is possible to be achieved. In general, using higher IP for both of the fuels resulted in lower TPN, probably due to better fuel and air mixing process. However, this trend is not significant for PM emissions from G75 combustion. This opens a topic about the nature of these particulates (by looking at their diameter).

Figure 5-26 shows the count median diameter of particulates emissions from G75 and diesel combustion. Based on these results, generally, diesel emissions are dominated by larger diameter particulates, as well as having higher nucleation and accumulation mode concentrations, compared to G75 emissions. Higher TPN observed for G75 at the IP of 500 bar is dominated by smaller particulates (total CMD is less than 30 nm) mainly in the nucleation mode. Using higher IPs of 600 and 700 for G75 resulted in increased particulate dimeters not because of the increased concentration in the accumulation mode but reduction in the TPN mostly due to reduced nucleation mode particulates. For diesel, more EGR valve opening resulted in larger particulates with CMD up to 83.7 nm indicating the dominance of larger agglomerates resulted from high equivalence ratio of local air-fuel packets and possible low rate of soot oxidation.

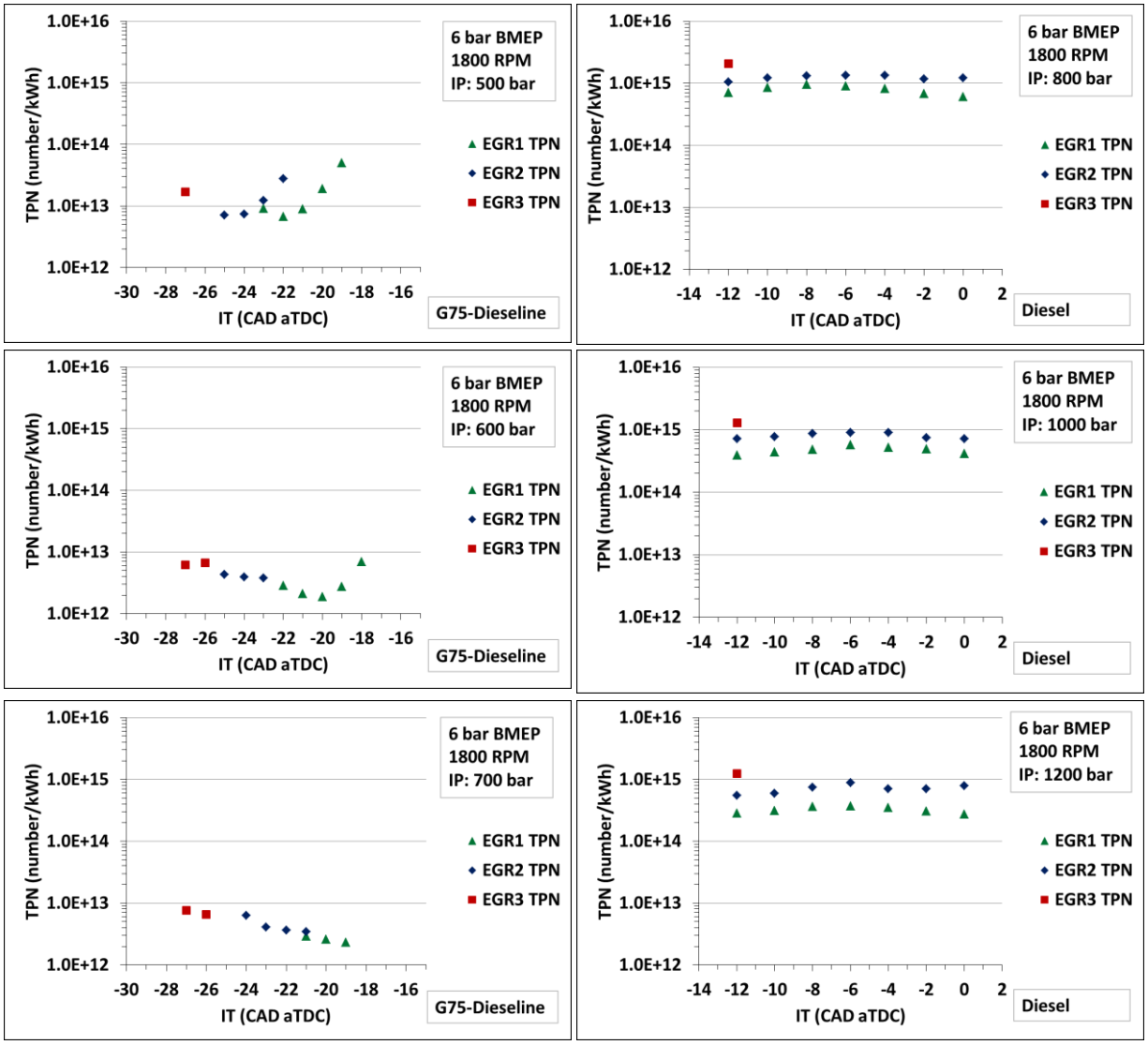


Figure 5-25 Brake specific total particulate number (TPN) for G75, left column, and diesel, right column, at different injection pressures, injection-timings and EGR valve positions at 6 bar BMEP (it should be noted that this graph is a semi-logarithmic plot)

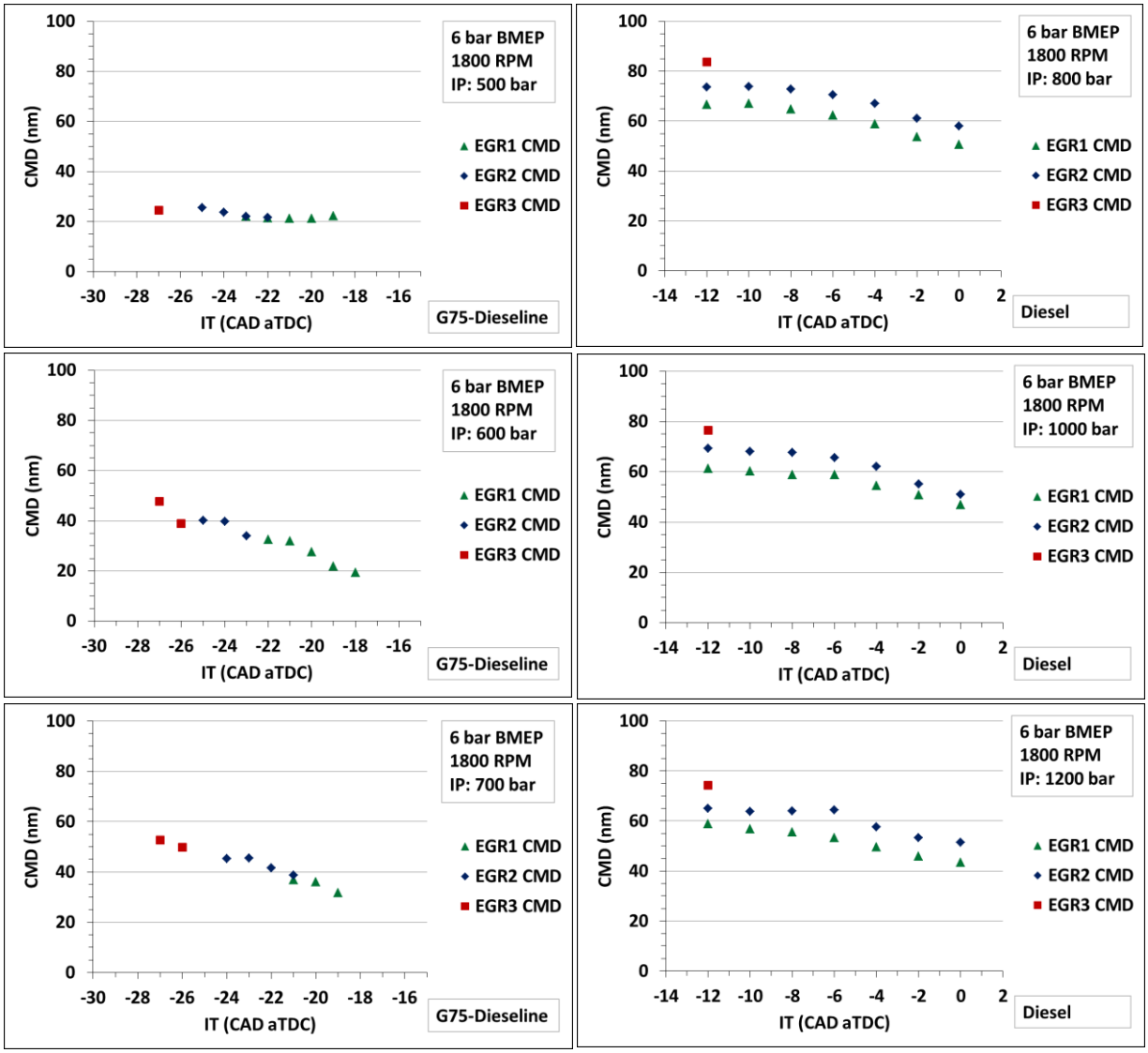
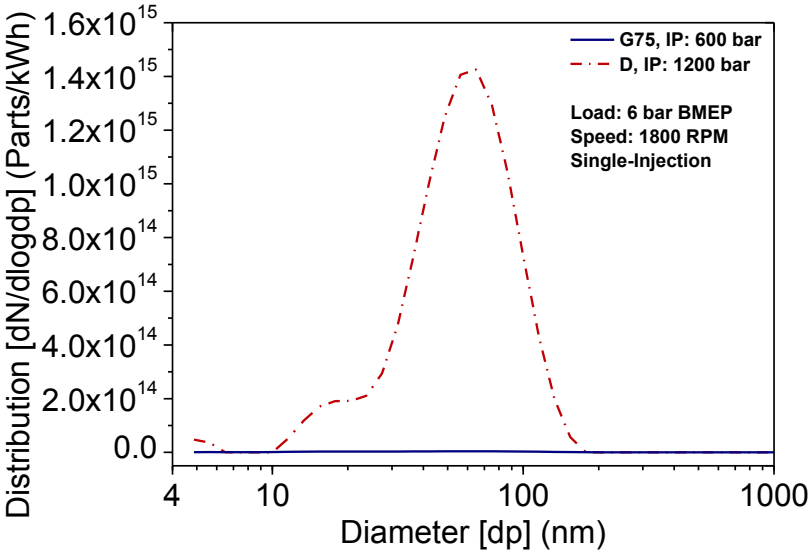


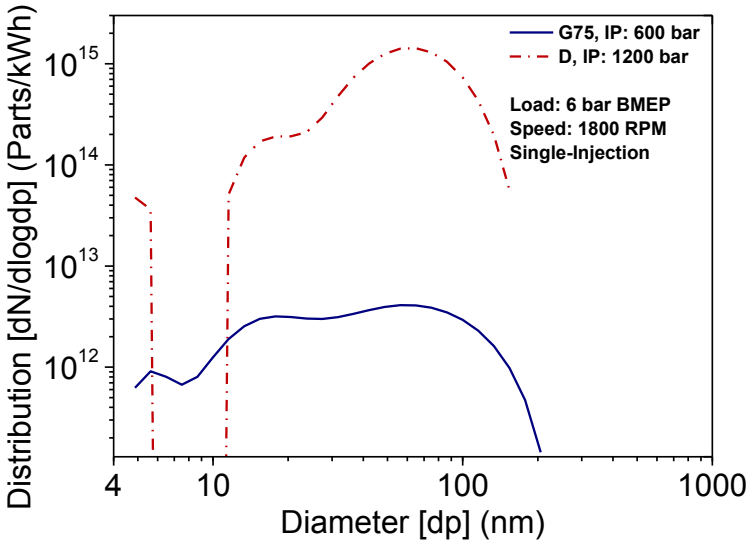
Figure 5-26 Particulates count median diameter (CMD) for G75, left column, and diesel, right column, at different injection pressures, injection-timings and EGR valve positions at 6 bar BMEP

Figure 5-27 illustrates the brake specific particulate number and size distribution comparing emissions of G75 and diesel fuels at two selected points. These points were selected based on achieving minimum smoke and maximum BTE while meeting the target of $BSNO_x$<0.4 g/kWh. Settings for G75 are IP of 600 bar and IT of -24 CAD aTDC and for diesel are IP of 1200 bar and IT of -4 CAD aTDC with the EGR2 valve setting for both. With these settings diesel and G75 have almost the same BTE (38.21% for diesel and 38.41% for G75) and

$BSNO_x$ while smoke of diesel is 84 times more than smoke of G75 (1.428 FSN for diesel and 0.017 FSN for G75) as shown before. Compared to diesel, Acc. BSPM and BSTPN emitted from of G75 combustion were around 99.5% lower. Based on Figure 5-27, particulates emitted from diesel combustion are mainly accumulation mode.



(a)



(b)

Figure 5-27 Brake specific particulate number and size distributions for G75 and diesel at 6 bar BMEP; (a) semi-logarithmic plot and (b) log-log plot

In general, G75 combustion resulted in higher BSTHC and BSCO emissions as illustrated in Figure 5-28 and Figure 5-29, respectively, compared to diesel combustion. In contrast to the case of G75 combustion, variations of BSTHC emissions from diesel combustion were not significant and BSTHC stayed at less than around 0.5 g/kWh regardless of the utilised IP, EGR valve opening and IT. Variations of BSCO emissions for diesel were also insignificant compared to G75, although for both fuels EGR valve opening can influence BSCO results. At the selected points discussed earlier, BSTHC and BSCO emissions of G75 was around 4 and 2.3 times higher than diesel, respectively, due to possible overmixing.

Based on the results presented for this engine load, changes in combustion and emissions characteristics of G75 when varying the IT is more significant compared to diesel. This indicates the importance of the AHR-50 for G75 due to its longer ignition delay. There is a trade-off between THC-CO reduction and NO_x reduction when operating on G75. The main issue for diesel combustion at this load is high smoke emissions which can be reduced at the expense of either increased $BSNO_x$ or reduced BTE. For both fuels there is a trade-off between increasing BTE and reducing NO_x.

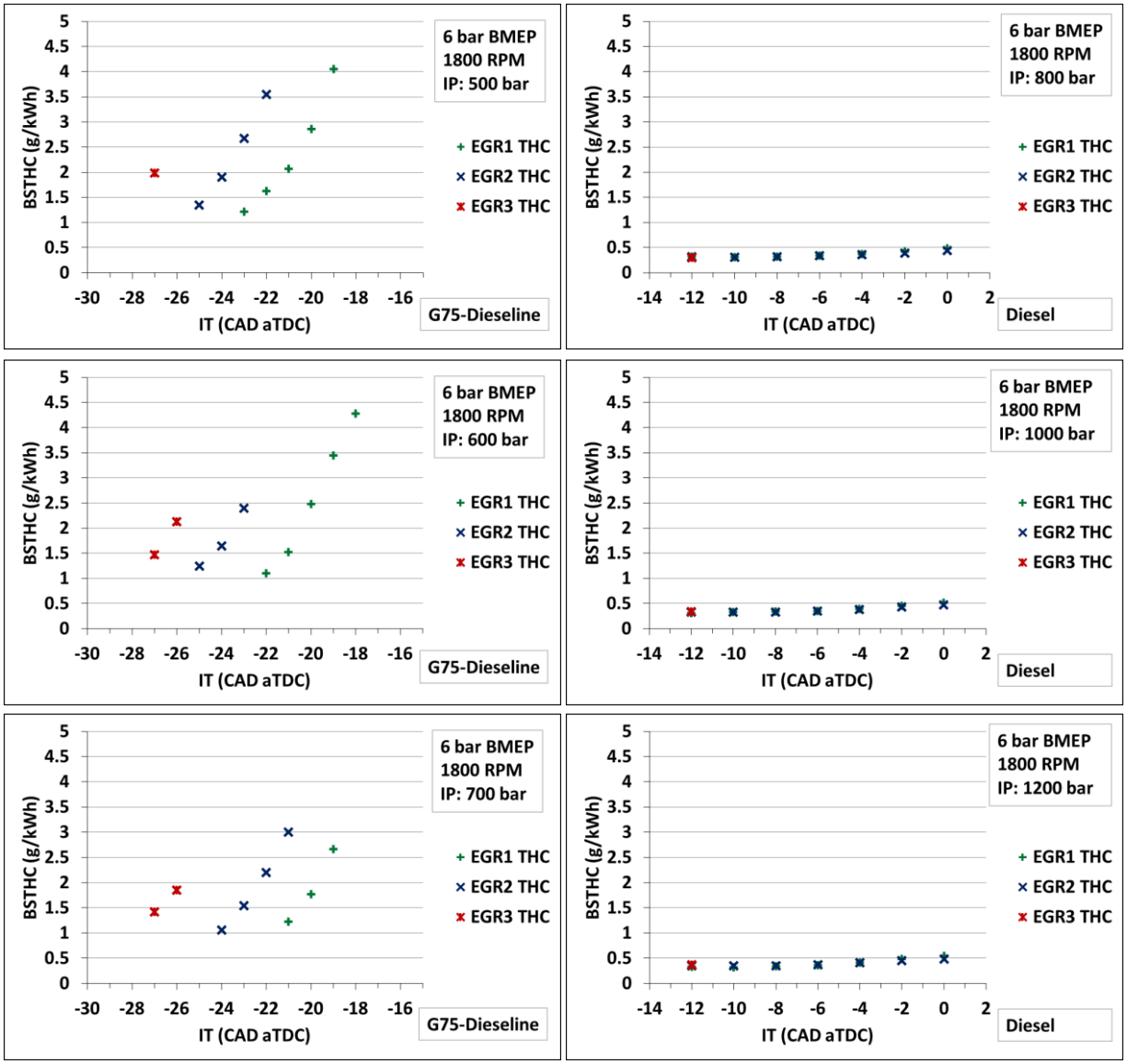


Figure 5-28 Brake specific total hydrocarbons (BSTHC) for G75, left column, and diesel, right column, at different injection pressures, injection-timings and EGR valve positions at 6 bar BMEP

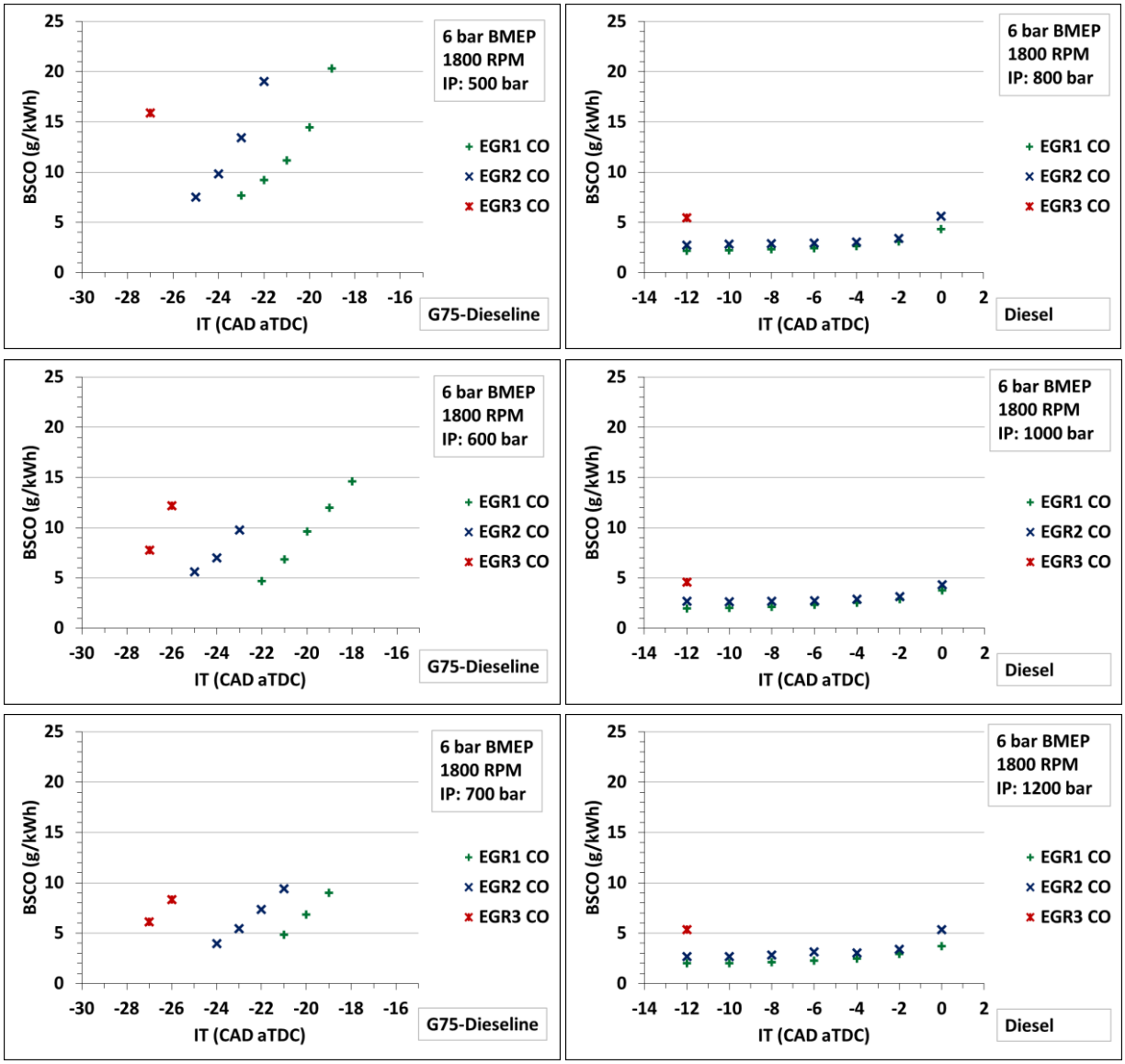


Figure 5-29 Brake specific carbon monoxide (BSCO) for G75, left column, and diesel, right column, at different injection pressures, injection-timings and EGR valve positions at 6 bar BMEP

Figure 5-30 illustrates in-cylinder pressure, HRR and injection pulse of G75 and diesel at two selected points (similar to what was discussed earlier for minimum smoke and maximum BTE). The reason for shorter pulse duration for diesel fuel is the fact that it was injected at higher pressure compared to G75. It can be seen that the separation between EOI and SOC for G75 is more pronounced compared to diesel owing to its longer ignition delay at this load. These points have the same AHR-50 fixed at 12 CAD aTDC. G75 combustion resulted in

higher peak HRR and in-cylinder pressure compared to diesel due to more premixed combustion.

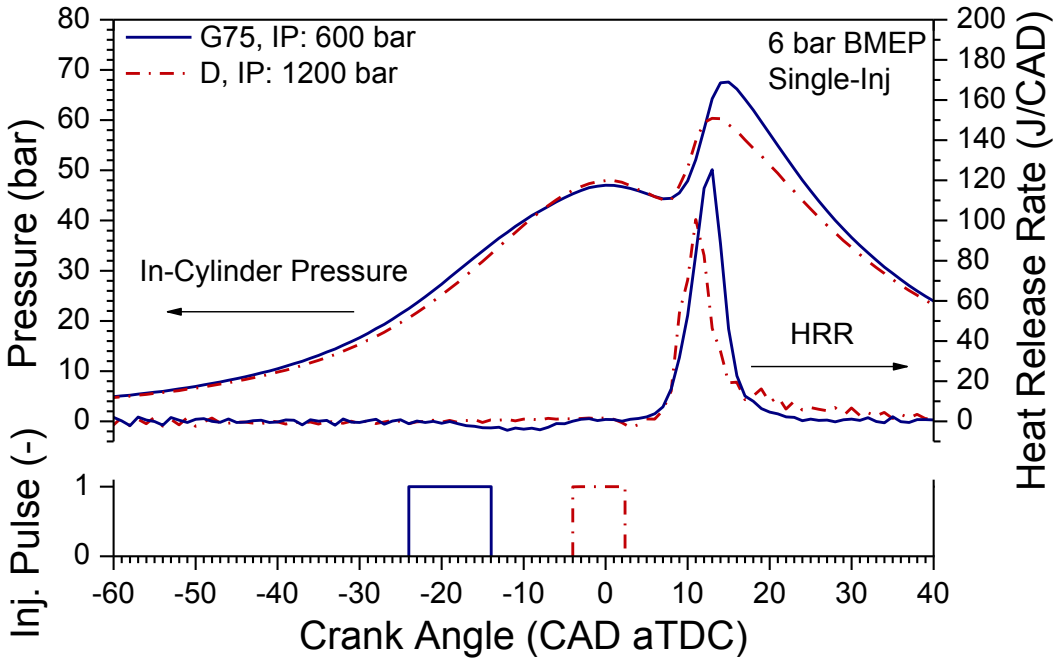


Figure 5-30 In-cylinder pressure, heat release rate and injection pulse for G75 and diesel at 6 bar BMEP using single-injection

5.3.3. Results at 12 bar BMEP

Some screening tests at 10 and 12 bar BMEP with G75 indicated that there are difficulties with achieving low-NO_x and low-smoke combustion. From the screening experiments, it was concluded that λ should be always more than 1.2; otherwise smoke emissions will be more than 3 FSN and combustion will be unstable for G75. Dependence of smoke emissions on this λ limit has a consequence on the $BSNO_x$ emissions as well. Using high rates of EGR in order to reduce $BSNO_x$ will lower λ and consequently higher intake pressure is required to compensate for the reduced intake O_2. Stock high-pressure EGR and VNT turbocharger

system used in this study has a limit in terms of delivering boost pressure. Moreover, more intake boost means more back pressure for the engine and therefore more pumping losses which may result in reduced BTE. Long ignition delay (ID) of G75, compared to diesel, shown at 1.4, 3 and 6 bar BMEP was less significant at 12 bar BMEP; e.g at 1.4 bar BMEP ID of 31 CAD was achieved while at 12 bar BMEP ID was mostly around 9 CAD while injection duration was generally longer. For these reasons, some tests at 12 bar BMEP at two EGR rates (while λ was fixed between 1.2 and 1.3) and different ITs were conducted; results are discussed below.

Figure 5-31 illustrates the results for single-injection of G75 with the IP of 1000 bar at two EGR rates, 15% and 18%, and three different ITs. Utilising IPs below 1000 bar resulted in high smoke values (more than 3 FSN). In this figure, there is also a base case for diesel single-injection with the same IP for comparison purposes. BTE of G75 combustion at this load was influenced by the IT; retarding IT reduced BTE at both rates of EGR. This is due to occurrence of combustion further after TDC, retarded AHR-50, which can reduce BTE as well as MPRR. Smoke emissions followed the same trend in response to retarding the IT, while higher EGR rate resulted in elevated smoke emissions. At this load, it was possible to achieve BTE of 40.54% while smoke was 0.870 FSN and $BSNO_x$ was 1.09 g/kWh for G75. In the case of diesel BTE, smoke and $BSNO_x$ were 40.19%, 2.236 FSN and 0.77 g/kWh respectively. Differences in BSTHC and BSCO emissions from combustion of G75 and diesel are insignificant as shown in Figure 5-31. These results indicate that G75 emissions are more similar to diesel as opposed to observations in the lower studied loads.

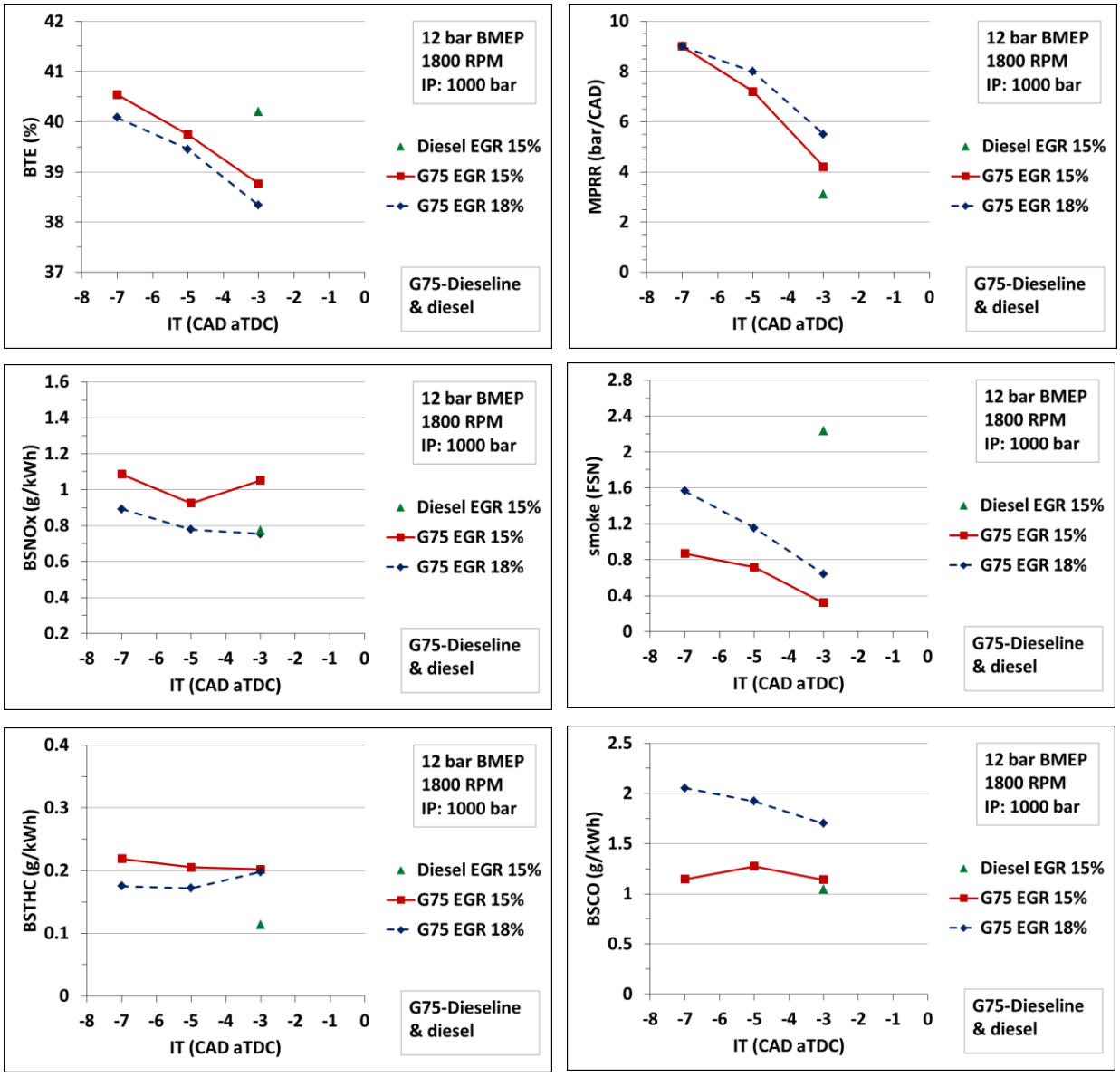


Figure 5-31 Comparison of results of G75 single-injection with the results of base line diesel single-injection at 12 bar BMEP with fixed injection pressure of 1000 bar

As an example, in-cylinder pressure, HRR and injection pulse of G75 was compared to diesel at the same IP, EGR rate and combustion-phasing (Figure 5-32). It is clear that using diesel resulted in a mixing-controlled combustion indicated by the negative ignition dwell and low peak of HRR. On the other hand, G75 combustion was more close to the premixed type combustion with a relatively longer ID, although ignition dwell was not significantly long.

The outcome of the difference between combustion of these two fuels is the higher smoke emissions of diesel shown in Figure 5-31. From these results, clearly MPRR for G75 combustion was higher than diesel at the same AHR-50, although it was <10 bar/CAD.

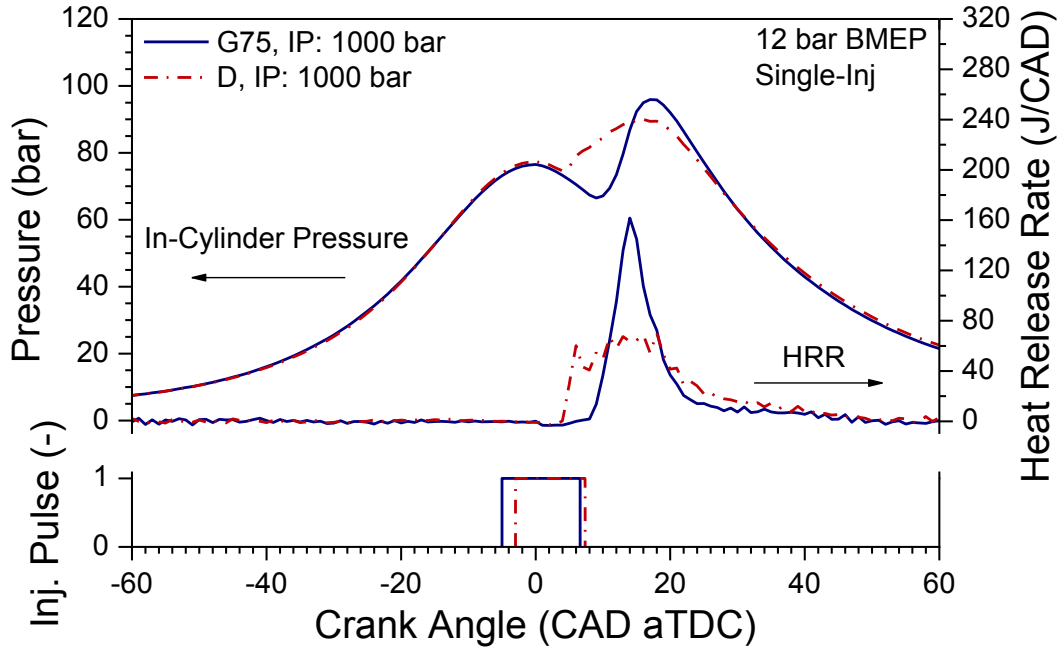


Figure 5-32 In-cylinder pressure, heat release rate and injection pulse for G75 and diesel at 12 bar BMEP, IP of 1000 bar and EGR rate of 15%

Increasing IP to 1200 bar for both fuels, with fixed λ and AHR-50 at 1.2 and 13 CAD aTDC, respectively, resulted in reduced BTE (Table 5-6) compared to results for IP of 1000 bar. While BTE of both fuels was in the same range, smoke emission of diesel combustion was higher than G75 by around 3.35 times. However, $BSNO_x$ emission of G75 was around 1.6 times more than the results for diesel. This means at this load, there is a trade-off between NO_x and smoke reduction for both of the studied fuels. It should be noted that combustion delay of G75 (as a fuel with low CN) at this condition is only 2 CAD longer than that of diesel which is an insignificant difference compared to observations at the lower studied

loads. In terms of brake specific particulate number and size distribution, presented in Figure 5-33, G75 fuel combustion resulted in less TPN (by around 79.5%) compared to diesel combustion while total CMD was 23.1 nm smaller. Distribution of particulates for both of the fuels has a similar profile but there is a difference in absolute values.

Table 5-6 Comparison of G75 and diesel at 12 bar BMEP with fixed injection pressure and combustion-phasing; IT for G75 and diesel were -5 and -3 CAD aTDC, respectively

Fuel	IP	BTE	$BSNO_x$	BSTHC	BSCO	smoke
(-)	bar	%	g/kWh	g/kWh	g/kWh	FSN
G75	1200	39.53	1.01	0.15	1.43	0.819
Diesel	1200	39.78	0.63	0.08	1.40	2.744

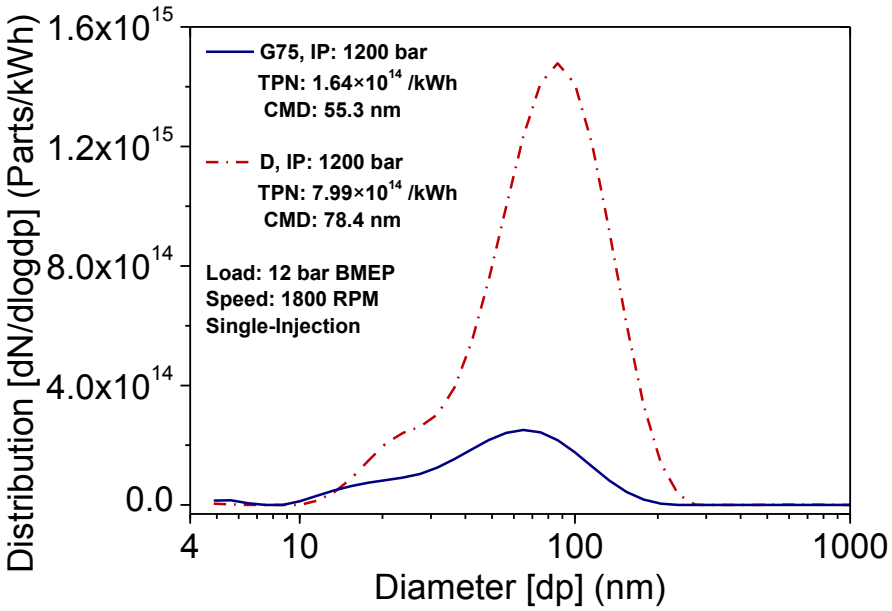


Figure 5-33 Brake specific particulate number and size distributions for G75 and diesel at 12 bar BMEP and IP of 1200 bar

Moreover, increasing IP had some effects on the in-cylinder pressure trace as well. Figure 5-34 shows that increasing IP to 1200 bar resulted in higher peak heat release rate for G75 (compared to the results for IP of 1000 bar) while smoke and $BSNO_x$ were in the same range. Similar to the results for IP of 1000, diesel combustion at this load is more mixing-controlled while G75 combustion is more close to the premixed combustion type indicated by the HRR profile.

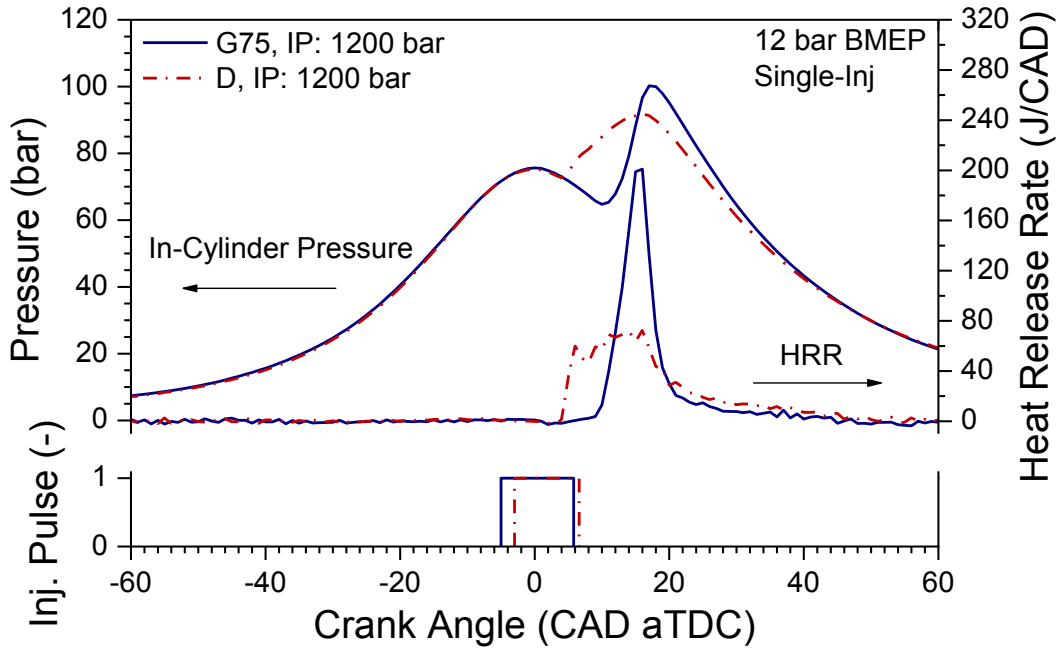


Figure 5-34 In-cylinder pressure, heat release rate and injection pulse for G75 and diesel at 12 bar BMEP and IP of 1200 bar

5.3.4. Results at 17.3 bar BMEP

Results at 17.3 bar BMEP showed similar trends to the results at 12 bar BMEP for G75 fuel combustion. When operating on G75 fuel, IPs above 1100 bar could not be achieved while this was not the case for the diesel fuel. It can be hypothesised that some properties of G75

fuel, most importantly lower viscosity and initial boiling point (IBP), could have some effects on the operation of the high pressure fuel pump. As a future work, addition of viscosity improver can be investigated to identify any improvements when using stock FIE.

Table 5-7 shows the results of G75 combustion at some selected operating conditions. Similar to the lower studied loads, IT can affect combustion and consequently emissions characteristics. Increase of EGR rate and retarding the IT reduced the BTE and $BSNO_x$ and increased smoke. It should be mentioned that absolute intake pressure at this load was more than around 2.5 bar and therefore ID was shorter [67]. Earlier ITs resulted in longer IDs, although for the entire studied cases ignition dwell was negative.

Table 5-7 G75 combustion performance and emissions results at 17.3 bar BMEP and IP of 1100 bar

IT	**EGR**	**BTE**	**$BSNO_x$**	**BSTHC**	**BSCO**	**smoke**	**TPN**	**Acc. PM**
CAD aTDC	%	%	g/kWh	g/kWh	g/kWh	FSN	Number/kWh	g/kWh
-3	4.79	39.25	2.46	0.14	1.02	0.935	2.08×10^{14}	0.068
-3	5.46	39.04	2.11	0.09	0.96	1.024	2.02×10^{14}	0.074
-1	5.02	37.77	1.76	0.07	1.60	2.144	3.15×10^{14}	0.130

Results of the G75 combustion were compared to results of the diesel combustion (listed in Table 5-8) with the same AHR-50 and EGR rate (4.7%). Compared to diesel results, using G75 can reduce smoke emissions by around 44.7% while $BSNO_x$ emissions were higher by around 1.43 times. It seems that properties of G75 fuel are not significantly helpful to reduce NO_x and smoke simultaneously at this high studied load. The mixing-controlled nature of the combustion for both fuels results in observing the trade-off for NO_x and soot reduction. Similar to the 12 bar BMEP, increasing the EGR rate was limited by the available intake boost from the stock VNT turbocharger.

Table 5-8 Comparison of G75 and diesel at 17.3 bar BMEP with the same AHR-50; IT of G75 and diesel were fixed at -3 and 0 CAD aTDC, respectively

Fuel	IP	BTE	$BSNO_x$	BSTHC	BSCO	smoke	TPN	Acc. PM
(-)	bar	%	g/kWh	g/kWh	g/kWh	FSN	Number/kWh	g/kWh
G75	1100	39.25	2.46	0.14	1.02	0.935	2.08×10^{14}	0.068
Diesel	1200	38.96	1.72	0.06	0.95	1.692	3.92×10^{14}	0.146

Figure 5-35 illustrates in-cylinder pressure, HRR and injection pulse for both fuels at 17.3 bar BMEP with settings used in Table 5-8. SOC for both fuels was before the EOI resulting in lower peak of HRR compared to 12 bar BMEP as less premixing was achieved. It can be concluded that G75 and diesel fuel illustrated similar combustion and emissions characteristics at this high studied load. It is suggested that, for both 12 and 17.3 bar BMEP, higher boost pressure should be investigated. It is expected that with higher intake pressure, more EGR can be used and therefore NO_x is reduced while intake O_2 concentration is high enough to either reduce soot formation or improve soot oxidation [34].

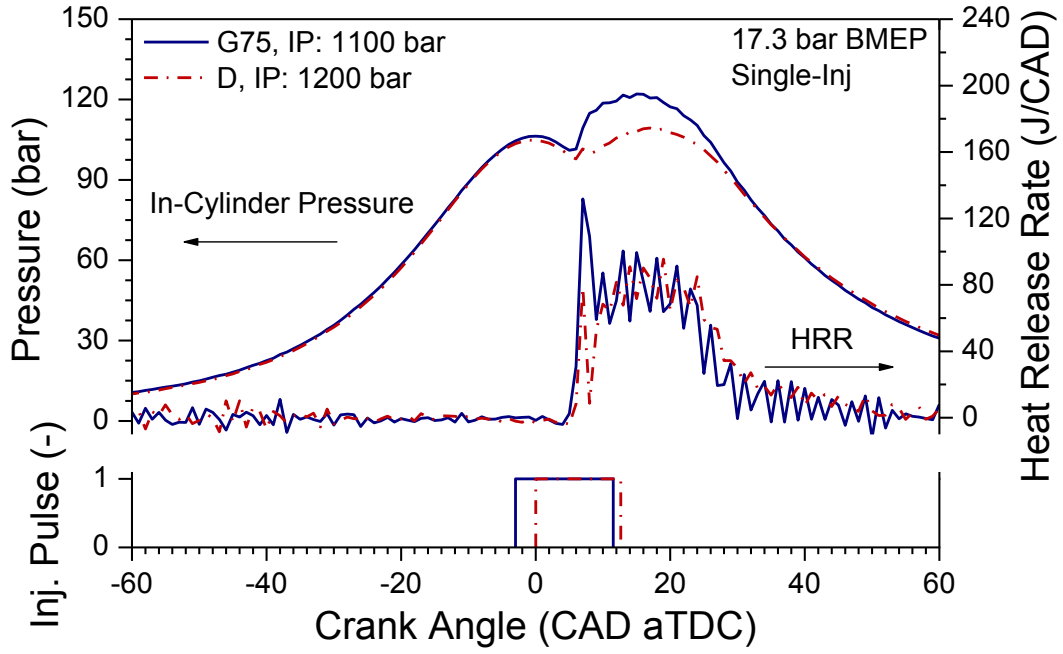


Figure 5-35 In-cylinder pressure, heat release rate and injection pulse for G75 and diesel at 17.3 bar BMEP

5.4. Investigation of double-injection strategies for Dieseline PCI combustion

In the previous section, effects of single-injection strategy on G75 combustion performance and emissions characteristics at different loads were investigated and results were compared to results for diesel. In this section, effects of double-injection strategies at engine operating loads of 1.4, 3, 6 and 12 bar BMEP when using G75 are investigated. Furthermore, some comparisons to double-injection of diesel and also single-injection of both fuels in the same operating loads are conducted. Engine rotational speed was fixed at 1800 RPM for all of the experiments.

5.4.1. Results at 1.4 bar BMEP

Figure 5-36 illustrates results of some selected operating points when using double-injection strategies for G75 and diesel at 1.4 bar BMEP. Double-injection is defined as two separated injection events with different ITs and various quantity-ratios (IQs). As an example for IQ definition, when first injection-quantity (IQ1) is 10%, it means 10% of the total injected quantity is injected in the first injection and 90% is injected in the second injection event.

For both fuels, three levels of IQ1 fixed at 10%, 30% and 50% were used. IQ1 of more than 50% was not studied due to the observed BTE reduction penalty discussed in Chapter 4. First injection-timing (IT1) for G75 was varied at -100, -80 and -60 CAD aTDC, while results at -60 CAD aTDC illustrated engine instability and therefore are not presented. For G75, second injection-timing (IT2) was fixed at -40 CAD aTDC, IP was fixed at 150 bar and hot-EGR strategy (fixed at 52%) was used; with these settings peak BTE is achieved when using single-injection strategy as discussed earlier in this chapter. Moreover, some screening experiments for double-injection strategies with IP more than 150 bar showed BTE reduction. Due to higher CN of diesel, apart from using the same IT1 range studied for G75, more retarded timings at -40 and -20 CAD aTDC were studied. For diesel, IP was fixed at 500 bar and IT2 was fixed at -10 CAD aTDC which helped to maintain combustion-phasing in the same range similar for G75. For comparison purposes, results of the selected points for the single-injection strategy for both G75 and diesel are listed in Table 5-9.

Using G75 with double-injection strategies resulted in lower levels of $BSNO_x$ and smoke emissions compared to using diesel fuel. In general, increasing the IQ1 for both fuels resulted in reduced BTE. Generally for diesel fuel, advancing the IT1 resulted in reduced BTE and increased BSTHC and BSCO emissions. This can be due to increased mixing and possible fuel wall-impingement. Apart from IT1 of -20 CAD aTDC, diesel smoke emissions were

normally less than 0.5 FSN when using double-injection strategies. However, these levels are higher than smoke emissions results for single-injection strategy (as it can be seen in Table 5-9). Results for diesel showed that with retarding the IT1, generally, AHR-50 gets closer to the TDC. This means that first portion of the injected fuel undergoes combustion closer to the TDC as it is injected in an environment with higher pressure and temperature [22]. Lower CN of diesel is responsible for these observations. For G75, AHR-50 always stayed at the same CAD, regardless of the IQ1 or IT1 variations, indicating the importance of IT2 for fixing AHR-50 for PCI mode as shown in Chapter 4. These mean that IT2 can control AHR-50 when there is no combustion from the first portion of the injected fuel in the double-injection strategy.

Peak BTE for G75 combustion using single-injection is higher than all of the achieved BTEs at this load with double-injection. Therefore, as smoke emissions and $BSNO_x$ emissions are low with both strategies, single-injection is preferred. For diesel, combustion and emission characteristics depend considerably on the IQ1 and IT1 as they can change the premixing level and combustion-phasing. In general, for diesel, as expected [2] lower $BSNO_x$ is achieved, while smoke is higher, with double-injection compared to using single-injection.

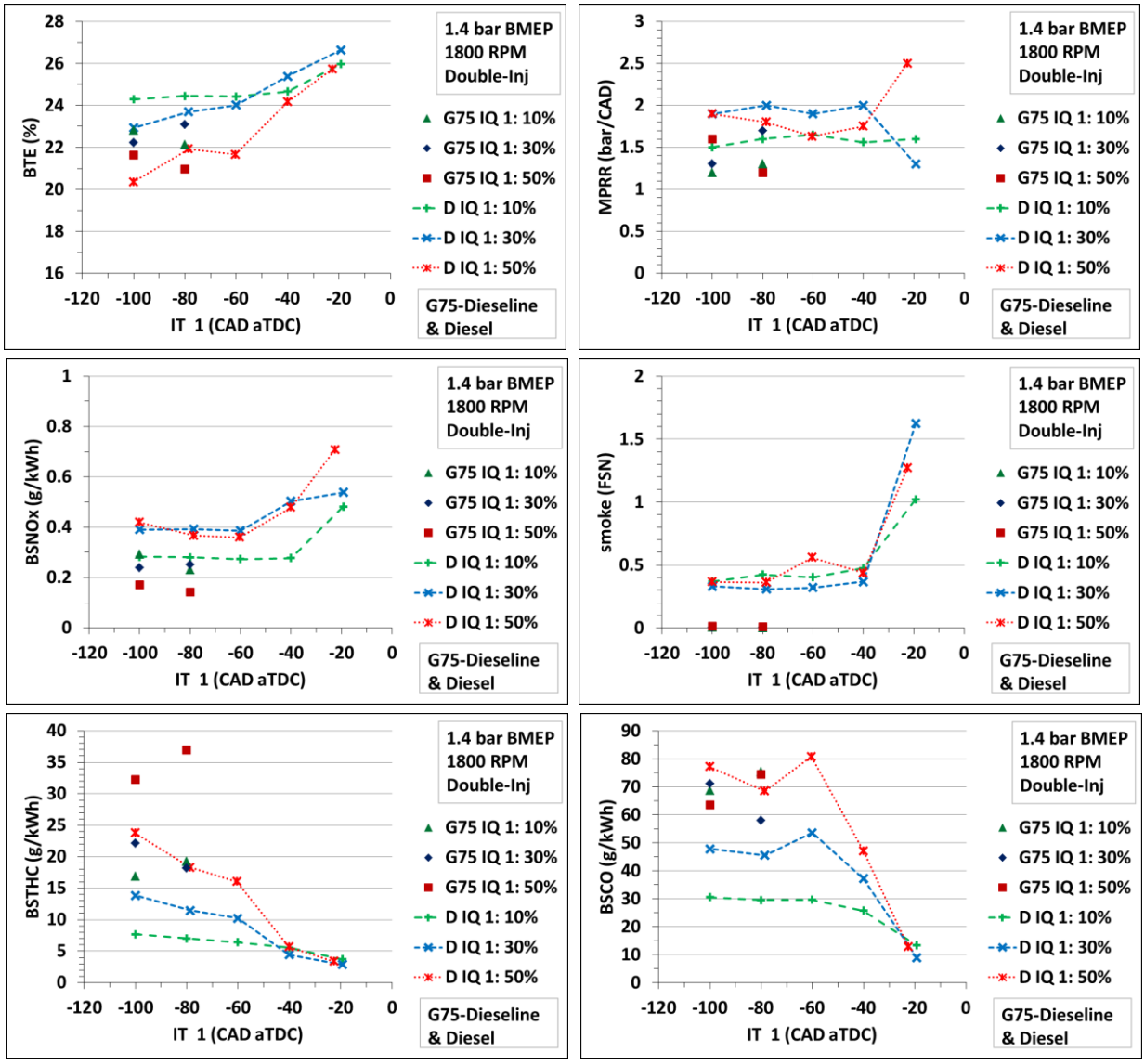


Figure 5-36 Comparison of G75 and diesel when using double-injection strategy at 1.4 bar BMEP

Table 5-9 Results of selected operating points of G75 and diesel fuels at 1.4 bar BMEP using single-injection strategy

Fuel	IP	BTE	$BSNO_x$	BSTHC	BSCO	smoke
(-)	bar	%	g/kWh	g/kWh	g/kWh	FSN
G75	150	24.31	0.25	11.66	57.73	0.001
Diesel	500	26.30	0.72	4.55	17.78	0.061

5.4.2. Results at 3 bar BMEP

Figure 5-37 compares double-injection results for G75 and diesel at 3 bar BMEP. IT2 was fixed at -32.5 and -8 CAD aTDC for G75 and diesel, respectively. IP was fixed at 350 and 700 bar for G75 and diesel, respectively, while hot-EGR was used for G75. These settings were selected based on results of single-injection and some screening tests for high BTE and low emissions. Very high smoke and AHR-50 before TDC limited experiments for the diesel fuel at IQ1 of 30% and 50% and IT1 after -60 CAD aTDC. For comparison purposes, results of the selected points when using single-injection strategy are listed in Table 5-10.

At this load, with the same level of IQ1, G75 and diesel combustion resulted in similar values of BTE. Lower IQ1 at the same IT1 resulted in higher BTE for both of the fuels. Smoke emissions, when using double-injection for G75, were normally lower than results of single-injection strategy (always remained below 0.009 FSN). While smoke emissions of G75 were low (which is in line with lower TPN and Acc. PM), smoke emissions of diesel showed an interesting trend. Increase of IQ1 resulted in elevated smoke emissions and this is believed to be due to occurrence of intense combustion from the first injected portion at the same time with the second injection event. Injection of fuel into an already combusting mixture can increase soot formation rate [2, 22]. $BSNO_x$ emissions from double-injected diesel combustion were higher than results for G75 and diesel single-injection strategy; for all of the studied points $BSNO_x$ was more than 0.4 g/kWh. For G75, at IT1 of -80 CAD aTDC and IQ1 of 10%, maximum BTE (33.30%) in the studied range was achieved while $BSNO_x$ was 0.31 g/kWh. With these settings, diesel combustion resulted in BTE of 33.12% while $BSNO_x$ and smoke were around 1.5 and 24.4 times higher than results of G75. Diesel double-injection compared to the single-injection resulted in around 2.2 times more and 52.9% less $BSNO_x$ and smoke emissions, respectively. Based on these results, double-injection strategy with low

IQ1 percentage for G75 competes with single-injection in order to achieve high efficiency and low emissions while diesel double-injection is limited by either high NO_x or smoke.

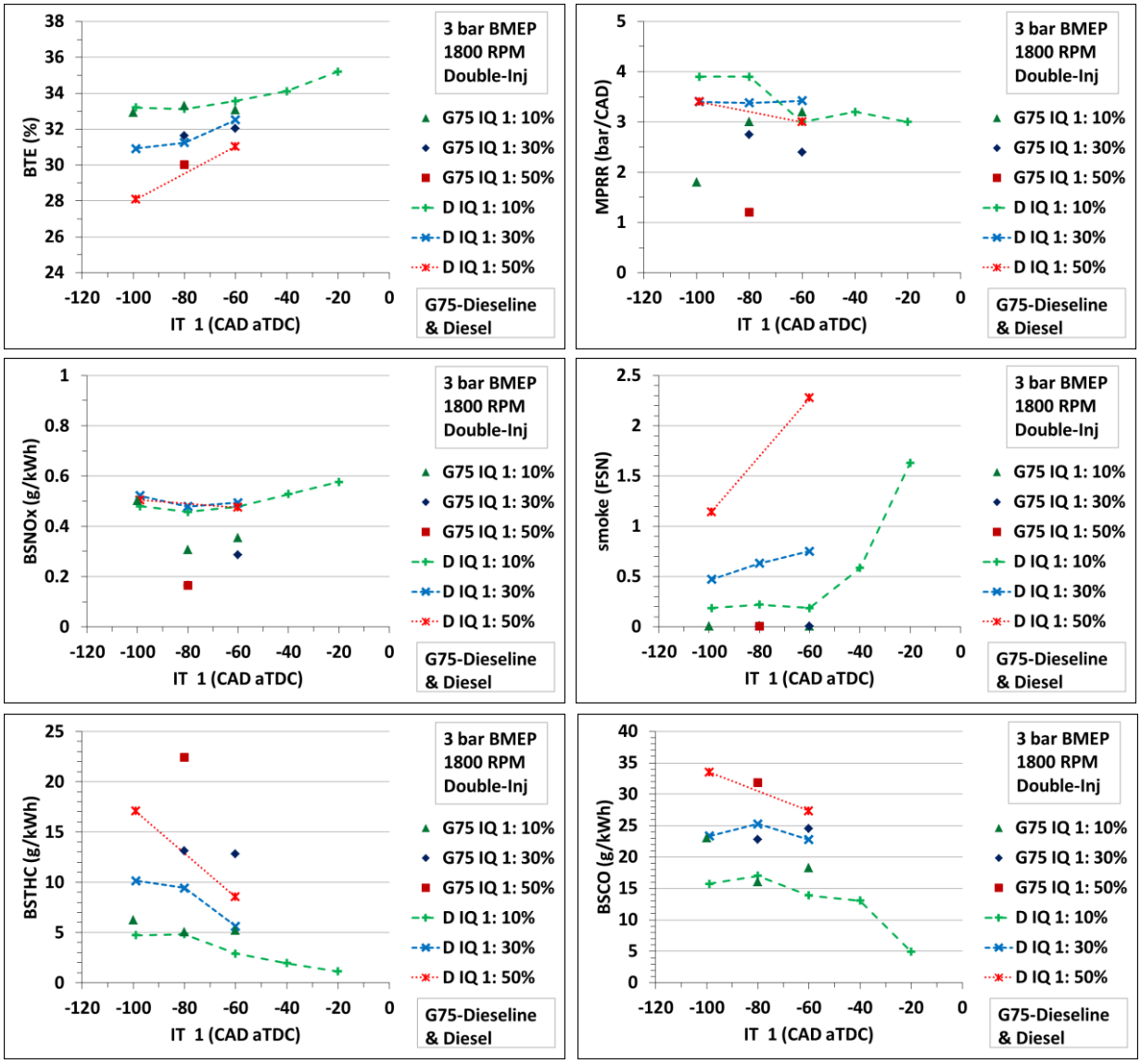


Figure 5-37 Comparison of G75 and diesel when using double-injection strategy at 3 bar BMEP

Table 5-10 Results of selected operating points of G75 and diesel fuels at 3 bar BMEP using single-injection strategy

Fuel	IP	BTE	$BSNO_x$	BSTHC	BSCO	smoke
(-)	bar	%	g/kWh	g/kWh	g/kWh	FSN
G75	350	33.09	0.21	5.58	17.20	0.006
Diesel	700	33.29	0.21	2.29	13.40	0.467

5.4.3. Results at 6 bar BMEP

Double-injection strategies were also investigated for G75 and diesel at 6 bar BMEP (Figure 5-38). IT2 was fixed at -26 and -3 CAD aTDC for G75 and diesel, respectively. When using diesel fuel with IQ1 of 30% and 50%, at any IT1, smoke was more than 3 FSN and for this reason only some selected points are presented. IP for G75 and diesel was fixed at 500 and 1200 bar, respectively, and cold-EGR rate was fixed at 32%.

For G75, using lower IQ1 resulted in higher BTE due to less overmixing of the first portion of the fuel. This claim is supported by the observed higher BSTHC emissions when using higher IQ1 percentage. Contrary to diesel, smoke emissions of G75 were almost zero and $BSNO_x$ emissions were <0.4 g/kWh at all of the studied operating settings. Issues discussed in Chapter 4 of this thesis regarding achievement of double-injection strategies at loads higher than 5 bar BMEP were resolved by using G75 fuel. These results indicate the possibility of achieving low-smoke and low-NO_x emissions while BTE can be more than 38% with low IQ1 for G75 similar to single-injection strategy; Table 5-11 shows the results of some selected points when using single-injection strategy. Diesel double-injection resulted in generally higher smoke emissions.

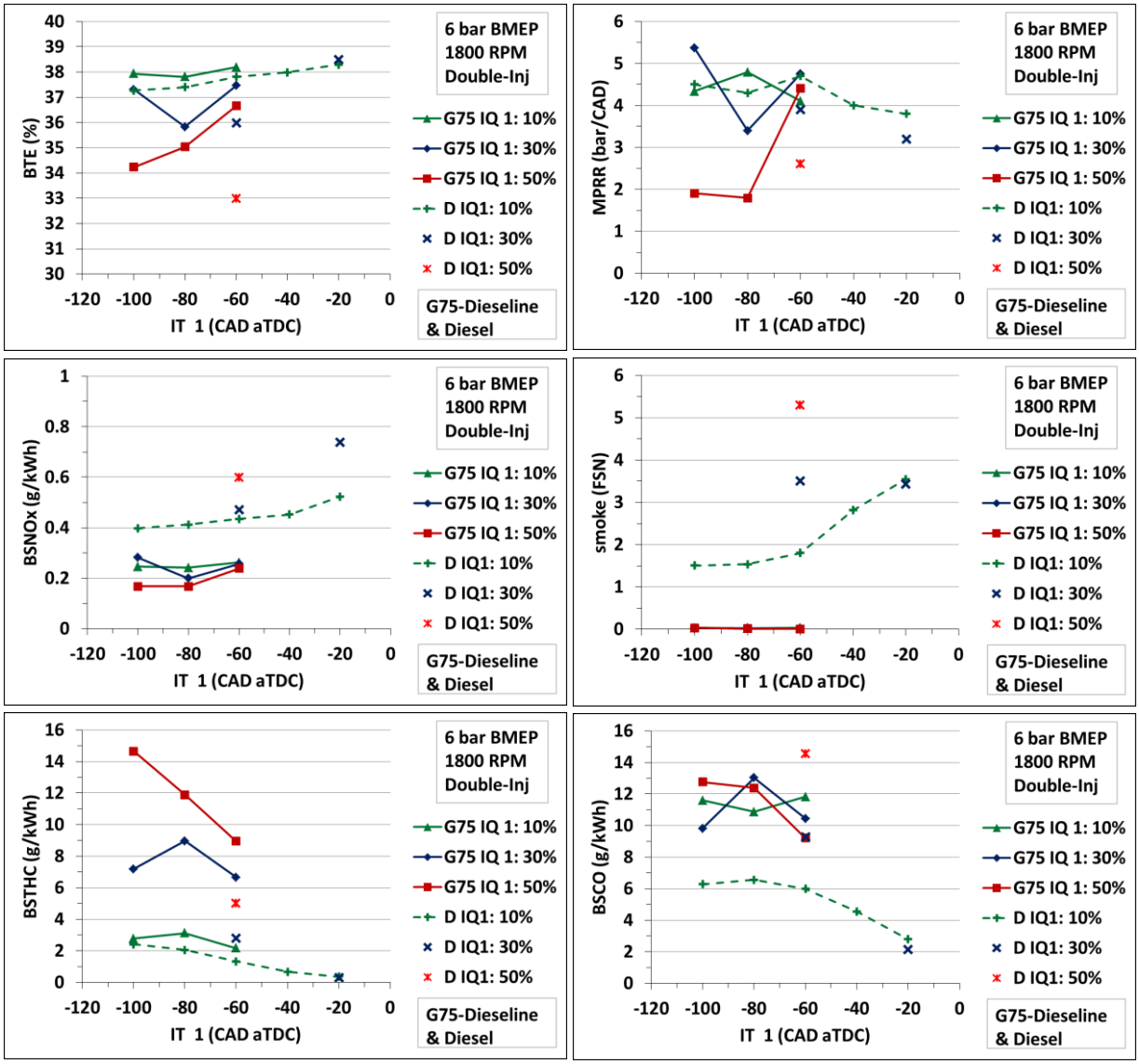


Figure 5-38 Comparison of G75 and diesel when using double-injection strategy at 6 bar BMEP; IP of G75 and diesel were fixed at 500 and 1200 bar, respectively

Table 5-11 Results of selected operating points of G75 and diesel fuels at 6 bar BMEP using single-injection strategy

Fuel	IP	BTE	$BSNO_x$	BSTHC	BSCO	smoke
(-)	bar	%	g/kWh	g/kWh	g/kWh	FSN
G75	500	38.01	0.34	1.91	9.83	0.012
Diesel	1200	38.21	0.34	0.41	3.05	1.428

Plotting in-cylinder pressure, HRR and injection pulse events reveals some more information about the difference between the studied fuels as shown in Figure 5-39. There was no sign of pre-combustion before TDC for the G75 fuel opposite to what was observed for G50 fuel with double-injection discussed in Chapter 4. SOC for G75 was isolated from the end of the second injection regardless of the utilised injection strategy. This can explain achievement of almost zero smoke emissions by enough premixing of fuel and air. In contrast to G75, low ID of diesel fuel resulted in the two-stage combustion event. Depending on the percentage of IQ1, a considerable fraction of heat from combustion was released before the TDC; increasing IQ1 resulted in a more pronounced peak of HRR. This first peak can increase in-cylinder mixture temperature and therefore shorten ID for the second portion of the injected fuel. First-stage of combustion may consume more of the available oxidiser inside the cylinder which will result in higher local equivalence ratios which can be sources of soot emissions. In-cylinder pressure trace profile was effectively influenced by the occurrence of the first-stage combustion. Higher IQ1 resulted in higher first and second pressure peaks for the diesel fuel. A comparison of particulate number and size distribution is illustrated in Figure 5-40 where injection settings are similar to Figure 5-39. In this figure, increase of particulate concentration and CMD with increase of IQ1 is obvious which supports the above discussions.

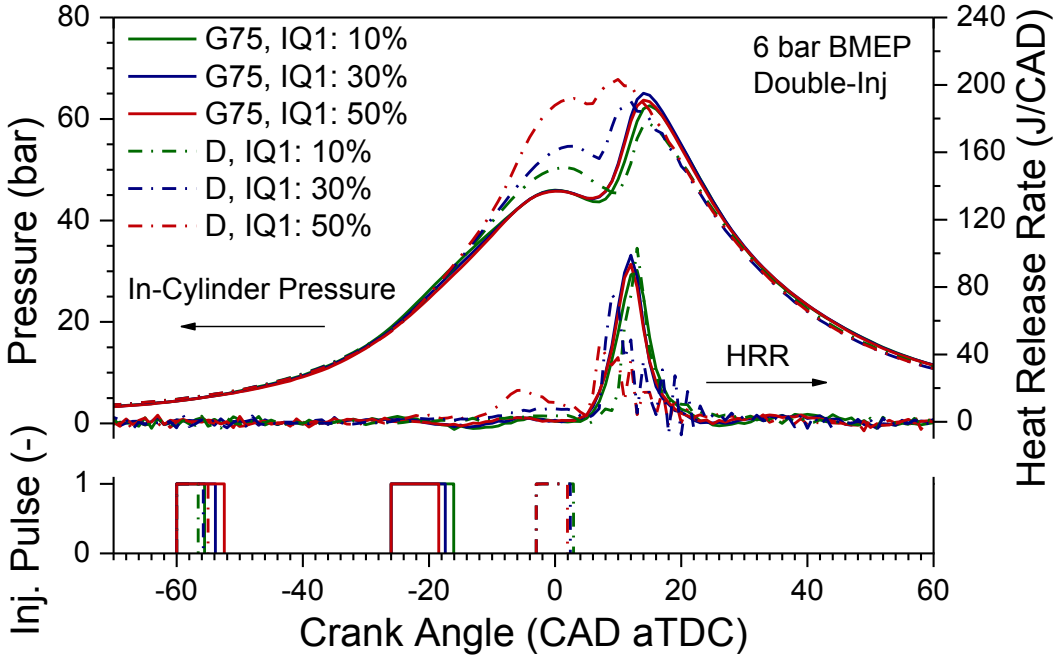


Figure 5-39 In-cylinder pressure, heat release rate and injection pulse for G75 and diesel at 6 bar BMEP with double-injection strategies

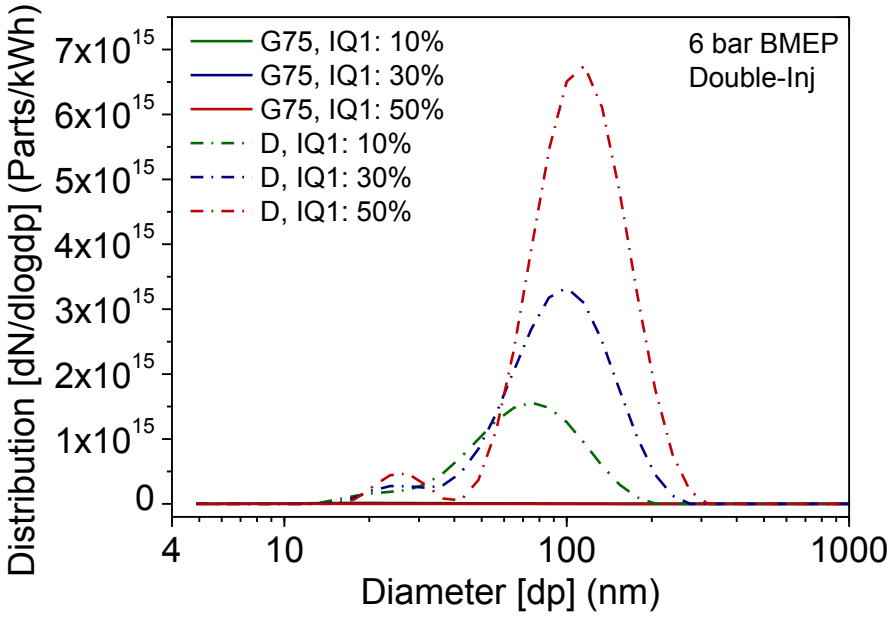


Figure 5-40 Particulate number and size distribution for G75 and diesel at 6 bar BMEP with double-injection strategies

5.4.4. Results at 12 bar BMEP

At 12 bar BMEP, using IQ1 of 50% resulted in high smoke as well as MPRR for both fuels where a major portion of combustion happened before the TDC. This means that even ID of G75 was not long-enough at this load to prevent ignition and combustion before the TDC. Even with lower IQ1, avoiding combustion before the TDC for both fuels was challenging. Similar to the single-injection strategy, smoke emissions of both fuels were high at this load (Figure 5-41). Using IQ1 of 30% for diesel fuel resulted in reduced BTE (around 36.5%) which can be due to negative work on the piston (combustion before TDC) and heat transfer losses (high in-cylinder temperature peak).

Figure 5-42 shows in-cylinder pressure, HRR and injection pulse. For G75, IQ1 of 10% showed similar trends to those of G75 single-injection while IQ1 of 30% resulted in a first-stage combustion peak as was observed for diesel fuel. As mentioned before, shorter ID of G75 at this load resulted in less possibility to achieve a premixed fuel-air mixture and therefore higher smoke was emitted. However, diesel first-stage combustion happened earlier compared to the G75 combustion. For the same points, particulate number and size distribution is illustrated in Figure 5-43. The size distribution of particulates, although observed at lower concentrations for G75, is generally similar for both fuels. Increase of IQ1from 10% to 30% increased CMD and Acc. PM as shown in this figure. At this operating condition where combustion event is more similar for G75 and diesel, there is a scope for studying fuel composition effects, e.g HC structure, aromatics content and oxygenates content, on particulate emissions [24, 141].

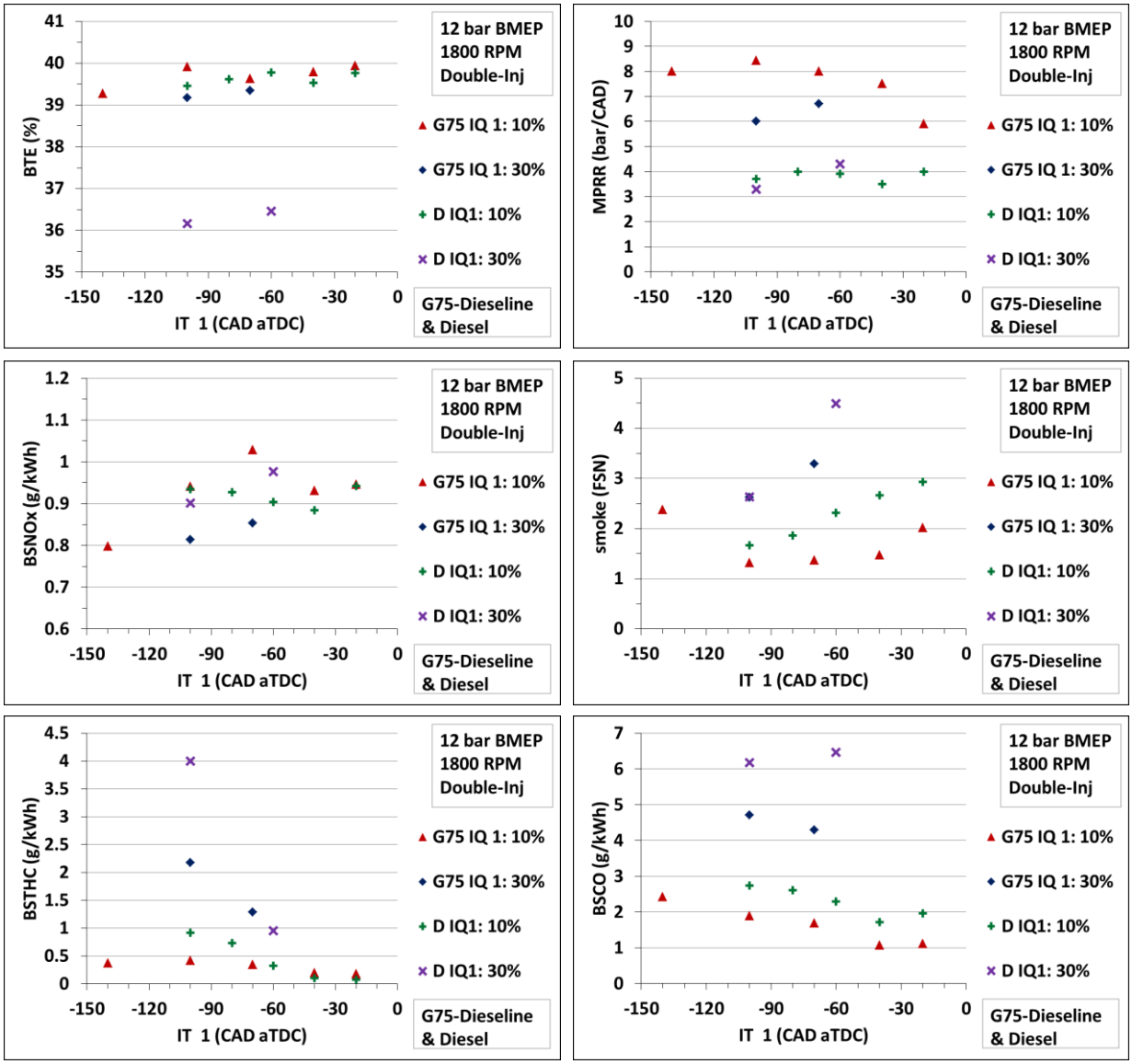


Figure 5-41 Comparison of G75 and diesel when using double-injection strategy at 12 bar BMEP; IP of G75 and diesel were fixed at 1000 and 1200 bar, respectively, and IT2 was maintained at -5 CAD aTDC for G75 and at -3 CAD aTDC for diesel and EGR rate was fixed at 15% for both fuels

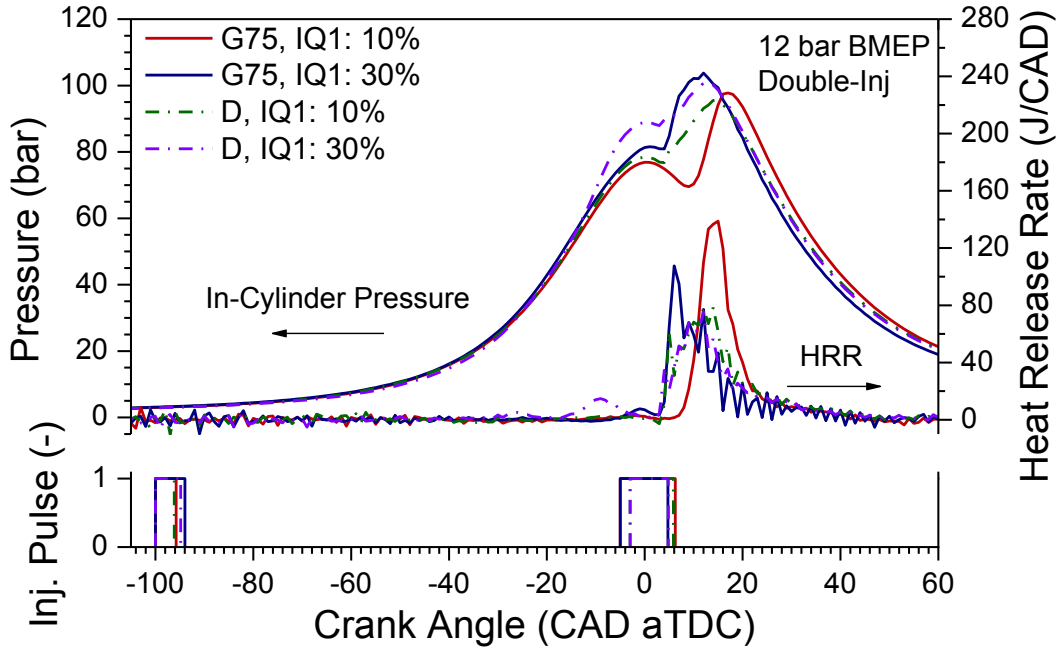


Figure 5-42 In-cylinder pressure, heat release rate and injection pulse for G75 and diesel at 12 bar BMEP with double-injection strategies. Injection pressures of G75 and diesel were fixed at 1000 bar and 1200 bar, respectively

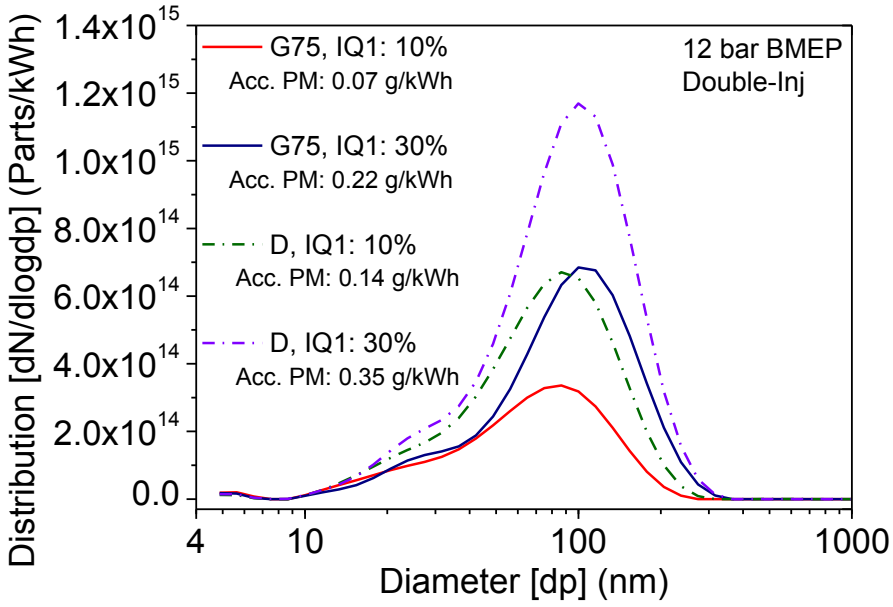


Figure 5-43 Particulate number and size distribution for G75 and diesel at 12 bar BMEP with double-injection strategies. Injection pressures of G75 and diesel were fixed at 1000 bar and 1200 bar, respectively

Lower and higher IPs were studied for G75 and results are listed in Table 5-12. Smoke emission was reduced when IP was increased, although this reduction was insignificant when increasing IP from 1000 to 1100 bar. The rest of the parameters were in the same range with different IPs. These results suggest that due to higher smoke emissions with double-injection and no improvements on other characteristics, single-injection is preferred at this load for both fuels.

Table 5-12 Comparison of different injection pressures for G75 double-injection at 12 bar BMEP. First and second injection-timings were fixed at -40 and -5 CAD aTDC, respectively. EGR rate was fixed at 15% and 10 % of the total injected fuel was injected in the first injection

Fuel	**IP**	**BTE**	**BSNOx**	**BSTHC**	**BSCO**	**smoke**
(-)	bar	%	g/kWh	g/kWh	g/kWh	FSN
G75	900	39.46	0.85	0.19	1.30	2.17
G75	1000	39.79	0.93	0.20	1.07	1.469
G75	1100	39.71	1.08	0.17	1.04	1.37

In addition to Table 5-12, in-cylinder pressure, HRR and injection pulse for these studied IPs are illustrated in Figure 5-44. Minor reduction in the injection duration as a result of elevated IP resulted in a slightly longer ignition dwell which was not significantly helpful for smoke reduction.

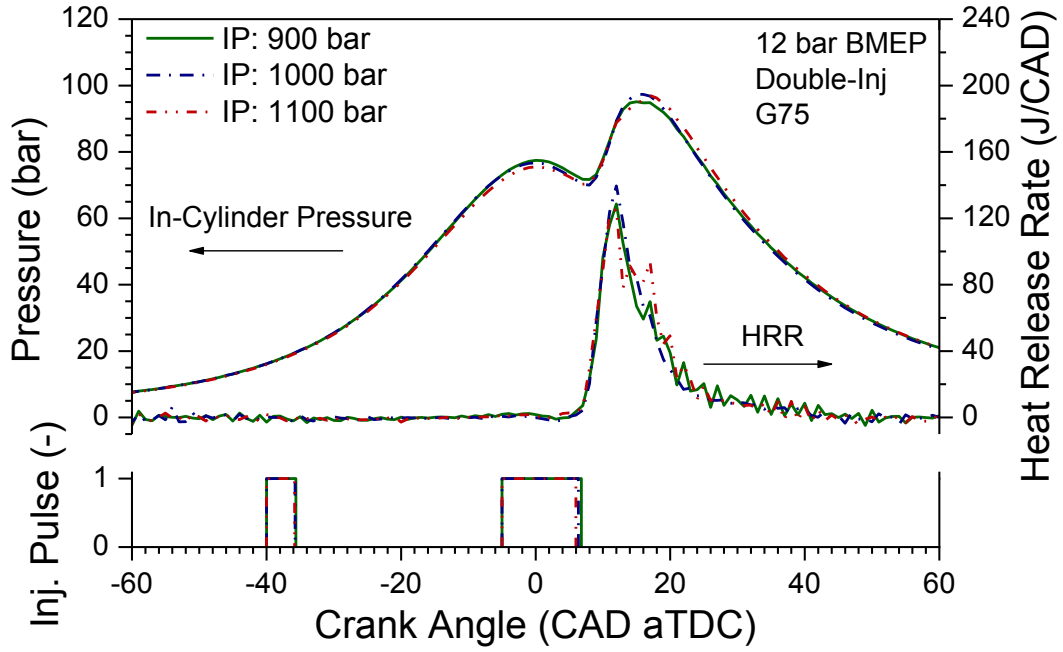


Figure 5-44 In-cylinder pressure, heat release rate and injection pulse for G75 at 12 bar BMEP with different injection pressures and double-injection strategy

5.5. Summary/Conclusions

This chapter investigated G75-Dieseline (G75) PCI combustion and emission characteristics at 1800 RPM and various operating loads: 1.4, 3, 6, 12 and 17.3 bar BMEP. Results were compared to results of diesel combustion. First, some techniques were developed to reduce CO and HC emissions in addition to the combustion instability at 1.4 and 3 bar BMEP. The investigation was followed by studying effects of various injection settings (injection pressure (IP), injection-timing (IT), single-injection and double-injection strategies) and intake/exhaust handling strategies at each of the studied loads. The major findings are as follows:

5.5.1. Effects single-injection with different injection and intake/exhaust handling strategies

- At 1.4 and 3 bar BMEP, hot-EGR strategy was investigated with an incentive to increase engine intake temperature to enhance PCI combustion and reduce CO and HC emissions. Without utilising hot-EGR, G75 PCI combustion is significantly unstable. For diesel, compared to cold-EGR, hot-EGR can reduce both BSTHC and BSCO by more than 30%. However, it can increase smoke considerably (by up to 3.9 times) for diesel with two possible mechanisms: thermal effect and throttling effect (reduced intake O_2 concentration). Changes in the smoke emissions while varying the EGR rate are minimal for G75 as opposed to diesel. Increasing EGR rate to reduce $BSNO_x$ from diesel combustion was accompanied with reduced BTE and increased smoke and THC emissions. Better fuel-air mixing (for lean mixture) due to longer ignition delay and consequently lower HRR peak for G75 compared to diesel can explain these results.

- At 1.4 and 3 bar BMEP, using IPs of more than 350 bar for G75 resulted in elevated cyclic variations, HC and CO emissions probably due to excessive overmixing and fuel wall-impingement. COV of NIMEP of G75 PCI can be reduced from around 60% to less than 2% with using low IP (between 150 and 350 bar) and hot-EGR. It can be hypothesised that with the utilised low IPs for G75, higher degree of stratification, shorter penetration and liquid length and reduced wall-impingement can be some benefits apart from lower cost of the fuel injection system. In attempts to reduce high smoke emissions from high-EGR driven low-NO_x combustion of diesel by using higher IPs, it was found that there is a penalty of reduced BTE probably due to higher parasitic losses, fuel wall-impingement and overmixing. Higher BSTHC and BSCO emissions is the penalty of using G75 compared to diesel; however, these emissions are well-reduced by a DOC as

discussed in Chapter 7. Therefore, it can be concluded that at low engine loads, hot-EGR and low IP are helpful for improving the combustion efficiency of the low-cetane fuel (G75) PCI combustion while smoke emissions are low. However, using diesel fuel needs cold-EGR and higher IP or otherwise particulate emissions will be high.

- At 6 bar BMEP, IP>500 bar and cold-EGR are required to benefit from low smoke and high BTE of the G75 PCI. At each studied IP, BTE and $BSNO_x$ were functions of IT and EGR settings for both G75 and diesel. Either of advancing IT or increasing IP or increasing λ shifted combustion-phasing towards the TDC and therefore increased BTE, MPRR and $BSNO_x$. Compared to diesel combustion with higher IP (more than 800 bar) while $BSNO_x$ was below 0.4 g/kWh and BTE was in the same range, BS particulate mass and BS total particulate number (TPN) emitted from G75 combustion were lower by up to 99.5%. Particulates emitted from diesel combustion are mainly dominated by larger agglomerates while both nucleation and accumulation mode particulates are low from G75 combustion. Changes in combustion and emission characteristics of G75 when varying the IT is more significant compared to diesel. This indicates the importance of the combustion-phasing for G75 due to its longer ignition delay. There is a trade-off between THC-CO reduction and NO_x reduction when operating on G75. These highlight the need for optimising engine controlling parameters as well as cylinder geometry for PCI combustion. The main issue for diesel combustion at this load is high smoke emissions which can be reduced at the expense of either increased $BSNO_x$ or reduced BTE. For both fuels there is a trade-off between increasing BTE and reducing NO_x. Finally, it is concluded that with the same $BSNO_x$ and BTE, compared to diesel, G75 fuel can reduce particulate emissions significantly due to longer ignition delay and higher volatility.

- At 12 bar BMEP when using G75, it was found that λ should be always more than 1.2; otherwise smoke emissions and combustion instability will be high. Due to limitations of the turbocharging system of the stock engine, this implies some difficulties with using higher EGR rates to lower down NO_x. At this load, the difference between ignition delay of G75 and diesel was less significant compared to the lower studied loads due to higher in-cylinder pressure and temperature. Therefore, IP was required to be more than 1000 bar to improve fuel-air mixing and to shorten injection duration to avoid high soot emissions. However, compared to the slightly less-efficient diesel combustion, more-premixed type G75 combustion resulted in less BSTPN and smoke by around 79.5% and 61.1%, respectively, while diesel $BSNO_x$ was lower by around 29.4%. Therefore, although it is possible to reduce particulate emissions with using G75 compared to diesel at this load, it is challenging to reduce NO_x and smoke simultaneously and the need for a more robust boosting system is obvious.

- At 17.3 bar BMEP, using G75 resulted in mixing-controlled dominated combustion while particulate emissions were lower by more than 45% compared to diesel. Simultaneous NO_x and smoke reduction is challenging and it is recommended to study intake boost pressures higher than 2.5 bar absolute with high EGR rates.

5.5.2. Effects of double-injection strategies

- At 1.4 bar BMEP, increasing the first injection-quantity (IQ1) resulted in lower BTE for both G75 and diesel due to possible overmixing and wall-impingement. Using G75 with double-injection strategies resulted in lower levels of $BSNO_x$ and smoke emissions compared to diesel. Due to the occurrence of two-stage combustion, using the studied double-injection strategies for diesel showed higher smoke. For diesel, combustion and

emissions characteristics depend considerably on the IQ1 and IT1 as they can change the premixing level and combustion-phasing. When using G75, peak BTE of the double-injection (23.09%) was lower than single-injection (24.31%). Using single-injection strategy for G75 showed low levels of smoke and NO_x emissions and therefore at this load, considering the BTE penalty, double-injection strategy is not recommended.

- At 3 bar BMEP, increase of IQ1 reduced BTE for both fuels. For diesel, injecting more than 30% of the total fuel quantity in the first injection resulted in intense combustion of this portion before the TDC and therefore high smoke emissions due to double-stage combustion. For G75, the range of BTE values was similar to the results of single-injection of G75 and diesel. Both $BSNO_x$ and smoke emissions from G75 combustion were considerably lower than diesel. Similar to the previous load, IT2 can effectively control the combustion-phasing for G75. Based on these results, double-injection strategy with low IQ1 percentage for G75 competes with single-injection in order to achieve high efficiency and low emissions and therefore there is no preference on the injection strategy. However, diesel double-injection is limited by either high NO_x or high smoke.

- At 6 bar BMEP, limitations with double-injection strategy for achieving single-stage combustion discussed in Chapter 4 were overcome by using G75 instead of G50. In contrast to high smoke emissions from diesel combustion, G75 PCI resulted in near-zero smoke emissions while $BSNO_x$ was less than 0.4 g/kWh. Similar range of BTE levels for single-injection and low-IQ1 double-injection was observed for G75 while $BSNO_x$ was slightly lower and BSTHC and BSCO were slightly higher for double-injection. Therefore, as the differences are small, there is no preference on the injection strategy for G75. For diesel fuel, increase of particulate concentration and CMD with increase of IQ1 was obvious. Therefore, double-injection strategy is not recommended for diesel at this load due to high smoke emissions.

- At 12 bar BMEP, when using double-injection strategy for both G75 and diesel, a HRR peak was observed for the first injected fuel portion before the TDC due to the short ignition delay. Under the boosted-high-load conditions, ignition delay of G75 was not significantly longer than diesel. Achievement of simultaneous low-smoke and low-NO_x was challenging at this load in the studied multi-cylinder stock CI engine. These results suggest that due to higher smoke emissions with double-injection and no improvements on other characteristics, single-injection is preferred at this load for both fuels.

Finally, it was shown that by using the developed techniques, G75 PCI can reduce particulate emissions at all of the studied loads while maintaining the same range of BTE and NO_x compared to diesel fuel combustion. Combustion of G75 was shown to be more sensitive to the changes of engine controlling parameters and this highlights the need for a comprehensive optimisation of engine to suite PCI combustion. It can be concluded that if there is a long-enough ignition dwell then it is better to use low IP to enhance PCI combustion. In general as smoke and NO_x emissions from PCI combustion are already low, single-injection is favoured over double-injection to avoid complexity, high HC/CO (at low loads) and possible high smoke (at high loads). The need for detailed in-cylinder optical studies and simulation of chemical kinetics under the studied PCI conditions is obvious.

Chapter 6
NAPHTHA FUELLED PREMIXED COMPRESSION IGNITION COMBUSTION ENGINE

6.1. Introduction

Results of G75-Dieseline (G75) fuel combustion, compared to diesel fuel, illustrated benefits of reduced $BSNO_x$ and smoke with similar BTE in a wide load range from 1.4 to 17.3 bar BMEP. Earlier introduction provided for the naphtha fuel, in Chapter 2, discussed the possibility for this fuel to be a candidate in the upcoming years. This chapter focuses on the naphtha PCI/GCI combustion and compares it to G75 and diesel combustions. The main objective is to investigate effects of the narrower boiling range of naphtha compared to G75 on PCI/GCI combustion performance and emission characteristics. For this reason, the studied naphtha fuel has almost similar derived cetane number (DCN) as the studied G75; full specification of this fuel was provided in Chapter 3.

6.2. Investigation of single-injection strategy at different operating loads

In this section, results of single-injection of naphtha at different engine operating loads of 1.4, 3, 6, 12 and 17.3 bar BMEP are presented. Engine rotational speed was fixed at 1800 RPM for all these experiments. The intention of these tests was to repeat similar engine operating conditions studied for G75 and diesel fuels in Chapter 5. In some conditions minor modifications to engine controlling parameters were inevitable as some properties of the

naphtha fuel and its performance in the engine are different compared to G75 and diesel; if applicable, these are clarified for each operating load.

6.2.1. Investigation of different injection pressures and timings at 1.4 bar BMEP

Combustion and emission characteristics of naphtha CI at 1.4 bar BMEP while using single-injection are illustrated in Figure 6-1. Studied conditions were kept similar to the case of G75, e.g. three injection pressures (IPs) of 150, 250 and 350 bar while varying injection-timing (IT) at -20, -30 and -40 CAD aTDC. At this load, similar to the case of G75, usage of cold-EGR resulted in very unstable combustion and therefore hot-EGR strategy, explained in depth in Chapter 5, was used.

The main issue at this load with the combustion of naphtha was high coefficient of variation (COV) of net indicated mean effective pressure (NIMEP) with IPs of 250 and 350 bar. Even with IP of 150 bar at IT of -20 CAD aTDC, results showed high COV of NIMEP (around 49%). This cyclic variation is linked with misfire/incomplete-combustion and some random sudden combustion events causing smoke emissions to be unexpectedly high at some conditions as shown in Figure 6-1. COV of NIMEP was increased as the IP was increased from 150 to 350 bar. These were expected to some extent as naphtha is more volatile (has a narrower boiling range) compared to G75. Moreover, the probability of having higher fraction of long-chain n-alkanes, which easily auto-ignite and help to proceed to the combustion event, is lower for naphtha. Additionally, more volatility of naphtha favours overmixing phenomenon which can cause misfire and combustion instability. It can be hypothesised that these properties of naphtha reduce the degree of stratification and consequently result in overmixing at low loads and rapid combustion at higher loads (discussed later in this chapter) which are, normally, issues with the HCCI type combustion [63]. It can be concluded that at

this load, under the studied engine controlling parameters settings, usage of only IP of 150 bar, and to some extent 250 bar, resulted in acceptable levels of BSTHC, BSCO and COV of NIMEP (below 10%). However, these levels are higher than results of G75 and diesel presented in the previous chapter.

Generally, at every injection-timing, BTE was the highest for the IP of 150 bar. $BSNO_x$ emission target of less than 0.4 g/kWh was difficult to be achieved for IPs of 250 and 350 bar at ITs of -20 and -30 CAD aTDC which had high COV of NIMEP. In general, usage of lower IP resulted in lower BSTHC and BSCO emissions. It can be concluded that for naphtha single-injection, very low IPs can be studied. However, there is a lower limit for the diesel engine conventional common rail fuel injection equipment (FIE) and for the case of the current studied engine it is 150 bar and therefore it was not possible to study lower IPs. Outside this range of studied ITs and IPs, results were not acceptable in terms of COV and THC and CO emissions.

Compared to the selected point of G75 results in Chapter 5 with the same settings, at the peak BTE settings for naphtha, BTE was 2.54% lower (in absolute value), BSCO and BSTHC were higher by around 1.4 and 2.5 times, respectively, while smoke was the same. This shows better performance of G75 compared to naphtha in the studied engine at this load.

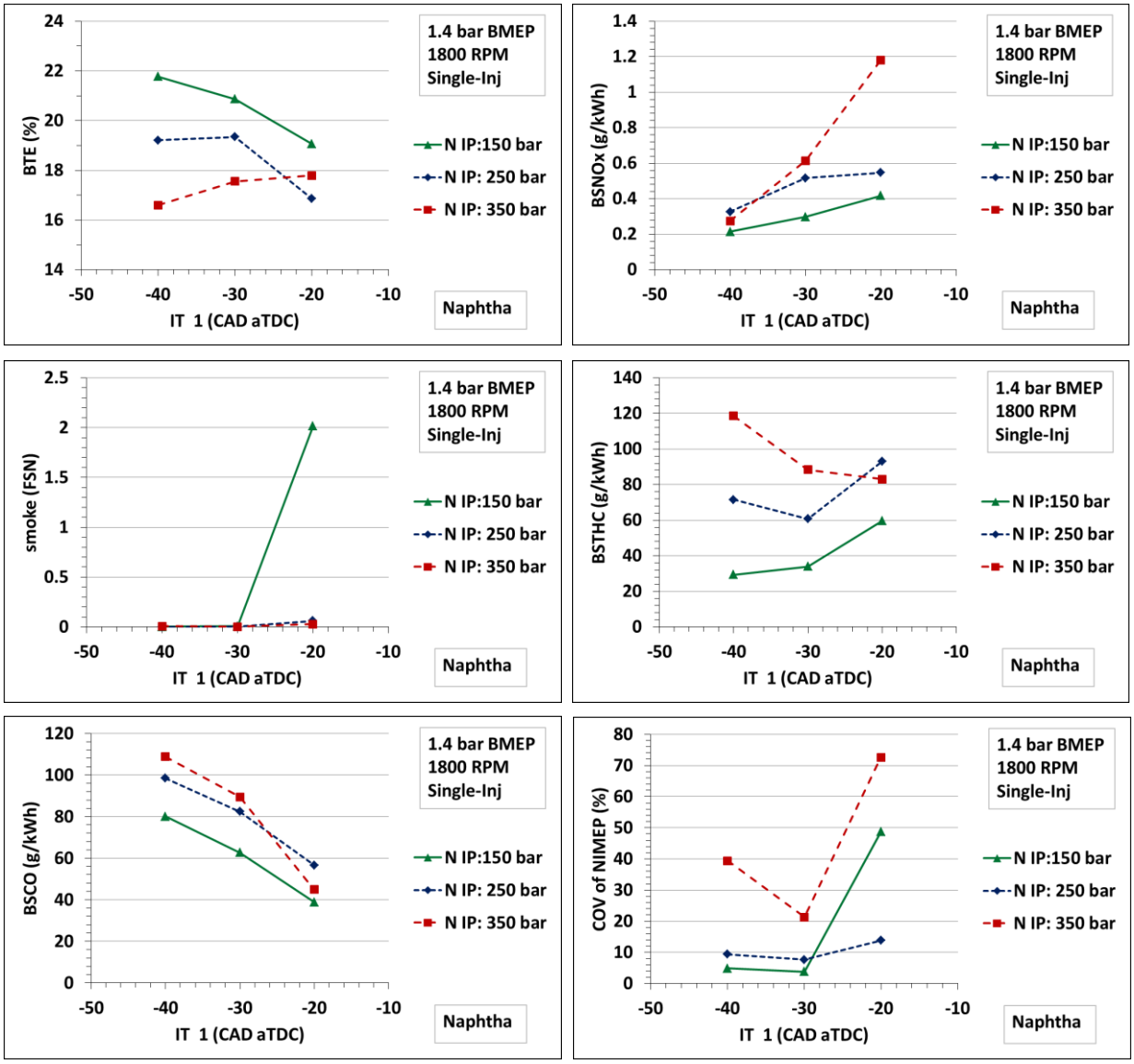


Figure 6-1 Combustion and emissions characterises of naphtha compression ignition at 1.4 bar BMEP while using single-injection strategy

6.2.2. Investigation of different EGR rates at 1.4 bar BMEP

In addition to the discussed experiments, some more experiments at two IPs of 150 and 250 bar were conducted to identify effects of the hot-EGR rate sweep (Figure 6-2). IT for these experiments was fixed at -40 and -30 CAD aTDC for IPs of 150 and 250 bar, respectively, selected based on the results presented in Figure 6-1 for maximum BTE at each IP.

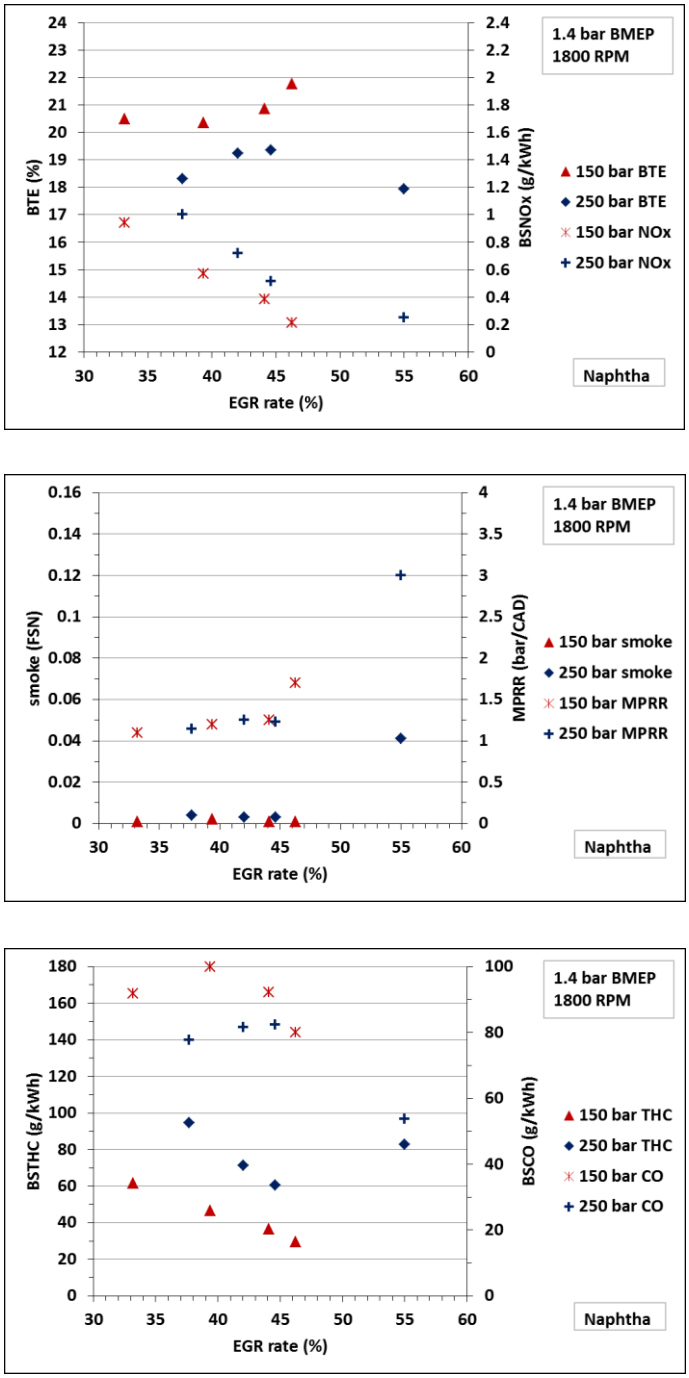


Figure 6-2 Effect of varying EGR rate for naphtha compression ignition at 1.4 bar BMEP while using single-injection

Figure 6-2 shows that increasing EGR rate reduces $BSNO_x$ emissions monotonically. In general, increasing EGR rate improved BTE and this is due to the fact that increasing hot-EGR rate increases the intake temperature and therefore helps reduce BSTHC and COV of

NIMEP. More discussion on this topic was provided in Chapter 5. However, the increase in BTE has a limit where using more EGR rate reduces BTE. This can be observed for the IP of 250 bar and EGR rate of 55%. At these settings, BTE dropped to less than 18% and BSTHC increased probably due to excessive dilution. Smoke emissions for all these cases stayed at very low levels (close to zero).

6.2.3. Investigation of different injection pressures and timings at 3 bar BMEP

At 3 bar BMEP, similar to the case of G75, three IPs of 150, 250 and 350 bar at three ITs of -52.5, -42.5 and -32.5 CAD aTDC while hot-EGR rate was fixed at 45% were studied (Figure 6-3). At this operating condition, similar trends to the case of G75 were observed. Retarding the IT, generally, resulted in elevated BTE levels and reduced BSTHC and BSCO emissions. High COV of NIMEP was not an issue at this load in contrast to the lower studied load. Increase of IP increased BSTHC and BSCO emissions which can be due to overmixing and fuel wall-impingement (due to longer penetration length of the fuel spray). Regardless of the IP, results at IT of -32.5 CAD aTDC showed higher BTE levels and lower BSTHC and BSCO values. This can be due to shorter ignition delay and possibly less interaction between fuel spray and walls which needs to be confirmed with optical studies.

Results for $BSNO_x$ emissions of naphtha CI showed very similar trends to those of G75 while absolute values were, in general, significantly higher for naphtha. This is believed to be due to more intense peak of HRR and high MPRR resulting in high in-cylinder peak temperature. This is another proof that the narrower boiling range of naphtha can bring the combustion more close to the HCCI type combustion in the current engine. Higher IP, in general, resulted in lower $BSNO_x$ emissions while the reduction amount was IT dependant. This may indicate the presence of some spray-wall interactions. For instance at -42.5 CAD aTDC, smoke

emissions for IP of 350 bar was unexpectedly high, almost 0.4 FSN. Higher IPs at this IT, such as 650 bar, resulted in lower smoke values (0.164 FSN) which is still higher than that of naphtha's expected characteristics at this load. Spray characteristics of naphtha may be different from G75 and can affect spray-wall interaction and consequently mixture formation; this needs to be confirmed with optical studies.

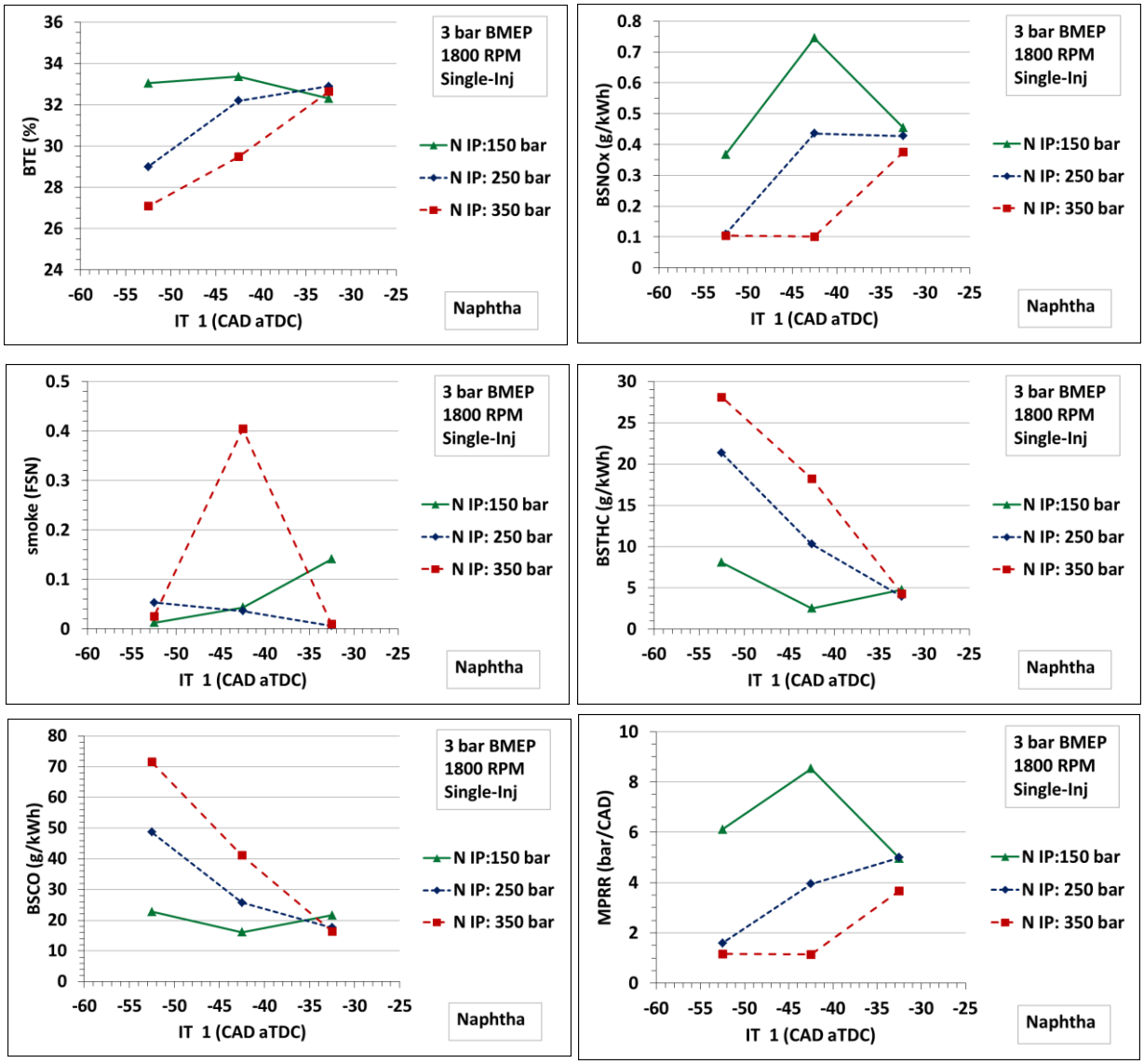


Figure 6-3 Combustion and emissions characterises of naphtha compression ignition at 3 bar BMEP while using single-injection

At this engine load, peak BTE while considering the $BSNO_x$ target of <0.4 g/kWh, was 33.04% at IT of -52.5 CAD aTDC with IP of 150. Referring back to Table 5-10 in Chapter 5, peak BTE for G75 was similar to this value; however, $BSNO_x$ is around 1.8 times higher and smoke and MPRR are 2 times higher for naphtha. Both BSTHC and BSCO are higher for naphtha fuel. Therefore, since smoke emissions are low for both fuels at this load, G75 is preferred as its combustion generally results in lower $BSNO_x$, BSTHC, BSCO and MPRR.

IP sweep was also investigated at this load while fixing the IT at -32.5 CAD aTDC, shown to generally result in higher BTE compared to the other studied ITs. Results illustrated in Figure 6-4 indicate that there is a general decreasing trend for BTE as IP is increased. This is in-line with the fact that BSTHC and BSCO were increasing in general. It should be mentioned that COV of NIMEP, as well, was increased as higher IP was used (e.g. from 1.76% for 150 bar to 18.73% for 650 bar). Overmixing, fuel wall-impingement and some parasitic losses linked with higher IP can all help explain the observed trends. Variations in smoke and $BSNO_x$ are not very sharp. Therefore, there is no incentive to use higher IPs for a fuel like naphtha since these results show that lower IPs are better for improved BTE, combustion stability and combustion efficiency at this load.

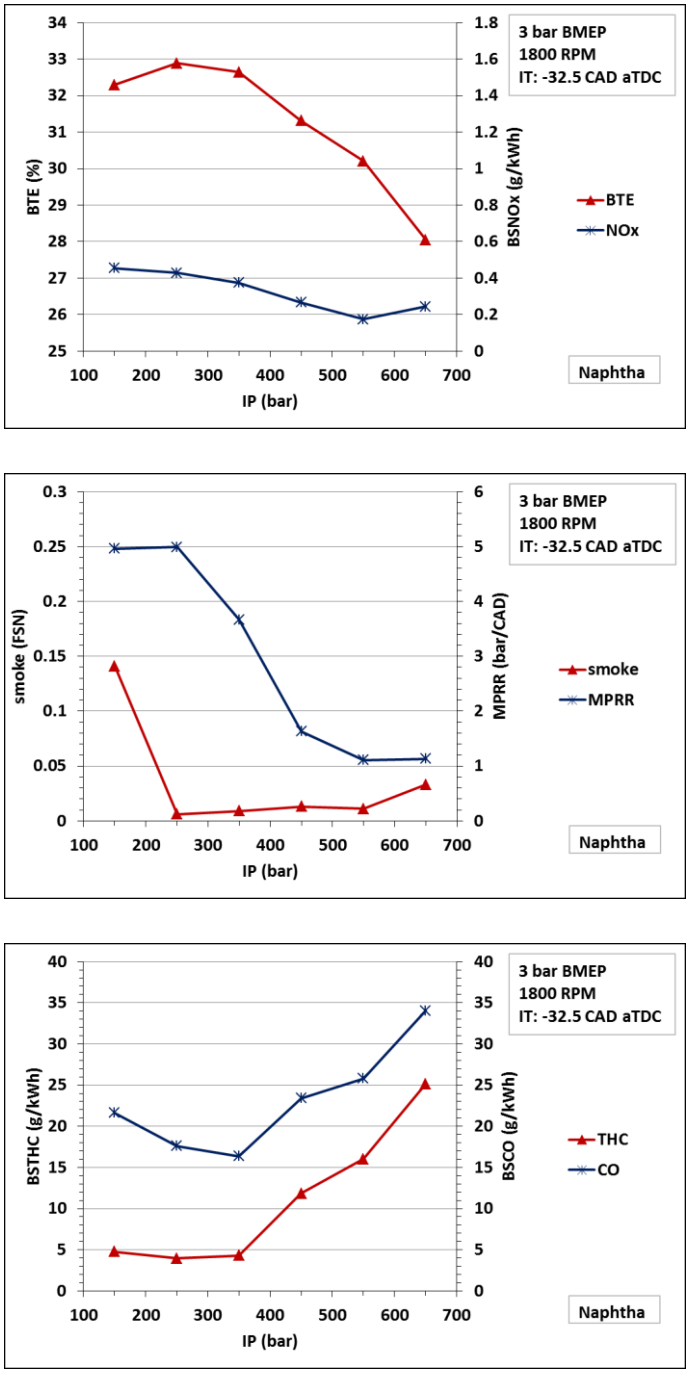


Figure 6-4 Effect of varying injection pressure for naphtha compression ignition at 3 bar BMEP while using single-injection

6.2.4. Results at 6 bar BMEP

Similar to the case of G75, different EGR (cold-EGR) valve settings and IPs were studied for single-injection strategy for naphtha compression ignition at 6 bar BMEP. Naphtha combustion with the exact EGR valve settings used for G75 had some issues. With more EGR valve opening (e.g. EGR2 and EGR3 settings for G75) λ was reduced to less than 1.2 and combustion became very unstable. Results of these test points are not presented due to severe engine instability and this shows the sensitivity of naphtha to the EGR rate. Therefore, a new batch of settings was developed for naphtha; EGR1 refers to 46.5% and EGR2 refers to 48.5% valve opening of the full opening position of the utilised EGR valve. With these settings, λ was between 1.2 and 1.4 and EGR was between 27% and 31%. Figure 6-5 illustrates BTE and $BSNO_x$ results using these two EGR valve settings with three IPs of 500, 600 and 700 bar. With IP of 700 bar, results for EGR2 valve setting showed combustion instability and therefore are not presented. IT limits, similar to the case of G75 discussed in Chapter 5, were selected based on two constraints: (a) MPRR must not exceed 12 bar/CAD and (b) BTE must be more than 33%.

Similar to G75 results, BTE and $BSNO_x$ were functions of IT, IP and EGR valve settings for naphtha. Advancing IT increased both BTE and $BSNO_x$ due to the fact that earlier IT advances combustion event towards to the TDC. With the same IT, increasing IP resulted in higher $BSNO_x$ and BTE as the combustion-phasing (AHR-50) was advanced. At IP of 700 bar, as opposed to the case for G75, achieving the $BSNO_x$ target of <0.4 g/kWh with BTE>33% was impossible. Generally, BSTHC and BSCO emissions from naphtha combustion were higher than the results for G75 and this is discussed later in this sub-section. Smoke emissions of naphtha CI were mostly less than 0.02 FSN and in the same range for G75.

Considering the defined $BSNO_x$ target (<0.4 g/kWh), BTE levels for naphtha were lower than those of G75 (Figure 5-21) at all of the studied IPs. Apart from higher BSTHC and BSCO, this can be hypothesised to be due to the lower charge stratification level when using naphtha, compared to G75, and therefore rapid combustion featuring sudden heat release events. This can increase $BSNO_x$ levels at this load which is a characteristic of HCCI type combustion [63]. It was shown that increasing the IP is helping this process and therefore some lower IPs were studied as presented below. At this load, lower IP is believed to increase stratification level and help to reduce $BSNO_x$ and MPRR for fuels such as naphtha.

IPs as low as 250 and 350 bar were studied and results show that smoke levels are high (in the range of 0.1 to 1 FSN) and BTE levels are low (less than 36%). Therefore, only results for the IP of 400 bar are presented in Figure 6-6. Lower IP helped to reduce $BSNO_x$ emissions while these reductions had the disadvantage of lower BTE at the same $BSNO_x$ levels shown for IPs of 500, 600 and 700 bar. BSTHC and BSCO emissions were increased monotonically as the IT was retarded due to retarded AHR-50. Considering the $BSNO_x$ target of <0.4 g/kWh, maximum BTE for naphtha in the studied conditions was 37.05% while smoke was 0.013 FSN. This BTE is 1.36% lower (in absolute value) compared to the peak BTE achieved for G75 with the same $BSNO_x$ target. BSTHC and BSCO of naphtha were more than two times higher than the results for G75 at the same conditions. Therefore, in view of simultaneously achieving high BTE and low $BSNO_x$, BSTHC and BSCO, G75 performed better than naphtha at this engine load condition probably due to higher degree of fuel-air mixture stratification.

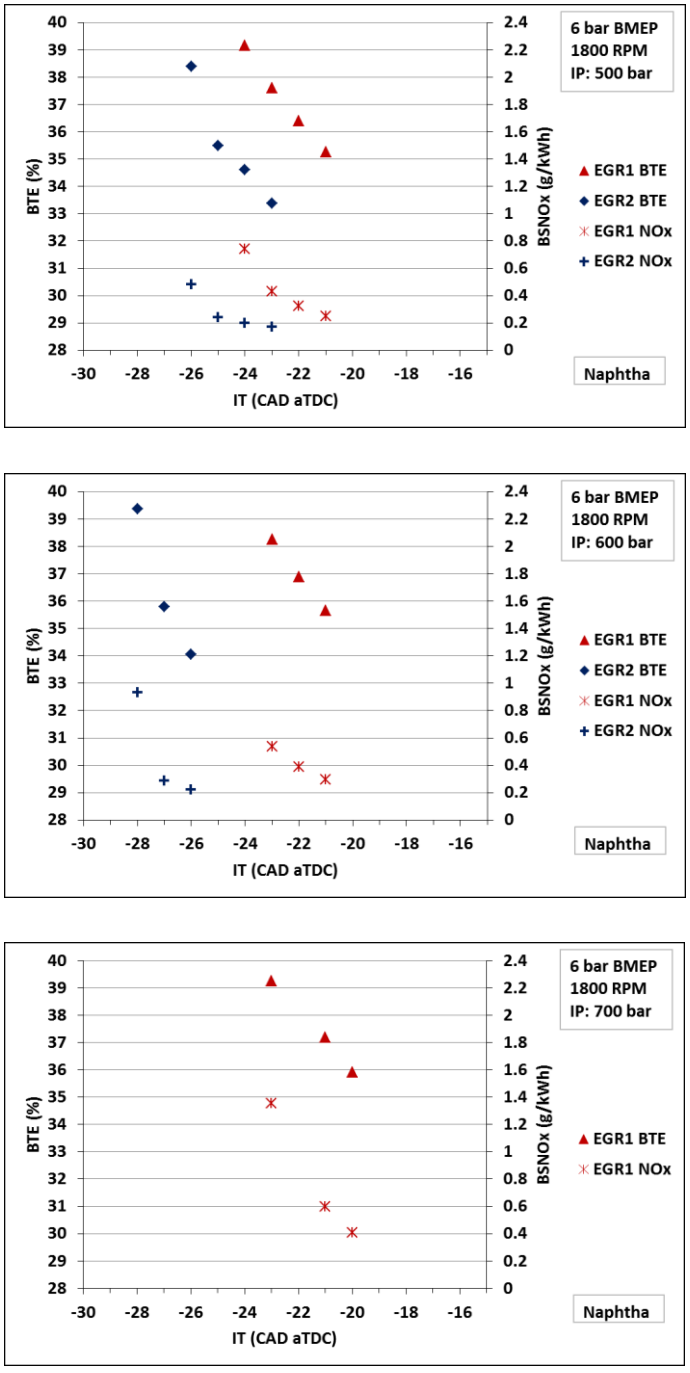


Figure 6-5 Brake thermal efficiency (BTE) and brake specific NO_x ($BSNO_x$) of naphtha compression ignition with different injection pressures and EGR settings at 6 bar BMEP

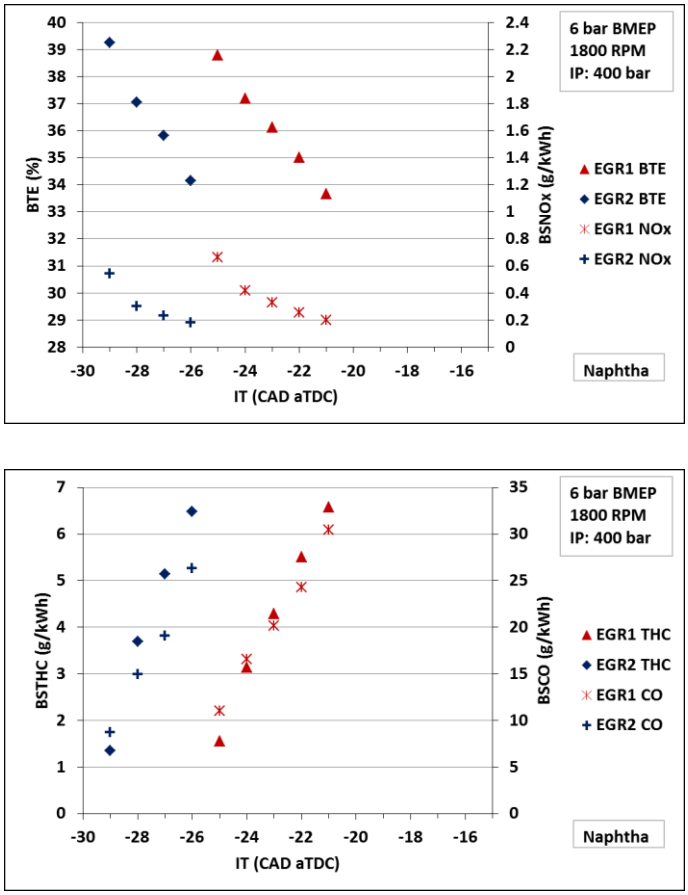


Figure 6-6 BTE, $BSNO_x$, BSTHC and BSCO of naphtha compression ignition with the injection pressure of 400 bar and different EGR settings at 6 bar BMEP

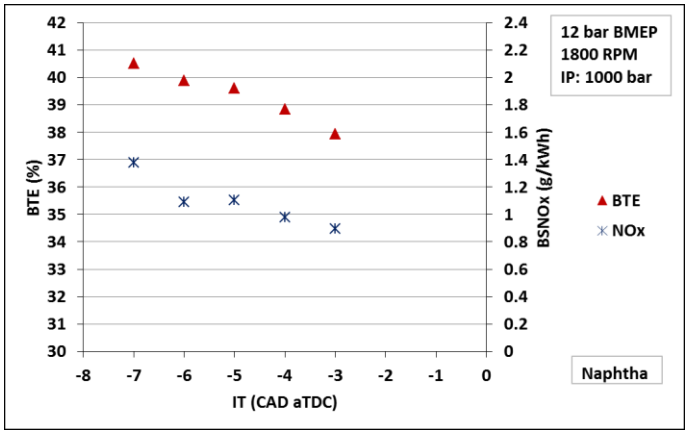
6.2.5. Results at 12 bar BMEP

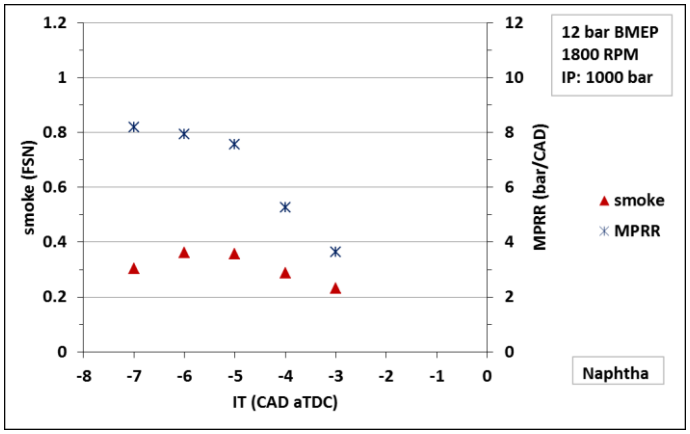
Effects of IT variation were investigated for naphtha CI at the load of 12 bar BMEP and results are shown in Figure 6-7. As expected, BTE, $BSNO_x$ and MPRR were reduced when IT was retarded. Compared to both G75 and diesel, naphtha combustion resulted in lower smoke emissions while $BSNO_x$ emissions were generally higher.

For naphtha, high BTE level of 40.50% with a relatively low smoke (for this load) of 0.303 FSN was achieved while $BSNO_x$ emission was 1.38 g/kWh. For G75, with the same IT and IP, BTE was 40.54%, $BSNO_x$ was 1.08 g/kWh and smoke was 0.870 FSN. As it can be seen in Figure 6-8, showing results for the aforementioned points, naphtha demonstrated slightly

longer combustion delay (by around 1 CAD) while its combustion HRR peak is higher than G75; these can help explain lower smoke and higher NO_x from the naphtha combustion. However, referring to particulate number and size distributions shown in Figure 6-9, there is a shift in the distribution towards smaller particulates for naphtha compared to G75. Particulates emitted from combustion of both fuels are dominated by accumulation mode while the peak is not significantly different. However, G75 particulates are mainly larger agglomerates compared to naphtha particulates. TPN from naphtha combustion was lower than G75 by only around 10.1% while Acc. PM was lower by around 48.8% and CMD was lower by 13.5 nm. It is believed that lower smoke values observed for naphtha combustion are not mainly due to lower number of particulates but smaller particulates which are linked with lower emitted particulate volume (they did not darken the filter of smoke meter as much as G75 particulates). This can be due to the higher volatility of naphtha fuel which can help reduce equivalence ratio of the local packets and/or absence of heavy HC compared to G75.

For naphtha (Figure 6-7), BSTHC and BSCO emissions variation trends were opposite. As the IT was retarded, BSTHC was reduced and BSCO was increased, although both emissions were varying at low levels. BSTHC and BSCO emissions are below 0.25 g/kWh and 1.5 g/kWh, respectively, which are in the same range of results discussed for G75 in Chapter 5.





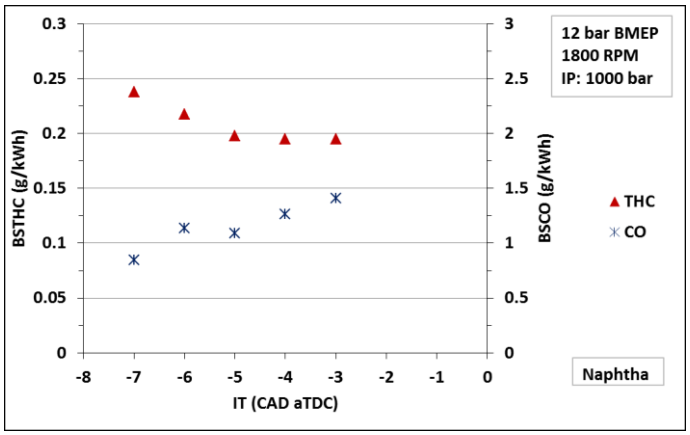


Figure 6-7 Combustion and emission characteristics of naphtha compression ignition with varying injection-timing at 12 bar BMEP; λ and EGR rate were fixed at around 1.25 and 8%, respectively.

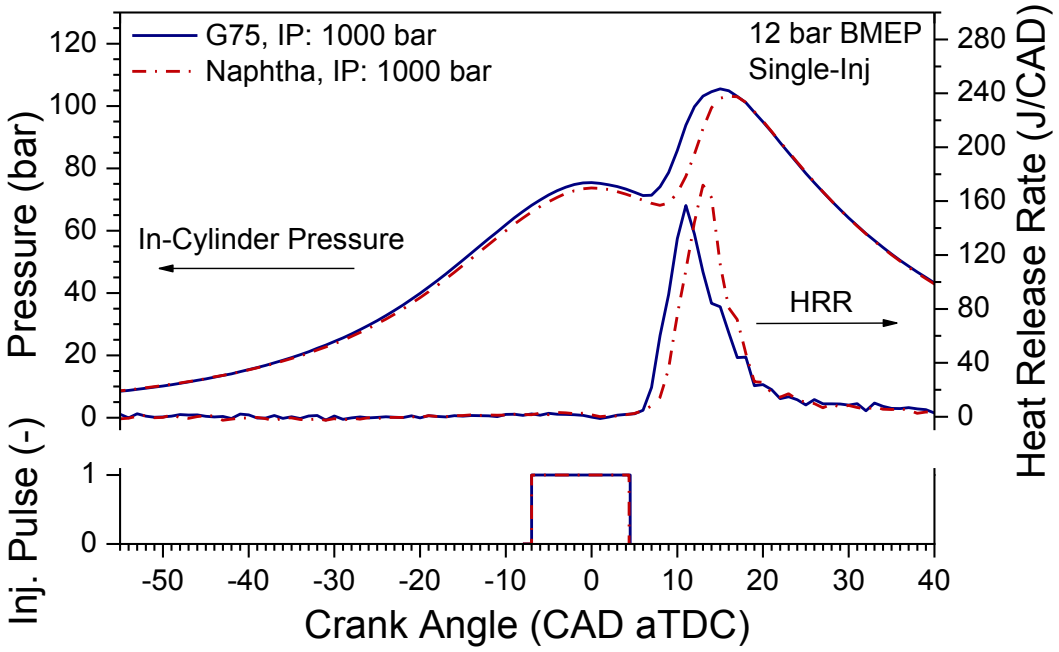


Figure 6-8 In-cylinder pressure, heat release rate and injection pulse for naphtha and G75 at 12 bar BMEP when using single-injection

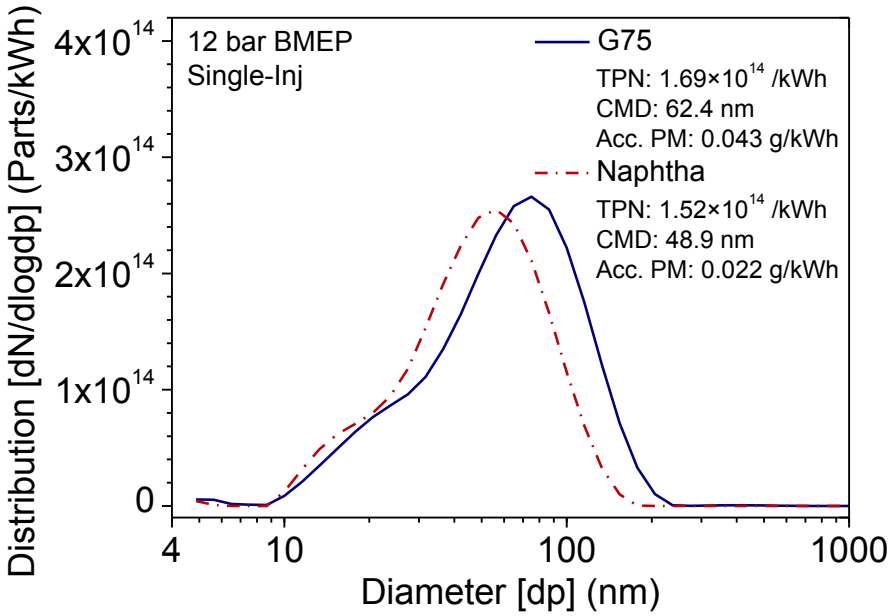


Figure 6-9 Particulate number and size distribution of naphtha and G75 at 12 bar BMEP when using single-injection

Furthermore, results of sweeping IP from 900 to 1200 bar while fixing IT at -6 CAD aTDC are illustrated in Figure 6-10. These results indicate that increasing IP can slightly decrease BTE and slightly increase $BSNO_x$ and MPRR levels. Therefore, based on this figure, variation of IP in the studied range did not have a significant effect on combustion performance and emission characteristics.

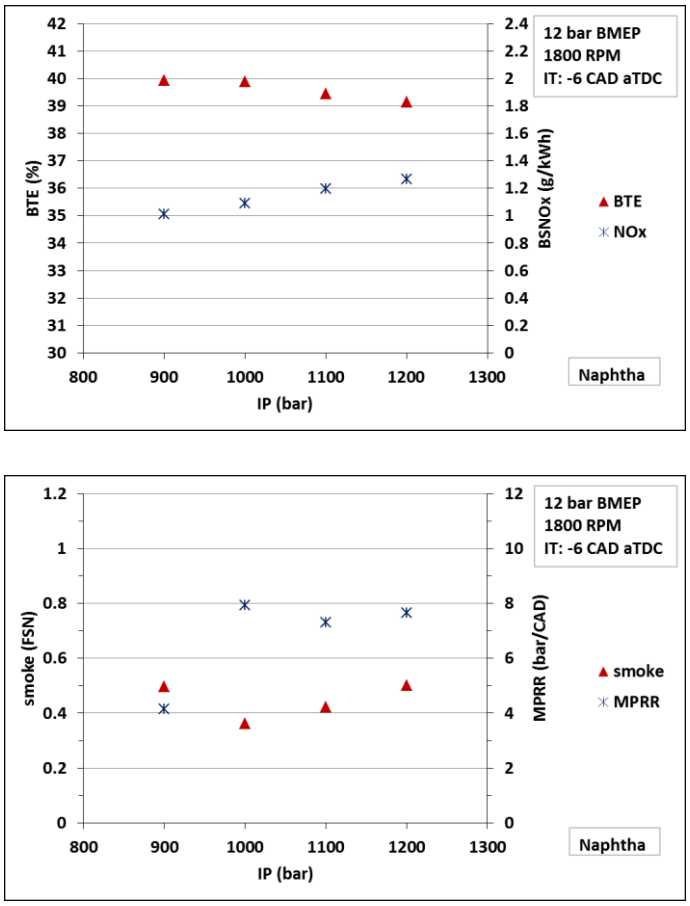


Figure 6-10 Combustion and emission characteristics of naphtha compression ignition with varying injection pressure at 12 bar BMEP

Increase of EGR rate at this load, while other settings were fixed, increased smoke emissions and reduced $BSNO_x$ emissions (Table 6-1). While BSTHC emissions were almost in the same level, BSCO emissions were increased with increasing EGR rate. BTE levels also were lower

for higher EGR rates. These are due to two reasons: increasing EGR, first, reduces oxidiser availability inside the cylinder and second, slightly prolongs ignition delay and combustion delay which means combustion occurs further from the TDC.

Table 6-1 Combustion and emission characteristics of naphtha compression ignition with varying EGR rate at 12 bar BMEP; IT and IP were fixed at -7 CAD aTDC and 1000 bar, respectively

EGR rate	BSCO	BSTHC	$BSNO_x$	smoke	BTE
(%)	(g/kWh)			(FSN)	(%)
10.23%	2.34	0.28	0.86	0.871	39.74
9.51%	1.23	0.24	1.12	0.489	40.13
6.92%	0.84	0.24	1.38	0.303	40.50

6.2.6. Results at 17.3 bar BMEP

Some tests at 17.3 bar BMEP were conducted and it was found that smoke emission results of naphtha compression ignition were "out-of-character" as they were generally higher (some results are listed in Table 6-2) than results for both diesel and G75. In general, BTE and $BSNO_x$ levels were lower compared to G75 and diesel (please refer to section 5.3.4 for comparison). This shows the well-known trade-off between NO_x and particulate emissions reduction normally observed for diesel compression ignition. With the same EGR level, IP and AHR-50, compared to G75, naphtha CI combustion emitted around 2.7 and 2.9 times more TPN and Acc. PM, respectively, while BTE was lower by 0.23% in absolute value.

Similar to G75, ignition delay and combustion delay of naphtha at this high and boosted studied load were significantly shorter when compared to lower studied loads and were close to those of diesel. Results of the HRR analysis indicated the presence of a diffusive (mixing-controlled) combustion rather than a premixed combustion (with a single sharp peak of HRR)

observed in the lower studied loads. This is due to the fact that there was an overlap between injection and combustion events. Higher smoke emissions might be due to the weakness of soot oxidation process because of lower temperature of combustion [20] confirmed by lower $BSNO_x$ emissions. This needs further investigation to understand the process of soot formation and oxidation at this high load. IT had some effects on combustion and emission characteristics. Compared to using IT of -2 CAD aTDC, using IT of -4 CAD aTDC resulted in lower smoke and BSCO emissions and higher $BSNO_x$ and BTE levels. These results are in-line with the principle that the location of AHR-50 is an effective factor in determining engine performance and emissions.

Table 6-2 Combustion and emissions characteristics of naphtha compression ignition at 17.3 bar BMEP; IP and EGR rate are fixed at 1100 bar and 5.5%, respectively

IT	**BSCO**	**BSTHC**	**$BSNO_x$**	**smoke**	**BTE**	**TPN**	**Acc. PM**
(CAD aTDC)	(g/kWh)			(FSN)	(%)	Number/kWh	g/kWh
-2	3.78	0.07	1.33	3.72	36.63	9.41×10^{14}	0.456
-4	1.86	0.12	1.75	2.32	38.81	5.41×10^{14}	0.214

6.3. Investigation of double-injection strategies at different operating loads

In this section, results of naphtha compression ignition while using double-injection strategies at various engine operating loads of 1.4, 3, 6 and 12 bar BMEP with an engine rotational speed of 1800 RPM are presented. Generally, three first injection quantity-ratios (IQ1s) at three different first injection-timings (IT1s) were studied. In general, IQ1 percentage was varied at 10%, 30% and 50% and IT1 was varied at -100, -80 and -60 CAD aTDC similar to what were studied for G75 and diesel fuels in the previous chapter. Results are compared to

results of some selected naphtha single-injection, G75 double-injection and diesel double-injection strategies at each engine operating load.

6.3.1. Results at 1.4 bar BMEP

Naphtha CI when using double-injection strategies at 1.4 bar BMEP was accompanied with high COV of NIMEP (more than 10%) regardless of the utilised IP, injection-timings and IQ1 and therefore, results are not presented here. This problem was observed for the single-injection strategy as discussed earlier in this chapter and is believed to be due to possible overmixing and fuel-wall interaction when using advanced injection-timings.

6.3.2. Results at 3 bar BMEP

At 3 bar BMEP, second injection-timing (IT2), IP and hot-EGR rate were fixed at -32.5 CAD aTDC, 350 bar, and 43%, respectively, similar to the case for investigation of double-injection for G75. Results for IQ1 of 50% at IT2 of -60 and -80 CAD aTDC showed high combustion instability and BSTHC emissions and therefore are excluded from discussions. Figure 6-11 illustrates combustion and emission characteristics results. Generally, using IQ1 of 10% resulted in the highest obtained BTE levels; however, $BSNO_x$ values were high. Only with IT1 of -60 CAD aTDC, at which the maximum BTE was achieved (32.36%) in the studied range, $BSNO_x$ was below 0.4 g/kWh. This BTE is slightly less than the maximum BTE achieved for single-injection with IP of 350 bar (32.64%). BSTHC and BSCO at the same point were around 1.97 and 1.21 times, respectively, higher than the single-injection results. Smoke emissions were below 0.02 FSN for all of the settings. It can be concluded that at this

load, there is no significant difference between single and double injection strategies for naphtha and due to lower HC and CO, single-injection is preferred.

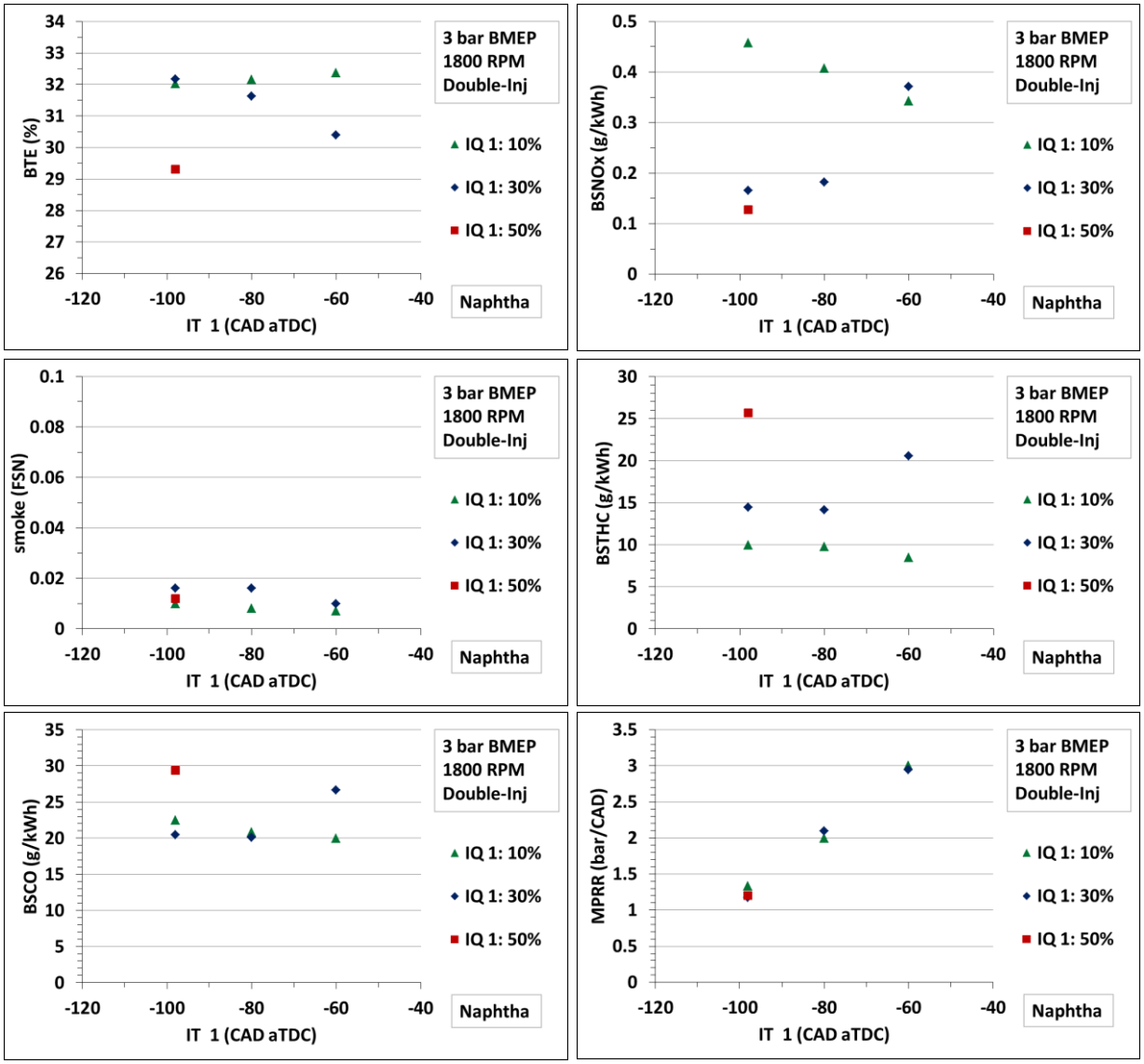


Figure 6-11 Combustion and emission characteristics of naphtha at 3 bar BMEP with double-injection strategies

6.3.3. Results at 6 bar BMEP

At 6 bar BMEP, results illustrated interesting trends as it is shown in Figure 6-12. IT2 and IP were fixed at -28.5 CAD aTDC and 500 bar, respectively. Cold-EGR technique was used while λ was between 1.27 and 1.3.

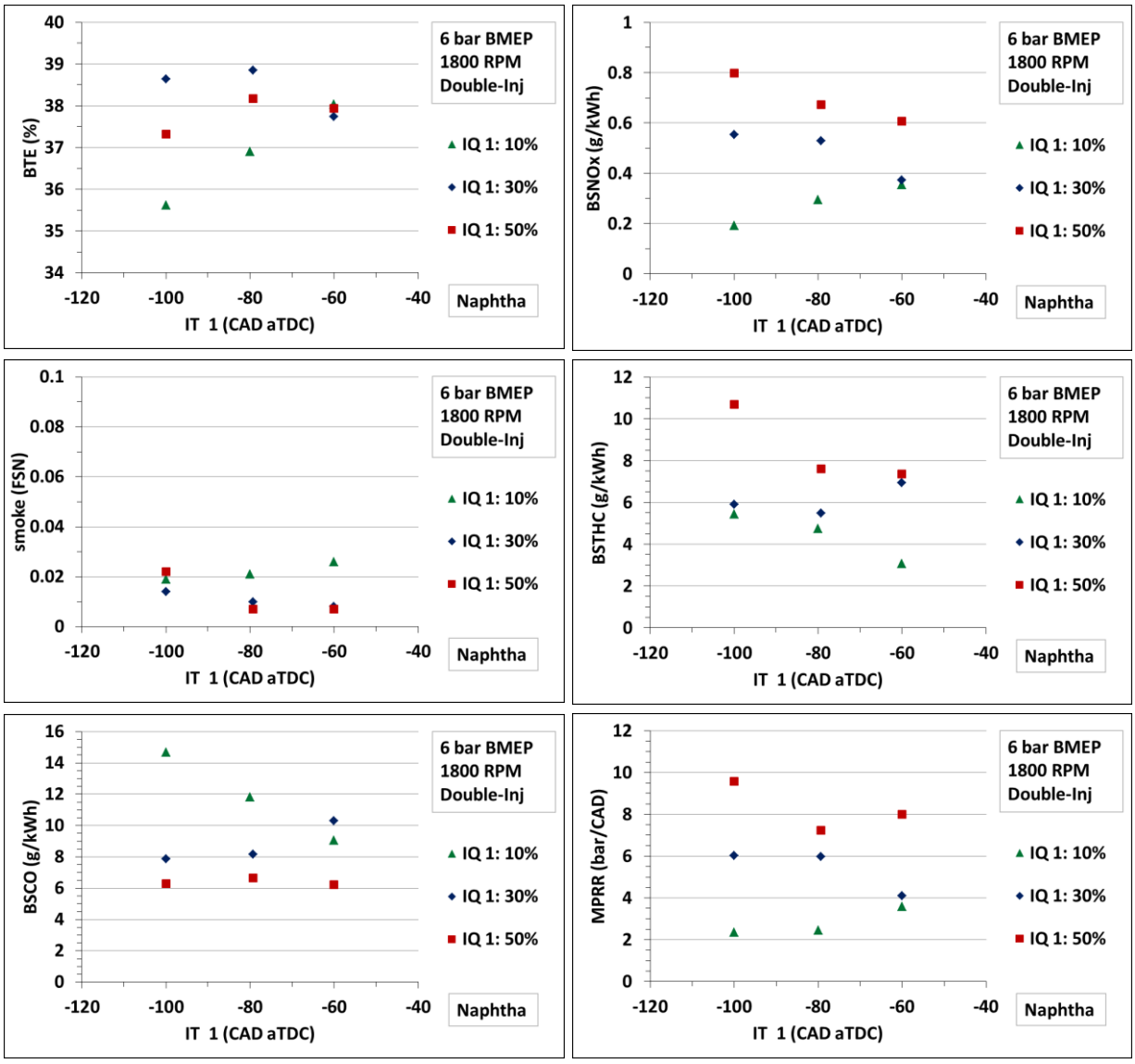


Figure 6-12 Combustion and emission characteristics of naphtha at 6 bar BMEP with double-injection strategies

At this load, generally, using IQ1 of 30%, compared to 10% and 50%, resulted in higher BTE levels. These results can be explained by the overmixing level, indicated by BSTHC emissions, and combustion-phasing, supported by $BSNO_x$ emissions. Increasing IQ1 from 10% to 50% advanced combustion-phasing. At a fixed EGR rate and λ, if combustion occurs closer to the TDC, BTE and NO_x will be higher and THC and CO will be lower. This is mainly due to the higher in-cylinder temperature at the point of combustion and also more expansion work drawn from the combusting mixture. Results shown in Figure 6-12 indicate that increasing IQ1 resulted in elevated $BSNO_x$ emissions and MPRR which can support the claimed hypothesis. In order to support results achieved for BTE levels, in addition to the combustion-phasing, fuel-air overmixing and/or possible fuel wall-impingement should be considered. Increasing IQ1 resulted in higher BSTHC which can be a sign of overmixing or under-mixing. Therefore, it can be hypothesised that combustion-phasing and overmixing are competing to influence combustion and emission characteristics at this load with double-injection. This behaviour was not observed for G75 and diesel combustion presented in Chapter 5.

BSCO emissions showed an opposite variation trend compared to BSTHC emissions. Bonds between fuel hydrocarbons should be broken and some reactions are required in order to produce CO [22]. However, if THC emissions are mostly unburned fuel, there was no chance for CO to be produced and therefore lower CO emissions will be measured in the engine exhaust. Smoke emissions for all of the settings were below 0.026 FSN. $BSNO_x$ emissions of IQ1 of 10% was below 0.4 g/kWh while using higher IQ1 generally resulted in higher $BSNO_x$ values than the target due to advanced combustion-phasing as discussed earlier. Compared to the peak BTE for single-injection at the same IP with $BSNO_x$<0.4 g/kWh, using double-injection with IQ1 of 10% and IT1 of -60 CAD aTDC resulted in higher BTE (38.03%) by 1.63% in absolute value. This is believed to be due to the effect of the first injection on

lowering the main peak of HRR (with an earlier AHR-50) and therefore achieving lower NO_X and higher BTE. Compared to G75 results with the same IP and IT1 settings, similar BTE was achieved for naphtha while $BSNO_x$ was higher by around 1.35 times. Optimisation of engine controlling parameters is out of the scope of this work; however, from these results it can be observed that changes in controlling settings can efficiently influence engine outputs. Compared to single-injection, double-injection is more suitable for naphtha to benefit from high BTE and low NO_x at 6 bar BMEP in the studied engines. There is no significant difference between the performance of naphtha and G75 with double-injection at peak BTE and low NO_x conditions at this load.

6.3.4. Results at 12 bar BMEP

At the studied load of 12 bar BMEP for double-injection strategies, similar to results for G75 and diesel presented in Chapter 5, smoke emissions were high from naphtha combustion (Figure 6-13). Indeed, due to high smoke emissions, results at IQ1 of 30% and 50% are not presented for most of the studied first injection-timings. For these tests, IT 2, IP, λ and EGR rate were fixed at -6 CAD aTDC, 1000 bar, around 1.25 and 8%, respectively.

In general, using IQ1 of 10%, compared to 30% and 50%, resulted in higher levels of BTE. BSTHC emissions were lower for IQ1 of 10% compared to 30% and 50%. Apart from higher possibility of overmixing, these can be due to the fact that some part of combustion occurred before the TDC and therefore did not contribute to the useful work on the piston. Similar trends of overmixing was observed at 6 bar BMEP when using double-injection. Ignition and combustion delays of naphtha, similar to G75, are shorter in the higher studied load. Compared to single-injection strategy results for naphtha, usage of double-injection resulted

in higher smoke emissions (by more than 3.5 times) and no major improvement on BTE and NO_x reduction. Therefore, single-injection is the preferred strategy for naphtha at this load.

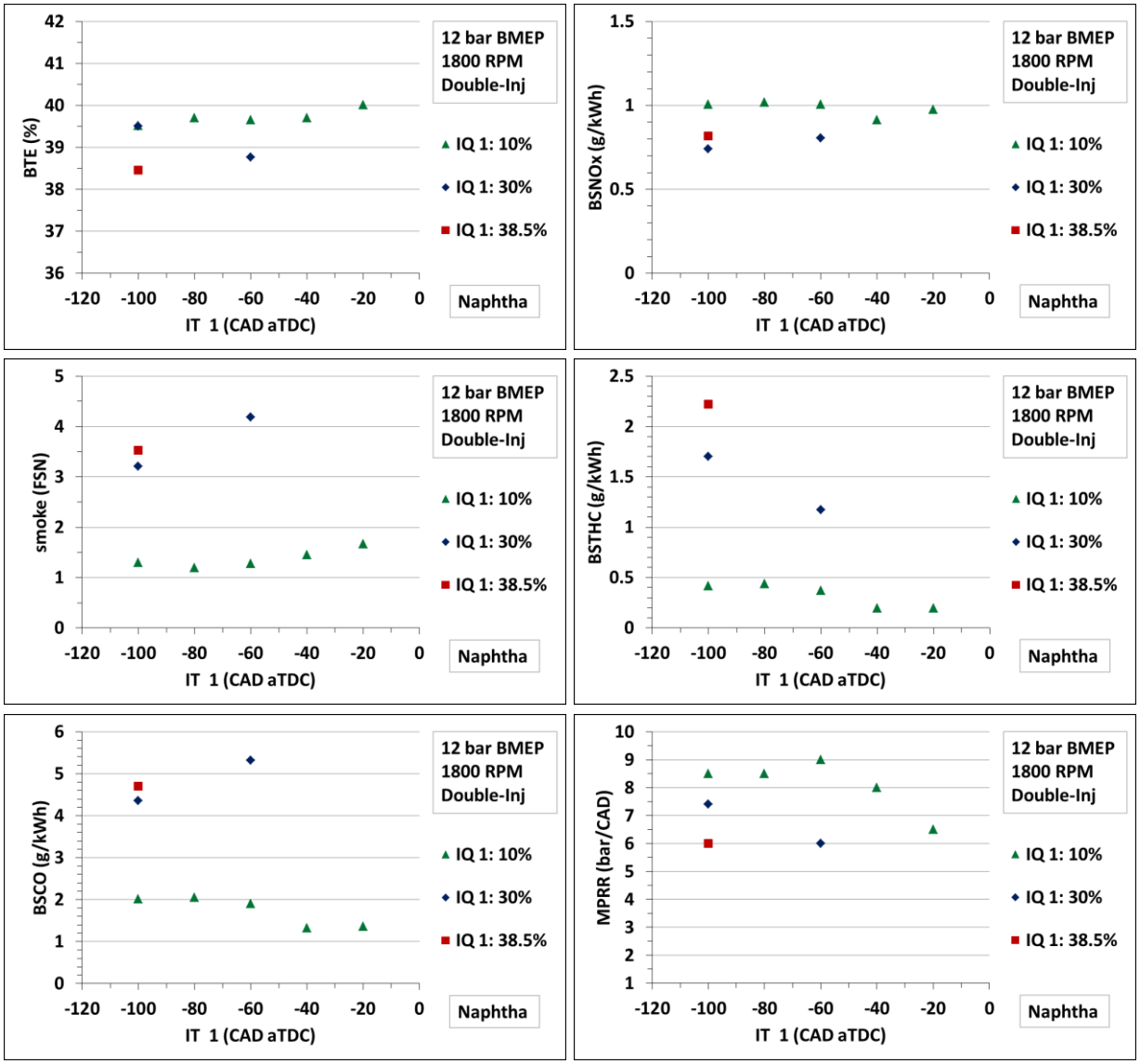


Figure 6-13 Combustion and emission characteristics of naphtha at 12 bar BMEP with double-injection strategies

Retarding the IT1 further than -60 CAD aTDC to -40 and -20 CAD aTDC helped to slightly reduce BSTHC and BSCO emissions and increase BTE levels, while smoke emissions were

higher. Later fuel injection affect the results by two main roots: first, fuel is injected in a denser and higher temperature environment, compared to earlier injection-timings, and therefore physical and chemical processes required to achieve ignition and combustion occur faster [22] and second, shorter time is available for the fuel to be well-mixed with air in order to achieve premixed combustion. In support of these hypotheses, start of combustion (SOC) and combustion-phasing results showed that later injection-timings resulted in earlier SOC and AHR-50 and therefore proved the kinetically controlled nature of the combustion under these conditions.

Altering IT2 while IT1 is fixed can affect results as listed in Table 6-3. Compared to IT2 of -6 CAD aTDC, advancing IT2 resulted in lower smoke emissions while retarding IT2 increased smoke emissions. $BSNO_x$ and BSCO emissions were reduced with retarding IT2. Higher smoke emissions with retarded IT2 can be attributed to the fact that lower combustion temperature as a result of retarded centre of combustion will reduce in-cylinder soot oxidation possibility and the generated carbonaceous solid emissions leave the exhaust valve not fully oxidised.

Table 6-3 Variation of second injection-timing (IT2) for naphtha at 12 bar BMEP while first injection-timing was fixed at -100 CAD aTDC

IT 2	**BTE**	**$BSNO_x$**	**BSTHC**	**BSCO**	**smoke**
CAD aTDC	%	g/kWh			FSN
-10.5	39.62	1.27	1.67	3.90	2.492
-6	39.50	0.74	1.70	4.36	3.211
-1	38.42	0.46	1.70	6.84	4.514

6.4. Summary/Conclusions

The main objective of this chapter is to investigate effects of the narrower boiling profile of naphtha compared to G75-Dieseline (G75) on combustion performance and emissions in a wide engine operating load range. Engine control settings were kept similar to the settings used for G75 in Chapter 5 and major findings are provided below:

6.4.1. Results of single-injection strategies

- At 1.4 bar BMEP, hot-EGR strategy and low injection pressure (IP) were necessary to be used, similar to the case of G75, for reducing combustion instability. Higher intake temperature effect on improving the combustion behaviour at this load, caused by using high hot-EGR rates, is obvious. However, even with IP as low as 150 bar at some injection-timings (ITs), high COV of NIMEP (more than 10%) remained the major issue at this low operating load for naphtha. This is hypothesised to be due to lower degree of stratification of charge and higher overmixing caused by higher volatility of naphtha compared to G75. It is recommended to use IPs less than 150 bar for naphtha. IT is an important factor for controlling the cyclic variation. Compared to the selected point of G75 results, from Chapter 5, with the same settings as the peak BTE settings for naphtha, BTE was 2.54% lower (in absolute value), BSCO and BSTHC were higher by around 1.4 and 2.5 times, respectively, while smoke was the same. This shows better performance of G75 compared to naphtha in the current studied engine at this load.

- At 3 bar BMEP, high COV of NIMEP was less problematic; while utilisation of hot-EGR strategy is a necessary requirement. Similar to G75, low IP is preferred for naphtha.

Compared to G75 and diesel, combustion was shorter and more intense which resulted in generally higher NO_x emissions and MPRR believed to be due to the narrower boiling profile of naphtha. At this load, peak BTE value, while considering the $BSNO_x$ target of <0.4 g/kWh, was 33.04% with IP of 150. Peak BTE value of G75 was similar to this value, however, $BSNO_x$ was around 1.8 times and smoke and MPRR were 2 times higher for naphtha. Moreover, both BSTHC and BSCO were generally higher for naphtha. Therefore, since smoke emissions are low for both G75 and naphtha at this load, G75 is preferred as its combustion generally results in lower $BSNO_x$, BSTHC, BSCO and MPRR.

- At 6 bar BMEP, naphtha CI combustion is sensitive to the IT and EGR settings. Advancing IT regardless of the selected IP and cold-EGR rate increased both BTE and $BSNO_x$ mainly by advancing the combustion-phasing. Achieving high BTE, while meeting the $BSNO_x$ target of <0.4 g/kWh, was challenging at this load for naphtha. This can be hypothesised to be due to the lower charge stratification level when using naphtha, compared to G75, and therefore rapid combustion featuring sudden heat release events. For this reason, studying lower injection pressures seemed a promising option to increase stratification level and help to reduce $BSNO_x$ and MPRR. IP of 400 bar resulted in the peak BTE, with $BSNO_x$<0.4 g/kWh, which is 1.36% lower (in absolute value) compared to the G75 results. BSTHC and BSCO of naphtha were more than two times higher than the results for G75 at the same conditions. It is believed that using Dieseline helped to improve stratification level of the charge. Therefore, in view of simultaneously achieving high BTE and low $BSNO_x$, BSTHC and BSCO, G75 performed better than naphtha at this engine load condition.

- At 12 bar BMEP, compared to G75, it is possible to reduce smoke emissions by approximately 65% at the expense of higher $BSNO_x$ (by around 28%) while BTE is similar. Higher EGR rate can be used to reduce NO_x, however even naphtha combustion showed the trade-off of NO_x and smoke reduction at this load and therefore there is no significant difference from G75 results. Particulate emissions from naphtha combustion, compared to G75, have a smaller diameter accumulation mode peak. However, total emitted particulate number was not significantly different (was lower by around 10% for naphtha) while accumulation mode particulate mass, on the other hand, was lower by around 49%. This can be due to the higher volatility of naphtha fuel which can help reduce equivalence ratio of the local packets and/or absence of heavy HC compared to G75. So at this load, compared to G75, lower smoke emissions are achievable with the same BTE but higher $BSNO_x$ emissions for naphtha.

- At 17.3 bar BMEP, naphtha combustion resulted in increased smoke emissions and reduced BTE compared to both G75 and diesel combustion. There is a further scope to understand the nature of particulates formation and oxidation process at this load. With the same EGR level, IP and combustion-phasing, compared to G75, naphtha combustion emitted around 2.7 and 2.9 times more total particulate number and accumulation mode particulate mass, respectively. Ignition and combustion delay of naphtha were similar to diesel and G75 and therefore combustion was mixing-controlled.

6.4.2. Results of double-injection strategies

- At 1.4 bar BMEP, results showed COV of NIMEP of more than 10% for all of the studied settings regardless of the utilised IP, IT and first injection-quantity (IQ1) for

naphtha. It is suggested to investigate IPs less than 150 bar for double-injection at this operating load.

- At 3 bar BMEP, results indicated no significant difference between single and double injection strategies for naphtha. Maximum BTE was achieved with IQ1 of 10% (32.36%) while $BSNO_x$ was less than 0.4 g/kWh. This BTE is slightly less than the maximum BTE achieved for single-injection with IP of 350 bar (32.64%). BSTHC and BSCO at the same point were around 1.97 and 1.21 times, respectively, higher for double-injection. It can be concluded that at this load, single-injection is preferred for naphtha due to lower HC and CO.

- At 6 bar BMEP, when using double-injection strategies, it was found that premixing and variation of the combustion-phasing are two competing factors for influencing the combustion and emission characteristics. Variations in the IQ1 and IT1 can change both of these factors. Using IQ1 of 30%, compared to 10% and 50%, resulted in achieving higher BTE. Using IQ1 of 10% resulted in more retarded combustion-phasing compared to using IQ1 of 50%; while BSTHC levels of IQ1 of 50% were higher. This behaviour was not observed for G75 and diesel combustion presented in Chapter 5. Compared to single-injection, double-injection is more suitable for naphtha to benefit from higher BTE and lower NO_x at this load in the studied engine. There is no significant difference between the performance of naphtha and G75 with double-injection at peak BTE and low NO_x conditions.

- At 12 bar BMEP, smoke emissions from naphtha combustion were in the same range of G75 results (more than 1 FSN) for the studied settings. Increase of IQ1 advanced the

combustion-phasing and increased smoke emissions due to the pre-TDC combustion events. Retarding the IT2 resulted in higher smoke emissions hypothesised to be due to poor in-cylinder soot oxidation. Ignition and combustion delays of naphtha, similar to G75, are shorter in this higher studied load. Compared to single-injection strategy results for naphtha, usage of double-injection resulted in higher smoke emissions (by more than 3.5 times) and no major improvement on BTE and NO_x reduction. Therefore, single-injection is the preferred strategy for naphtha at this load.

In general, it was found that the only benefit of using naphtha over G75 in the current studied engine was reduction of smoke emissions at 12 bar BMEP when using single-injection with the penalty of higher $BSNO_x$ emissions.

Chapter 7
EFFECTS OF THE DOC ON EMISSIONS FROM A PREMIXED COMPRESSION IGNITION ENGINE

7.1. Introduction

Relatively higher levels of hydrocarbons (HC) and carbon monoxide (CO) emissions from premixed compression ignition (PCI) combustion mode compared to diesel CI combustion, especially at lower operating loads, were discussed in the previous chapters. One effective method to reduce these gaseous emissions is by utilising a diesel oxidation catalyst (DOC) after-treatment system. Moreover, DOC can help to reduce volatile fraction of particulate emissions [95]. DOC induced oxidation of gas phase HC may also reduce chances of HC nucleation and/or condensation and adsorption on soot particulates when there is a temperature gradient in the exhaust system or later when they are released to the atmosphere. HC nucleation can increase particulate number (PN) and particulate mass (PM) while condensation/adsorption can increase PM [90]. The importance of semi-volatile organic compounds (SVOC) for these processes was discussed in Chapter 2. In this sense, DOC can contribute to the reduction of both PM and PN emitted from the exhaust tailpipe.

However, despite the possibility of achieving high conversion efficiency with a DOC, various operating factors must be present to guarantee its efficient operation. One of the most important parameters for efficient reduction capability of a DOC is its operating temperature [16]. This temperature dependence of the DOC operation can be troublesome at lower engine operating loads and speeds when exhaust gas temperatures are relatively low. At these low

engine loads, using premixed low temperature combustion (LTC) mode featuring high cold-EGR levels will add “insult to the injury”, since the exhaust gas temperatures are lower and CO and HC levels are higher compared to low EGR conditions [140].

Using a production (stock) DOC for the exhaust of a CI engine fuelled with G75-Dieseline (G75) for PCI combustion and diesel at the same settings is investigated in this chapter. As it was shown in earlier chapters, particulate emissions from the G75 PCI combustion mode, which are very low in terms of both number and mass, are mostly believed to be nuclei which have high volatility and therefore the DOC should aid to the reduction of these emissions. This chapter put this thought in practice with examining the properties of particulates before and after the DOC. Experiments focusing on investigation of the effectiveness of a DOC on reducing both gaseous and particulate emissions comparing G75 and diesel fuels are conducted at 1.4, 3 and 6 bar BMEP and a fixed engine speed of 1800 RPM.

7.2. Test Procedure

For these experiments, two studied fuels discussed in Chapter 5, G75 and diesel, were utilised. Considerable contribution of the engine lubricating oil to the emitted particulates from the engine was highlighted in Chapter 2. In order to completely separate the effect of oil contribution when using G75 and diesel, oil was changed before conducting the batch of experiments for each fuel. At each of the studied loads, the engine was completely warmed and stable in order to meet conditions of steady state testing. Emissions, temperature and pressure were measured before and after the DOC at the locations described in Chapter 3. Apart from the online measurement techniques, gas adsorption tubes were collected at each of the studied conditions in order to study the effect of the DOC on the composition of SVOC in the gas phase.

7.3. Effects of the DOC on emissions of Dieseline and diesel CI combustion at 1.4 bar BMEP

At the lower studied load (1.4 bar BMEP), the major challenge for the good functionality of the DOC is the low temperature of exhaust gas. This section examines the effects of the stock DOC on emissions from combustion strategies developed in Chapter 5 for G75 and diesel fuels at this load.

7.3.1. Results for G75-Dieseline operation

At 1.4 bar BMEP, G75 PCI combustion was achieved by the strategies (mainly hot-EGR and low injection pressure (IP)) discussed in details in Chapter 5. For the case of these experiments, IP was fixed at 150 bar, a double-injection strategy with first injection-quantity (IQ1) of 10% was used and hot-EGR rate was fixed at 52%. These settings were selected for high brake thermal efficiency (BTE) and low emissions from results discussed in Chapter 5. However, this does not mean that these settings necessarily result in the lowest or highest obtainable values of each characteristics. For instance in terms of particulates emissions, a sweep of IP is shown in Figure 7-1 when using single-injection strategy. It can be seen that with the two studied injection-timings, increase of IP from 150 bar to 450 bar resulted in elevated particulates emissions which is in-line with increase of COV of NIMEP and reduction of BTE as discussed in Chapter 5. Misfiring events can be sources of high particulate emissions both in terms of number and mass.

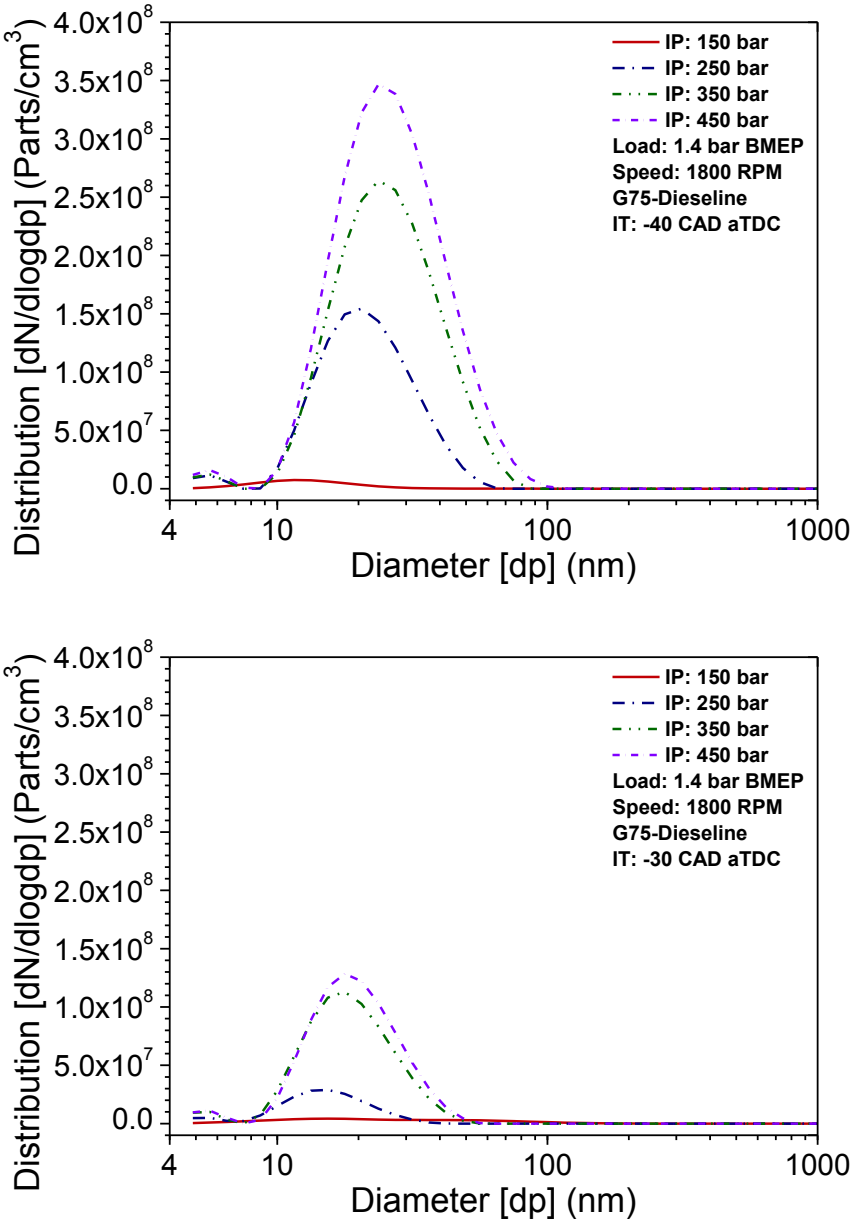


Figure 7-1 Injection pressure (IP) sweep effect on particulate number and size distribution for G75-Dieseline at 1.4 bar BMEP at two injection-timings (IT)

Emissions and exhaust gas temperature (Ex. Temp.) results measured before and after the DOC and their reduction percentages over the DOC are listed in Table 7-1. DOC efficiently converted the two high-level emissions of THC and CO which are signatures of most of the premixed combustion modes at low loads. Conversion efficiencies of CO and THC were 99.95% and 95.98%, respectively, accompanied by consumption of O_2 and production of

CO_2. In terms of brake specific (BS) results, BSCO was reduced from 76.33 g/kWh to 0.03 g/kWh which is significant. Compared to before DOC, exhaust temperature was increased by more than 83 ^oC after DOC resulting from exothermic reactions (combustion) of CO and HC with oxidising species. This temperature increase can be useful for activation and regeneration purposes if a diesel particulate filter is to be assembled after the DOC. Although NO_x levels are relatively low using this combustion technique and it is difficult to comment on any changes, NO_2 levels were lower after the DOC while NO emissions increased. This may indicate NO_2 consumption in the DOC. Moreover, it should be borne in mind that NO to NO_2 conversion depends on the operating temperature and properties of the DOC, e.g. the utilised precious metals [100]. Normally, NO to NO_2 conversion is lower at lower operating temperatures [100]. Smoke emissions stayed at very low levels before and after DOC. These results, at this studied low operating load, confirm the robust operation of a production DOC when used as a PCI/GCI engine exhaust after-treatment system.

Exhaust temperature before DOC for G75 PCI was higher than the diesel case with the same EGR, owing to the hot-EGR strategy discussed in details in Chapter 5. Results presented in the next subsection illustrate the significant importance of the exhaust temperature gain for DOC when using hot-EGR instead of cold-EGR. These make the hot-EGR technique a "win-win" strategy for improving both engine and exhaust after-treatment system operation at lower loads when using low-cetane-number fuelled PCI combustion.

Table 7-1 Emissions and exhaust temperature before and after DOC when using G75 at 1.4 bar BMEP

	O_2	**CO_2**	**CO**	**THC**	**NO**	**NO_2**	**NO_x**	**smoke**	**Ex. Temp.**
	%v	%v	ppmv	ppmv	ppmv	ppmv	ppmv	FSN	^oC
Before DOC	10.72	6.78	7840.00	3784.01	13.07	3.04	16.10	0.006	209.26
After DOC	9.68	8.11	3.59	152.17	18.74	0.59	19.33	0.004	293.09
Reduction %	9.70	-19.76	99.95	95.98	-43.46	80.73	-20.04	33.33	-40.06

Figure 7-2 and Table 7-2 illustrate physical characteristics of the particulates emissions from G75 PCI combustion. Data are presented in terms of total and modal particulates characteristics. Total number concentration presented in the table is calculated from the discrete spectrum while log-normalisation was used for nucleation and accumulation mode concentrations. It can be seen that DOC had a pronounced effect on helping to reduce particulate emissions, although it should be mentioned that these emissions are in very low levels at this operating point. Particulates at this condition are dominated by the nucleation mode and therefore, as discussed before, this would allow DOC to help reduce them easier compared to carbonaceous fraction. Both PN and PM measured after the DOC were considerably lower than the emissions measured upstream of the DOC (see reduction percentages in Table 7-2). It seems that particulate emissions at this operating point are mainly driven by HC as concentrations of the accumulation mode (more likely to be carbonaceous particulates with less volatility) are very low. Some analyses were conducted to identify the mass-ratio of elemental carbon to organic carbon (EC/OC) of particulates before and after the DOC. The EC/OC of particulates collected on the quartz filter before DOC was only 0.02 at this operating point. Nucleation mode particulates can be originated either from the combustion chamber itself or from nucleation mechanism in the exhaust system (with a temperature gradient) and/or in the dilution system where the exhaust sample is diluted and cooled [24, 142]. It can be "hypothesised" that some mechanisms can explain this considerable reduction of particulates by using the DOC:

i. High HC levels are being effectively removed from the exhaust stream via the DOC and therefore there is less chance for the nucleation phenomenon, from HC, to occur.
ii. Moreover, as the concentration of available sink media (carbonaceous core or ash) is low, there is less chance for condensation/adsorption of HC to occur during dilution.

iii. Lower particulates concentration before DOC helps adsorption and conversion of the volatile species inside the DOC as the gaseous phase has a higher diffusion rate compared to the particulate phase [24, 95].

iv. Direct oxidation of nucleation mode particulates is possible as these have small diameters and can enter the active sites of the DOC.

Higher exhaust temperature, compared to the diesel operation with cold-EGR, combined with higher volatility of the emissions helped to achieve this efficient reduction. This means that when using the developed PCI combustion techniques at this load, apart from reducing PM and PN considerably, their size profile is shifted towards smaller and more volatile particulates which can be effectively controlled by the application of a DOC.

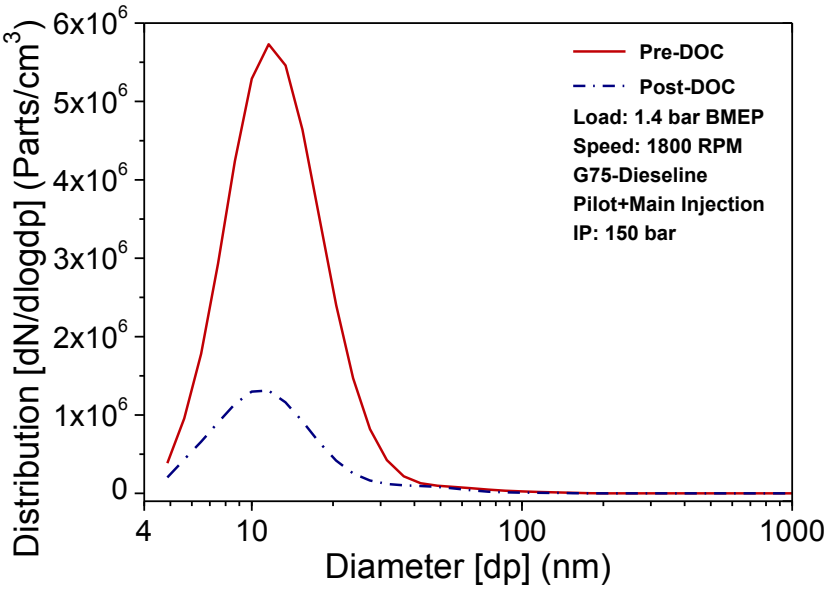


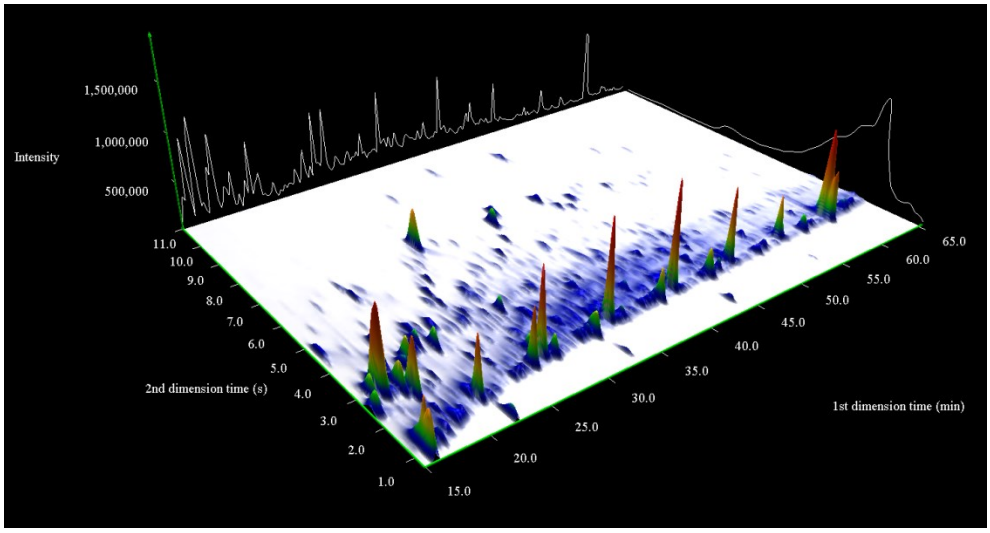
Figure 7-2 Particulate number and size distribution before and after DOC when using G75 at 1.4 bar BMEP

Table 7-2 Particulate emissions physical concentration characteristics for G75 at 1.4 bar BMEP

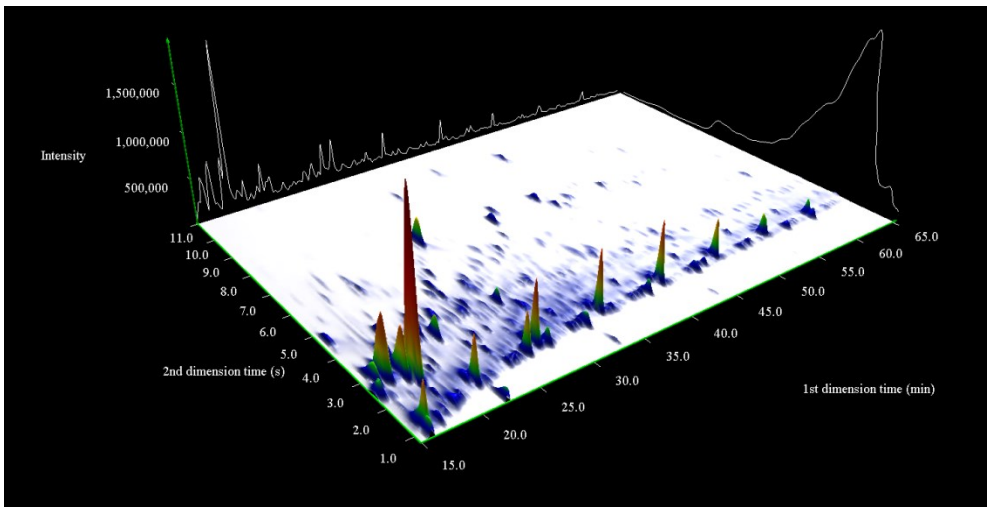
	Total (N/cc)	Nucleation Mode			Accumulation Mode		
		Concentration (N/cc)	Mass (µg/cc)	CMD (nm)	Concentration (N/cc)	Mass (µg/cc)	CMD (nm)
Before DOC	2.53E+06	2.50E+06	4.49E-06	12.0	4.61E+04	4.68E-06	46.6
After DOC	6.22E+05	6.02E+05	8.60E-07	10.9	3.00E+04	2.47E-06	45.4
Reduction %	75.44	75.94	80.84	9.44	34.95	47.36	2.60

In order to identify the effects of the DOC on SVOC emissions, this part investigates the concentration of some selected pronounced compound classes upstream and downstream of the DOC. These analyses are focused on the SVOC collected in the gas phase using adsorption tube and analysed on the TD-GC×GC-TOF-MS described in Chapter 3. SVOC are believed to be the major driving factor for the chemical behaviours of the particulates. Normally, in the exhaust of a diesel engine, SVOC are hydrocarbons sourced from either diesel fuel (lighter HC) and lubricating oil (heavier HC). The major classes of SVOC in the ULSD fuel are alkanes and cycloalkanes while the mass-based concentration of alkanes is around 5 times of the cycloalkanes confirmed with GC×GC-TOF-MS analysis [94]. Straight-chain or normal-alkanes contribute significantly to the mass of the total measured alkanes [94]. More volatile species (with carbon number below 10) can as well contribute to the total particulates emissions; however, their contribution compared to SVOC is hypothesised to be relatively lower as SVOC can change phase frequently from gas to liquid/solid or vice versa. Moreover, the focus of this work is on high molecular weight (HMW) SVOC (>C_{10}) as this has not been investigated comprehensively in the literature for any combustion mode [86].

Figure 7-3 illustrates the three-dimensional plots for the total ion chromatogram (TIC) related to the analysis of gas phase SVOC with the TD-GC×GC-TOF-MS. From this figure it is clear that the measured concentration of SVOC was significantly lower after the DOC.



(a)



(b)

Figure 7-3 Three-dimensional plots of the total ion chromatogram (TIC) for gas phase SVOC emissions from G75 combustion at 1.4 bar BMEP, (a) before DOC and (b) after DOC

The SVOC characterisation starts with gas phase alkanes. Figure 7-4 illustrates the normal alkanes (n-alkanes) and total alkanes (including normal and branched alkanes) measured before and after the DOC at this operating load. Concentrations presented in these figures are mass of the specific specie in the diluted collected gas. Although there is no specific baseline

to compare these emission results with, alkane emissions from G75 combustion were generally lower than emissions from the diesel combustion presented later in this section.

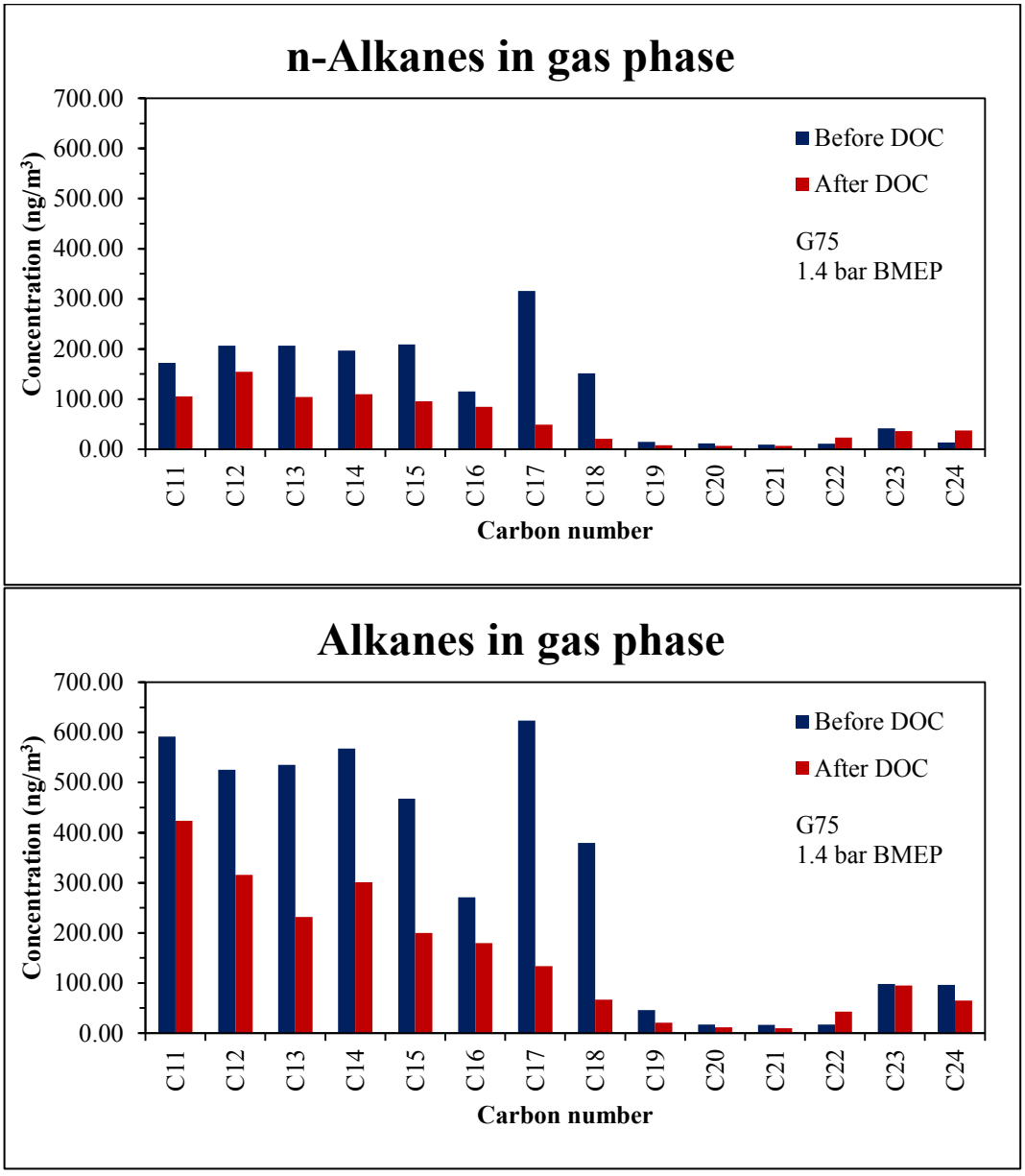


Figure 7-4 Normal alkanes (n-alkane) and total alkanes emissions before and after the DOC when using G75 fuel at 1.4 bar BMEP

Based on Figure 7-4, contribution of n-alkanes to the total alkanes is significant (more than 30% before and after the DOC). Apart from the contribution from the diesel fuel which can be seen as SVOC with C<20 [86, 94], a low secondary concentration peak after C_{22} was observed in alkanes. This is believed to be the contribution from the lubricating oil which was addressed in some earlier studies [94]. Conversion efficiency of the total measured n-alkanes (from C_{11} to C_{24}) using the DOC was around 50%. This conversion efficiency is calculated using the mass of SVOC before and after the DOC. C_{17} and C_{18} n-alkanes had the highest conversion efficiencies using the DOC; their conversion efficiency was around 85%. Conversion efficiency of n-alkanes with carbon number below C_{17} and above C_{18} was below 50%. This trend was similar for the total alkanes. It should be mentioned that it is expected to observe less HMW HC in the exhaust stream of the G75 combustion as G75 fuel is dominated by gasoline content which normally contains HC with carbon number <10. Hypotheses regarding the trend of these SVOC reductions are provided later in this section.

There can be an argument when comparing these SVOC conversion efficiencies to the conversion efficiency of THC measured by the hot wet flame ionisation detector (FID) presented in Table 7-1. Although, SVOC characterisation showed different conversion efficiencies for different compounds (sometimes up to 100%), in total it was lower than what was measured for THC by the FID (around 96%). However, results after the DOC showed some leftover of the THC emissions. It can be hypothesised that part of these THC leftovers after the DOC are indeed HMW organic species which were not converted completely to CO_2 and water when compared to hydrocarbons with carbon numbers <10. The low concentration of the HMW SVOC (measured in this work) is a support for this claim. However, this needs further investigation with measuring a wider spectrum of carbon numbers for HC, probably from C_4 to C_{40}, which was out of scope and resources of the current work.

n-Alkyl-cyclohexane concentrations were lower compared to n-alkanes as shown in Figure 7-5; the peak concentration value was for C_{13} (91.43 ng/m^3) before DOC. Total conversion efficiency of this class was around 47%, while individual compounds had different conversion efficiencies. For example, for C_{13}, as the main emitted n-alkyl-cyclohexane, conversion efficiency was around 59%. In general, total alkyl-cycloalkanes emissions were lower than total alkanes. C_{12} had the highest concentration among the analysed alkyl-cycloalkanes, while its conversion efficiency was only 37.5%. Maximum conversion efficiency in this class belongs to C_{18} (around 75%). Total conversion efficiency of this class was around 41%. In general, light molecular weight (LMW) HC are pronounced in the gas phase and HMW HC are expected to be more pronounced in the particulate phase for all of the studied species [24, 86, 94]. This can be due to the fact that LMW HC have lower boiling point and higher vapour pressure [86].

As discussed in Chapter 2, theory and experimental results related to the conversion efficiency of different classes of HC with different apparent carbon number do not necessarily agree with each other [105]. In theory, LMW HC, which have higher diffusion rate, must be converted easier with a DOC. However, experimental results sometimes show that HMW HC are converted more efficiently over a DOC. It should be mentioned that HMW HC have lower light-off temperature compared to LMW HC [95]. Therefore, there seems to be a competition between adsorption rate and required temperature needed for efficient conversion of SVOC. This needs further modelling and lab-based experimental studies to be confirmed. Moreover, there might be an active partitioning between gas and solid phase SVOC which needs further study. Furthermore, as discussed later in this chapter, conversion efficiency seems to be fuel dependent as well.

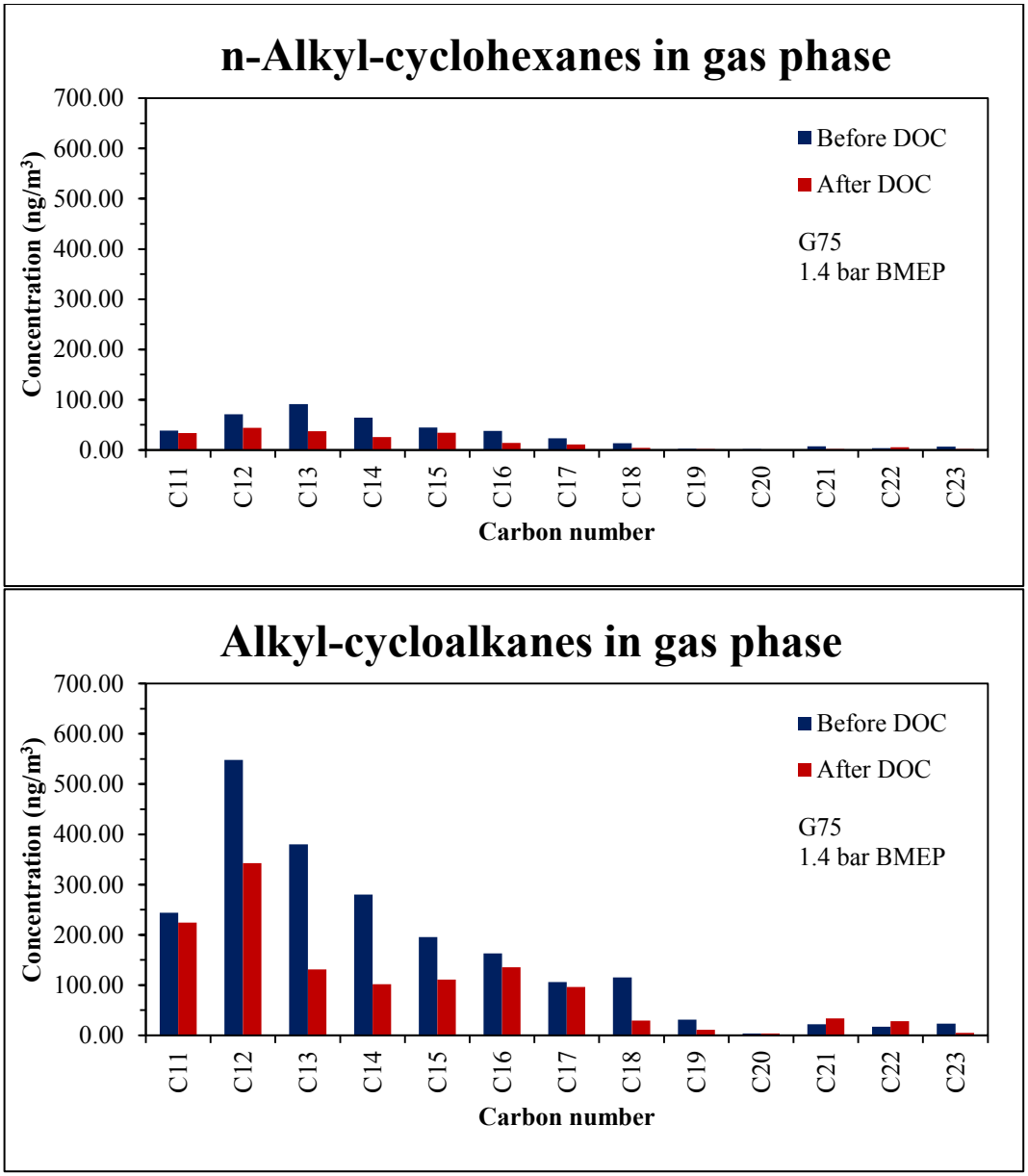


Figure 7-5 Normal (n)-alkyl-cyclohexanes and total alkyl-cycloalkanes emissions before and after the DOC when using G75 fuel at 1.4 bar BMEP

Polycyclic aromatic hydrocarbons (PAH) emissions including Naphthalene (NAP), Acenaphthylene (ACY), Acenaphthene (ACE), Fluorene (FLU), Anthracene (ANT), Phenanthrene (PHE), Fluoranthene (FLR) and Pyrene (PYR) are illustrated in Figure 7-6. NAP is the most pronounced polycyclic hydrocarbon (160.12 ng/m^3 before DOC) and its

conversion efficiency was around 39.5%. For all other PAH, with the exception of PHE, the concentrations were below 3 ng/m^3.

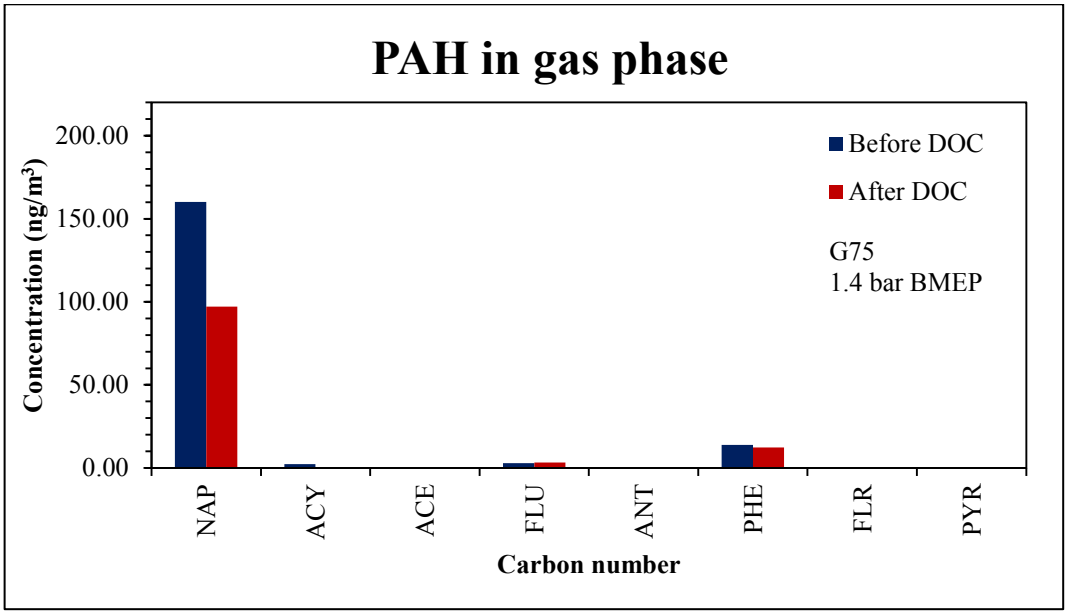


Figure 7-6 PAH emissions before and after the DOC when using G75 fuel at 1.4 bar BMEP

Among all the studied classes of SVOC, not necessarily presented here, alkanes had the highest mass-based concentrations in the exhaust of the G75 PCI combustion. This is in line with the analysis of the fuel SVOC composition [94]. Moreover, the highest conversion efficiency in the studied classes belongs to the alkanes (more than 50% in total).

7.3.2. Results for diesel operation

Results for diesel operation with cold-EGR showed poor conversion efficiencies for CO and THC using the DOC at this load (please see Table 7-3). Based on the conclusions drawn in Chapter 5, cold-EGR strategy and IP of 500 bar were used for diesel operation which are also

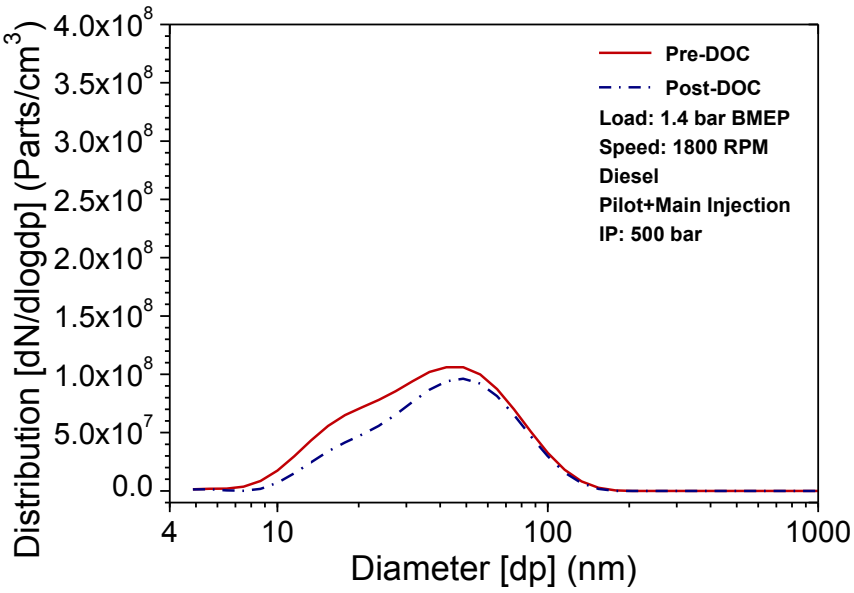
normally being practised for diesel engines. Similar to G75, double-injection strategy with IQ1 of 10% and EGR rate of 52% were used for this operating condition. Lower conversion efficiencies compared to the case of G75 are believed to be primarily due to the lower exhaust temperature which did not help the DOC to reach the light-off temperature for converting all of the volatile species. Although both CO and THC emissions are lower than those of G75 before the DOC, their conversion efficiencies are only 26.58% and 13.45%, respectively. This means that their concentration will be higher than the case of G75 after DOC. For instance, BSCO of diesel after DOC was 23.21 g/kWh which is around 774 times more than what was measured for G75. It should be emphasised again that smoke emission of diesel operation is higher than G75 results; as discussed in Chapter 5.

Table 7-3 Emissions and exhaust temperature before and after DOC when using diesel at 1.4 bar BMEP

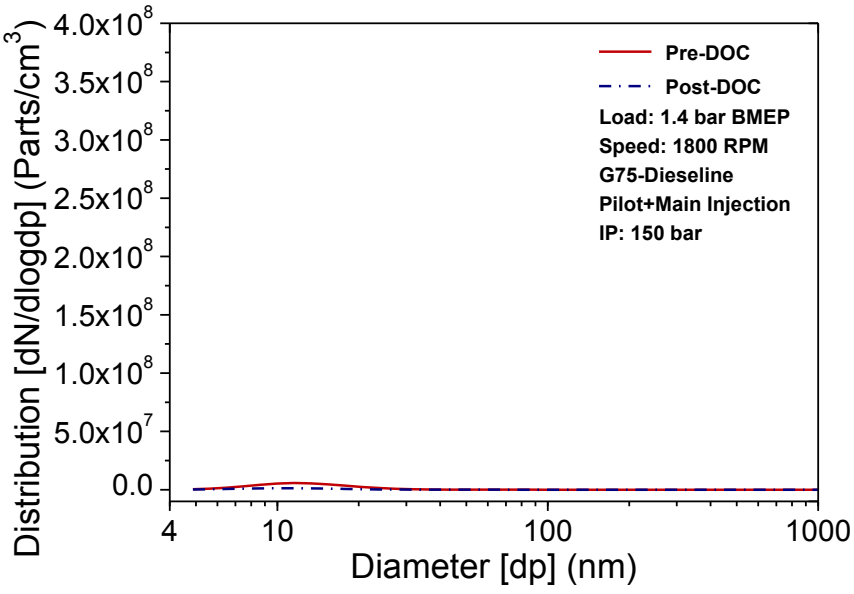
	O_2	**CO_2**	**CO**	**THC**	**NO**	**NO_2**	**NO_x**	**smoke**	**Ex. Temp.**
	%v	%v	ppmv	ppmv	ppmv	ppmv	ppmv	FSN	^oC
Before DOC	10.94	6.87	3160.00	1640.14	13.52	7.43	20.95	0.367	184.73
After DOC	10.93	6.98	2320.00	1419.51	20.07	0.03	20.10	0.313	166.26
Reduction %	0.12	-1.62	26.58	13.45	-48.49	99.65	4.05	14.71	10.00

In terms of particulate emissions, while both PN and PM are higher for diesel compared to G75, their reduction using DOC was not significant. Figure 7-7 shows particulate number and size distribution for both diesel and G75 with the same scale. Compared to the G75, total particulates concentration from diesel combustion with larger diameters is around 31 times higher while its reduction efficiency was only 20.37% using the DOC. Concentration characteristics are listed in Table 7-4. For diesel, accumulation mode is more pronounced compared to the nucleation mode while reduction of concentrations of both modes is

relatively low. Lower exhaust temperature coupled with the fact that particulates are believed to be of a less volatile nature can be used to justify these results.



(a)



(b)

Figure 7-7 Particulate number and size distribution before and after DOC when using: (a) diesel and (b) G75 at 1.4 bar BMEP

Table 7-4 Particulate emissions physical concentration characteristics for diesel at 1.4 bar BMEP

	Total (N/cc)	Nucleation Mode			Accumulation Mode		
		Concentration (N/cc)	Mass (µg/cc)	CMD (nm)	Concentration (N/cc)	Mass (µg/cc)	CMD (nm)
Before DOC	7.76E+07	3.72E+07	5.31E-04	21.9	3.59E+07	5.65E-03	55.3
After DOC	6.18E+07	3.02E+07	7.42E-04	26.0	2.80E+07	4.67E-03	58.2
Reduction %	20.37	18.89	-39.87	-18.52	22.12	17.25	-5.23

Although it was shown in Chapter 5 that using the hot-EGR technique for diesel increases smoke emissions; in order to identify the effect of higher exhaust temperature this technique was investigated for 1.4 bar BMEP (please see Table 7-5). It is shown that using hot-EGR strategy led to an increase in exhaust temperature by approximately 30 ^{o}C, and therefore THC and CO conversion efficiencies were increased to the levels achieved for G75 fuel. This confirms the importance of the exhaust temperature for improving the conversion efficiencies when using the DOC. It should be noted that smoke emissions when using hot-EGR was around 3.6 times higher compared to cold-EGR results at the same EGR rate.

Table 7-5 Emissions and exhaust temperature before and after DOC when using hot-EGR for diesel at 1.4 bar BMEP

	O_2	**CO_2**	**CO**	**THC**	**NO**	**NO_2**	**NO_x**	**smoke**	**Ex. Temp.**
	%v	%v	ppmv	ppmv	ppmv	ppmv	ppmv	FSN	^{o}C
Before DOC	9.16	8.20	2540.37	1157.37	14.16	10.18	24.34	1.314	214.99
After DOC	8.91	8.61	5.79	42.99	20.70	0.91	21.61	1.179	208.93
Reduction %	2.75	-5.00	99.77	96.29	-46.20	91.09	11.21	10.27	2.82

Particulate number and size distribution results are illustrated in Figure 7-8. Particulate concentration is considerably higher than cold-EGR and to a much larger extent G75 results. For this condition, using lognormal bimodal analysis for particulates, it was not possible to separate the nucleation mode as particulates were mostly accumulation mode with high

concentrations. As listed in Table 7-6, particulates total number concentration reduction was in the same range for the case of cold-EGR technique. Therefore, increased exhaust temperature by using hot-EGR technique had the benefit of better THC and CO catalytic reductions at the expense of increased PN and PM. It can be hypothesised that reduction efficiency depends on two separate factors: 1-exhaust temperature and 2-volatility level of the particulates which is linked with the presence of volatile species (which can form nucleation mode particulates).

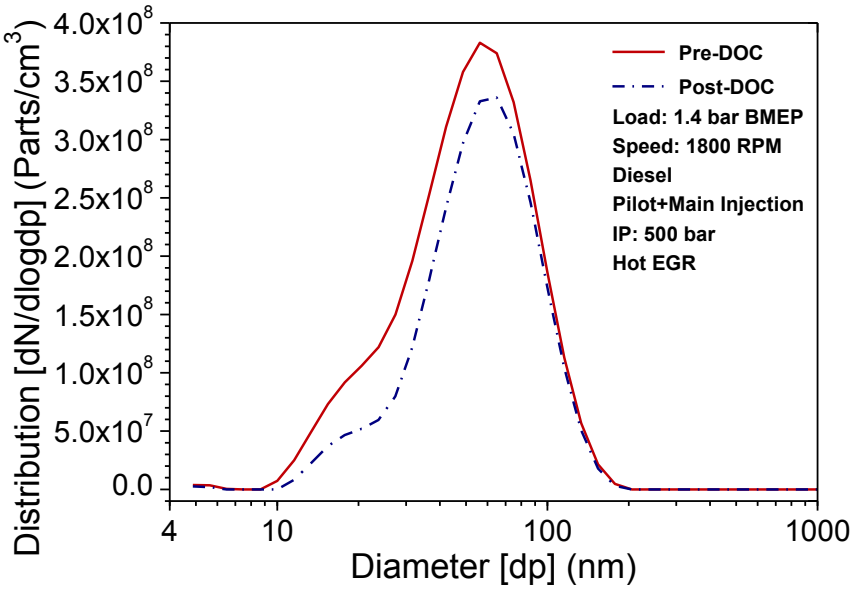


Figure 7-8 Particulate number and size distribution before and after DOC when using hot-EGR for diesel at 1.4 bar BMEP

Table 7-6 Particulate emissions physical concentration characteristics for hot-EGR diesel at 1.4 bar BMEP

	Total (N/cc)	Nucleation Mode			Accumulation Mode		
		Concentration (N/cc)	Mass (µg/cc)	CMD (nm)	Concentration (N/cc)	Mass (µg/cc)	CMD (nm)
Before DOC	2.18E+08	n/a	n/a	n/a	1.83E+08	3.42E-02	52.3
After DOC	1.70E+08	n/a	n/a	n/a	1.40E+08	2.77E-02	58.7
Reduction %	22.03	n/a	n/a	n/a	23.90	19.00	-12.05

Considering the case of cold-EGR strategy for diesel, similar gas phase SVOC characterisation performed for G75 operation was conducted. Figure 7-9 illustrates the results for n-alkanes and total alkanes which are the major components of total measured SVOC emissions. Compared to SVOC emissions from G75 PCI, concentrations of n-alkanes and total alkanes are generally higher before and after the DOC. A bimodal distribution of concentration based on carbon number for alkanes can be seen with two main peaks at C_{14} and C_{23} for SVOC measured before the DOC. It can be hypothesised that these peaks are from diesel fuel and engine lubricating oil respectively [86, 94]. Similar to the case of G75, alkanes with carbon number less than 18 are pronounced in these results.

Total conversion efficiencies for n-alkanes and alkanes were around 30% and 38%, respectively, which are lower than what was achieved for G75 with even lower concentrations before the DOC. Alkanes with carbon number between 18 and 21 had negative conversion efficiencies, although they have relatively lower concentrations. This might be due to desorption of SVOC adsorbed on the surface of particulates [86] or active partitioning into the particulate phase (for results measured before the DOC) [86] or reproduction of these species from other HC inside the DOC [95]; these need further investigation. Maximum positive conversion efficiencies for the alkanes were achieved for C_{23} and C_{12} with values of around 62% and 56% respectively. It might be worthy to mention that, for diesel fuel, conversion efficiencies of LMW HC with higher concentrations, in the studied carbon number range, were generally higher than heavier hydrocarbons. Comparing these conversion efficiencies with the conversion efficiency measured for THC emissions with the hot FID (Table 7-3), it can be seen that, generally, DOC is converting alkanes with 11<carbon number<24 better than THC. Another point to mention is the HC storage mechanism for HMW HC (with higher boiling points) in the DOC at temperatures below light-off [95]. Therefore, one possible explanation for this trend can be HC storage rather than catalytic HC conversion [95].

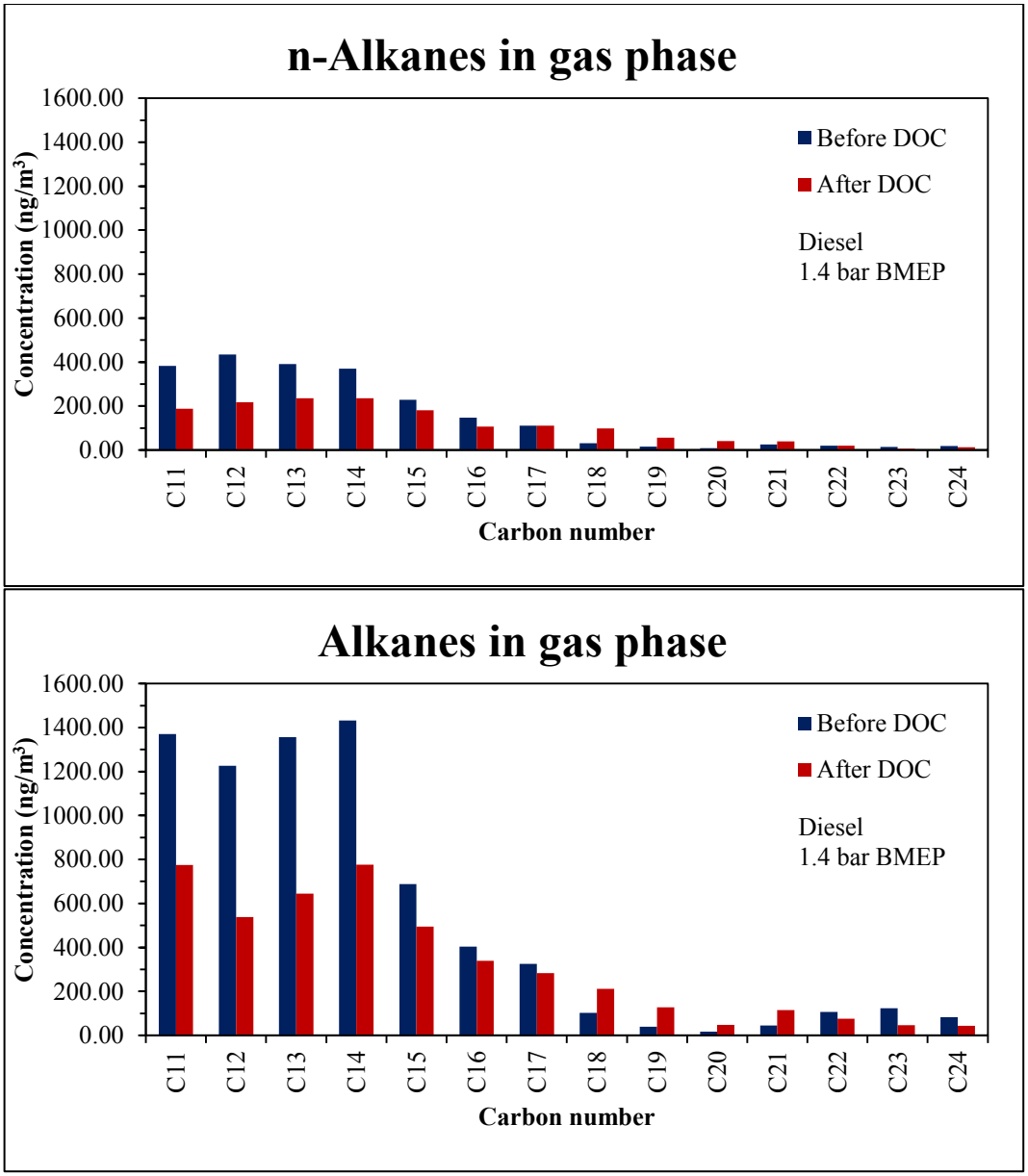


Figure 7-9 Normal alkanes (n-alkane) and total alkanes emissions before and after the DOC when using diesel fuel at 1.4 bar BMEP

Figure 7-10 illustrates the results of n-alkyl-cyclohexanes and total alkyl-cycloalkanes emissions from diesel combustion. Similar to the alkanes, alkyl-cycloalkanes emissions from diesel combustion were larger than that of G75 combustion at this engine operating load. The peak concentration belongs to the C_{12} alkyl-cycloalkanes while its conversion efficiency using DOC was around 44.5%. Total conversion efficiencies of the n-alkyl-cyclohexanes and alkyl-

cycloalkanes were around 40.5% and 41.5% respectively. Similar to alkanes, conversion efficiencies of lighter SVOC were higher than heavier SVOC for alkyl-cycloalkanes.

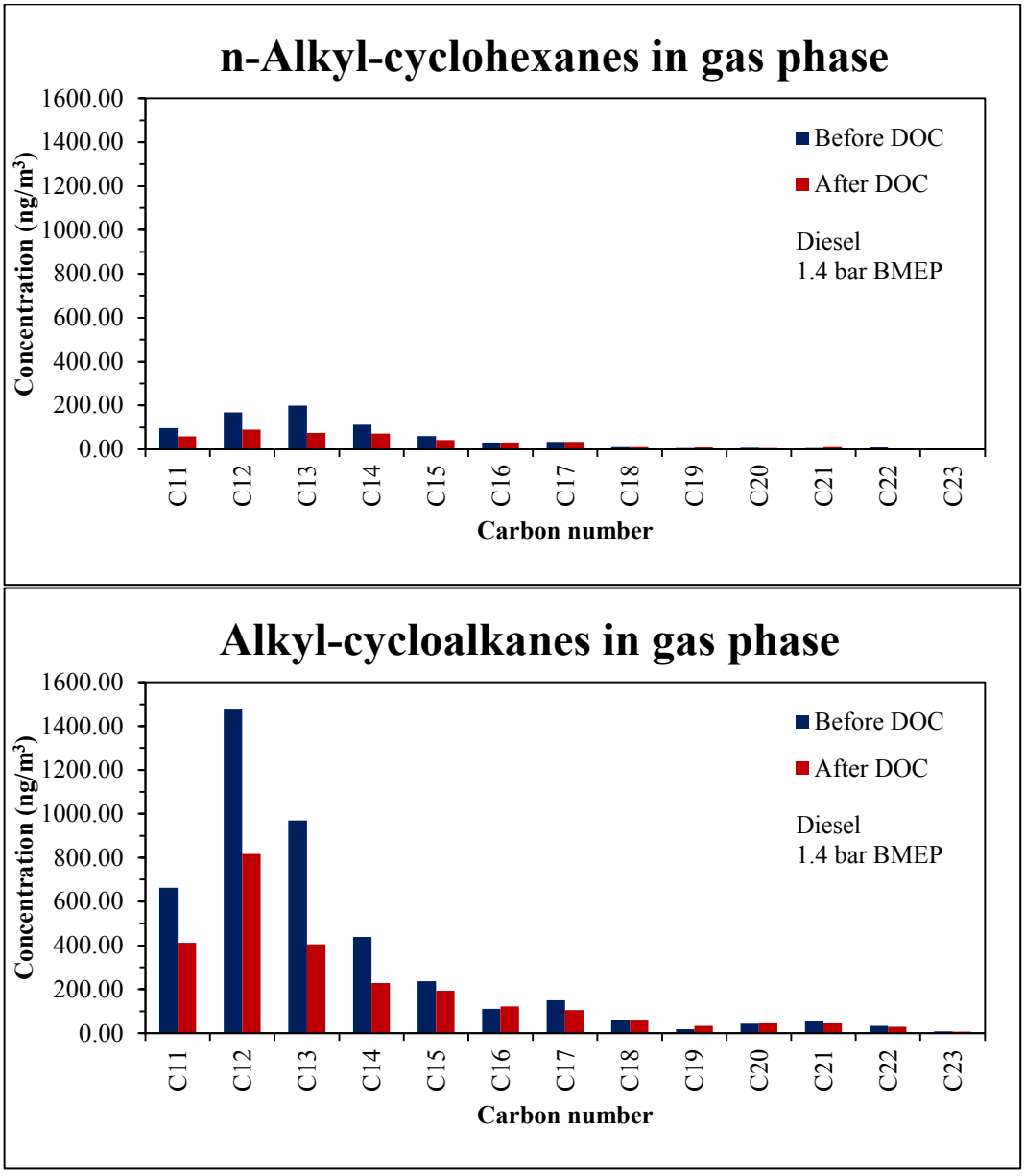


Figure 7-10 Normal (n)-alkyl-cyclohexanes and total alkyl-cycloalkanes emissions before and after the DOC when using diesel fuel at 1.4 bar BMEP

PAH emissions from diesel combustion were, in general, higher than G75 combustion as shown in Figure 7-11. ACE, ANT, FLR and PYR were not found in the exhaust of the G75 PCI, while they were present in the diesel emissions. Total conversion efficiency of PAH emissions of diesel was more than 50% at this operating load. NAP with the maximum concentration in the studied PAH, was reduced by around 49.5% using the DOC.

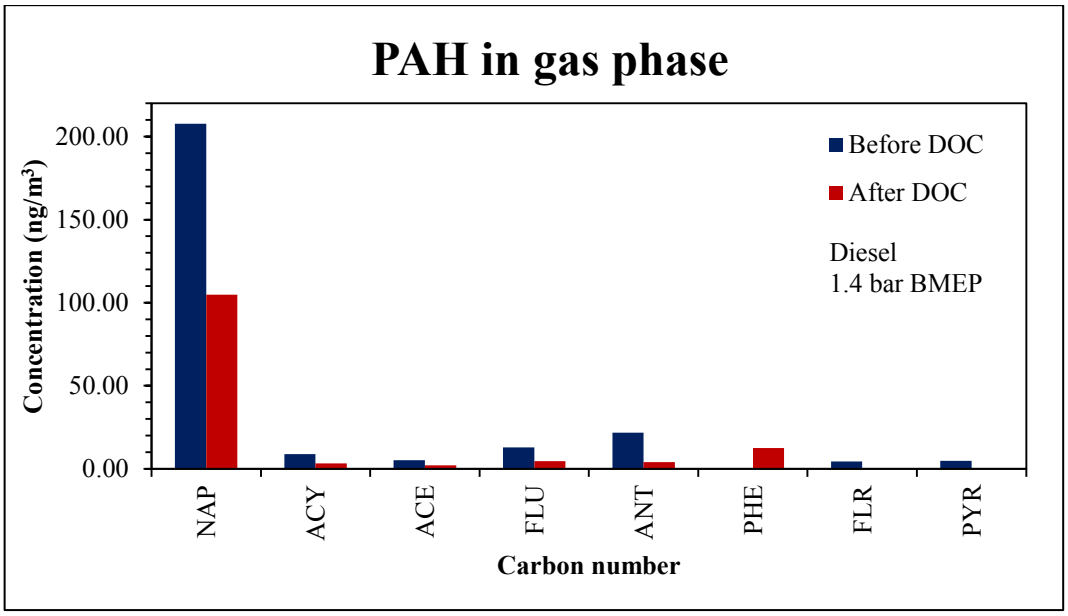


Figure 7-11 PAH emissions before and after the DOC when using diesel fuel at 1.4 bar BMEP

7.4. Effects of the DOC on emissions of Dieseline and diesel CI combustion at 3 bar BMEP

This section investigates effects of the DOC on engine emissions while using hot-EGR for G75 and cold-EGR for diesel at 3 bar BMEP. Double-injection with IQ1 of 10% was used for both fuels while second injection-timing (IT2) for diesel was more retarded compared to G75 due to higher cetane number.

7.4.1. Results for G75-Dieseline operation

Effects of the DOC on the emissions from G75-Dieseline combustion were analysed at 3 bar BMEP while IP was fixed at 350 bar and hot-EGR rate of 45% was used. These settings were concluded from the results presented in Chapter 5. Emissions and exhaust temperature results are listed in Table 7-7. At this load, conversion efficiency of CO and THC emissions are 99.88% and 96.83% respectively. Compared to the lower studied load, increase of exhaust temperature, from the value measured at the inlet of the DOC, was lower after the DOC. This may be due to the THC and CO concentrations being relatively lower and therefore less exothermic reactions take place on the surface of the DOC.

Table 7-7 Emissions and exhaust temperature before and after DOC when using G75 at 3 bar BMEP

	O_2	**CO_2**	**CO**	**THC**	**NO**	**NO_2**	**NO_x**	**smoke**	**Ex. Temp.**
	%v	%v	ppmv	ppmv	ppmv	ppmv	ppmv	FSN	^oC
Before DOC	7.57	9.42	3069.90	1919.37	31.92	7.57	39.49	0.008	281.91
After DOC	7.16	9.95	3.54	60.77	41.26	5.79	47.05	0.009	283.51
Reduction %	5.40	-5.60	99.88	96.83	-29.27	23.51	-19.16	-12.50	-0.57

The particulate number and size distribution and concentration characteristics results are shown in Figure 7-12 and Table 7-8, respectively. Reduction of total particulate number was lower compared to the case of 1.4 bar BMEP. This may be due to the fact that particulates are at very low levels and less amount of volatile compounds are present in the exhaust gases. However, the concentration of nucleation mode particulates was reduced by almost 24%. At this load, the accumulation mode concentration was more pronounced compared to the lower studied load. Although absolute values for particulate concentrations are relatively low, there seemed to be a shift towards larger particulates which have probably more carbonaceous solid

fractions. EC and OC analysis for this condition revealed that almost 5% of the total mass of the collected particulates are EC.

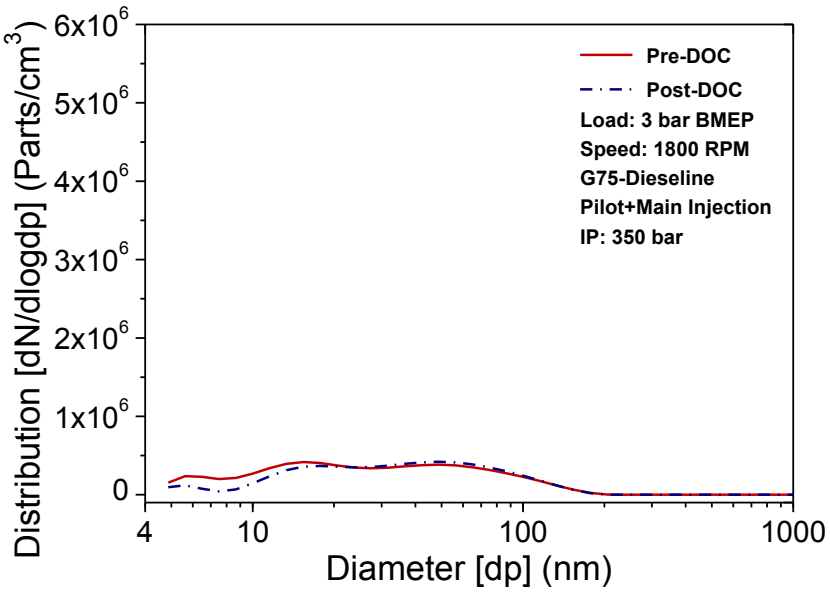


Figure 7-12 Particulate number and size distribution before and after DOC when using G75 at 3 bar BMEP

Table 7-8 Particulate emissions physical concentration characteristics for G75 at 3 bar BMEP

	Total (N/cc)	Nucleation Mode			Accumulation Mode		
		Concentration (N/cc)	Mass (µg/cc)	CMD (nm)	Concentration (N/cc)	Mass (µg/cc)	CMD (nm)
Before DOC	4.50E+05	1.85E+05	7.58E-07	14.3	1.93E+05	4.53E-05	52.5
After DOC	4.06E+05	1.41E+05	7.93E-07	16.8	1.96E+05	4.43E-05	54.0
Reduction %	9.88	23.78	-4.59	-17.16	-1.68	2.22	-2.76

Alkanes emissions measured before and after the DOC are shown in Figure 7-13 for this operating load. From this point, major discussion on effects of the DOC on SVOC emissions is focused on the homologous series of alkanes only, which is present in abundance in the fuel and emissions as discussed earlier. A bimodal concentration of alkanes was observed at this

load similar to the lower studied load, while alkanes with carbon number below 18 were present in abundance in the gas phase. Total conversion efficiency of the alkanes using the DOC was around 49% which is close to the conversion efficiency achieved at 1.4 bar BMEP for G75. In general, conversion efficiencies of different alkanes were higher than 40% with a mean conversion efficiency of around 47.5%. Conversion efficiency of the C_{14}, which had the second abundant concentration in the distribution, was around 57.5%.

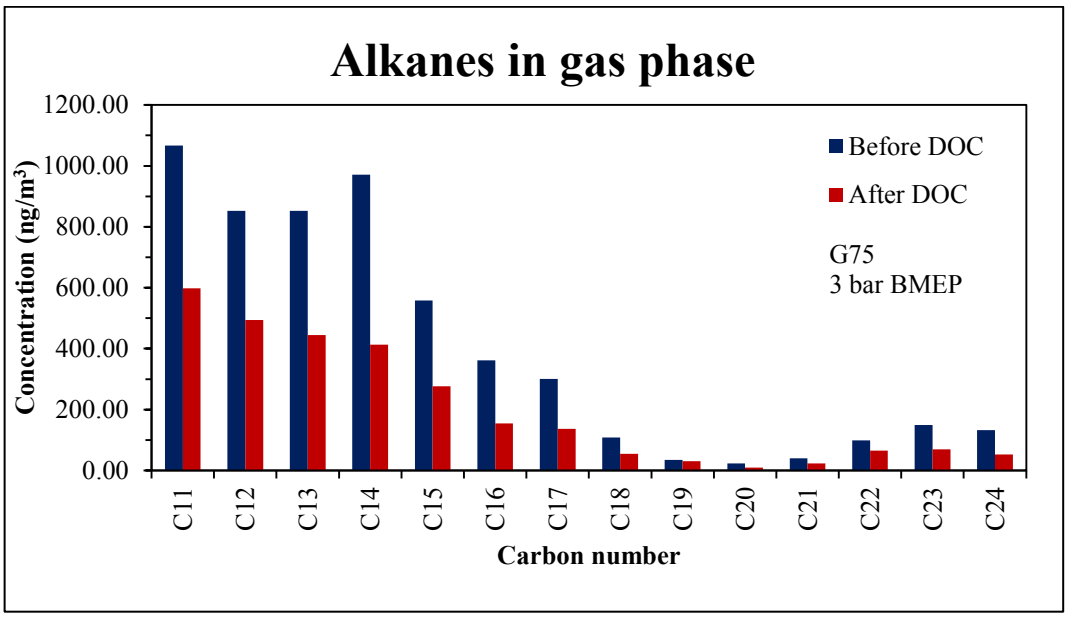


Figure 7-13 Alkanes emissions before and after the DOC when using G75 fuel at 3 bar BMEP

7.4.2. Results for diesel operation

Emissions and exhaust gas temperature results at 3 bar BMEP are listed in Table 7-9 for diesel with the IP of 700 bar and the same EGR rate as G75. It should be noted that as cold-EGR strategy was used for diesel, exhaust gas temperature measured upstream of the DOC was lower than G75 by around 19 ^{o}C. Conversion efficiencies of CO and THC were high at this

load as the exhaust temperature before DOC was sufficiently high. However, smoke emission of diesel is around 73 times higher than G75 after the DOC. Investigations at this operating condition can help understand effects of the DOC when its inlet temperature is sufficiently high for efficient conversion of the existing volatile species and the carbonaceous fraction concentration is significant.

Table 7-9 Emissions and exhaust temperature before and after DOC when using diesel at 3 bar BMEP

	O_2	**CO_2**	**CO**	**THC**	**NO**	**NO_2**	**NO_x**	**smoke**	**Ex. Temp.**
	%v	%v	ppmv	ppmv	ppmv	ppmv	ppmv	FSN	^oC
Before DOC	8.93	8.38	2419.90	1345.07	30.46	12.89	43.35	0.722	263.05
After DOC	8.64	8.78	5.28	37.78	41.19	7.06	48.25	0.660	264.41
Reduction %	3.30	-4.80	99.78	97.19	-35.22	45.27	-11.29	8.59	-0.52

Particulates emissions of diesel combustion at this load were dominated by the accumulation mode as illustrated in Figure 7-14. Results of measurements downstream of the DOC, compared to upstream, showed slight reductions in the accumulation mode and to a higher extent in the nucleation mode. Particulates emissions of diesel was higher than G75 both in terms of number and mass at the same load while using a lower IP (350 bar) for G75. These are supported by the results listed in Table 7-10. Although the nucleation mode peak was not very pronounced, a good reduction of more than 50% for nucleation mode concentration was observed. However, nucleation mode concentration (upstream of the DOC) for diesel was around 145 times higher than that of G75. This means post DOC nucleation mode concentration for diesel is higher than the G75 case. Reduction in accumulation mode particulates was not significant. Based on the results presented in this chapter, it can be concluded that the DOC is effective for reducing nucleation mode particulates (if the operating temperature is sufficiently high) and not for the accumulation mode particulates.

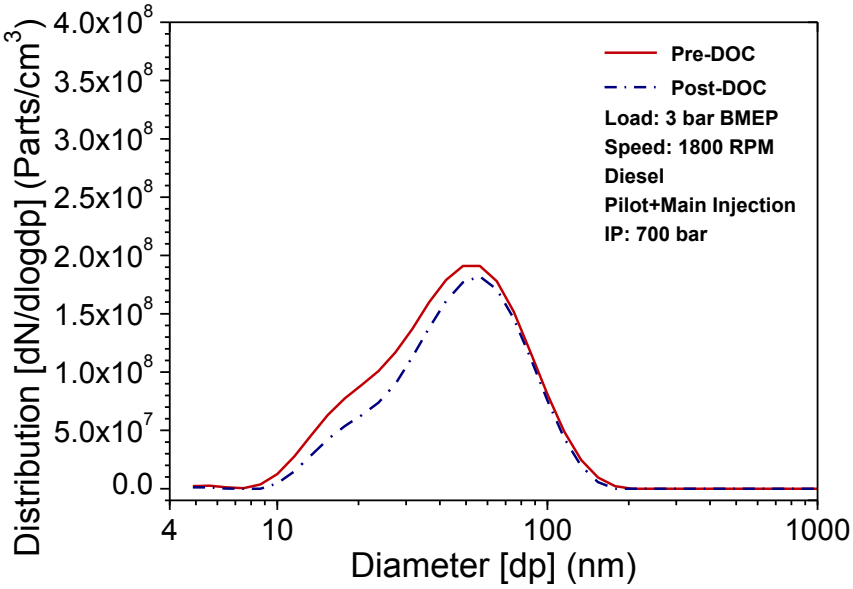


Figure 7-14 Particulate number and size distribution before and after DOC when using diesel at 3 bar BMEP

Table 7-10 Particulate emissions physical concentration characteristics for diesel at 3 bar BMEP

	Total (N/cc)	Nucleation Mode			Accumulation Mode		
		Concentration (N/cc)	Mass (µg/cc)	CMD (nm)	Concentration (N/cc)	Mass (µg/cc)	CMD (nm)
Before DOC	1.26E+08	2.69E+07	3.98E-04	22.0	8.35E+07	1.39E-02	53.3
After DOC	1.06E+08	1.34E+07	4.20E-05	17.1	8.10E+07	1.28E-02	53.3
Reduction %	16.09	50.12	89.46	22.51	3.05	8.03	0

Concentration distribution of total alkanes emissions, based on the carbon number, from the diesel combustion is illustrated in Figure 7-15. In general, conversion efficiency of different carbon number alkanes was lower compared to the case of G75. Total conversion efficiency for the alkanes was around 28.5% which is lower than the achieved value for the G75 operation (around 49%) and diesel operation at 1.4 bar BMEP (around 38%). Peak conversion efficiency, with the value of around 58.5%, was achieved for C_{19} alkanes. Gas phase alkanes emissions from diesel combustion at this operating mode were dominated by the alkanes with carbon numbers below 18. It is expected that a significant concentration of the SVOC can be

found in the particulate phase at this condition. This is hypothesised based on the fact that particulate emission concentration is high at this load; particulates are good sinks for SVOC [86] on which they can be condensed.

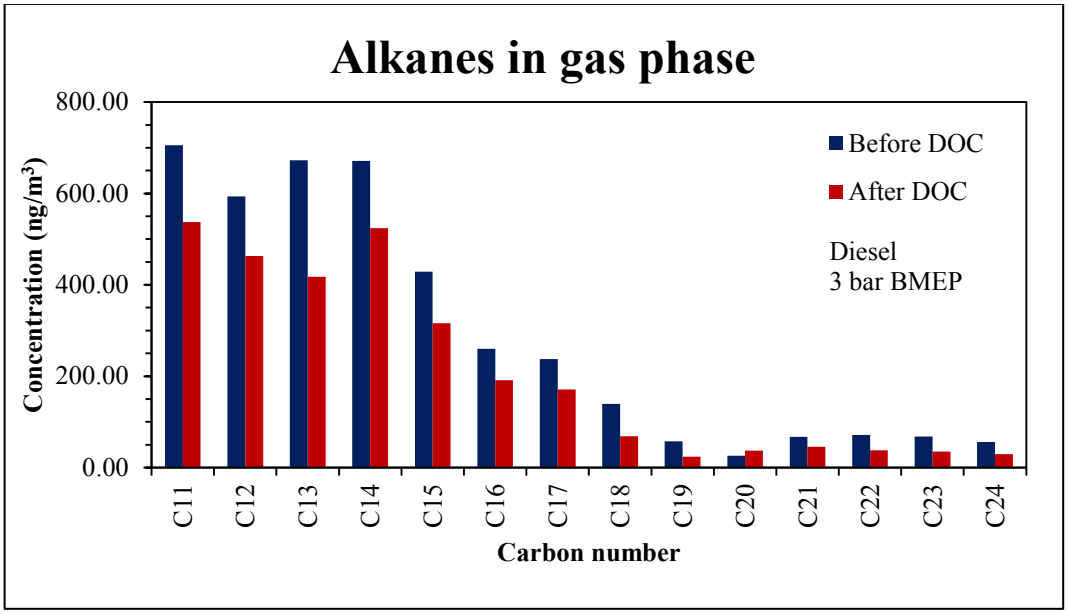


Figure 7-15 Alkanes emissions before and after the DOC when using diesel fuel at 3 bar BMEP

7.5. Effects of the DOC on emissions of Dieseline and diesel CI combustion at 6 bar BMEP

Exhaust temperature at 6 bar BMEP, with the studied EGR rates described in Chapter 5, was generally in the excess of 360 ^{o}C. The intention of the tests at this load condition was to identify effects of this high temperature on the effectiveness of the DOC. Cold-EGR strategy was used which was concluded to be beneficial for both G75 and diesel fuels in Chapter 5. Double-injection strategy with IQ1 of 10% was used for both fuels.

7.5.1. Results for G75-Dieseline operation

At 6 bar BMEP, featuring a high exhaust temperature of 379 ^{o}C, conversion efficiencies of CO and THC were high (Table 7-11), similar to the lower studied loads for G75. It should be noted as the engine load is increased, O_2 concentration in the exhaust gas is reduced and this means less oxidiser is available which may weaken the DOC performance. This, however, was not observed in the studied conditions (please see Table 7-11).

Table 7-11 Emissions and exhaust temperature before and after DOC when using G75 at 6 bar BMEP

	O_2	**CO_2**	**CO**	**THC**	**NO**	**NO_2**	**NO_x**	**smoke**	**Ex. Temp.**
	%v	%v	ppmv	ppmv	ppmv	ppmv	ppmv	FSN	^{o}C
Before DOC	5.01	11.33	2462.77	1125.08	55.23	5.91	61.14	0.017	379.07
After DOC	4.81	11.65	5.59	30.58	64.57	4.10	68.67	0.016	359.83
Reduction %	4.03	-2.85	99.77	97.28	-16.92	30.59	-12.33	5.88	5.08

Particulate size and number distribution results measured before and after the DOC are illustrated in Figure 7-16 for G75. There is an obvious reduction of nucleation mode particulates (with smaller diameters) using the DOC. This is in line with observations in the previous studied loads. Particulates physical characteristics concentrations are listed in Table 7-12. There are reductions in both particulate number and mass when comparing results of before and after the DOC. Total particulate number concentration was reduced by around 20%.

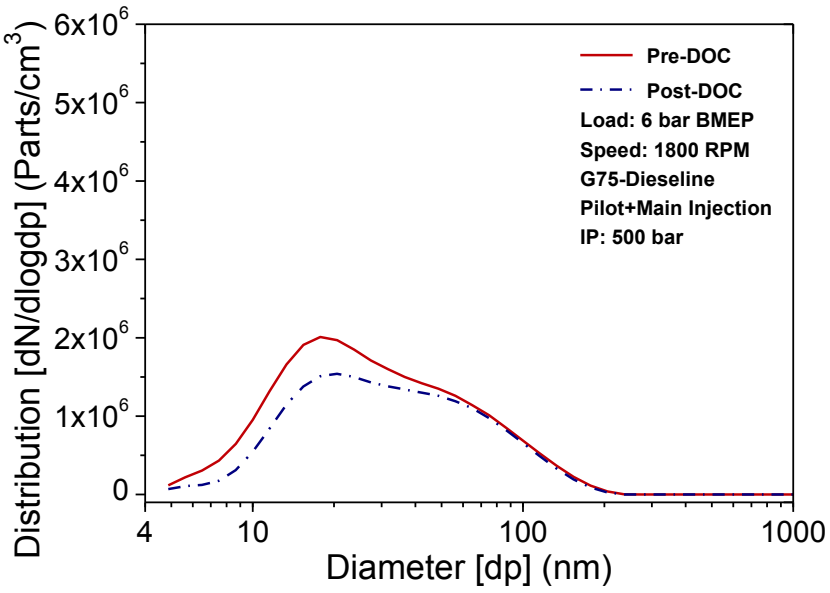


Figure 7-16 Particulate number and size distribution before and after DOC when using G75 at 6 bar BMEP

Table 7-12 Particulate emissions physical concentration characteristics for G75 at 6 bar BMEP

	Total (N/cc)	Nucleation Mode			Accumulation Mode		
		Concentration (N/cc)	Mass (µg/cc)	CMD (nm)	Concentration (N/cc)	Mass (µg/cc)	CMD (nm)
Before DOC	1.70E+06	8.32E+05	4.77E-06	16.5	7.41E+05	1.50E-04	47.4
After DOC	1.36E+06	6.28E+05	4.71E-06	18.0	6.33E+05	1.33E-04	50.7
Reduction %	19.63	24.61	1.24	-9.17	14.48	11.26	-7.09

Effects of the DOC on total alkanes emissions can be seen in Figure 7-17. Even at 6 bar BMEP, when using G75, alkanes with lower carbon number (within the studied range) had larger concentrations. Total conversion efficiency of the alkanes was around 22%. As opposed to normally good conversion efficiencies observed for C_{16} to C_{19} alkanes in the lower studied loads, negative conversion efficiencies were observed at this condition. Although, exhaust temperature is higher at this condition, SVOC concentration itself and also O_2 concentrations are relatively lower. Moreover, characterisation of the particulate phase SVOC is an interesting case study to identify any partitioning between gas and particulate phase [86].

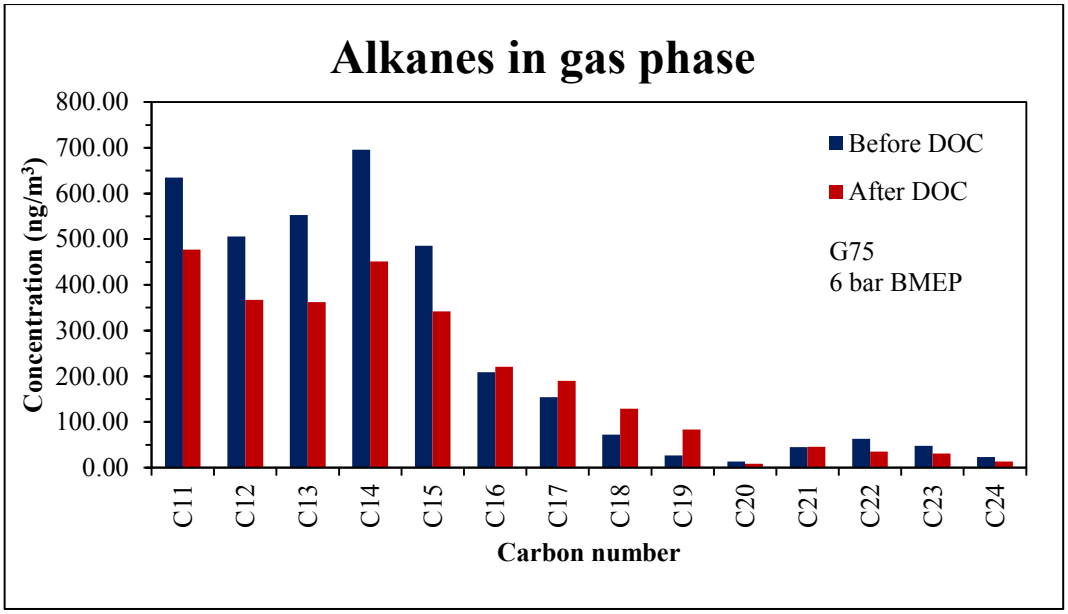


Figure 7-17 Alkanes emissions before and after the DOC when using G75 fuel at 6 bar BMEP

7.5.2. Results for diesel operation

Diesel combustion smoke emission was around 112 times higher than G75 combustion at 6 bar BMEP with the studied settings. CO and THC conversion efficiencies using the DOC were considerably high (please see Table 7-13). Temperature measured after the DOC was around 20 ^{o}C lower than before the DOC. This may indicate that relatively lower concentrations of the consumed CO and HC did not increase the temperature considerably. Moreover, possible heat losses through the surfaces of the DOC can help explain these results.

Table 7-13 Emissions and exhaust temperature before and after DOC when using diesel at 6 bar BMEP

	O_2	CO_2	CO	THC	NO	NO_2	NO_x	smoke	Ex. Temp.
	%v	%v	ppmv	ppmv	ppmv	ppmv	ppmv	FSN	^{o}C
Before DOC	6.77	10.14	1163.02	555.36	92.84	8.33	101.17	1.906	377.57
After DOC	6.69	10.30	5.54	14.21	103.36	2.28	105.64	1.854	358.15
Reduction %	1.09	-1.66	99.52	97.44	-11.33	72.63	-4.42	2.73	5.14

Particulate number and size distribution and physical characteristics concentrations are shown in Figure 7-18 and Table 7-14, respectively. Distribution was heavily dominated by larger accumulation mode particulates which did not change significantly after the DOC. For both of the measurement locations, through lognormal bimodal analysis, it was not possible to detect a nucleation mode peak. Reduction of diesel particulate emissions at this load using the DOC was minimal and it is believed that application of a diesel particulate filter (DPF) will be more helpful for the case of these carbonaceous particulates. EC and OC analysis at this load for diesel showed that up to 22% of the mass of total collected particulates were EC.

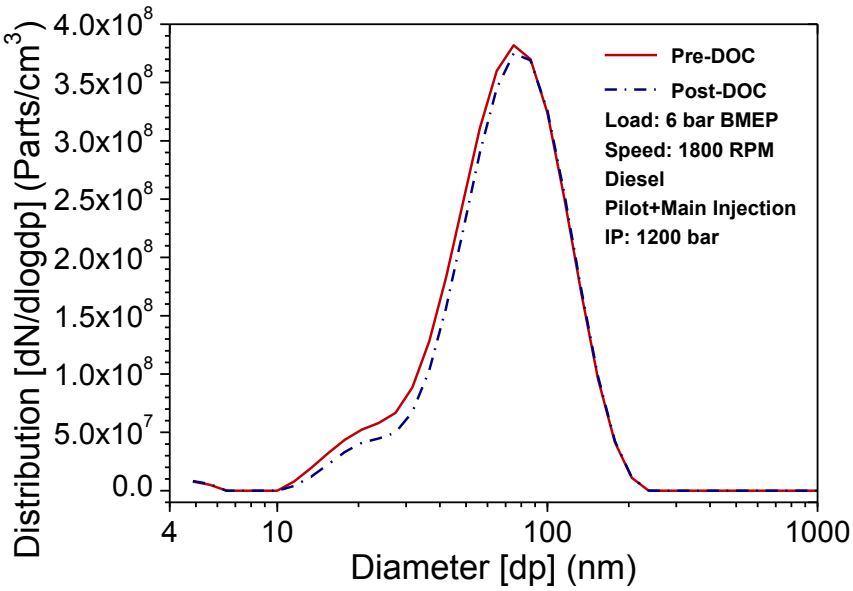


Figure 7-18 Particulate number and size distribution before and after DOC when using diesel at 6 bar BMEP

Table 7-14 Particulate emissions physical concentration characteristics for diesel at 6 bar BMEP

	Total (N/cc)	Nucleation Mode			Accumulation Mode		
		Concentration (N/cc)	Mass (µg/cc)	CMD (nm)	Concentration (N/cc)	Mass (µg/cc)	CMD (nm)
Before DOC	2.03E+08	n/a	n/a	n/a	1.65E+08	6.17E-02	66.7
After DOC	1.91E+08	n/a	n/a	n/a	1.52E+08	5.65E-02	70.4
Reduction %	6.14	n/a	n/a	n/a	7.95	8.36	-5.55

Alkanes emissions from diesel combustion at 6 bar BMEP are illustrated in Figure 7-19. The total conversion efficiency of total alkanes was around 26% and generally was higher for alkanes with carbon numbers larger than 21. Similar to the results shown for G75 operation at 6 bar BMEP, there were negative conversion efficiencies for C_{16} to C_{19} alkanes. There can be several hypotheses about why the differences in the conversion efficiencies are observed. Normally at higher engine loads, the ratio of EC to OC of particulate matter is higher [24]. This means that there is more sink media available for organic vapours to be condensed and adsorbed onto under the right temperature and pressure. This reduces the chance of DOC to convert these adsorbed vapours as they have partitioned into the particulate phase. Even during sampling, part of the gases can be adsorbed on the already collected particulates on the sampling filter (acting as the sink media) upstream of the adsorption tube. Moreover, it is possible that the gas phase species measured after the DOC are partitioned from the particulate phase within the DOC. These highlight the necessity for measuring SVOC in the particulate phase in addition to the gas phase to confirm these hypotheses.

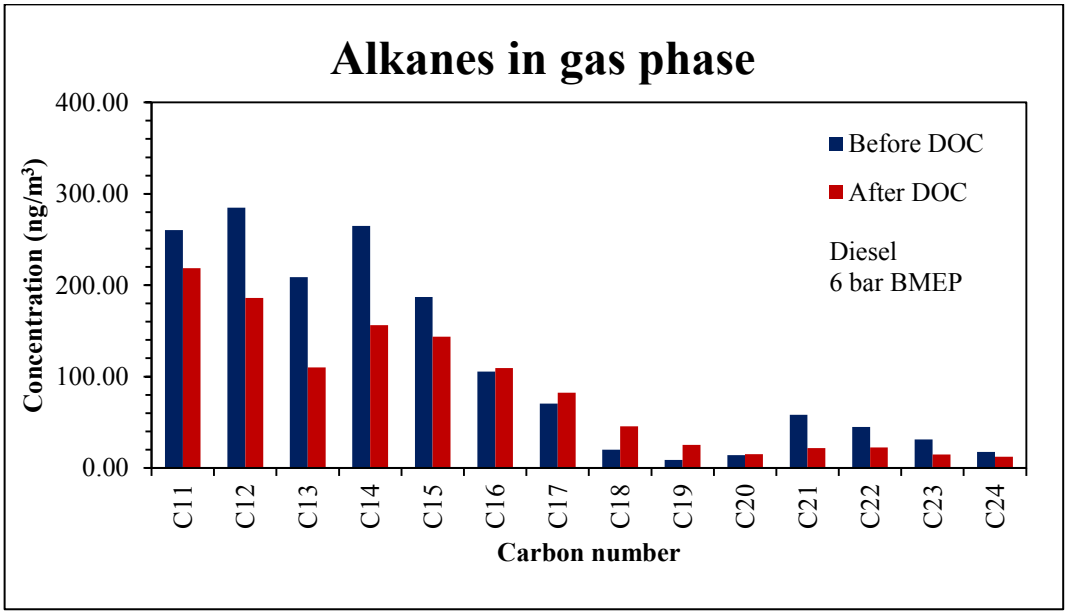


Figure 7-19 Alkanes emissions before and after the DOC when using diesel fuel at 6 bar BMEP

7.6. Summary/Conclusions

Due to the nature of the PCI combustion featuring longer ignition delays, compared to diesel, HC and CO emissions, especially at low loads, are relatively higher. This chapter investigated effects of a production DOC on the emissions from a G75-Dieseline (G75) fuelled PCI engine at three loads of 1.4, 3 and 6 bar BMEP and a fixed speed of 1800 RPM. Results were compared to the results collected when using diesel fuel. The major findings at each studied-load are as follows:

1.4 bar BMEP:

- The major challenge for the good functionality of the DOC at this low load, featuring high concentrations of volatile species, is the low exhaust temperature. It was found that, compared to cold-EGR, using hot-EGR increases the exhaust temperature (to values more than 200 ^{o}C) and consequently improves the catalytic reduction of volatile species.
- Conversion efficiencies of CO and THC emissions from the G75 PCI combustion with the hot-EGR strategy were 99.95% and 95.98%, respectively. Although, particulate emissions measured before the DOC are low at this PCI condition, total particulate number, nucleation mode mass and accumulation mode mass were reduced by more than 75%, 81% and 47%, respectively, by using the DOC. The more volatile nature of particulates (with less elemental carbon fractions present in the exhaust) emitted from the G75 PCI coupled with high exhaust temperature are believed to have helped achieve these reductions. Therefore, hot-EGR technique is a “win-win” strategy for both in-cylinder and out-cylinder CO and HC reduction, without the penalty of higher smoke emissions, for PCI combustion with low-cetane fuels.

- For diesel, using hot-EGR strategy to increase exhaust temperature increased smoke emissions by approximately 3.6 times (reasons were discussed in Chapter 5) while using cold-EGR strategy resulted in low CO and THC conversion efficiencies; 26.58% and 13.45% respectively. Moreover, particulate emissions reduction was not significant due to lower exhaust temperature and less volatility of the particulates. Thus, volatile species catalytic reduction for diesel operation is problematic at this load.
- For both G75 and diesel, gas phase SVOC emissions characterisation revealed that there is a bimodal distribution of concentrations based on the carbon number (molecular weight) for each SVOC class. The higher peaks related to the lighter hydrocarbons (with C<20) are believed to be originated from the fuel. The smaller peaks related to the heavier hydrocarbons (with C>22) are believed to be sourced from the engine lubricating oil. Low molecular weight (LMW) HC are pronounced in the gas phase and high MW HC are expected to be more pronounced in the particulate phase. This can be due to the fact that LMW HC have lower boiling point and higher vapour pressure. Alkanes were found to be the major contributor to the total gas phase SVOC emissions as expected by their abundance in the automotive fuels. Conversion efficiencies of SVOC with different MW within the same class and of different classes are different. Moreover, using different fuels (G75 or diesel) can change these values.
- All abundant classes of SVOC emissions, e.g. alkanes, alkyl-cycloalkanes and PAH, from G75 combustion were generally lower than diesel. Moreover, generally, SVOC conversion efficiencies for G75 operation are higher than those for diesel operation which can be due to lower exhaust temperature of diesel. For example, the conversion efficiency of alkanes when using G75 and diesel were 51% and 38%, respectively.
- Due to the difference observed for THC and gas phase SVOC reduction values when using the DOC, HMW HC storage possibility when the temperature is below light-off for

some compounds was highlighted in this chapter. This brings a scope for further characterisation of a wider range of HC (e.g. from C_4 to C_{40}).

3 bar BMEP:

- Higher exhaust temperature at this load helped achieve efficient conversion of CO and THC (by more than 95%) using the DOC for both fuels. It was found that most of the reductions in the particulates number and mass are related to the nucleation mode which is believed to be more volatile. Due to the short ignition delay of diesel, total emitted particulate number from diesel combustion was 280 times higher than the value for G75.
- For G75, total conversion efficiency of the alkanes using the DOC was around 49% while it was around 28.5% for diesel. It is expected that a significant concentration of SVOC can be found in the particulate phase at this condition for the diesel combustion as the particulate concentration (dominated by the accumulation mode) is relatively high. SVOC can be condensed on the particulates present in the exhaust and dilution system.
- It was found that the conversion efficiency of some HMW HC is higher than the LMW HC (within the studied range). In theory LMW HC, which have higher diffusion rate, are expected to be converted easier. While it is known that HMW HC have lower light-off temperature. Therefore, there seems to be a competition between adsorption rate and required temperature needed for efficient conversion of SVOC which needs to be confirmed with further modelling and experimental work.

6 bar BMEP:

- Reduced exhaust oxygen concentration (resulted from using high EGR rates) observed at this higher studied load did not affect the conversion efficiency of CO and THC. Total particulate number and accumulation mode mass emitted from the diesel combustion were around 119 and 411 times, respectively, higher than the values for G75 mainly due to its longer ignition delay and higher volatility. Up to 22% of the mass of total collected particulates from the diesel combustion exhaust were elemental carbons (dominated by the accumulation mode). This reduces the chance of their number reduction by using the DOC (around only 6%) while G75 particulates (more volatile) were reduced more efficiently (by around 20%).
- Some negative conversion efficiencies were observed at this condition for both fuels and mainly for alkanes with carbon number between C_{16} and C_{19}. This can be hypothesised to be due to the higher ratio of EC to OC of particulate matter at higher loads. EC is a good sink media for adsorption of the organic vapours and it is possible that the gas phase species measured after the DOC are partitioned from the particulate phase or formed from other HC within the DOC. These highlight the necessity for measuring SVOC in the particulate phase in addition to the gas phase to confirm this hypothesis.

Finally, it was confirmed that using the DOC for the exhaust of the developed G75 PCI combustion technique is useful for reducing THC (including gas phase SVOC), CO and particulate emissions at all of the studied loads. However, results collected for diesel showed poor conversion efficiency of HC and CO at low loads and low reduction of particulates when using the DOC.

Chapter 8
SUMMARY, CONCLUSIONS & FUTURE WORK

8.1. Introduction

The overall aim of this research work was to reduce emissions from the production multi-cylinder light-duty compression-ignition engine while maintaining its high fuel-conversion efficiency. This includes utilisation of low-cetane number fuels (Dieseline (a blend of diesel and gasoline) and naphtha) combined with high EGR rates for the premixed compression-ignition (PCI) combustion mode. Furthermore, the effectiveness of a diesel oxidation catalyst (DOC) for reducing volatile species emitted from the PCI combustion was investigated. Summary of the approaches and main conclusions are provided in the next section.

8.2. Summary and conclusions

In this thesis, experimental results were reported and discussed in four different chapters. Experiments were conducted for three fuels: Dieseline (at two volumetric blend-ratios of diesel-gasoline; 50-50 (G50) and 25-75 (G75)), naphtha and diesel. Chapters 4, 5 and 6 mainly focused on the PCI techniques incorporating long ignition delay and high volatility of the fuels and high EGR rates for in-cylinder simultaneous reduction of particulate matter (PM) and oxides of nitrogen (NO_x) emissions. It was found that due to the nature of the PCI combustion featuring longer ignition delays compared to diesel, hydrocarbons (HC) and carbon monoxide (CO) emissions, especially at low loads, are relatively higher. Therefore, Chapter 7 investigated an out-cylinder technique (by using a DOC) to reduce total HC (THC)

and CO emissions. In this manner, an overall NO_x, PM, THC and CO emissions abatement solution was developed. Major findings of the conducted case studies are presented below:

Parametric Analysis of Split-injection

Two-stage split-injection (double-injection) strategies were investigated to improve fuel-air premixing quality and consequently reduce NO_x and PM, in comparison to the results of the single-injection strategy, at low-medium loads for a G50-Dieseline (G50) fuelled partially PCI (PPCI) engine. A parametric analysis, by using the Taguchi design-of-experiment, was conducted to quantitatively identify individual effects of each under-study injection parameter (injection timings and quantity-ratios) on the combustion and emission characteristics. Furthermore, optimum operating values of injection parameters for obtaining the minimum and maximum of the combustion and emission characteristics were identified.

At 1.37 and 2.97 bar BMEP, variations of the NO_x emissions were dominated by the first injection event. Variations of the brake thermal efficiency (BTE), CO and THC were mainly influenced by the first injection-timing. Variations of the combustion-phasing (AHR-50) were governed by the second injection-timing. Variations of the smoke emissions were load dependant, although the main contributor was second injection-timing.

Double-injection strategies developed in this case study for the G50 fuelled PPCI engine improved the fuel-air premixing process when compared to the single-injection strategy; it was possible to simultaneously reduce brake specific NO_x ($BSNO_x$) and smoke emissions by approximately 50% and 90%, respectively. However, due to possible fuel-air overmixing and fuel wall-impingement when using advanced injection-timings, THC emissions can be higher. At higher loads, ignition delay of G50 is not long enough to avoid pre-TDC and double-stage

combustion when using double-injection. Therefore, in order to achieve a low-smoke combustion at higher operating loads, it was suggested to use a less reactive fuel in combination with enhanced air/exhaust handling strategies; thus the two following case studies were conducted.

G75-Dieseline Fuelled PCI Engine

G75-Dieseline (G75) PCI combustion was investigated at various loads from 1.4 to 17.3 bar BMEP while using single and double injection strategies with various intake/exhaust handling techniques. In general, as smoke and NO_x emissions from G75 PCI combustion are low, single-injection is favoured over double-injection to avoid complexity, high HC/CO (caused by overmixing and wall-impingement at low loads) and possible high smoke (caused by two-stage combustion at high loads). At each operating load, combustion performance and emission characteristics are functions of the injection event and intake/exhaust handling strategies which affect both premixing level and combustion-phasing. It was concluded that, as particulate emissions are lower compared to the diesel combustion results, lower injection pressures (IPs) must be used at all loads for G75 (especially below 12 bar BMEP) to reduce parasitic losses, overmixing and wall-impingement and increase the degree of charge stratification. In other words, if there is a long-enough ignition dwell then it is better to use low IP to enhance the PCI combustion. It was shown that using the developed techniques, G75 PCI can reduce particulate emissions at a wide load range from 1.4 to 17.3 bar BMEP, mainly due to longer ignition delay and consequently better fuel-air premixing, while maintaining the same range of BTE compared to the diesel fuel combustion.

Combustion instability and high CO and THC emissions mainly due to the long ignition delay of low-cetane fuels are the challenges with the PCI combustion at low loads. Utilisation of the

hot-EGR strategy to increase intake temperature and low IP (between 150 and 350 bar) were shown to enhance the G75 PCI combustion at 1.4 and 3 bar BMEP while smoke and NO_x emissions were close to zero. However, using the hot-EGR strategy for diesel with shorter ignition delay increased smoke emissions by up to 3.9 times due to the thermal throttling effect. In attempts to reduce high smoke emissions from the high-EGR driven low-NO_x combustion of diesel by using higher IPs, it was found that there is a penalty of reduced BTE probably due to higher parasitic losses, fuel wall-impingement and overmixing. Therefore, using diesel fuel needs cold-EGR and higher IP or otherwise particulate emissions will be high. Higher BSTHC and BSCO emissions are the penalties of using G75 compared to diesel; however, these emissions are well-reduced by a DOC (discussed later in this section).

At medium loads (above 6 bar BMEP), cold-EGR strategy and IP>500 bar are required to avoid high particulate emissions from the G75 PCI combustion. Due to longer ignition delay and higher volatility of the G75 compared to diesel, particulate emissions, in terms of number and mass, were reduced by up to 99.5% while maintaining $BSNO_x$ below 0.4 g/kWh. High particulate emissions from the diesel combustion can be reduced at the expense of either increased $BSNO_x$ or reduced BTE. Limitations with double-injection strategy for G50 at medium loads for achieving single-stage combustion were overcome by using G75 (which has a lower cetane number). Double-injection strategy helped to advance combustion-phasing towards the TDC at medium-high loads by the combustion of the first injected portion of the fuel which increases in-cylinder temperature before/during the second injection.

At loads above 12 bar BMEP, the difference between ignition delay of G75 and diesel was less significant compared to the lower studied loads due to the higher in-cylinder pressure and temperature. Therefore, IP>1000 bar was required to improve fuel-air mixing and to shorten injection duration to avoid high soot emissions from the less-premixed combustion. Particulate emissions were reduced by up to 79% when using G75 instead of diesel fuel.

Although it is possible to reduce particulate emissions with using G75 instead of diesel at higher loads, it is challenging to reduce NO_x and smoke simultaneously. Thus there is a need for a more efficient turbocharging system to avoid very low specific air-fuel ratios while using high EGR rates to suppress NO_x formation. Using double-injection strategy for G75 and diesel resulted in high smoke emissions due to the double-stage combustion.

Combustion of G75 was shown to be more sensitive to the changes of engine controlling parameters and this highlights the need for a comprehensive optimisation of engine to suite PCI combustion. The need for detailed in-cylinder optical studies and simulation of chemical kinetics under the studied PCI conditions is obvious.

Naphtha Fuelled PCI Engine

Naphtha was compared to G75 in order to investigate the effects of its gasoline-like (narrower) boiling profile on the combustion performance and emission characteristics of the PCI engine. Particulate emissions from naphtha PCI combustion, similar to G75 PCI combustion, were generally lower than diesel combustion results.

The main issue with the naphtha fuelled PCI combustion at very low loads is the high cyclic variations of the combustion. Even with using hot-EGR strategy and low IP (e.g. 150 bar), CO and THC emissions were considerably high and obtaining a COV of IMEP<10% was challenging. This is hypothesised to be due to the lower degree of stratification of charge and higher overmixing caused by higher volatility of naphtha compared to G75. Peak obtained BTE was 2.54% lower (in absolute value) compared to the results of an equivalent G75 PCI condition. It is recommended to investigate IP<150 bar for naphtha.

At loads above 3 and below 17.3 bar BMEP, in general, combustion is shorter and more intense compared to the G75 combustion. This is believed to be due to the lower charge stratification level caused by the higher volatility of naphtha which results in a more rapid combustion with some accompanied issues such as increased NO_x emissions due to possible high in-cylinder peak temperature. This imposes some challenges for obtaining high BTE and low NO_x simultaneously as the combustion-phasing is required to be delayed to reduce NO_x emissions and therefore BTE is reduced. It is recommended to use lower IP for naphtha (lower than what was used for G75) to help increase stratification level. Similar to G75 results, at most of the studied loads, due to lower THC and CO levels, single-injection is favoured over double-injection.

Similar to G75, ignition delay of naphtha was shortened as the load was increased, while in general, G75 performed better in all of the studied loads for simultaneously achieving high BTE and low NO_x, smoke, THC and CO. It is believed that using Dieseline improved stratification level of the charge useful for the PCI combustion.

DOC Effects on Emissions from the PCI Engine

High THC and CO emissions, especially at low operating loads, from the G75 PCI combustion are efficiently reduced by a production DOC.

At 1.4 bar BMEP, exhaust gas temperature of the diesel combustion with cold-EGR was below 200 ^{o}C, resulting in low catalytic reductions of CO and THC (<30%). Using hot-EGR for diesel to increase the exhaust temperature resulted in elevated smoke emissions; however, using hot-EGR for G75 resulted in near-zero smoke emissions and conversion efficiency of >96% for THC and CO. Therefore, utilisation of the hot-EGR is a “win-win” strategy to

enhance the PCI combustion process and reduction of the volatile/semi-volatile compounds using the DOC at low loads. For both fuels at higher loads, THC and CO conversion efficiencies are high as the exhaust temperature is sufficiently high.

DOC helped reduce low-level particulate number and mass emissions from the G75 PCI combustion by up to 75% and 64%, respectively. Major reductions were achieved for nucleation mode particulates believed to be mainly volatile. When operating on the PCI combustion, more volatile nature of particulates, as opposed to the case of diesel, can explain these DOC-induced reductions.

Gas phase semi-volatile organic compounds (SVOC) characterisation revealed that there is a bimodal distribution of concentrations based on the molecular weight (MW) for each SVOC class. Higher peaks related to the lighter HC (carbon-number<20) and smaller peaks related to the heavier HC (carbon-number>22) are believed to be originated from fuel and engine lubricating oil, respectively. Low MW (LMW) SVOC and high MW (HMW) SVOC are pronounced in gas phase and particulate phase, respectively. Alkanes are the major contributor to the total gas phase SVOC emissions as expected by their abundance in the automotive fuels. DOC-induced reductions of SVOC with different MW within the same class and of different classes are different. It was found that the conversion efficiency of some HMW SVOC is higher than the LMW SVOC (within the studied range). In theory LMW HC, which have higher diffusion rate, are expected to be converted easier. While it is known that HMW HC have lower light-off temperature. Therefore, there seems to be a competition between adsorption rate and required temperature needed for efficient conversion of SVOC which needs to be confirmed with further modelling and experimental work.

Some negative conversion efficiencies, especially at higher engine operating loads when the elemental carbon (EC) fraction is higher, were observed for SVOC emissions (mainly for

alkanes with 16<carbon-number<19). EC is a good sink media for adsorption of the organic vapours and it is possible that the gas phase species measured after the DOC are partitioned from the particulate phase or formed from other HC within the DOC. These highlight the necessity for measuring SVOC in the particulate phase in addition to the gas phase to confirm this hypothesis.

8.3. Possible implications for fuel/automotive industries and suggested future work

Major suggestions for further research and development work raised from the investigations conducted in this thesis are as follow:

Technologies for PCI/GCI Engines

At low-medium engine loads, hot-EGR strategy and low IP are interesting technologies for the future low-cetane fuelled PCI engines. Results presented in this thesis highlight the necessity for some detailed in-cylinder optical analysis of the effects of hot-EGR and/or low IP on the fuel spray, combustion and emissions characteristics in a CI engine. Various enhancements suiting PCI engines, such as optimised control strategy, combustion chamber geometry and injection system (e.g. reducing the included-angle of the injector), can be further studied to lower HC emissions sourced from the fuel wall-impingement.

At high engine loads, when using high EGR rates, more powerful intake boosting systems, compared to the current systems, are required for reducing particulate emissions further. Moreover, it is beneficial to investigate high volumetric blend-ratios of gasoline (>90%) in

the Dieseline fuel for the PCI combustion. However, the issues with the high cyclic variations of combustion at lower operating loads must be taken into account. Optimising the gas exchange process (e.g. via valve timings) and increasing the in-cylinder temperature can be further areas of research at low loads; it might be helpful to use a sparking system or a powerful glow-plug. Utilisation of PCI engines in hybrid electric powertrains might be beneficial as the low load operation (when fuel conversion efficiency is lower) can be assisted by an electric motor. Cold start, transient and low-load low-speed operation of the CI engine using low-cetane PCI strategies are interesting case studies.

Future Fuels for PCI/GCI Engines

It is suggested that the future low-cetane fuels for PCI/GCI engines have a small fraction of heavy distillates (diesel-like), proved to be useful for enhancing the combustion at low-medium loads in this work. It is believed that higher stratification level of the charge resulted from using fuels with a wider boiling range can help avoid rapid (HCCI-type) combustion. There is a further scope for studying fuel composition effects, e.g HC structure, aromatics content and oxygenates content, on combustion and emission characteristics of the PCI mode.

SVOC Conversion Mechanism Using a DOC

Results discussed in the Chapter 7 of this thesis highlighted the requirement for some theoretical and lab-based research into the detailed conversion mechanisms of SVOC in a DOC. Moreover, it is suggested to measure a wide spectrum of HC based on the carbon-number, e.g. from C_4 to C_{40}, to identify the contribution of SVOC to THC emissions. Investigation of the competition between adsorption rate and required temperature needed for

efficient conversion of SVOC with different molecular weights and structures is an interesting case study. There is a scope for further characterisation of particulate emissions form the PCI combustion, e.g. morphology and size-resolved characterisation with impaction based particulate collectors, to understand the DOC effects.

AUTHOR'S PUBLICATIONS RELATED TO THIS WORK

Papers Published:

- **Soheil Zeraati Rezaei**, Fan Zhang, Hongming Xu, Akbar Ghafourian, Jose M. Herreros, Shijin Shuai, *Investigation of Two-stage Split-injection Strategies for a Dieseline Fuelled PPCI Engine*, Fuel, 107 (2013) 299-308.

  This paper was awarded as the Engineering and Physical Sciences (EPS) Best Publication of the Month (Research Impact Award) for papers published in May 2013 from the University of Birmingham.
- Mohammed S. Alam, **Soheil Zeraati Rezaei**, Christopher P. Stark, Zhirong Liang, Hongming Xu, Roy M. Harrison, *The Characterisation of Diesel Exhaust Particles - Composition, Size Distribution and Partitioning*, Faraday Discussions, 189 (2016) 69-84.
- Fan Zhang, **Soheil Zeraati Rezaei**, Hongming Xu, Shijin Shuai, *Experimental Investigation of Different Blends of Diesel and Gasoline (Dieseline) in a CI Engine*, SAE International Journal of Engines, 7 (2014) 1920-30.
- Fan Zhang, Hongming Xu, **Soheil Zeraati Rezaei**, Gautam Kalghatgi, Shijin Shuai, *Combustion and Emission Characteristics of a PPCI Engine Fuelled with Dieseline*, SAE International, Technical Paper 2012-01-1138 (2012).

Papers in Preparation as the Lead Author:

- **Soheil Zeraati Rezaei**, Yasser Al Qahtani, Hongming Xu, *Investigation of Low-injection-pressures and Hot-EGR for a Dieseline(RON-75) Fuelled PCI Engine – Part I: Combustion Performance and Gaseous Emissions*, (Prepared for the Journal of Fuel).
- **Soheil Zeraati Rezaei**, Yasser Al Qahtani, Hongming Xu, Jose M. Herreros, *Investigation of the Diesel, Dieseline and Naphtha Fuelled Premixed Compression-ignition Engine – Part I: Low-load Operation*, (Prepared for the Journal of Applied Energy).

- **Soheil Zeraati Rezaei**, Yasser Al Qahtani, Hongming Xu, Jose M. Herreros, *Investigation of the Diesel, Dieseline and Naphtha Fuelled Premixed Compression-ignition Engine – Part II: Medium-high-load Operation*, (Prepared for the Journal of Applied Energy).
- **Soheil Zeraati Rezaei**, Jose M. Herreros, Mohammed S. Alam, Manju Tanwar, Roy M. Harrison, Hongming Xu, *Effects of the Oxidation-catalyst on Emissions from a Premixed Compression-ignition Engine – Part I: Regulated Emissions*, (Prepared for the Journal of Applied Catalysis B: Environmental).
- **Soheil Zeraati Rezaei**, Jose M. Herreros, Mohammed S. Alam, Manju Tanwar, Roy M. Harrison, Hongming Xu, *Effects of the Oxidation-catalyst on Emissions from a Premixed Compression-ignition Engine – Part II: Unregulated Emissions*, (Prepared for the Journal of Applied Catalysis B: Environmental).
- **Soheil Zeraati Rezaei**, Shahin Neishabouri, Hongming Xu, Jose M. Herreros, *Investigation of 2-methylfuran for Dual-fuel Compression-Ignition Combustion*, (Prepared for the Journal of Biofuels Engineering).

Oral Presentations:

- **Soheil Zeraati Rezaei**, Mohammed S. Alam, Zhirong Liang, Christopher P. Stark, Roy M. Harrison, Hongming Xu, *Investigation of SVOC in Diesel Fuel, Engine Lubricating Oil and Diesel Engine Emissions*, Cambridge Particle Meeting 2016, University of Cambridge UK, 10th of June 2016.
- **Soheil Zeraati Rezaei**, Fan Zhang, Hongming Xu, Shijin Shuai, *Experimental Investigation of Different Blends of Diesel and Gasoline (Dieseline) in a CI Engine*, SAE 2014 International PFL Meeting, Birmingham UK, 20th of October 2014.
- **Soheil Zeraati Rezaei**, Fan Zhang, Hongming Xu, Akbar Ghafourian, Jose M. Herreros, *Investigation of Injection Strategies for a Dieseline Fuelled PPCI Engine*, UnICEG Meeting, University of Bath UK, 11th of April 2013.

REFERENCES

1. Stone, R., *Introduction to Internal Combustion Engines*. Third ed1999: MACMILLAN PRESS LTD.
2. Kalghatgi, G., *Fuel/Engine Interactions*2013: SAE International.
3. IEA. *Energy and Air Pollution*. 2016 [cited 2016 01/07/2016]; Available from: http://www.iea.org/publications/freepublications/publication/WorldEnergyOutlookSpecialReport2016EnergyandAirPollution.pdf.
4. IEA. *WORLD ENERGY OUTLOOK 2015 FACTSHEET - Global energy trends to 2040*. 2015 [cited 2016 26/06/2016]; Available from: http://www.worldenergyoutlook.org/media/weowebsite/2015/WEO2015_Factsheets.pdf.
5. IEA. *World Energy Outlook 2015 - Executive Summary*. 2015 [cited 2016 26/06/2016]; Available from: http://www.iea.org/publications/freepublications/publication/WEB_WorldEnergyOutlook2015ExecutiveSummaryEnglishFinal.pdf.
6. Sawyer, R.F., *Science based policy for addressing energy and environmental problems.* Proceedings of the Combustion Institute, 2009. **32**(1): p. 45-56.
7. Dockery, D.W., et al., *An Association between Air Pollution and Mortality in Six U.S. Cities.* New England Journal of Medicine, 1993. **329**(24): p. 1753-1759.
8. *Handbook of Diesel Engines*, K. Mollenhauer and H. Tschöke, Editors. 2010, Springer-Verlag Berlin Heidelberg.
9. DieselNet. *Emission Standards - European Union - Cars and Light Trucks*. 2016 [cited 2016 18/06/2016]; Available from: https://www.dieselnet.com//standards/eu/ld.php.
10. ExxonMobil. *The Outlook for Energy: A View to 2040*. 2016 [cited 2016 05/07/2016]; Available from: http://cdn.exxonmobil.com/~/media/global/files/outlook-for-energy/2016/2016-outlook-for-energy.pdf.
11. Dearman. *The Dearman Engine*. 2016 [cited 2016 06/07/2016]; Available from: http://dearman.co.uk/dearman-technologies/the-dearman-engine/.
12. Anitescu, G., T.J. Bruno, and L.L. Tavlarides, *Dieseline for Supercritical Injection and Combustion in Compression-Ignition Engines: Volatility, Phase Transitions, Spray/Jet Structure, and Thermal Stability.* Energy & Fuels, 2012. **26**(10): p. 6247-6258.
13. SMMT. *MOTOR INDUSTRY FACTS 2015*. 2015 [cited 2016 05/07/2016]; Available from: http://www.smmt.co.uk/wp-content/uploads/sites/2/100049_SMMT-Facts-Guide-2015.pdf.
14. Campanari, S., G. Manzolini, and F. Garcia de la Iglesia, *Energy analysis of electric vehicles using batteries or fuel cells through well-to-wheel driving cycle simulations.* Journal of Power Sources, 2009. **186**(2): p. 464-477.
15. Amjad, S., S. Neelakrishnan, and R. Rudramoorthy, *Review of design considerations and technological challenges for successful development and deployment of plug-in hybrid electric vehicles*, in *Renew. Sust. Energ. Rev.*2009. p. 1104-1110.
16. Heywood, J.B., *Internal combustion engine fundamentals*1988: McGraw-Hill.
17. Burger, J.L., R.V. Gough, and T.J. Bruno, *Characterization of Dieseline with the Advanced Distillation Curve Method: Hydrocarbon Classification and Enthalpy of Combustion.* Energy & Fuels, 2013. **27**(2): p. 787-795.
18. Al-Abdullah, M.H., G.T. Kalghatgi, and H. Babiker, *Flash points and volatility characteristics of gasoline/diesel blends.* Fuel, 2015. **153**: p. 67-69.

19. Dec, J.E., *A Conceptual Model of DI Diesel Combustion Based on Laser-Sheet Imaging**, 1997, SAE International, SAE Technical Paper 970873.
20. Kamimoto, T. and M.-h. Bae, *High Combustion Temperature for the Reduction of Particulate in Diesel Engines*, 1988, SAE International, SAE Technical Paper 880423.
21. Dec, J.E., *Advanced compression-ignition engines—understanding the in-cylinder processes.* Proceedings of the Combustion Institute, 2009. **32**(2): p. 2727-2742.
22. Musculus, M.P.B., P.C. Miles, and L.M. Pickett, *Conceptual models for partially premixed low-temperature diesel combustion.* Progress in Energy and Combustion Science, 2013. **39**(2-3): p. 246-283.
23. Bruneaux, G., *Combustion structure of free and wall-impinging diesel jets by simultaneous laser-induced fluorescence of formaldehyde, poly-aromatic hydrocarbons, and hydroxides.* International Journal of Engine Research, 2008. **9**(3): p. 249-265.
24. Eastwood, P., *Particulate emissions from vehicles*2008: SAE International and Wiley-PEPublishing Series.
25. Higgins, B. and D.L. Siebers, *Measurement of the Flame Lift-Off Location on DI Diesel Sprays Using OH Chemiluminescence*, 2001, SAE International, SAE Technical Paper 2001-01-0918.
26. Siebers, D.L. and B. Higgins, *Flame Lift-Off on Direct-Injection Diesel Sprays Under Quiescent Conditions*, 2001, SAE International, SAE Technical Paper 2001-01-0530.
27. Plee, S.L., T. Ahmad, and J.P. Myers, *Flame Temperature Correlation for the Effects of Exhaust Gas Recirculation on Diesel Particulate and NOx Emissions*, 1981, SAE International, SAE Technical Paper 811195.
28. Plee, S.L., et al., *Nineteenth Symposium (International) on Combustion Diesel NOx emissions—A simple correlation technique for intake air effects.* Symposium (International) on Combustion, 1982. **19**(1): p. 1495-1502.
29. Ladommatos, N., et al., *The Dilution, Chemical, and Thermal Effects of Exhaust Gas Recirculation on Diesel Engine Emissions - Part 1: Effect of Reducing Inlet Charge Oxygen*, 1996, SAE International, SAE Technical Paper 961165.
30. Ladommatos, N., et al., *The Dilution, Chemical, and Thermal Effects of Exhaust Gas Recirculation on Diesel Engine Emissions - Part 2: Effects of Carbon Dioxide*, 1996, SAE International, SAE Technical Paper 961167.
31. Ladommatos, N., et al., *The Dilution, Chemical, and Thermal Effects of Exhaust Gas Recirculation on Diesel Engine Emissions - Part 3: Effects of Water Vapour*, 1997, SAE International, SAE Technical Paper 971659.
32. Ladommatos, N., et al., *The Dilution, Chemical, and Thermal Effects of Exhaust Gas Recirculation on Diesel Engine Emissions - Part 4: Effects of Carbon Dioxide and Water Vapour*, 1997, SAE International, SAE Technical Paper 971660.
33. Ladommatos, N., et al., *The Effects on Diesel Combustion and Emissions of Reducing Inlet Charge Mass Due to Thermal Throttling with Hot EGR*, 1998, SAE International, SAE Technical Paper 980185.
34. Ladommatos, N., S. Abdelhalim, and H. Zhao, *The effects of exhaust gas recirculation on diesel combustion and emissions.* International Journal of Engine Research, 2000. **1**(1): p. 107-126.
35. Kalghatgi, G.T., et al., *Surrogate fuels for premixed combustion in compression ignition engines.* International Journal of Engine Research, 2011. **12**(5): p. 452-465.
36. Kanda, T., et al., *PCCI Operation with Early Injection of Conventional Diesel Fuel*, 2005, SAE International, SAE Technical Paper 2005-01-0378.

37. Kashdan, J.T., S. Mendez, and G. Bruneaux, *On the origin of Unburned Hydrocarbon Emissions in a Wall Guided, Low NOx Diesel Combustion System*, 2007, SAE International, SAE Technical Paper 2007-01-1836.
38. Hotta, Y., et al., *Achieving Lower Exhaust Emissions and Better Performance in an HSDI Diesel Engine with Multiple Injection*, 2005, SAE International, SAE Technical Paper 2005-01-0928.
39. Zhang, L., *A Study of Pilot Injection in a DI Diesel Engine*, 1999, SAE International, SAE Technical Paper 1999-01-3493.
40. Reitz, R.D. and G. Duraisamy, *Review of high efficiency and clean reactivity controlled compression ignition (RCCI) combustion in internal combustion engines.* Progress in Energy and Combustion Science, 2015. **46**: p. 12-71.
41. Zhang, F., et al., *Experimental Investigation of Different Blends of Diesel and Gasoline (Dieseline) in a CI Engine.* SAE International Journal of Engines, 2014. **7**(4): p. 1920-1930.
42. Algunaibet, I.M., et al., *Flammability and volatility attributes of binary mixtures of some practical multi-component fuels.* Fuel, 2016. **172**: p. 273-283.
43. Zeraati Rezaei, S., et al., *Investigation of two-stage split-injection strategies for a Dieseline fuelled PPCI engine.* Fuel, 2013. **107**: p. 299-308.
44. Ma, X., et al., *High Speed Imaging Study on the Spray Characteristics of Dieseline at Elevated Temperatures and Back Pressures.* SAE International Journal of Fuels and Lubricants, 2014. **7**(1): p. 159-166.
45. Ma, X., et al., *Throttleless and EGR-controlled stoichiometric combustion in a diesel–gasoline dual-fuel compression ignition engine.* Fuel, 2014. **115**: p. 765-777.
46. Zhang, F., et al., *Combustion and Emission Characteristics of a PPCI Engine Fuelled with Dieseline*, 2012, SAE International, SAE Technical Paper 2012-01-1138.
47. Zhang, F., et al., *Investigation into Light Duty Dieseline Fuelled Partially-Premixed Compression Ignition Engine.* SAE International Journal of Engines, 2011. **4**(1): p. 2124-2134.
48. Zhang, F., *Spray, combustion and emission characteristics of dieseline fuel*, 2013, PhD Thesis, University of Birmingham.
49. Turner, D., et al., *An Experimental Study of Dieseline Combustion in a Direct Injection Engine*, 2009, SAE International, SAE Technical Paper 2009-01-1101.
50. Wang, J., Z. Wang, and H. Liu, *Combustion and emission characteristics of direct injection compression ignition engine fueled with Full Distillation Fuel (FDF).* Fuel, 2015. **140**: p. 561-567.
51. Liu, H., et al., *Effects of gasoline research octane number on premixed low-temperature combustion of wide distillation fuel by gasoline/diesel blend.* Fuel, 2014. **134**: p. 381-388.
52. Methanol-Safe-Handling. *Using Physical and Chemical Properties to Manage Flammable Liquid Hazards*. 2016 [cited 2016 01/04/2016]; Available from: http://www.methanol.org/Health-And-Safety/Technical-Bulletins/Technical-Bulletins/UsingPhysicalandChemicalPropertiestoManageFlam-(1).aspx.
53. Pickett, L.M., D.L. Siebers, and C.A. Idicheria, *Relationship Between Ignition Processes and the Lift-Off Length of Diesel Fuel Jets*, 2005, SAE International, SAE Technical Paper 2005-01-3843.
54. Viollet, Y., J. Chang, and G. Kalghatgi, *Compression Ratio and Derived Cetane Number Effects on Gasoline Compression Ignition Engine Running with Naphtha Fuels.* SAE International Journal of Fuels and Lubricants, 2014. **7**(2): p. 412-426.

55. Chang, J., et al., *Enabling High Efficiency Direct Injection Engine with Naphtha Fuel through Partially Premixed Charge Compression Ignition Combustion*, 2012, SAE International, SAE Technical Paper 2012-01-0677.
56. Chang, J., et al., *Fuel Economy Potential of Partially Premixed Compression Ignition (PPCI) Combustion with Naphtha Fuel*, 2013, SAE International, SAE Technical Paper 2013-01-2701.
57. Zhu, H., et al., *Effect of biodiesel and ethanol on load limits of high-efficiency premixed low-temperature combustion in a diesel engine.* Fuel, 2013. **106**: p. 773-778.
58. Han, X., M. Zheng, and J. Wang, *Fuel suitability for low temperature combustion in compression ignition engines.* Fuel, 2013. **109**: p. 336-349.
59. Campos-Fernandez, J., et al., *Performance tests of a diesel engine fueled with pentanol/diesel fuel blends.* Fuel, 2013. **107**: p. 866-872.
60. Liu, H., et al., *Effects of fuel properties on combustion and emissions under both conventional and low temperature combustion mode fueling 2,5-dimethylfuran/diesel blends.* Energy, 2013. **62**: p. 215-223.
61. Benajes, J., et al., *An Investigation on Mixing and Auto-ignition using Diesel and Gasoline in a Direct-Injection Compression-Ignition Engine Operating in PCCI Combustion Conditions.* SAE Int. J. Engines, 2011. **4**(2): p. 2590-2602.
62. Dijkstra, R., et al., *Assessment of the Effect of Low Cetane Number Fuels on a Light Duty CI Engine: Preliminary Experimental Characterization in PCCI Operating Condition*, 2011, SAE International, SAE Technical Paper 2011-24-0053.
63. Lu, X., D. Han, and Z. Huang, *Fuel design and management for the control of advanced compression-ignition combustion modes.* Progress in Energy and Combustion Science, 2011. **37**(6): p. 741-783.
64. Manente, V., B. Johansson, and W. Cannella, *Gasoline partially premixed combustion, the future of internal combustion engines?* International Journal of Engine Research, 2011. **12**(3): p. 194-208.
65. Kalghatgi, G., L. Hildingsson, and B. Johansson, *Low NOx and Low Smoke Operation of a Diesel Engine Using Gasolinelike Fuels.* Journal of Engineering for Gas Turbines and Power, 2010. **132**(9): p. 092803-092803.
66. Yang, Y., et al., *Partial Fuel Stratification to Control HCCI Heat Release Rates: Fuel Composition and Other Factors Affecting Pre-Ignition Reactions of Two-Stage Ignition Fuels.* SAE Int. J. Engines, 2011. **4**(1): p. 1903-1920.
67. Dec, J.E., et al., *Effects of Gasoline Reactivity and Ethanol Content on Boosted, Premixed and Partially Stratified Low-Temperature Gasoline Combustion (LTGC).* SAE International Journal of Engines, 2015. **8**(3).
68. Ciatti, S., et al., *Efficiency and Emissions performance of Multizone Stratified Compression Ignition Using Different Octane Fuels*, 2013, SAE International, SAE Technical Paper 2013-01-0263.
69. Han, D., et al., *Attainment and Load Extension of High-Efficiency Premixed Low-Temperature Combustion with Dieseline in a Compression Ignition Engine.* Energy & Fuels, 2010. **24**(6): p. 3517-3525.
70. Yang, H., et al., *Fuel octane effects on gasoline multiple premixed compression ignition (MPCI) mode.* Fuel, 2013. **103**: p. 373-379.
71. Kim, K., et al., *Load expansion of naphtha multiple premixed compression ignition (MPCI) and comparison with partially premixed compression ignition (PPCI) and conventional diesel combustion (CDC).* Fuel, 2014. **136**: p. 1-9.
72. Tuner, M., et al., *Multi Cylinder Partially Premixed Combustion Performance Using Commercial Light-Duty Engine Hardware*, 2014, SAE International, SAE Technical Paper 2014-01-2680.

73. Han, D., et al., *HC and CO emissions of premixed low-temperature combustion fueled by blends of diesel and gasoline.* Fuel, 2012. **99**: p. 13-19.
74. Sellnau, M., et al., *Development of a Gasoline Direct Injection Compression Ignition (GDCI) Engine.* SAE International Journal of Engines, 2014. **7**(2): p. 835-851.
75. Sellnau, M., et al., *Gasoline Direct Injection Compression Ignition (GDCI) - Diesel-like Efficiency with Low CO2 Emissions.* SAE International Journal of Engines, 2011. **4**(1): p. 2010-2022.
76. Sellnau, M.C., et al., *Full-Time Gasoline Direct-Injection Compression Ignition (GDCI) for High Efficiency and Low NOx and PM.* SAE International Journal of Engines, 2012. **5**(2): p. 300-314.
77. Sellnau, M.C., et al., *Part-Load Operation of Gasoline Direct-Injection Compression Ignition (GDCI) Engine*, 2013, SAE International, SAE Technical Paper 2013-01-0272.
78. Cracknell, R.F., et al., *Modelling a Gasoline Compression Ignition (GCI) Engine Concept*, 2014, SAE International, SAE Technical Paper 2014-01-1305.
79. Kalghatgi, G.T., P. Risberg, and H.-E. Ångström, *Advantages of Fuels with High Resistance to Auto-ignition in Late-injection, Low-temperature, Compression Ignition Combustion*, 2006, SAE International, SAE Technical Paper 2006-01-3385.
80. Kalghatgi, G.T., et al., *Some advantages and challenges of running a Euro IV, V6 diesel engine on a gasoline fuel.* Fuel, 2013. **108**: p. 197-207.
81. Hildingsson, L., et al., *Fuel Octane Effects in the Partially Premixed Combustion Regime in Compression Ignition Engines*, 2009, SAE International, SAE Technical Paper 2009-01-2648.
82. Won, H.W., et al., *Sufficiently premixed compression ignition of a gasoline-like fuel using three different nozzles in a diesel engine.* Proceedings of the Institution of Mechanical Engineers, Part D: Journal of Automobile Engineering, 2012. **226**(5): p. 698-708.
83. Inagaki, K., et al., *Dual-Fuel PCI Combustion Controlled by In-Cylinder Stratification of Ignitability*, 2006, SAE International, SAE Technical Paper 2006-01-0028.
84. Kokjohn, S.L., et al., *Experiments and Modeling of Dual-Fuel HCCI and PCCI Combustion Using In-Cylinder Fuel Blending.* SAE Int. J. Engines, 2009. **2**(2): p. 24-39.
85. Kittelson, D.B., *Engines and nanoparticles: a review.* Journal of Aerosol Science, 1998. **29**(5–6): p. 575-588.
86. Alam, M.S., et al., *The characterisation of diesel exhaust particles - composition, size distribution and partitioning.* Faraday Discussions, 2016. **189**(0): p. 69-84.
87. Laurence, R.B., V.W. Wong, and A.J. Brown, *Effects of Lubrication System Parameters on Diesel Particulate Emission Characteristics*, 1996, SAE International, SAE Technical Paper 960318.
88. Funkenbusch, E.F., D.G. Leddy, and J.H. Johnson, *The Characterization of the Soluble Organic Fraction of Diesel Particulate Matter*, 1979, SAE International, SAE Technical Paper 790418.
89. Black, F. and L. High, *Methodology for Determining Particulate and Gaseous Diesel Hydrocarbon Emissions*, 1979, SAE International, SAE Technical Paper 790422.
90. Ning, Z., C.S. Cheung, and S.X. Liu, *Experimental investigation of the effect of exhaust gas cooling on diesel particulate.* Journal of Aerosol Science, 2004. **35**(3): p. 333-345.
91. Donahue, N.M., et al., *Coupled Partitioning, Dilution, and Chemical Aging of Semivolatile Organics.* Environmental Science & Technology, 2006. **40**(8): p. 2635-2643.

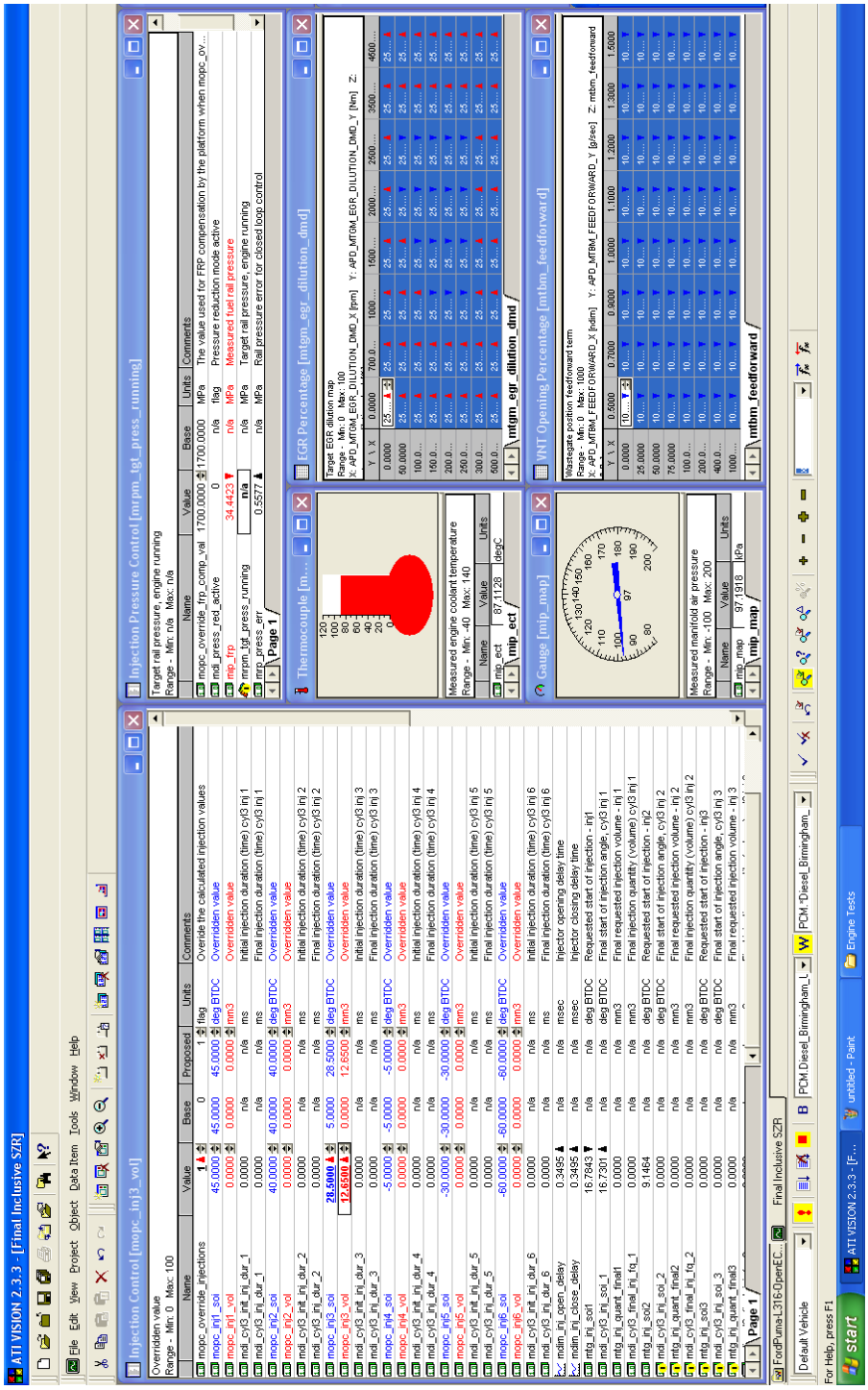
92. Huang, L., et al., *Effects of fuels, engine load and exhaust after-treatment on diesel engine SVOC emissions and development of SVOC profiles for receptor modeling.* Atmos Environ (1994), 2015. **102**: p. 229-238.
93. Sakurai, H., et al., *On-line measurements of diesel nanoparticle composition and volatility.* Atmospheric Environment, 2003. **37**(9-10): p. 1199-1210.
94. Zeraati-Rezaei, S., et al. *Investigation of SVOC in diesel fuel, engine lubricating oil and diesel engine emissions*. in *Cambridge Particle Meeting (on 10/06/2016)*. 2016. University of Cambridge.
95. Majewski, W.A. and M.K. Khair, *Diesel Emissions and Their Control*2006: SAE International.
96. Hasegawa, R. and H. Yanagihara, *HCCI Combustion in DI Diesel Engine*, 2003, SAE International, SAE Technical Paper 2003-01-0745.
97. Kimura, S., et al., *New Combustion Concept for Ultra-Clean and High-Efficiency Small DI Diesel Engines*, 1999, SAE International, SAE Technical Paper 1999-01-3681.
98. Kimura, S., et al., *Ultra-Clean Combustion Technology Combining a Low-Temperature and Premixed Combustion Concept for Meeting Future Emission Standards*, 2001, SAE International, SAE Technical Paper 2001-01-0200.
99. Kimura, S., et al., *An experimental analysis of low-temperature and premixed combustion for simultaneous reduction of NOx and particulate emissions in direct injection diesel engines.* International Journal of Engine Research, 2002. **3**(4): p. 249-259.
100. Kim, C.H., et al., *The Effect of Pt-Pd Ratio on Oxidation Catalysts Under Simulated Diesel Exhaust*, 2011, SAE International, SAE Technical Paper 2011-01-1134.
101. Lefort, I., *Thermally efficient advanced diesel exhaust aftertreatment for cleaner vehicles*, 2015, PhD Thesis, University of Birmingham.
102. Guan, B., et al., *Review of the state-of-the-art of exhaust particulate filter technology in internal combustion engines.* J Environ Manage, 2015. **154**: p. 225-58.
103. Spivey, J.J., *Complete catalytic oxidation of volatile organics.* Industrial & Engineering Chemistry Research, 1987. **26**(11): p. 2165-2180.
104. Russell, A. and W.S. Epling, *Diesel Oxidation Catalysts.* Catalysis Reviews, 2011. **53**(4): p. 337-423.
105. Johnson, J.E. and D.B. Kittelson, *Physical Factors Affecting Hydrocarbon Oxidation in a Diesel Oxidation Catalyst*, 1994, SAE International, SAE Technical Paper 941771.
106. Veser, G., M. Ziauddin, and L.D. Schmidt, *Ignition in alkane oxidation on noble-metal catalysts.* Catalysis Today, 1999. **47**(1–4): p. 219-228.
107. Hunter, K.C. and A.L.L. East, *Properties of C−C Bonds in n-Alkanes: Relevance to Cracking Mechanisms.* The Journal of Physical Chemistry A, 2002. **106**(7): p. 1346-1356.
108. Diehl, F., et al., *Catalytic oxidation of heavy hydrocarbons over Pt/Al2O3. Influence of the structure of the molecule on its reactivity.* Applied Catalysis B: Environmental, 2010. **95**(3-4): p. 217-227.
109. Hug, H.T., A. Mayer, and A. Hartenstein, *Off-Highway Exhaust Gas After-Treatment:Combining Urea-SCR, Oxidation Catalysis and Traps*, 1993, SAE International, SAE Technical Paper 930363.
110. Pi-Innovo. 2016 [cited 2016 28/07/2016]; Available from: http://pi-innovo.com/product/.
111. Axiomatic-global-electronic-solutions. 2016 [cited 2016 28/07/2016]; Available from: http://www.axiomatic.com/.

112. Accurate-Technologies. 2016 [cited 2016 28/07/2016]; Available from: https://www.accuratetechnologies.com/ECUCalibration/VISIONSoftware.
113. Accurate-Technologies. *VISION Software*. 2016 [cited 2016 28/07/2016]; Available from: https://www.accuratetechnologies.com/DataAcquisition/VISIONHub.
114. Zhang, J., *Particle matter emission control and related issues for Diesel engines*, 2011, PhD Thesis, University of Birmingham.
115. National-Instruments. *NI USB-6218*. 2016 [cited 2016 29/07/2016]; Available from: http://sine.ni.com/nips/cds/view/p/lang/en/nid/203484.
116. Variohm. *EPT3100 - Pressure Sensors For Motorsport*. 2016 [cited 2016 29/07/2016]; Available from: http://www.variohm.com/motorsports/sensors-detail.php?mid=50&did=EPT3100.
117. Wallner, T., *Correlation Between Speciated Hydrocarbon Emissions and Flame Ionization Detector Response for Gasoline/Alcohol Blends.* Journal of Engineering for Gas Turbines and Power, 2011. **133**(8): p. 082801-082801.
118. AVL, *SMOKE VALUE MEASUREMENT WITH THE FILTER-PAPER-METHOD - Application Note*, 2005.
119. AVL, *AVL 415S - VARIABLE SAMPLING SMOKE METER Operating Manual*, 2007.
120. CAMBUSTION, *DMS500 Fast Particulate Analyzer - User Manual - Version 4.03*, 2015.
121. CAMBUSTION. *Cambustion Application Note DMS01 - Particulate Mass Measurement with DMS Series Fast Spectrometers*. 2015 [cited 2016 30/07/2016]; Available from: http://www.cambustion.com/sites/default/files/applications/DMS/dms01v05.pdf.
122. Alam, M.S., et al., *Application of 2D-GCMS reveals many industrial chemicals in airborne particulate matter.* Atmospheric Environment, 2013. **65**: p. 101-111.
123. Alam, M.S. and R.M. Harrison, *Recent advances in the application of 2-dimensional gas chromatography with soft and hard ionisation time-of-flight mass spectrometry in environmental analysis.* Chemical Science, 2016. **7**(7): p. 3968-3977.
124. Sunset-Laboratory. *Lab OC-EC Aerosol Analyzer*. 2016 [cited 2016 30/07/2016]; Available from: http://www.sunlab.com/lab-oc-ec-aerosol-analyzer/.
125. Randolph, A.L., *Methods of Processing Cylinder-Pressure Transducer Signals to Maximize Data Accuracy*, 1990, SAE International, SAE Technical Paper 900170.
126. Silvis, W.M., *An Algorithm for Calculating the Air/Fuel Ratio from Exhaust Emissions*, 1997, SAE International, SAE Technical Paper 970514.
127. Ciatti, S. and S.N. Subramanian, *An Experimental Investigation of Low-Octane Gasoline in Diesel Engines.* Journal of Engineering for Gas Turbines and Power, 2011. **133**(9): p. 092802-092802.
128. Win, Z., et al., *24 Noise, Emissions and Fuel Economy Investigation on a Small DI Diesel Using Taguchi Methods*, 2002, SAE International, SAE Technical Paper 2002-32-1793.
129. Garcia-Diaz, A. and D. Phillips, *Principles of experimental design and analysis*1995, London: Chapman & Hall.
130. Park, S. and J. Anthony, *Robust Design for quality engineering and six sigma*2008, Singapore: World Scientific.
131. Muether, M., et al., *Advanced Combustion for Low Emissions and High Efficiency Part 1: Impact of Engine Hardware on HCCI Combustion*, 2008, SAE International, SAE Technical Paper 2008-01-2405.
132. Park, S.H., H.J. Kim, and C.S. Lee, *Effect of Multiple Injection Strategies on Combustion and Emission Characteristics in a Diesel Engine.* Energy & Fuels, 2016. **30**(2): p. 810-818.

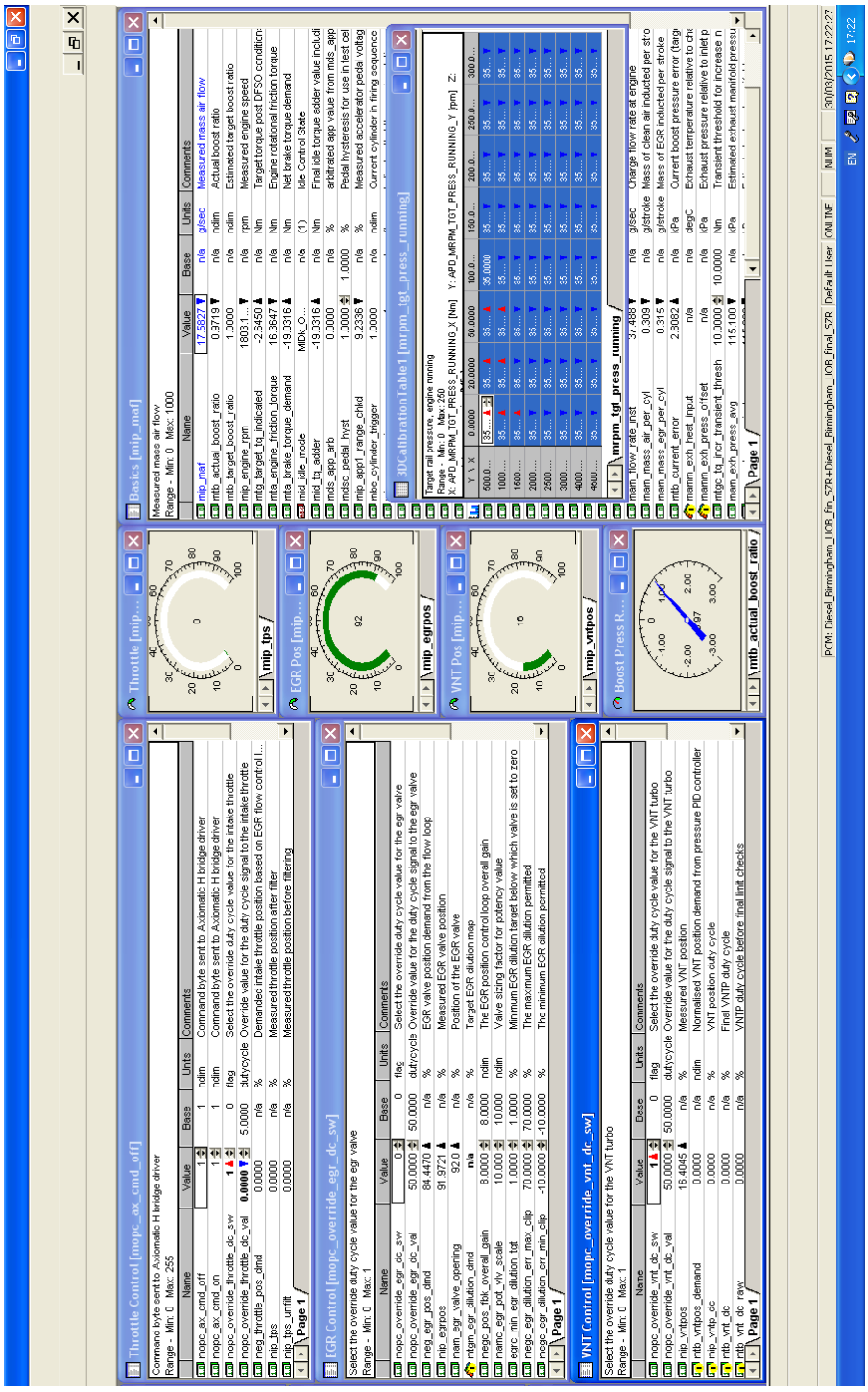
133. Park, S.H., I.M. Youn, and C.S. Lee, *Influence of ethanol blends on the combustion performance and exhaust emission characteristics of a four-cylinder diesel engine at various engine loads and injection timings.* Fuel, 2011. **90**(2): p. 748-755.
134. Shi, Y. and R.D. Reitz, *Optimization of a heavy-duty compression–ignition engine fueled with diesel and gasoline-like fuels.* Fuel, 2010. **89**(11): p. 3416-3430.
135. Kook, S., et al., *The Effect of Swirl Ratio and Fuel Injection Parameters on CO Emission and Fuel Conversion Efficiency for High-Dilution, Low-Temperature Combustion in an Automotive Diesel Engine*, 2006, SAE International, SAE Technical Paper 2006-01-0197.
136. Weall, A. and N. Collings, *Highly Homogeneous Compression Ignition in a Direct Injection Diesel Engine Fuelled with Diesel and Biodiesel*, 2007, SAE International, SAE Technical Paper 2007-01-2020.
137. Armas, O., A. Gómez, and J.M. Herreros, *Uncertainties in the determination of particle size distributions using a mini tunnel–SMPS system during Diesel engine testing.* Measurement Science and Technology, 2007. **18**(7): p. 2121.
138. Adams, C.A., et al., *Effects of biodiesel–gasoline blends on gasoline direct-injection compression ignition (GCI) combustion.* Fuel, 2013. **111**: p. 784-790.
139. DieselNet. *Heavy-Duty Truck and Bus Engines - Regulatory Framework*. 2012 [cited 2016 18/06/2016]; Available from: https://www.dieselnet.com/standards/eu/hd.php.
140. Jacobs, T.J. and D.N. Assanis, *Characteristic Response of a Production Diesel Oxidation Catalyst Exposed to Lean and Rich PCI Exhaust.* Journal of Engineering for Gas Turbines and Power, 2008. **130**(4): p. 042805.
141. Ladommatos, N., P. Rubenstein, and P. Bennett, *Some effects of molecular structure of single hydrocarbons on sooting tendency.* Fuel, 1996. **75**(2): p. 114-124.
142. Shi, J.P. and R.M. Harrison, *Investigation of Ultrafine Particle Formation during Diesel Exhaust Dilution.* Environmental Science & Technology, 1999. **33**(21): p. 3730-3736.

APPENDIX

A1. Engine control with ATI VISION interface



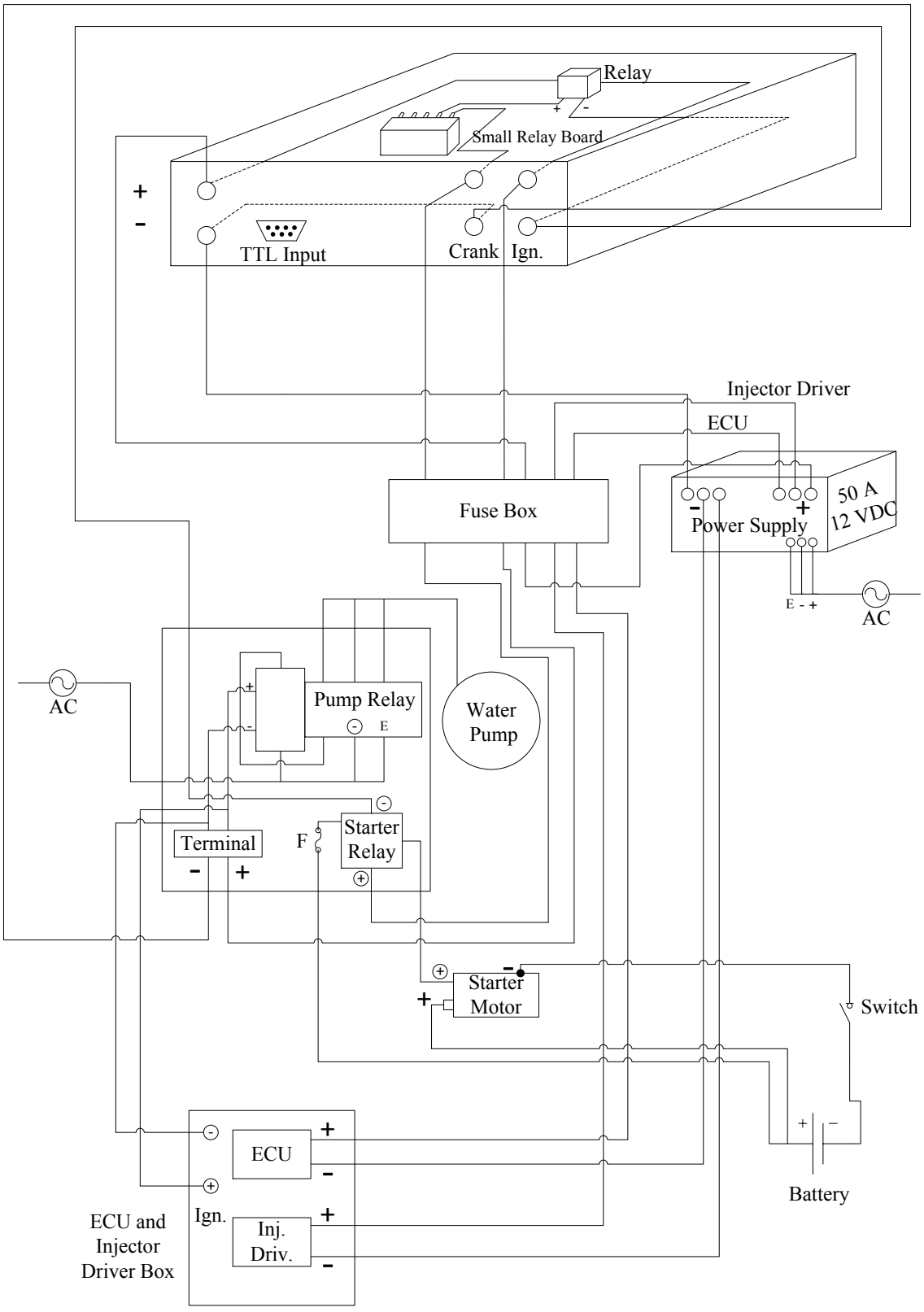
(a)



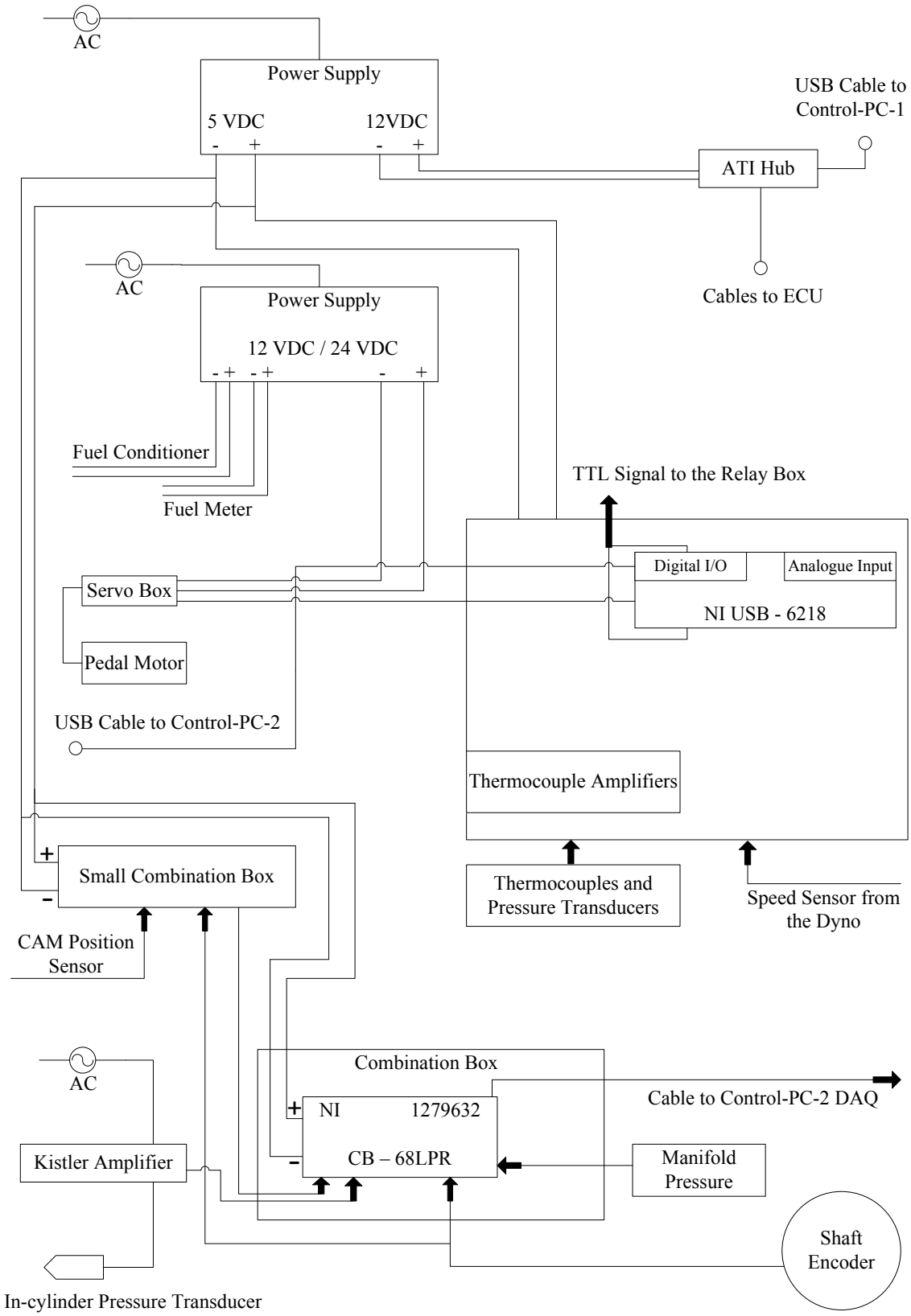
(b)

Figure A-1 ATI VISION interface (a) part 1 and (b) part 2

A2. Electrical and signal connections of the engine test cell



(a)



(b)

Figure A-2 Electrical and signal connections of the engine test cell (a) part 1 and (b) part 2

A3. Extraction Procedure for GC×GC-TOF-MS Analysis

Internal standard mix (this is prepared prior to extraction). The internal standard mix is composed of:

- *n*-Dodecane-d26 (1.0 mg/mL in 1.1 mL isooctane)
- *n*-Pentadecane-d32 (1.0 mg/mL in 1.1 mL isooctane)
- *n*-Eicosane-d42 (1.0 mg/mL in 1 mL isooctane
- *n*-Pentacosane-d52 (1.0 mg/mL in 1.1 mL isooctane)
- *n*-Triacontane-d62 (1 mg/mL in 1.1 mL isooctane)
- *p*-Terphenyl-d14 (100 μg/mL in 1 mL toluene)

All internal standards can be purchased from Greyhound ChemService (Birkenhead, UK) and were mixed together in isooctane.